

STOPBANK PERFORMANCE DURING THE  
2010 – 2011 CANTERBURY EARTHQUAKE SEQUENCE

---

A thesis submitted in partial fulfilment of the requirements for the Degree  
of Master of Science in Engineering Geology

in the University of Canterbury

by

Sophie Elizabeth Bainbridge

University of Canterbury

2013

---

For my grandad

**Deryck Wallis**

Who has always taught me that educational capital is the  
best investment you can make

## I. ACKNOWLEDGMENTS

Firstly, I would like to thank my supervisors Misko Cubrinovski, Tim McMorran and Jarg Pettinga for their assistance during the data processing phase and their reviews of this manuscript. I appreciate the time afforded to me as I understand the pressures that my supervisors have been under following the 2010 – 2011 Canterbury earthquake sequence. Tim in particular was always on hand to discuss issues as they came up and for this I am extremely grateful. Thanks also to Matthew Hughes, who I consider an unofficial supervisor. His assistance with GIS, his support and guidance in marrying a life of academic research and consultancy together and his encouraging words were a constant throughout the entire project.

I would also like to extend my gratitude towards local consultancies and authorities GHD Pty Ltd., Riley Consultants, Christchurch City Council and Environment Canterbury for their assistance in providing data for use in this thesis. Tom Parsons from GHD was always willing to open the door to his office and his data for me as a student, rather than a rival consultant, and for that I am extremely grateful.

A great deal of thanks goes to my Golder family (GANZL). As a part time student I tend to do most of my work in the weekends or after work in the office. These people around me have been so supportive that I am somewhat overwhelmed by the level of encouragement and practical support that has been offered to me. I'd like to thank the whole geotechnical team as everyone has at some point asked me how it is going and smiled empathetically when I discuss my trials and tribulations, I really appreciate that. Some real standouts who went out of their way to help either by undertaking a review or frequent mediation sessions include Marie-Claude Hébert, Krystle-Rae Brooks, Ian Lloyd, Natalie Connor, Dave Barry-MacCaulay, Michael Kerkham, Rich Little and Matt Howard. I would also like to thank the managing director Hannah Hamling, who approved two weeks of paid study leave for me.

Above all, I would like to thank the people in my life who make it all worthwhile. The people who have supported me through this and will continue to support me through everything I do. My wonderful and fun friends, Louise Vick, Courtney, Tash, Fi, Locksley, Louise Moody, Amanda, Maddy, Stacey, Mat and Laura. Alex's family; Nick, Denise, Luke, Beth, John and Katrina, the cheery voices at the end of skype. And of course, my family, my grandparents Deryck and Maureen, my Uncle David and Auntie Penny, my amazing parents who I love so much and am just so humbled by and my sister and brother who are the best. I feel like I'm forgetting someone... Oh! I know... Alex, the love of my life, who has been there for me throughout my whole thesis, reviewing my work, walking the dogs, taking me out for brunch and having dance parties with me in the kitchen. I love all of you and I'm so grateful to have you in my life.

## II. TABLE OF CONTENTS

I.	Acknowledgments .....	3
II.	Table of Contents .....	4
III.	List of Figures and Tables .....	8
IV.	List of Tables .....	12
V.	Abstract .....	13
1.0	Introduction .....	15
1.1	Project Background and Objective .....	15
1.2	Objectives .....	15
1.3	Thesis Format .....	16
2.0	Site Setting and 2010-2011 Canterbury Earthquakes .....	17
2.1	Geology and Geomorphology of the Study Area .....	18
2.1.1	Christchurch Geomorphology .....	19
2.1.2	Kaiapoi Geomorphology .....	21
2.2	Groundwater .....	22
2.2.1	Groundwater Depth .....	23
2.2.2	Tectonic Setting .....	24
2.2.3	Tectonic Setting of Canterbury and the Study Sites .....	25
2.3	Canterbury Earthquake Sequence .....	25
2.3.1	Observed Ground Motions .....	26
2.3.2	Observed Liquefaction and Lateral Spread .....	28
2.3.3	Spatial distribution of Liquefaction .....	28
2.3.4	Lateral Spreading .....	30
2.3.5	Earthquake-Induced Vertical and Horizontal Change .....	31
2.4	Summary of Earthquake Damage observed .....	34
3.0	Literature Review .....	35
3.1	Current Practice in Levee Construction .....	36
3.2	Review of Seismic Design Methods in Major Codes of Practice .....	37



3.2.1	Performance-Based Design Philosophy .....	38
3.2.2	Risk-Based Design Philosophy .....	38
3.3	Review of Seismic Failure Mechanisms .....	39
3.3.1	Experimental Tests .....	41
3.3.2	Case Studies .....	42
3.4	local failures of levees .....	43
3.5	Summary .....	44
4.0	Observed Damage Performance of the Flood Protection System during the Canterbury Earthquake Sequence .....	45
4.1	Introduction .....	45
4.2	Overview of Observed Damage .....	45
4.2.1	Avon River .....	46
4.2.2	Waimakariri and Kaiapoi Rivers .....	47
4.2.3	Comparison of seismic demand .....	47
4.3	Data Collection .....	50
4.3.1	Kaiapoi and Waimakariri River .....	50
4.3.2	Avon River .....	51
4.4	Typical Cross Sections of Stopbanks and Construction Histories .....	52
4.4.1	Avon River .....	52
4.4.2	Kaiapoi and Waimakariri Rivers .....	55
4.5	Distribution of Crest Settlement .....	57
4.6	Distribution of Ground Cracks .....	62
4.7	Changes in River Capacity .....	66
4.7.1	Halswell River .....	66
4.7.2	Kaiapoi River .....	67
4.7.3	Avon River .....	68
5.0	Geotechnical Stopbank Deformation Modes Observed During the Canterbury Earthquake Sequence ...	69
5.1	Introduction .....	69
5.1.1	Scope and Objectives .....	69
5.2	Observed Stopbank Deformation Modes .....	70
5.3	Liquefaction-Induced Deformation of Stopbanks .....	73
5.3.1	Liquefaction and Lateral Spreading .....	73

5.3.2	Initial Stress State of the Stopbank and Native Soils .....	74
5.3.3	Pore Water Pressure .....	75
5.3.4	Effect of Soil Profile on Stopbank Deformation .....	76
5.3.5	Deformation Mode 1 – Bearing Capacity Deformation .....	78
5.3.6	Deformation Mode 2 – Minor Central Crest Settlement .....	81
5.3.7	Deformation Mode 3 – Slumping .....	83
5.3.8	Deformation Mode 4 – Lateral Stretch / Foundation Extension .....	87
5.3.9	Deformation Mode 5 – Differential settlement (due to liquefaction) .....	89
5.4	Deformation Mode 6 – Rotational Deformation .....	92
5.5	Deformation Mode 7 – Damage to Engineered Structures .....	93
5.6	Summary and Conclusions .....	96
6.0	Analysis of Geotechnical Factors Influencing Stopbank Deformation .....	97
6.1	Introduction .....	97
6.2	Scope and Objectives .....	97
6.3	Sampling Procedure .....	98
6.4	Calculated Parameters .....	100
6.4.1	CPT Analysis Methodology .....	100
6.4.2	Peak Ground Accelerations .....	101
6.4.3	Event specific depth to groundwater .....	103
6.4.4	Liquefaction Potential Index (LPI) .....	103
6.4.5	Calculated Settlement .....	103
6.4.6	non-liquefiable crust thickness .....	103
6.4.7	depth and thickness to and of the critical liquefiable layer .....	104
6.4.8	cone resistance ( $q_c$ ) .....	104
6.4.9	Soil Behaviour Type ( $I_c$ ) .....	105
6.4.10	Factor of Safety (FoS) .....	105
6.5	Land Damage Parameters and Damage Index .....	105
6.5.1	Observed Ground Cracks (A) .....	105
6.5.2	Global Lateral Ground Movement (B) .....	106
6.5.3	Vertical Elevation Change .....	106
6.5.4	EQC Land Damage Category .....	106

6.5.5	Damage Index .....	107
6.6	Stopbank Damage Parameters and Severity Classification .....	108
6.6.1	Stopbank Deformation Mode .....	108
6.6.2	Repair Index .....	108
6.6.3	Severity Classification .....	108
6.7	Geomorphology Parameters .....	111
6.7.1	Height of channel .....	111
6.7.2	Angle of slope .....	111
6.7.3	Stopbank distance to river .....	111
6.7.4	Location on the river .....	111
6.8	Analysed Dataset and CPT Samples .....	112
6.9	Primary Dataset Results .....	114
6.9.1	Liquefaction .....	115
6.9.2	Lateral Spreading .....	119
6.10	Summary .....	125
7.0	Discussion, Conclusions and Recommendations .....	127
7.1	Conclusions .....	127
7.2	Discussion .....	130
7.2.1	Liquefaction Triggering .....	131
7.2.2	Geotechnical Properties of the Critical Layer .....	131
7.2.3	Lateral Spreading .....	132
7.3	Recommendations .....	133
8.0	References .....	134

## APPENDICES

Appendix A – Case Studies

Appendix B – Riley Stopbank Damage Maps

Appendix C – Riley Test Pit Logs

Appendix D – Kaiapoi and Avon River Cross Sections

Appendix E – CPT Liquefaction Analysis (Data CD)

Appendix F – Complete Analysis Dataset (Data CD)

### III. LIST OF FIGURES AND TABLES

Figure 1: Area of Study .....	17
Figure 2: Geological Map of the Canterbury Plains and Christchurch Region, South Island, New Zealand (Forsyth et al., 2008).....	18
Figure 3: Diagrammatic cross section through Quaternary deposits underlying Christchurch. After (Brown and Weeber, 1992; Browne and Naish, 2003).....	19
Figure 4: Compiled from Christchurch City Swamps and Vegetation Cover ‘Black Map’ (1856), Christchurch Drainage Board.....	20
Figure 5: Evolution of the Waimakariri River since European Settlement (Adapted from Environment Canterbury, (2011)) .....	22
Figure 6: Event specific groundwater surface elevations (CGD0800 – 11 Feb 2013).....	23
Figure 7: New Zealand Tectonic Setting ( <a href="http://data.gns.cri.nz/geoatlas/text.jsp">http://data.gns.cri.nz/geoatlas/text.jsp</a> ). Arrows indicate movement of the pacific plate realtive to the Australian Plate. ....	24
Figure 8: Experienced aftershocks Magnitude and Location (2010 - 2012).....	26
Figure 9: Comparison of PGA’s corrected to M7.5 experienced following the major earthquake. Adapted from Bradley and Hughes, 2012.....	27
Figure 10: Observed Liquefaction Interpreted from Aerial Photography. CGD0200 - 11 Feb 2013. ....	29
Figure 11: High-resolution lliquefaction map (Cubrinovski & Taylor, 2011).....	30
Figure 12: Vertical Elevation Change Canterbury Earthquake Sequence - Avon River .....	32
Figure 13: Vertical Elevation change Canterbury Earthquake Sequence - Kaiapoi River.....	33
Figure 14: Logic tree approach for integrating the results of various assumptions (Rosidi, 2007). ....	39
Figure 15: Typical Failure Modes (Towhata, 2008).....	40
Figure 16: Definition of wave at the crest (Kano et al., 2007).....	43
Figure 17: Damaged lengths of stopbank within WEC surveyed area .....	48
Figure 18: Damaged lengths of stopbank with Avon surveyed area .....	49
Figure 19: Typical Avon River Geometries. ....	53
Figure 20: Proposed Typical Avon River Cross Sections, Adapted from GHD, 2012. ....	54
Figure 21: Evolution of Stopbank morphology along the Waimakariri and Kaiapoi Rivers .....	55

Figure 22: Typical Kaiapoi River Stopbank Geometries, Taken from Hisotrical ECan River Stopbank Design Drawings.....	56
Figure 23: Coutts Island (Kaiapoi) example of stopbank settlement being significantly greater than that of adjacent native soils.....	57
Figure 24: Vertical Elevation Change Canterbury Earthquake Sequence - Avon River .....	58
Figure 25: Location of DLS survey points (GHD, 2011) .....	59
Figure 26: North Kaiapoi River Crest Surveys (Environment Canterbury, 2011).....	60
Figure 27: Horizontal settlement vs. time along the Lower Avon River .....	61
Figure 28: Kaiapoi River Observed Cracks - Post 22 February 2011 (CGD0400).....	64
Figure 29: Avon River observed cracks, post 22 February 2011 (CGD0400).....	65
Figure 30: Typical Halswell River bank condition prior to the Septemebr earthquake event (ECan, 2012) .....	66
Figure 31: Typical Halswell River Bank condition after the September Earthquake Event (McCracken and Surman, 2012) .....	67
Figure 32: WEC System Stopbank Deformation Modes .....	71
Figure 33: Avon River Stopbank Deformation Modes .....	72
Figure 34: Schematic examples of Deformation modes of ‘limited’ liquefaction-induced lateral Spreading .....	74
Figure 35: Distribution of Principal Stresses within the stopbank and underlying foundation soils Prior to Earthquake Loading (Huang et Al., 2008).....	75
Figure 36: Excess pore water pressure ratio of a stopbank at the end of an earthquake (Huang et Al., 2008) .....	75
Figure 37: Excess Pore water Pressure Vs. Time during an Earthquake A) Below an embankment and B) Within the Free field (Huang et Al., 2008).....	76
Figure 38: Boundary curves relating thickness of A nonliquefiable surface layer to thickness of the liquefied zone, as a function of peak earthquake accelerations required to induce venting or ground rupturing at the surface (Ishihara, 1985). .....	77
Figure 39: Deformation Mode 1 - Bearing Capacity Deformation.....	78
Figure 40: Example of Bearing Capactiy Deformation (DM1-BC). Photo provided by Environment Canterbury, 2011. ....	78
Figure 41: CPT Plots for CPT-KGA-01 (CGD, 2012) .....	80
Figure 42: Deformation Mode 2 - Minor Central Crest Settlement.....	82
Figure 43: Example OF Minor Crest Settlement (DM2-MCCS). Photo provided by Environment Canterbury. .	82
Figure 44: Deformation Mode 3 - Slumping .....	83

Figure 45: Examples OF Slumping Deformation (DM3-S). PHOTO 1 (Kaiapoi South Bank) provided by Environment Canterbury; Photo 2 (Avon River South Bank) provided by GHD.....	84
Figure 46: Aerial photo indicating 1865 Kaiapoi river banks, red box indicates zone of partial slumping. ....	85
Figure 47: Plan view of corner slumping deformation on the Avon River, approximately 1.3 km North of Avon-Heathcote Estuary Mouth (CGD 0100) .....	86
Figure 48: Deformation Mode 4 – Lateral stretch / foundation Extension .....	88
Figure 49: Example OF Lateral stretch / foundation Extension (DM4-LE). Photos provided by Environment Canterbury, 2011. ....	88
Figure 50: Deformation Mode 5 - Differential Settlement of the Stopbank .....	89
Figure 51: EXAMPLE OF Differential Settlement (DM5-DS). Photo provided by Environment Canterbury. ....	89
Figure 52: CPT_1337 CLIQ analysis Depicting Liquefaction behaviour of Predominantly Fine Grained Soils .	91
Figure 53: CPT_1341 CLIQ analysis depicting behaviour of liquefiable soils with a crust.....	91
Figure 54: Settlement of Gabion Basket and slumping of retained land .....	94
Figure 55: Slumping of land behind reinforced concrete retaining wall, wall has bulged out slightly and there are minor cracks .....	94
Figure 56: Outward rotation of gabion basket and associated slumping of retained land .....	95
Figure 57: Collapse of gabion basket and subsequent slumping of land into accommodation space .....	95
Figure 58: Locations of CPTs used for analysis .....	99
Figure 59: Conditional median PGA predicted in Canterbury from a) the 4 September 2010 earthquake and b) the 22 February 2011 earthquake (Bradley and Hughes, 2012).....	102
Figure 60: Visual explanation of Crust Thickness (C), Depth to Critical Layer (T) and Thickness of Critical Layer (Z).....	104
Figure 61: Damage Severity Map - Avon River .....	110
Figure 62: Damage Severity Map - WEC System .....	110
Figure 63: Definition of cut bank and point bar deposit .....	111
Figure 64: Location of angle of slope and Hff.....	111
Figure 65: Damage index for damaged and non-damaged sites (A + C). ....	114
Figure 66: Damage Index for damaged and non-damaged sites (B + C). ....	115
Figure 67: Distribution of PGAM7.5 for Primary and Secondary Events .....	116
Figure 68: Typical Qc Values of the Critical Layer.....	117
Figure 69: Typical Qc Values of the Critical Layer for DM7-EFD.....	117

Figure 70: Average $I_c$ of the Critical Layer.....	118
Figure 71: Average FoS of the Critical Layer .....	119
Figure 72: Location of cracks in relation to damage severity .....	120
Figure 73: EQC liquefaction and lateral spreading observations in areas of a) No or Low Damage and b) Major or Severe Damage of stopbanks .....	121
Figure 74: Damage severity map for the WEC system showing location of abandoned river channels.....	122
Figure 75: Location on river comparing distribution of cut-bank, point bar or straight lengths of the river. ....	123
Figure 76: Comparison of lateral spreading measurements within specific areas along the Avon River (solid symbols correspond to 4 September 2010 data, hollow symbols correspond to 22 February 2011 data); taken from Robinson et al., 2012. ....	124

## IV. LIST OF TABLES

Table 1: Calibration of the initial LiDar point cloud sets .....	31
Table 2: Earthquake Damage Observed .....	34
Table 3: Summary of Levee Design Requirements (Adapted from EM 1110-2-1913) .....	36
Table 4: CASE HISTORIES OF PERFORMANCE OF LEVEES DURING EARTHQUAKES .....	42
Table 5: Approximate Cumulative lengths of damage for the primary rivers and Stopbank System .....	46
Table 6: Experienced $PGA_{M7.5}$ (Comparison of Seismic Demand) .....	47
Table 7: RILEY Classification Guide for Stopbank Damage .....	50
Table 8: Predicted Annual Exceedance probability for the Avon River (GHD, 2012).....	52
Table 9: Stopbank performance summary along Waimakariri and Kaiapoi Rivers.....	67
Table 10: Summary of Stopbank deformation Modes .....	70
Table 11: Summary of stopbank Deformation Modes / mechanisms .....	96
Table 12: Distribution of Cone Penetration Tests.....	98
Table 13: Canterbury Geotechnical Database data used in analysis.....	98
Table 14: Additional data used in analysis .....	98
Table 15: Definition of Primary and Secondary Earthquake Events .....	101
Table 16: Damage Index.....	107
Table 17: Damage Severity Classification.....	109
Table 18: Sample CPTs .....	112



## V. ABSTRACT

In the period between September 2010 and December 2011, Christchurch was shaken by a series of strong earthquakes including the  $M_w 7.1$  4 September 2010,  $M_w 6.2$  22 February 2011,  $M_w 6.2$  13 June 2011 and  $M_w 6.0$  23 December 2011 earthquakes. These earthquakes produced very strong ground motions throughout the city and surrounding areas that resulted in soil liquefaction and lateral spreading causing substantial damage to buildings, infrastructure and the community. The stopbank network along the Kaiapoi and Avon River suffered extensive damage with repairs projected to take several years to complete. This presented an opportunity to undertake a case-study on a regional scale of the effects of liquefaction on a stopbank system. Ultimately, this information can be used to determine simple performance-based concepts that can be applied in practice to improve the resilience of river protection works.

The research presented in this thesis draws from data collected following the 4<sup>th</sup> September 2010 and 22<sup>nd</sup> February 2011 earthquakes. The stopbank damage is categorised into seven key deformation modes that were interpreted from aerial photographs, consultant reports, damage photographs and site visits. Each deformation mode provides an assessment of the observed mechanism of failure behind liquefaction-induced stopbank damage and the factors that influence a particular style of deformation.

The deformation modes have been used to create a severity classification for the whole stopbank system, being ‘no or low damage’ and ‘major or severe damage’, in order to discriminate the indicators and factors that contribute to ‘major to severe damage’ from the factors that contribute to all levels of damage a number of calculated, land damage, stopbank damage and geomorphological parameters were analysed and compared at 178 locations along the Kaiapoi and Avon River stopbank systems.

A critical liquefiable layer was present at every location with relatively consistent geotechnical parameters (cone resistance ( $q_c$ ), soil behaviour type ( $I_c$ ) and Factor of Safety (FoS)) across the study site. In 95% of the cases the critical layer occurred within two times the Height of the Free Face ( $H_{FF}$ ). A statistical analysis of the geotechnical factors relating to the critical layer was undertaken in order to find correlations between specific deformation modes and geotechnical factors. It was found that each individual deformation mode involves a complex interplay of factors that are difficult to represent through correlative analysis.

There was, however, sufficient data to derive the key factors that have affected the severity of deformation. It was concluded that stopbank damage is directly related to the presence of liquefaction in the ground materials beneath the stopbanks, but is not critical in determining the type or severity of damage, instead it is merely the triggering mechanism. Once liquefaction is triggered it is the gravity-induced deformation that causes the damage rather than the shaking duration.

Lateral spreading and specifically the depositional setting was found to be the key aspect in determining the severity and type of deformation along the stopbank system. The presence or absence of abandoned or old river channels and point bar deposits was found to significantly influence the severity and type of deformation. A review of digital elevation models and old maps along the Kaiapoi River found that all of the 'major to severe' damage observed occurred within or directly adjacent to an abandoned river channel. Whilst a review of the geomorphology along the Avon River showed that every location within a point bar deposit suffered some form of damage, due to the depositional environment creating a deposit highly susceptible to liquefaction.

## 1.0 INTRODUCTION

### 1.1 PROJECT BACKGROUND AND OBJECTIVE

Approximately two-thirds of New Zealanders live in areas that are naturally prone to flooding, with nearly 70% of towns and cities with populations of over 20,000 having river flood problems (McSaveney, 2009). The Waimakariri River (Figure 2.1) situated just north of Christchurch poses the biggest flood hazard in New Zealand. The Avon River runs directly through Christchurch and poses a 1 in 50 year tidal flood risk to approximately 6,000 of 160,000 properties in Christchurch (CCC, 2012). Due to this risk there are over 580 kilometres of stopbanks and over 945,000 tonnes of bank protection rock works used as river protection in Canterbury.

In the period between September 2010 and December 2011 Christchurch was shaken by a series of strong earthquakes including the  $M_w$ 7.1 4 September 2010,  $M_w$  6.2 22 February 2011,  $M_w$ 6.3 13 June 2011 and  $M_w$ 6.0 23 December 2011 earthquakes. These earthquakes produced very strong ground motions throughout Christchurch and surrounding areas that resulted in soil liquefaction and lateral spreading which caused substantial damage to buildings, infrastructure and the community. The stopbank network suffered extensive damage with repairs projected to take several years.

### 1.2 OBJECTIVES

The primary objective of this study is to document the damage to the stopbank network resulting from the 2010-2011 Canterbury earthquake sequence and to use these observations to understand the mechanisms of liquefaction-induced stopbank damage and factors that influence the nature and severity of stopbank deformation during earthquakes.

It is important to document case studies of stopbank damage during earthquakes because there are similar settings throughout the world where there are seismic risks to stopbank and flood protection assets to improve assessment, construction and design practice. Having an understanding of the behaviour of our stopbanks and the modes of deformation during earthquakes can help engineers in these regions to design more resilient flood protection.

The seismic risk is relatively high in New Zealand and with thousands of kilometres of stopbanks in New Zealand understanding how future earthquake damage can be managed can greatly reduce associated costs to our society.

With this in mind the aims of this thesis are as follows:

1. To summarise and present the observed performance of the Canterbury stopbank system during the 2010 – 2011 Canterbury earthquake sequence.

2. To define the key modes of stopbank deformation that occurred as result of the 2010 – 2011 Canterbury earthquake sequence and to find out the mechanism of deformation that results in each specific style of deformation.
3. To evaluate the key geotechnical/geological/geomorphological factors which determine whether stopbank damage will occur.
4. To assess correlations between observed stopbank damage, land damage, geological and geomorphological conditions and geotechnical factors computed from CPT analysis.

### 1.3 THESIS FORMAT

This document is structured into seven chapters. The present chapter covers the introduction to this research. It provides the background, the objectives and motivation for the research and organisation of the thesis.

Chapter 2 introduces the geology, geomorphology and tectonic setting of the study sites and summarises the 2010 – 2011 Canterbury earthquake sequence.

A literature review is presented in Chapter 3. This reviews current standards for seismic design methods of stopbanks in major codes of practice. A review of commonly observed earthquake induced failure mechanisms is included as well as a comprehensive review of case studies in order to support these failure mechanisms.

Chapter 4 summarises the observed damage to the stopbank system in the greater Christchurch area as a result of the earthquakes. As this research project commenced following the 22<sup>nd</sup> February 2011 earthquake and draws from data collected following the 4<sup>th</sup> September 2010 earthquake and major aftershocks the key data sets are discussed in detail. Typical stopbank geometries and characteristics, river profiles and construction histories are presented. Earthquake-induced damage to the system including distribution of crest settlement, ground cracks and changes in river capacity, as well as the limitations on these data sets are also discussed.

Chapter 5 uses the recorded and observed performance data reviewed in Chapter 4 to define and characterise the damaged lengths of stopbank into characteristic deformation modes and to identify the driving mechanism for each of these. The identified deformation modes are compared and correlated with geotechnical and geomorphological data and post-earthquake ground deformation maps in order to assess the factors affecting deformation associated with a particular deformation mode. Seven deformation modes are introduced and characterised in Chapter 5.

Chapter 6 combines an analysis of 178 Cone Penetration Tests with the severity of the deformation modes presented in Chapter 5 and considers multiple geotechnical and geomorphological features in order to determine the indicators and factors that contribute to severe stopbank damage during an earthquake. A statistical analysis of these data is also undertaken to find correlations between specific deformation modes and geotechnical factors interpreted from the liquefaction analysis.

The final chapter (Chapter 7) presents a general summary of the study, a discussion and recommendations for future work.

## 2.0 SITE SETTING AND 2010-2011 CANTERBURY EARTHQUAKES

Christchurch and Kaiapoi (the study areas) are located on the Canterbury Plains in the South Island of New Zealand. The plains are approximately 160 km long and of varying width up to about 60 km and comprise overlapping alluvial fans of glacier-fed rivers issuing from the Southern Alps, the mountain range that runs in a north-east south-west direction along the axis of the South Island. Figure 1 illustrates the location of the two key study areas and the Canterbury Plains.

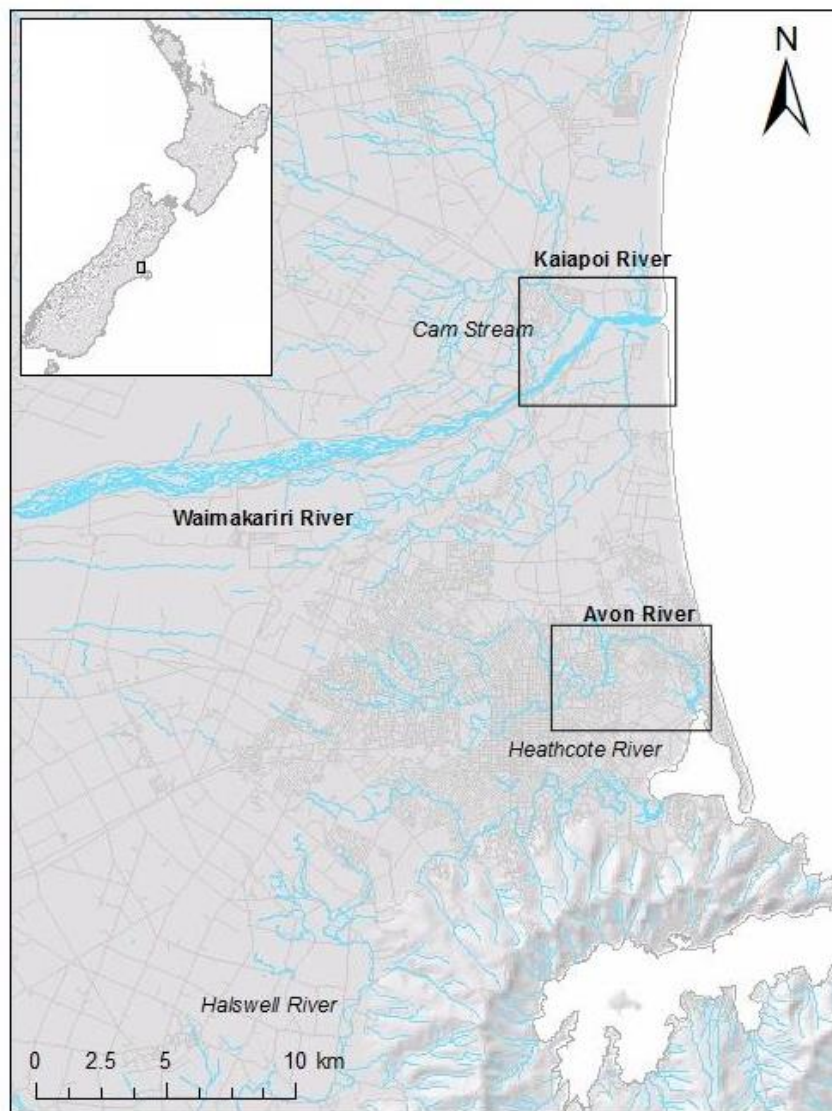
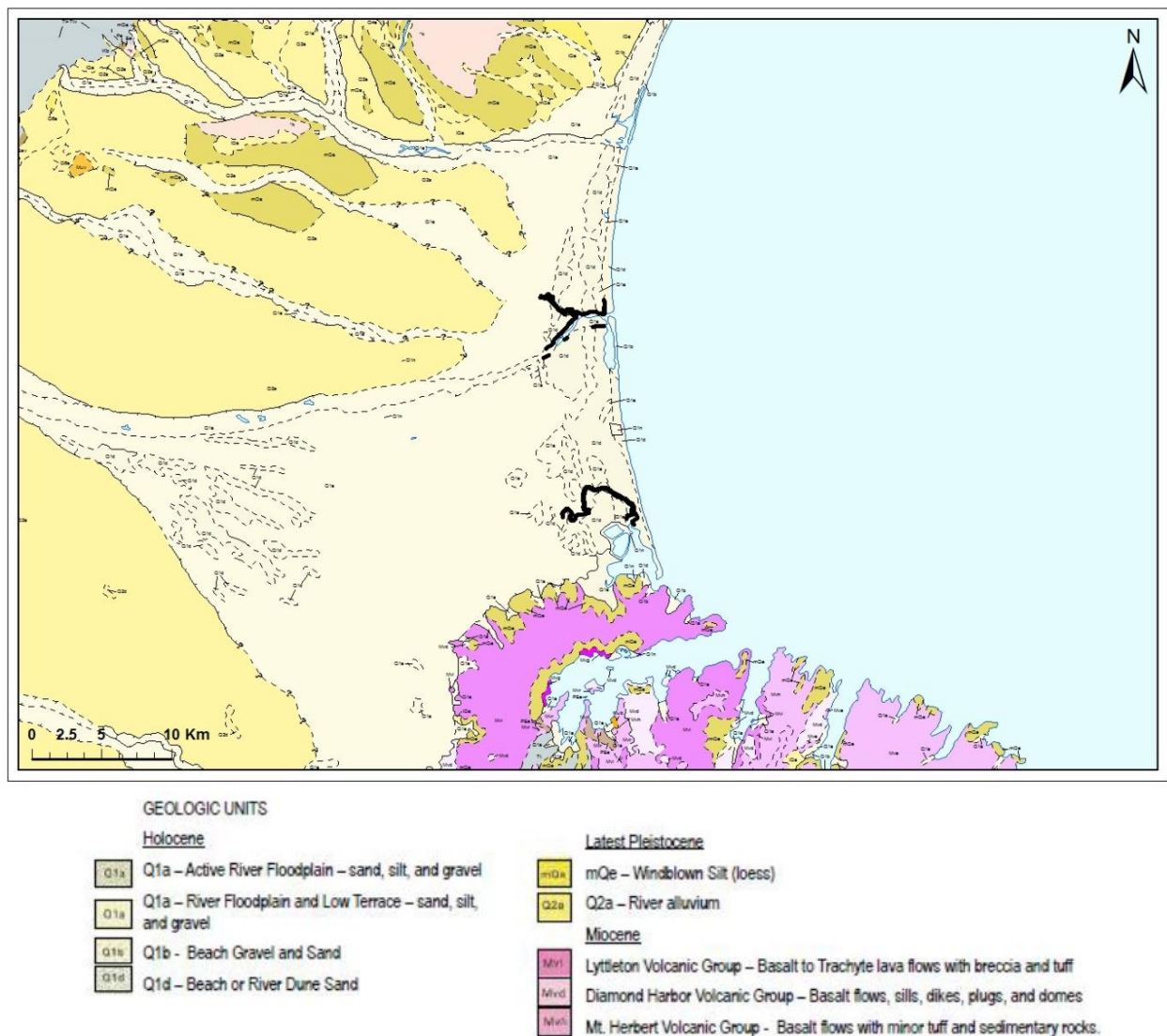


FIGURE 1: AREA OF STUDY

## 2.1 GEOLOGY AND GEOMORPHOLOGY OF THE STUDY AREA

The relatively rapid uplift of the Southern Alps, compared to the region to the east has resulted in rapid deposition during the late Quaternary and inundation of the Canterbury Plains by alluvial and fluvial deposits. The alluvial gravels underlying the Canterbury Plains typically are at least 500 m thick. Most are derived from the greywacke of the mountains or colluvium eroded from Banks Peninsula's volcanic rocks (Forsyth et al., 2008). Figure 2 shows the key geological units that comprise the Canterbury Plains (Forsyth et al., 2008).



**FIGURE 2: GEOLOGICAL MAP OF THE CANTERBURY PLAINS AND CHRISTCHURCH REGION, SOUTH ISLAND, NEW ZEALAND (FORSYTH ET AL., 2008)**

Due to the depositional environment of the Canterbury Plains, Christchurch and Kaiapoi are underlain by a stratigraphy of inter-bedded coarse and fine grained sedimentary deposits. The gravels and sands have been laid down by rivers, coastal processes and wind-blown deposits. Fine grained sediments have been deposited in near offshore marine environments, estuaries, lakes, wet lands and on flood plains. In the area of this study, the surface geological unit belongs to the Christchurch Formation and the Springston Formation (Brown and Weeber, 1992; Forsyth et al., 2008).

The Riccarton Gravel is a thick, widespread layer that is present at depth throughout much of the Christchurch urban area. This upper confined gravel formation was laid down during the last period of glacial advancement around 70,000 to 14,000 years ago. The Christchurch and Springston Formations overlie the Riccarton Gravels. The Christchurch Formation generally consists of marginal marine and coastal deposits including dune, beach, estuarine, lagoonal and coastal swamp deposits made up of gravel, sand, silt, clay, shell and peat. This formation extends as far inland as western Christchurch, to where the coast line was approximately 6,500 years ago and varies in thickness from several metres inland to 40 m at the coast (Brown and Weeber, 1992). This inland boundary represents the limit of progradation following postglacial sea level rise. The Springston Formation consists of postglacial fluvial channel and overbank deposits, accumulated inland of the Christchurch Formation. Figure 3 depicts the interbedded nature of the formations beneath Christchurch and shows the location of the Riccarton Gravels (Forsyth et al., 2008).

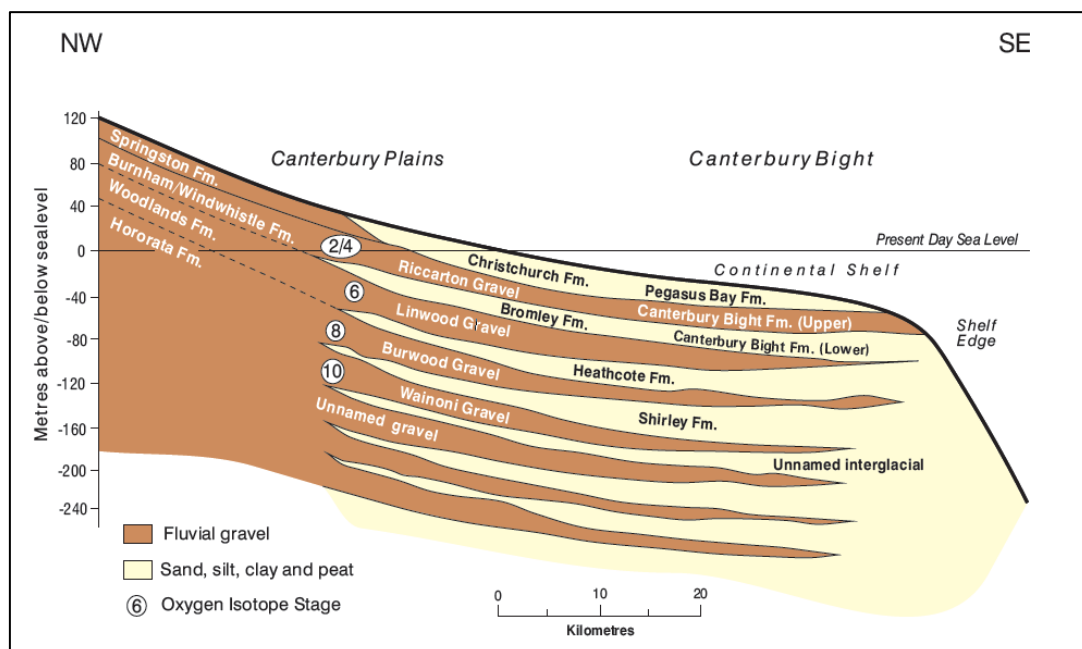


**FIGURE 3: DIAGRAMMATIC CROSS SECTION THROUGH QUATERNARY DEPOSITS UNDERLYING CHRISTCHURCH. AFTER (BROWN AND WEEBER, 1992; BROWNE AND NAISH, 2003)**

### 2.1.1 CHRISTCHURCH GEOMORPHOLOGY

Christchurch city is built on a Holocene low lying coastal margin, flanked by the eroded Tertiary volcanics of Banks Peninsula / Horomaka, with the wide braided riverbed of the Waimakariri River to the north of the city. Christchurch city lies within an area that was once predominantly swamps, estuaries and lagoons where drainage was impeded by sand dunes. Extensive areas of sand dunes and old dune ridges occur throughout the eastern city towards the coast (Forsyth et al., 2008). The Christchurch Drainage Board 'Black Map' (Figure 4) was produced in 1856 and shows the extent of streams, swamps and marshlands underlying large areas of what is now developed urban land.



The Avon River is a spring-fed river meandering from West to East through the Christchurch CBD and eastern suburbs and lying in former channels of the Waimakariri. The river terminates at the Avon-Heathcote Estuary, which is a former Waimakariri river mouth (Forsyth et al., 2008). The South New Brighton sand spit largely encloses the Avon-Heathcote estuary. The Avon River acts as a main drainage channel for Christchurch and has been historically modified for this purpose. With seventy-three percent of the Avon River catchment zoned for urban land use and development pressures over the last few decades, extensive modification to much of the river network has been undertaken (Fifield, 2011). Due to modifications, both natural and man-made, a series of abandoned ox-bow lakes and former channels surround the current channels.

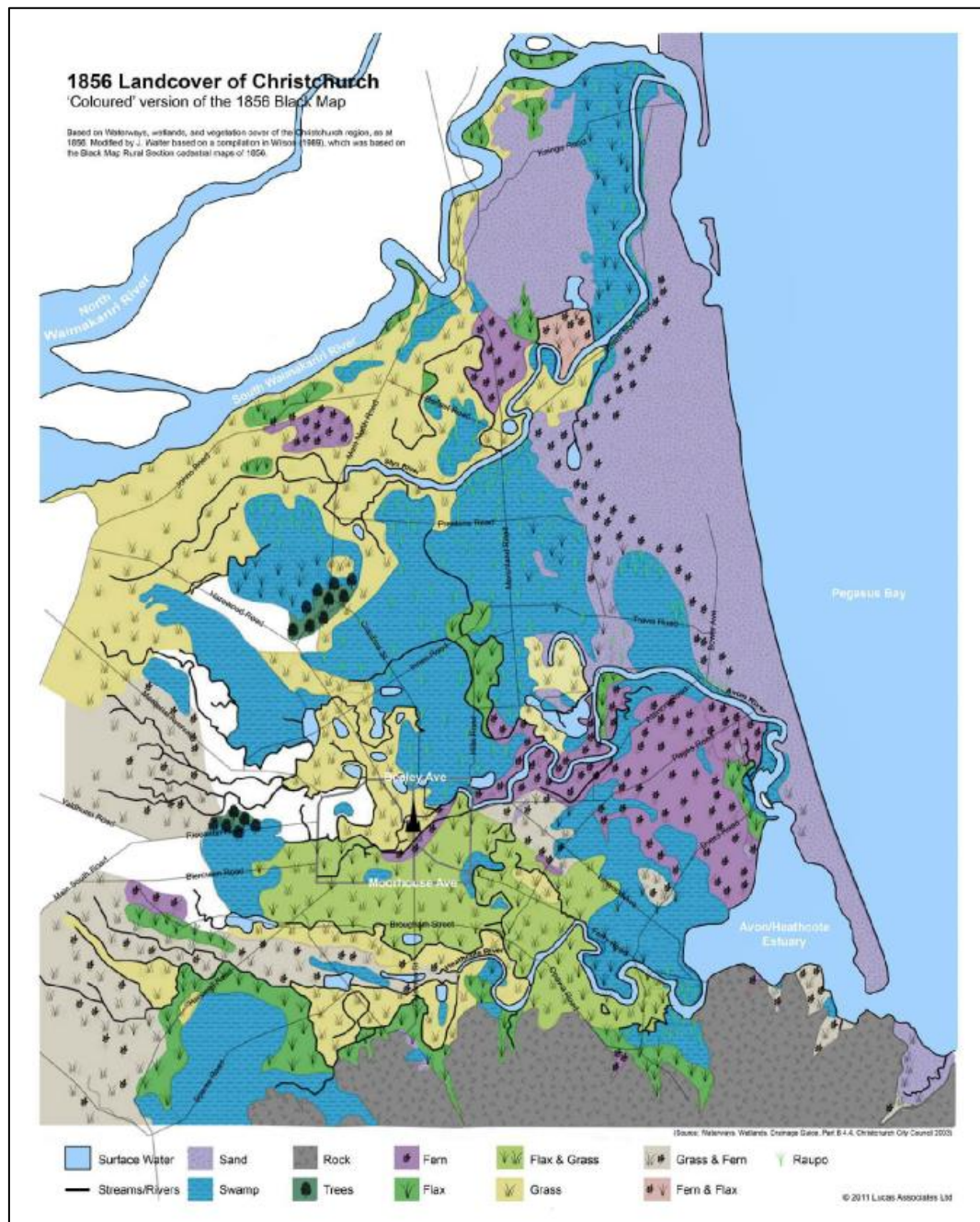


**FIGURE 4: COMPILED FROM CHRISTCHURCH CITY SWAMPS AND VEGETATION COVER 'BLACK MAP' (1856), CHRISTCHURCH DRAINAGE BOARD**



### 2.1.2 KAIAPOI GEOMORPHOLOGY

Kaiapoi developed as a port town on the Kaiapoi River, a tributary of the Waimakariri River. Hawkins (1957), describes Kaiapoi during the early days of its settlement, as swampy, low, damp and subject to flooding. He discusses the southern side of the river developing slower than the northern bank. However, by 1859 a number of buildings had 'grown out of the swamps, mud and flax which covered that part of the township'.

The Waimakariri River runs to the south of Kaiapoi and is one of several large braided rivers that run in a south-easterly direction from various catchments along the South Alps, flowing to the eastern coastline of the South Island of New Zealand. The Waimakariri River itself enters the Canterbury Plains from the Arthurs Pass area and drains a catchment of 3560 km<sup>2</sup>, 2490 km<sup>2</sup> of which are in the Southern Alps (Reinfelds and Nanson, 1993). The river is approximately 151 km long and has a large number of tributaries. Of particular interest to this project is the Kaiapoi River, a tributary that enters the Waimakariri River about 2.7 km from the coast.

Sedimentologically, the Waimakariri River reflects the geology of its catchment, comprising clasts of greywacke; well indurated sandstone and argillite with rare limestone, volcanics, conglomerate and coal measures. The mountain fed river experiences large flows with high sediment load during frequent flood events.

Over the history of its development the Waimakariri River and subsequently the town of Kaiapoi have been extensively modified both by human activities (river diversions, reclamation and stopbanks) and natural processes. The evolution of the Waimakariri River since European settlement is discussed in detail by Wotherspoon et al. (2011), and is summarised in Figure 5 below.

1. Prior to 1867 there were two branches of the Waimakariri River, with the North Branch (1) running through the town, supporting the majority of flow and the South Branch running south of the settlement (2). The high water flow through the town and the fact that any flood protection works were substandard meant that the settlement was exposed to numerous flooding events in its early years.
2. It was decided in 1868 that a canal would be constructed to re-direct a large amount of the water from the North Branch to the South Branch (3).
3. In 1879 – 1880, floods eroded the banks and changed the course of the south branch along Stewart's Gully at position 4, shifting the main flow of the river away from the town.
4. Due to the high incidence of flooding the Waimakariri River Trust was established in 1923. The Waimakariri River Trust implemented a major river improvement scheme known as the Hays No. 2 Scheme, which began construction in 1930. The scheme entailed excavation of a new channel and an overall improvement of the levee system along the Waimakariri River.
5. A channel was cut, in position 5, in order to re-route the majority of the water well clear of Kaiapoi. This completed the straightening of the river to its present course.

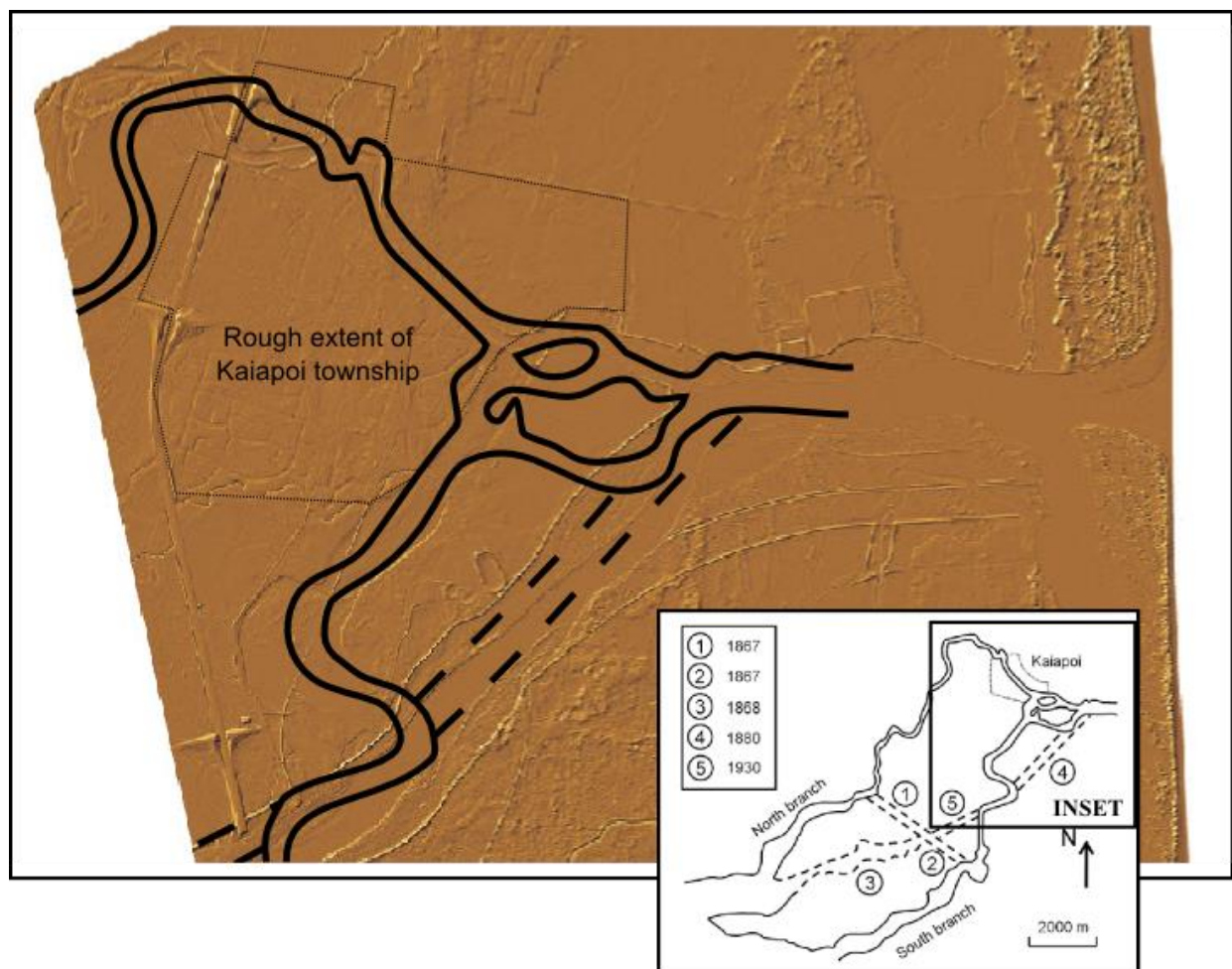


**FIGURE 5: EVOLUTION OF THE WAIMAKARIRI RIVER SINCE EUROPEAN SETTLEMENT (ADAPTED FROM ENVIRONMENT CANTERBURY, (2011))**

## 2.2 GROUNDWATER

The inter-bedded deposits beneath Christchurch make for a relatively complex hydrogeological system of unconfined and confined aquifers in the gravels and sands. Some aquifers are confined by extensive relatively impermeable, fine grained layers. The geotechnical properties of the inter-bedded deposits vary laterally and significant variability of behaviour can occur at the scales of metres and tens of metres.

The typical groundwater system of Christchurch and Kaiapoi is a shallow unconfined aquifer with a water table at less than 20 m depth and hydraulic connection with any nearby surface water courses. Groundwater depths tend to vary laterally over short distances, suggesting that localised channels of more permeable gravel are a significant feature of the groundwater flow regime. Confined aquifers tend to occur closer to the coast, where gravel strata are interbedded with fine-grained sediments that restrict vertical groundwater flow. Shallow groundwater levels vary seasonally and shallow aquifers may show considerable short-term fluctuations (Forsyth et al., 2008).

### 2.2.1 GROUNDWATER DEPTH

As levees are generally situated within close proximity of a waterway, the groundwater tables are subsequently usually quite high in the foundation soils. Liquefaction can only occur in saturated sediments, therefore having a higher groundwater means that sediments closer to the surface may have the potential to liquefy.

Groundwater depths derived from free surface elevations prior to each earthquake by subtracting the elevations from the most appropriate LiDAR-derived digital surface elevation model (CGD0800, 2012) indicate maximum depths to groundwater of 2 m during any of the earthquakes. However, the majority of the study area shows a depth to groundwater between 0 and 1 m. West of the damage zone the groundwater table rapidly becomes deeper, up to a maximum depth of 10 m. Figure 6 shows an example of the depth to groundwater during the February 2011 earthquake event.

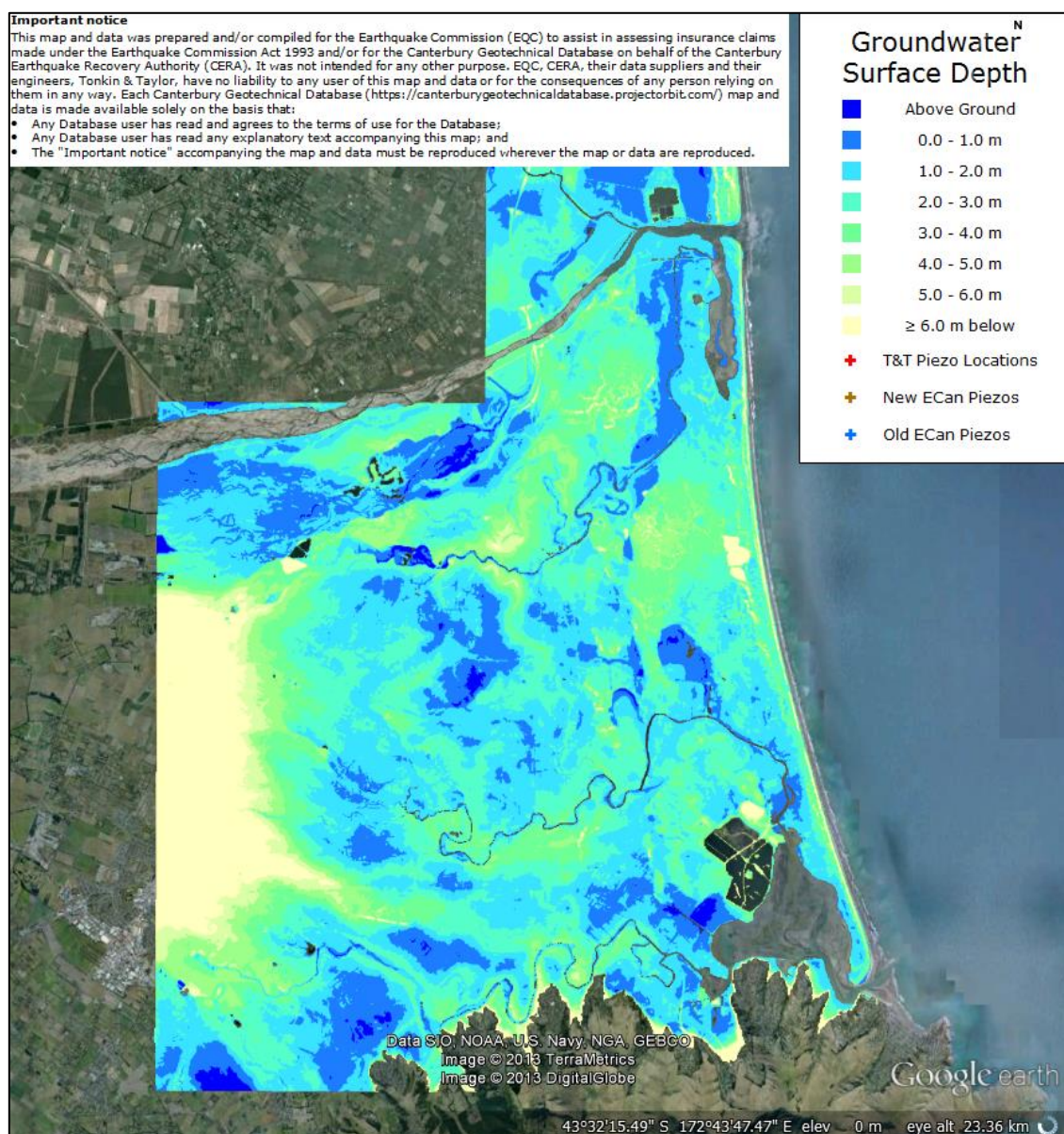


FIGURE 6: EVENT SPECIFIC GROUNDWATER SURFACE ELEVATIONS (CGD0800 – 11 FEB 2013)



### 2.2.2 TECTONIC SETTING

New Zealand straddles the boundary between the Pacific and Australian plates (Figure 7). The Pacific plate rotates anticlockwise relative to the Australian plate which causes variation in the behaviour of the plate boundary system along its length. To the north of New Zealand, the thin, dense, Pacific plate subsides beneath the thicker, lighter Australian plate in an oblique subduction style at the Hikurangi Margin and causes back-arc rifting in the Taupo Rift in the North Island. The Marlborough Fault System links the Hikurangi Margin to the Alpine Fault, where oblique convergence is building the Southern Alps in the Central South Island. The Marlborough Faults System comprises a series of splayed faults that display predominantly strike-slip behaviour. The plate boundary finishes with an opposite-sense subduction of the Australian plate under Fiordland at the northern termination of the Puysegur trench (Pettinga et al., 2001).



FIGURE 7: NEW ZEALAND TECTONIC SETTING ([HTTP://DATA.GNS.CRI.NZ/GEOATLAS/TEXT.JSP](http://data.gns.cri.nz/gEOATLAS/TEXT.JSP)). ARROWS INDICATE MOVEMENT OF THE PACIFIC PLATE RELATIVE TO THE AUSTRALIAN PLATE.

### 2.2.3 TECTONIC SETTING OF CANTERBURY AND THE STUDY SITES

Much of the Canterbury region is located within a wide zone of active earth deformation associated with oblique collision between the Australian and Pacific plates (Figure 7), where relative plate motion is obliquely convergent across the plate boundary at about 40 mm/yr at the latitude of Canterbury (De Mets et al., 1990). There are many mapped faults in this region, both expressed at the surface and ‘hidden’ beneath the surface, that pose a known earthquake hazard to Christchurch. Modelling of GPS-derived velocity fields suggests a strain rate of ~2 mm/yr of WNW-oriented permanent contraction for the region east of the Porter’s Pass Fault to offshore of Christchurch. Some of this slip is accommodated by several east-west trending and north-south to northeast-southwest trending active faults present throughout Canterbury and offshore on the Chatham Rise. In a general sense, east-west trending faults tend to be strike-slip faults while north-south to northeast-southwest trending faults tend to be oblique slip or reverse-slip faults with smaller components of strike-slip.

## 2.3 CANTERBURY EARTHQUAKE SEQUENCE

The Canterbury earthquake sequence, which began in September 2010 and continues at the time of writing, has included numerous significant earthquakes which have adversely affected the region.

The first major earthquake (the Darfield Earthquake) was a  $M_w 7.1$  and occurred on 4 September 2010 approximately 35 km west of the city of Christchurch in Darfield on a previously unrecognised strike-slip fault (Cubrinovski et al., 2010). The second significant earthquake (the Christchurch Earthquake) occurred on the 22 February 2011 with a magnitude of  $M_w 6.2$ . This earthquake occurred beneath Christchurch on a previously unrecognised reverse-oblique slip fault to the south-east of the city centre. This earthquake was particularly damaging, and resulted in 182 fatalities principally from the complete or partial collapse of several commercial buildings (Cubrinovski et al., 2011a). Other significant aftershocks include the  $M_w 6.3$  13 June 2011 earthquake and  $M_w 6.0$  23 December 2011 earthquake.

These earthquakes produced ground motion intensities equal to and exceeding those for which modern structures are designed in Christchurch. Consequently, such events resulted in substantial damage to buildings, infrastructure and lifelines. As a result of the strong ground motions, nonlinear response of surficial soils and in particular, severe liquefaction occurred over large regions of Christchurch, particularly to the east of the CBD. Each significant earthquake has been subsequently followed by a series of aftershocks as pictured in Figure 8.

Although there are many mapped faults in Canterbury, the Greendale Fault, which was the source of the Darfield Earthquake and Port Hills Fault, the source of the Christchurch earthquake, were not recognised prior to September 2010. Neither the generally east-west trending Greendale Fault, or the northeast-southwest trending Port Hills Fault are associated with distinct geomorphic expression at the surface that could have been recognized prior to the September and February earthquakes (Cubrinovski et al., 2010). The locations of these faults are depicted in Figure 8.

Although these faults were not specifically recognised prior to the Canterbury Earthquake Sequence they are accounted for in the New Zealand National Seismic Hazard Model (Stirling et al., 2012) as ‘background

seismicity'. The maximum magnitude of 'background' earthquakes which can occur off known faults was M7.0 in the seismicity model underlying NZS1170.5:2004. The current New Zealand Seismic Hazard Model has a maximum magnitude of M7.2 for the Canterbury Plains. Therefore, all earthquakes in the Canterbury sequence are of a size provided for by the current New Zealand seismicity model (Stirling et al., 2012).

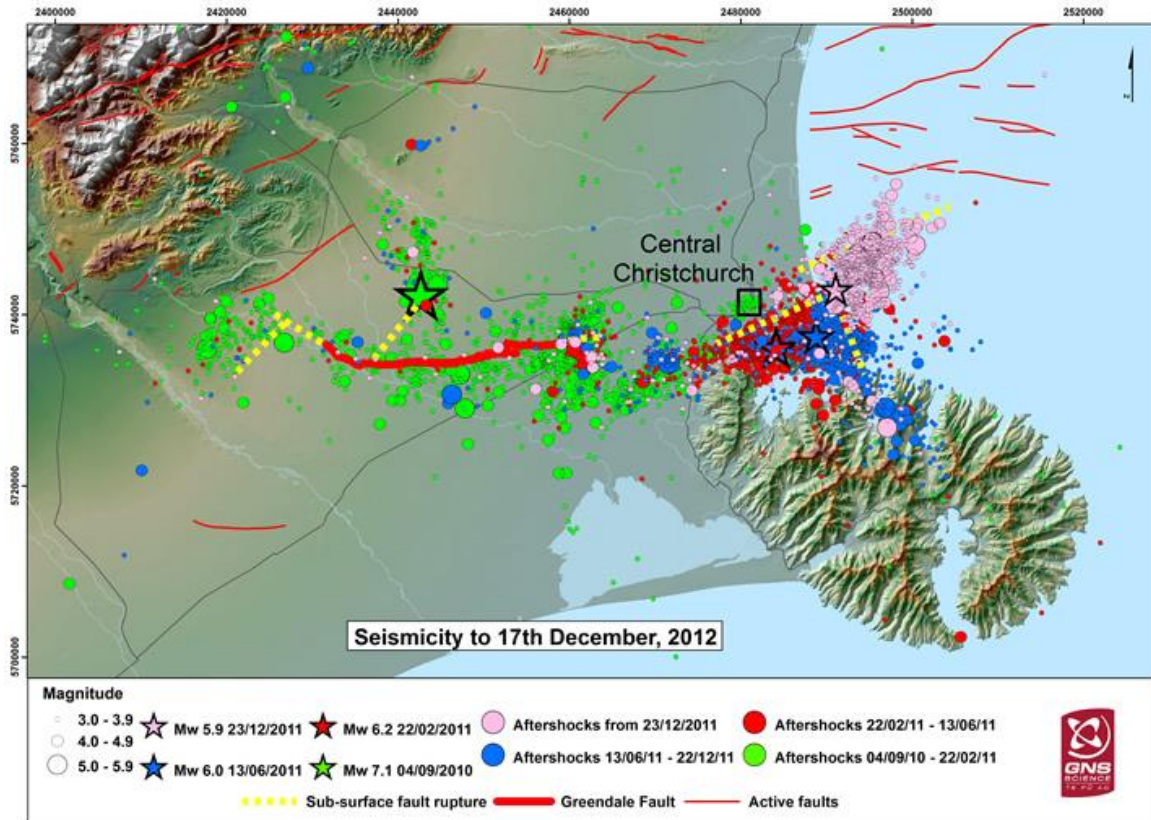


**Figure 8: Experienced aftershocks Magnitude and Location (2010 - 2012)**

<http://www.gns.cri.nz/Home/Our-Science/Natural-Hazards/Recent-Events/Canterbury-quake/Recent-aftershock-map>

### 2.3.1 OBSERVED GROUND MOTIONS

The Peak Ground Acceleration (PGA) which is the largest acceleration amplitude experienced during shaking is a good indicator, along with the magnitude of the earthquake, of the stresses the ground experienced during a particular earthquake event. Figure 9 illustrates the distribution of PGA's experienced during the September 2010 and February 2011 earthquakes, the PGA values have been corrected to a standard M7.5 for easy comparison.

The Canterbury Earthquake Sequence has produced the largest ground motions ever measured in New Zealand to date. The maximum PGA recorded during the 4 September 2010 Earthquake was greater than 1.25 g, which was experienced near the intersection of the triggering thrust fault, on which the rupture began, and the strike-slip Greendale Fault that carried most of the moment in the earthquake (Gledhill et al., 2011). PGA values in the Central Business District (CBD) of Christchurch averaged between about 0.2 and 0.3 g. The 22 February 2011 earthquake occurred about 7 km from the center of Christchurch. This earthquake produced extreme motions in Christchurch (Fry and Gerstenberger, 2011). The maximum

horizontal PGA was over 2.2 g with two other recordings in the city measuring greater than 1 g. Average PGA measured in the CBD was between about 0.6 and 0.8 g.

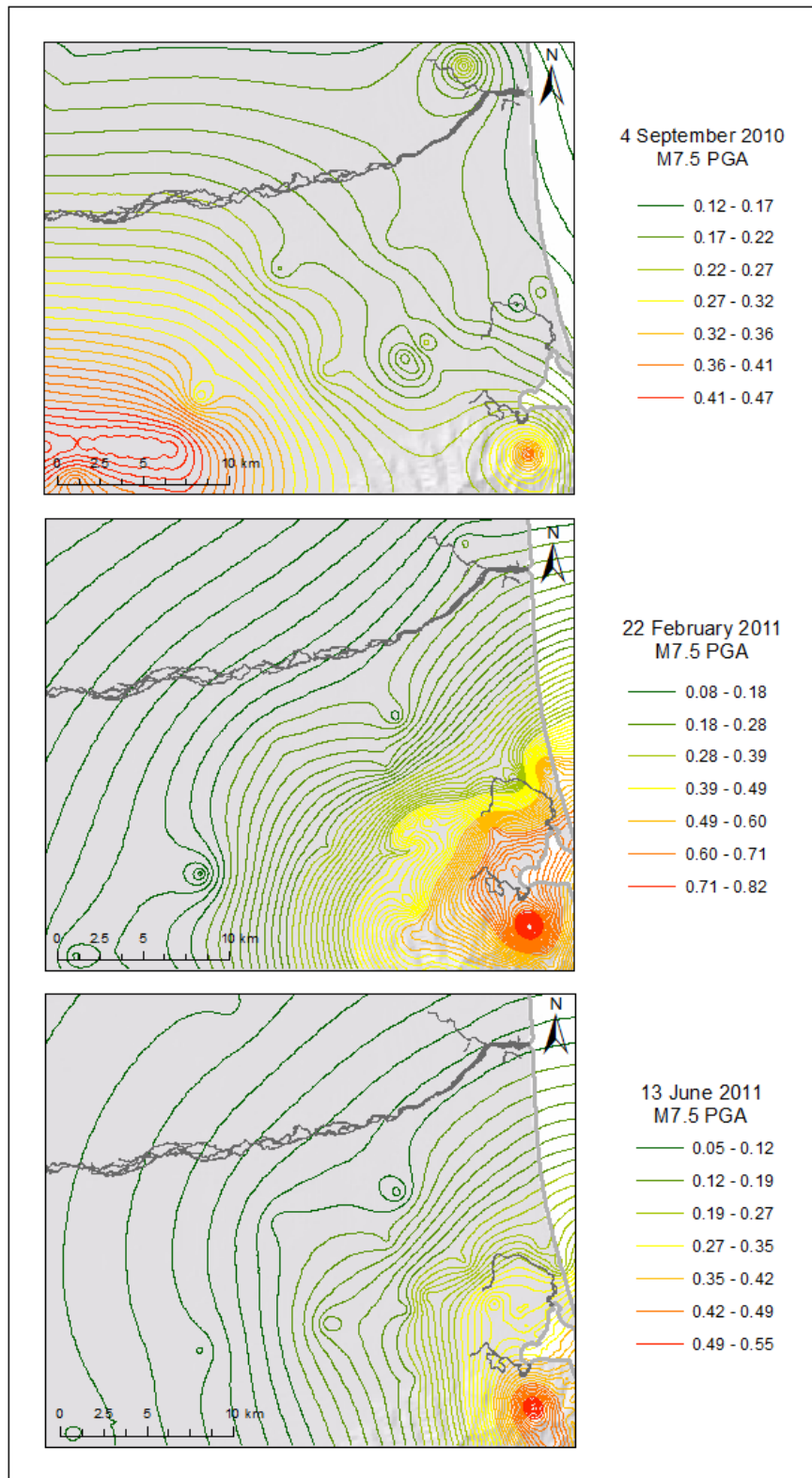


**FIGURE 9: COMPARISON OF PGA'S CORRECTED TO M7.5 EXPERIENCED FOLLOWING THE MAJOR EARTHQUAKE. ADAPTED FROM BRADLEY AND HUGHES, 2012.**

### 2.3.2 OBSERVED LIQUEFACTION AND LATERAL SPREAD

Liquefaction and lateral spreading were the most significant causes of damage to Christchurch and Kaiapoi during the Canterbury Earthquake Sequence. The liquefaction manifested itself as sand boils and large amounts of sand/silt ejecta and water. The M 7.1 Darfield earthquake caused liquefaction in Christchurch and adjacent areas in localised pockets adjacent to waterways or abandoned river channels and swamp, the  $M_w$  6.2 Christchurch earthquake however induced more widespread liquefaction affecting the majority of Christchurch. This was due to the fact that the Canterbury earthquake sequence was highly variable with unusually high PGA values, variable sub-surface geology and varying proximity to the epicentre for different events.

Kaiapoi was the worst-hit area following the M 7.1 Darfield Earthquake in terms of liquefaction severity. Investigations of old maps by Wotherspoon et al. (2011) showed that that much of the most significant liquefaction damage in and around Kaiapoi during the 2010 Darfield event occurred in areas where river channels had been reclaimed or in old channels that have had flow diverted away. As previously discussed, the highly modified nature of the Waimakariri River and its proximity to Kaiapoi meant that Kaiapoi is built on some of these reclaimed areas. After February 2011, most of the sand boils in areas close to the waterways were observed at existing/repairs cracks caused by the 2010 earthquake.

The Darfield Earthquake cause widespread liquefaction in the eastern suburbs of Christchurch along the Avon River, particularly in Avonside, Dallington, Burwood and Bexley. Other suburbs, particularly to the east and northeast of CBD, were also affected by liquefaction, but to a lesser extent. Following the M6.3 February Earthquake the manifestation of liquefaction was more widespread and primarily of moderate intensity with relatively extensive areas and volumes of sediment ejecta. There were also areas of low manifestation or only traces of liquefaction and pockets of severe liquefaction with very pronounced ground distortion, fissures, large settlements and substantial lateral ground movements (Cubrinovski et al., 2011b).

### 2.3.3 SPATIAL DISTRIBUTION OF LIQUEFACTION

Immediately following the two earthquakes, reconnaissance work was performed to investigate the extent and features of the damage. Figure 10 shows the distribution of liquefaction observed in the suburbs east of the CBD following the September 2010 and February 2011 earthquakes, respectively. These maps, which were constructed from visual identification of liquefaction using aerial photographs of varying quality and light conditions taken after each significant event, shows the extent of ejected material across the city. Liquefaction was categorised into the following classifications:

- Moderate to severe liquefaction
  - Roads had either ejected material or wet patches wider than a typical vehicle width
  - Ejected material in grass or on roads
  - Groups of 2 – 3 ejected material ‘boils’ within properties or parks
- Minor
  - Roads had either ejected material or wet patches narrower than a typical vehicle
  - Only one or two ejected material ‘boils’ within a property or park



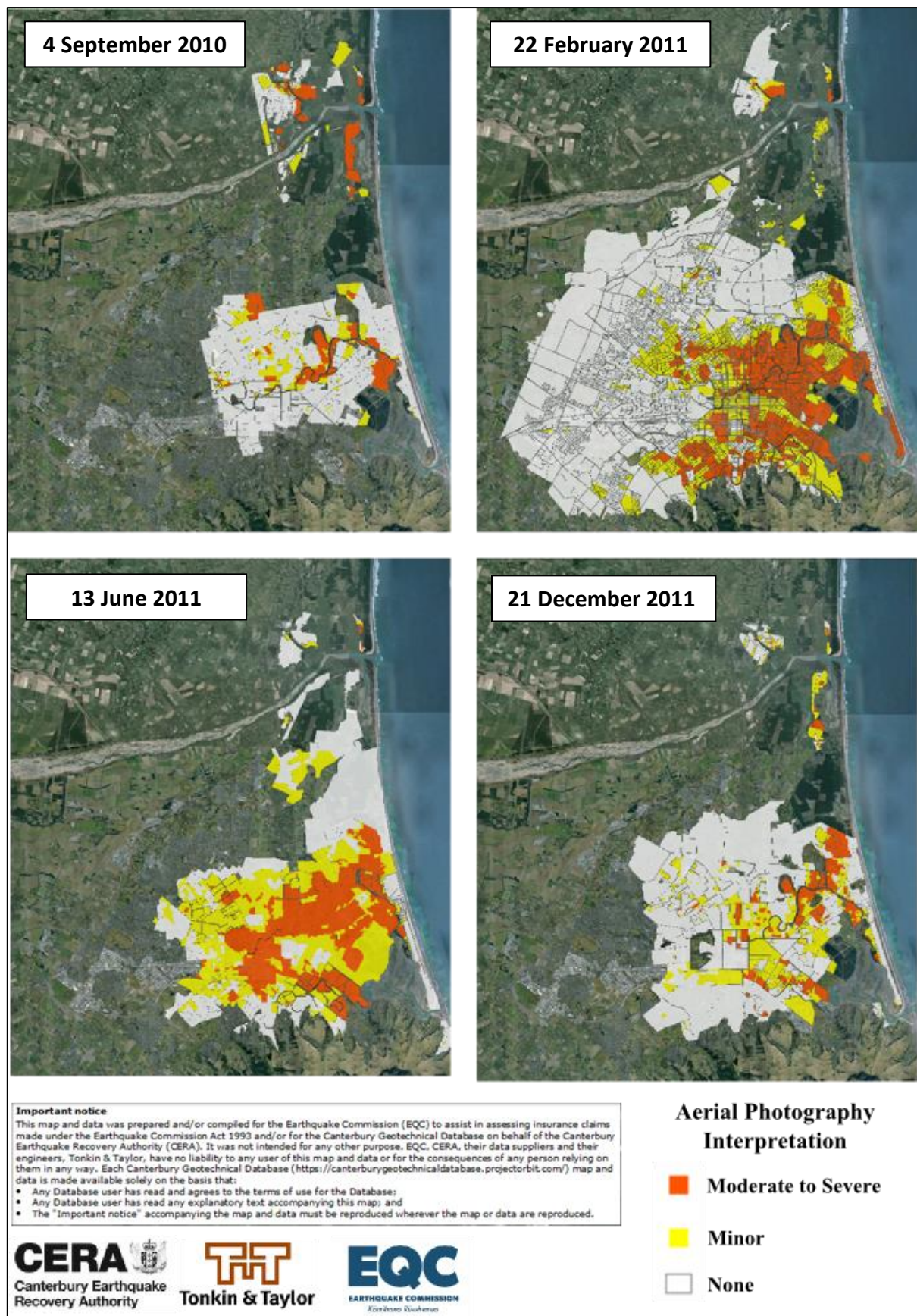


FIGURE 10: OBSERVED LIQUEFACTION INTERPRETED FROM AERIAL PHOTOGRAPHY. CGD0200 - 11 FEB 2013.



Higher resolution mapping was also undertaken following the earthquakes by personnel on foot and by car. Whilst these maps are of higher resolution they do not cover such extensive areas as the maps derived from aerial photographs. An example of one of the maps following the 22 February 2011 earthquake is shown in Figure 11.

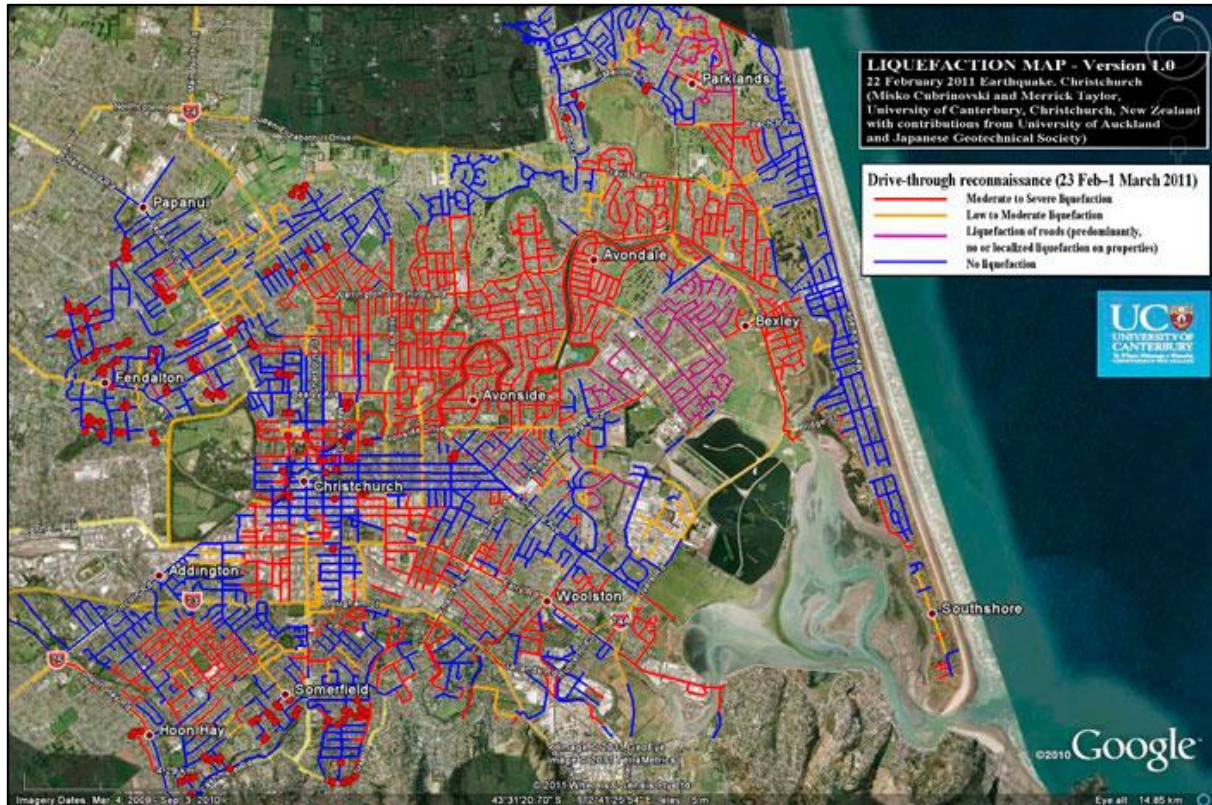


FIGURE 11: HIGH-RESOLUTION LIQUEFACTION MAP (CUBRINOSKVI & TAYLOR, 2011)

### 2.3.4 LATERAL SPREADING

Lateral spreading, associated with liquefaction, was observed in many areas adjacent to streams and waterways during the Canterbury earthquake sequence. Indications of lateral spreading during the earthquakes ranged from minor to very severe depending on proximity to waterways, the susceptibility of materials to liquefy and topographical variances. Much of South Kaiapoi, North Kaiapoi, Bexley and Spencerville were affected by severe lateral spreading.

Along the Avon River, particularly to the east of the CBD, lateral spreading occurred, causing horizontal displacements at the river bank of the order of several tens of centimeters to more than two meters. The lower Avon area displayed generally 'conventional' patterns of lateral spreading, with the majority of displacement occurring close to the free-face (or river bank). The Dallington/Avonside area displayed a very complex pattern of spreading as a result of the meandering features of the Avon River in this area (Robinson et al., 2011).

Field measurements of permanent lateral ground displacements were conducted along approximately 75 transects in urban areas affected by lateral spreading during the 2010 Darfield earthquake, by the methods of ground surveying, measuring the crack width in a perpendicular direction to the river and summing up the

crack widths (Robinson et al., 2011). The results indicate permanent lateral ground displacement measurements adjacent to the river bank of 0.3 – 0.9 m in Bexley, 0.6 – 0.9 m in Burwood, 0.5 – 1.8 m in Dallington/Avonside/Avondale, and 0.8 – 1.0 m in South Brighton.

At ten of these transect locations along the Avon River, lateral spreading displacements were carried out again after the February earthquake. It was found that the permanent lateral displacements were two to three times the displacements measured after the September earthquake indicating increased spreading movement which is in agreement with the more severe liquefaction observed in these areas during the February event (Cubrinovski et al., 2011a).

In South Kaiapoi, block-type movement was observed with atypical distribution of ground displacements where no cracks occurred close to the river bank, but very large ground fissures/cracks split the ground at distances of 120 to 200 m from the waterway. This feature significantly contributed to the severe damage of residential properties/houses in this area (Robinson et al., 2011). This damage is related to the old Waimakariri Channels as shown in Figure 5, the lateral spreading is occurring towards the abandoned channels as well as the current free faces.

### 2.3.5 EARTHQUAKE-INDUCED VERTICAL AND HORIZONTAL CHANGE

The extensive liquefaction and lateral spread also resulted in permanent vertical (and horizontal) ground movements. Figure 12 and Figure 13 show the vertical elevation changes over the entire Canterbury Earthquake Sequence, in lower Avon and Kaiapoi, respectively. A series of Digital Elevation Models (DEMs) were created following the earthquakes that summarize vertical elevation changes and horizontal ground movements (CGD0500). Vertical elevation changes were calculated from LiDAR acquired prior to the earthquakes and following each of the significant earthquake and are illustrated as colour banded DEMs. The horizontal ground movements for each earthquake were calculated using set points on infrastructure or on the ground to quantify the approximate horizontal movement of a particular point. The primary limitations of these data sets are the margin of accuracy accompanying each map. This was not provided post-survey, however statistics for calibration of the initial LiDAR point cloud sets are summarised in Table 1. It should be note that once DEMs are compared for relevant earthquakes, this error will increase.

TABLE 1: CALIBRATION OF THE INITIAL LIDAR POINT CLOUD SETS

Source LiDAR:	6-9 Jul 2003	5 Sep 2010	8-10 Mar 2011
<b>Average error</b>	-0.02 m	-0.04 m	0.03 m
<b>Standard Deviation</b>	0.13 m	0.13 m	0.06 m

Whilst there is a limitation in accuracy of the DEMs they do provide valuable information not only on the horizontal and vertical movement of the native ground but in some cases, where the data is of good enough quality, the approximate settlement of the stopbank.

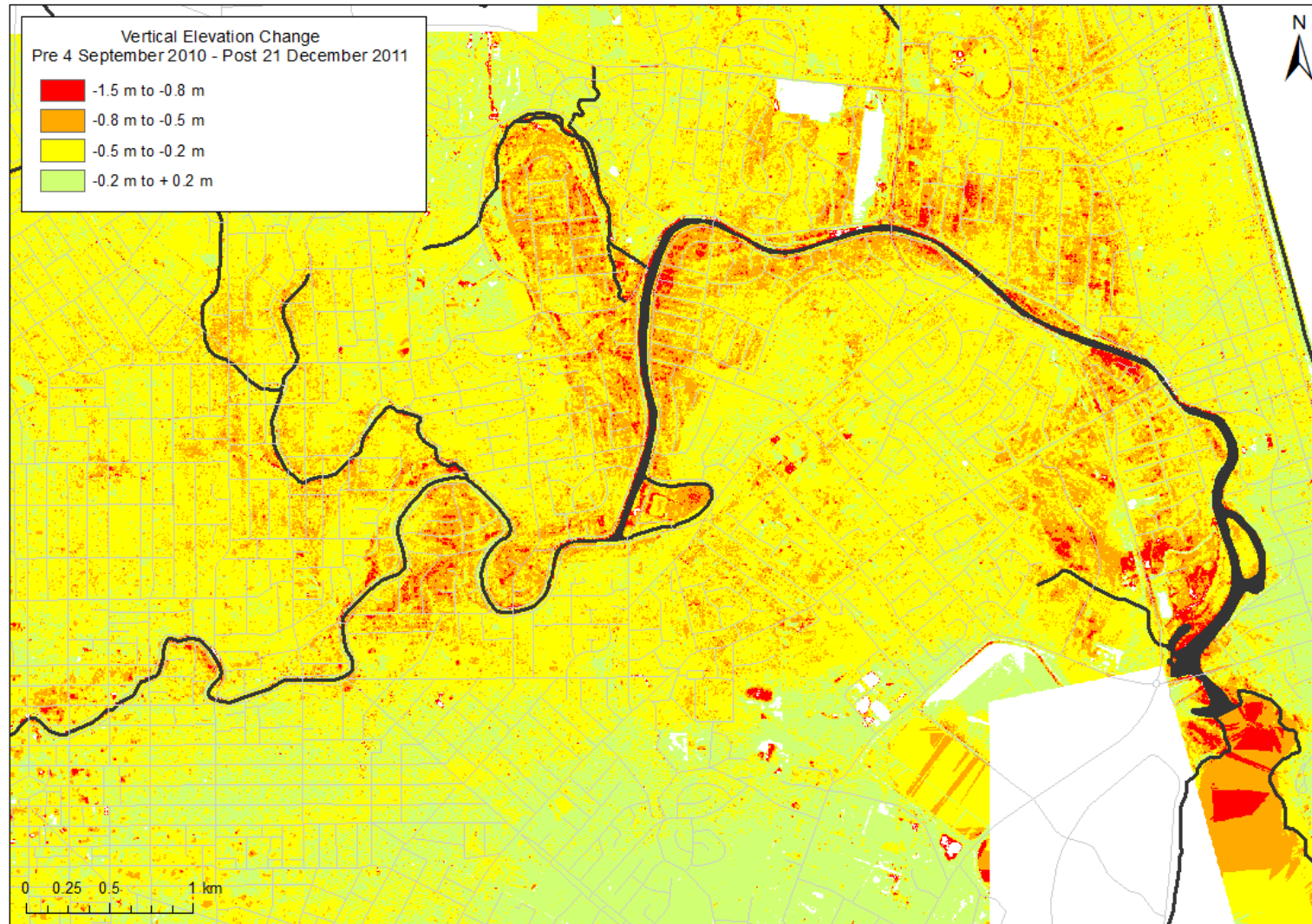


FIGURE 12: VERTICAL ELEVATION CHANGE CANTERBURY EARTHQUAKE SEQUENCE - AVON RIVER



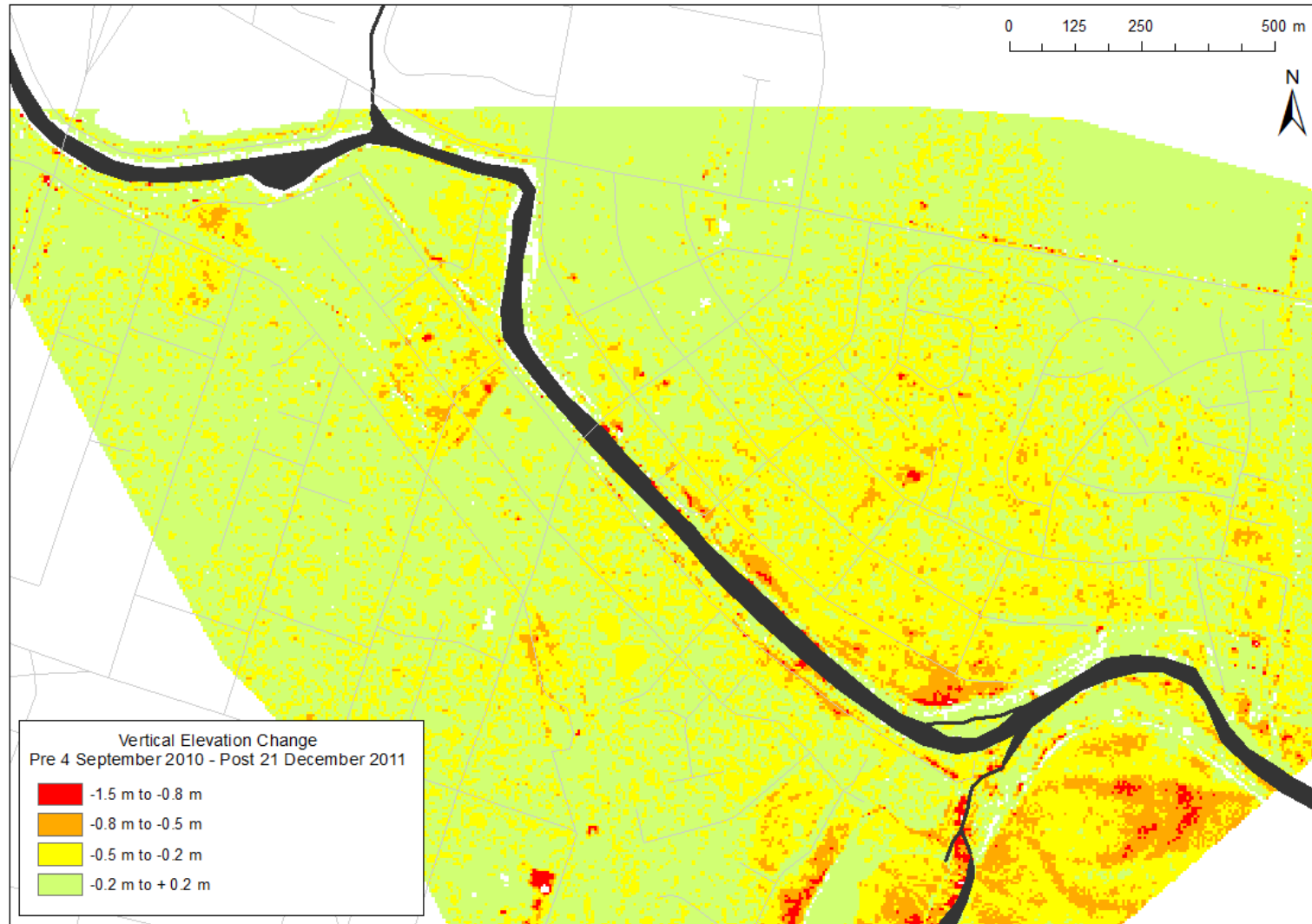


FIGURE 13: VERTICAL ELEVATION CHANGE CANTERBURY EARTHQUAKE SEQUENCE - KAIAPOI RIVER

## 2.4 SUMMARY OF EARTHQUAKE DAMAGE OBSERVED

A summary of the earthquake damage observed at each of the systems is presented in Table 2.

TABLE 2: EARTHQUAKE DAMAGE OBSERVED

<b>Location: Avon River</b>	
<b>Primary Earthquake Event:</b> 22 February 2011	<b>Secondary Earthquake Event:</b> 4 September 2010
<b>Observed Ground Motions:</b> <p>The maximum horizontal PGA during the 22 February 2011 event was over 2.2 g with two other recordings in the city measuring greater than 1 g and an average PGA between about 0.6 and 0.8 g. PGA values during the 4 September 2010 earthquake averaged between about 0.2 and 0.3 g.</p>	
<b>Observed Liquefaction and Lateral Spread:</b> <p>The 4 September 2010 earthquake caused in localised pockets adjacent to waterways or abandoned river channels and swamp, the 22 February 2011 earthquake, however, induced more widespread liquefaction affecting the majority of Christchurch. This was due to the more pronounced due to higher PGAs and closer proximity of the epicenter.</p>	
<b>Location: Kaiapoi/Waimakariri Rivers</b>	
<b>Primary Earthquake Event:</b> 4 September 2010	<b>Secondary Earthquake Event:</b> 22 February 2011
<b>Observed Ground Motions:</b> <p>PGAs observed in Kaiapoi were between 0.18 g and 0.30 g for the 4 September 2010 event, but we significantly lower at 0.16 g to 0.20 g for the 22 February 2011 event.</p>	
<b>Observed Liquefaction and Lateral Spread:</b> <p>Kaiapoi was the worst-hit area following the 4 September 2010 earthquake in terms of liquefaction severity, where extensive liquefaction and lateral spreading were observed. After February 2011, most of the sand boils in areas close to the waterways were observed at existing/repai red cracks caused by the 4 September 2010 earthquake.</p>	

### 3.0 LITERATURE REVIEW

Global awareness of the risk to flood protection infrastructure in seismically active areas has been increasing considerably as population growth sees substantial amounts of development occurring within active floodplains. Levee systems are often progressively upgraded using a staged funding approach to protect increasingly valuable residential and commercial infrastructure. This evolution usually involves the addition of material on the crest and batters of any given length of the levee rather than upgrading the structure's entire length at one time. For this reason, particularly given that systems can extend hundreds of kilometres, many levees fail to meet modern engineering standards.

Historically, literature on the performance of specific levees during large earthquakes is not extensive but recent scientific research and case studies from Japan have been instrumental in the development of an understanding of the behaviour of levees constructed in seismically active regions. The last 20 years has seen a marked increase in the number of publications documenting levee performance during large earthquakes and, extensive modeling has been undertaken in order to quantify the deformation mechanisms.

### 3.1 CURRENT PRACTICE IN LEVEE CONSTRUCTION

National design standards provide guidance for levee design in some countries. Noteworthy current levee design standards include the United States Army Corps of Engineers manual EM 1110-2-1913 (USACE, 2003) , Dike Design and Construction Guide – Best Management Practices for British Columbia (Golder, 2003), Urban Levee Design Criteria – Floodsafe California (DWR, 2012) and the Japanese Technical Standard and Guidelines for Planning and Design (DPWH, 2002).

These standards seek to provide guidance on best practices for site investigation, design, construction and maintenance of river levees. Based on these standards, predominantly EM 1110-2-1913, a summary of minor and major levee design requirements has been compiled and presented in Table 3.

**TABLE 3: SUMMARY OF LEVEE DESIGN REQUIREMENTS (ADAPTED FROM EM 1110-2-1913)**

Step	Procedure
1	Conduct geological study based on a thorough review of available data including analysis of aerial photographs. Initiate preliminary subsurface explorations.
2	Analyse preliminary exploration data and establish preliminary soil profiles, borrow locations, and embankment sections.
3	Initiate final exploration to provide: <ul style="list-style-type: none"><li>a. Additional information on soil profiles</li><li>b. Undisturbed strengths on foundation materials</li><li>c. More detailed information on borrow areas and other required excavations</li></ul>
4	Using the information obtained in Step 3: <ul style="list-style-type: none"><li>a. Determine both embankment and foundation soil parameters and refine preliminary sections where needed, noting all possible problem areas</li><li>b. Estimate quantities of suitable material and refine borrow area locations</li></ul>
5	Divide the entire levee into reaches of similar foundation conditions, embankment height, and fill material and assign a typical trial section to each reach
6	Analyse each trial section for: <ul style="list-style-type: none"><li>a) Under-seepage and through-seepage</li><li>b) Slope stability</li><li>c) Settlement</li><li>d) Trafficability of the levee surface</li></ul>
7	Design special treatment to preclude any problems as determined from Step 6. Determine surfacing requirements for the levee based on its expected future use.
8	Based on the results of Step 7, establish final sections for each reach
9	Calculate final fill quantities needed and determine final borrow area locations
10	Design embankment slope protection.



### 3.2 REVIEW OF SEISMIC DESIGN METHODS IN MAJOR CODES OF PRACTICE

Some earthquake prone countries around the world rely on “codes of practice” to mandate that levee constructions fulfils at least a minimum level of safety performance against future earthquakes. However, codes of practice are not universal, consistent or widely adapted. The USA procedures have neglected to consider seismicity except in California and in the Mississippi Delta (FEMA, 2008). In Japan there is a much greater appreciation for seismic design of levees and consequently there has been more focus on seismic considerations in levee design. The Netherlands is considered to be very benign with respect to earthquakes and because of the low probability, seismic effects on levees are not considered in their design criteria.

Locally, the NZS 4203:1984 code of practice for general structural design and design loadings for buildings provides guidance to geotechnical practitioners including a specific rule for “equivalent static method of analysis” of earth retaining structures. The seismic hazard in New Zealand has been described based on a probabilistic seismic hazard model developed by GNS Science. The output of this model is the basis for the current structural seismic design code (NZS1170.5:2004). However NZS 1170.5 specifically excludes design of soil retaining structures and civil structures including dams and bunds. The standard also excludes consideration of the effects of slope instability and soil liquefaction.

As the risks associated with building levees in seismically active regions are becoming better understood, towns and cities around the world now have greater awareness that their levee systems may be vulnerable to failure during earthquake shaking. Such seismic events could affect levee systems to the extent that there is risk to human life and significant adverse economic, infrastructure and environmental impacts. Some regions have identified the risk and preemptively commissioned geotechnical investigations of their flood protection systems e.g. earthquake risk assessment of flood protection assets in Wellington, New Zealand (Murashev et al., 2006) and preliminary seismic risk analysis associated with levee failures in the Sacramento – San Joaquin Delta (CBDA and CDWR, 2005).

In the USA, current thinking for levees that infrequently experience loading from high retained water levels is to accommodate the earthquake risk by providing efficient and prompt post-earthquake levee repair and flood response. Ground remediation for liquefaction prevention is also considered in some extreme cases (FEMA, 2008). For repair and improvement work associated with levees in urban and developing areas, seismic ground motions having a return period of 200 years are being proposed as the design level (FEMA, 2008). Repairs for improvements primarily for the purpose of seismic strengthening are generally not considered to be justifiable for levees that are subjected to only rare high water loading.

In Japan, the ‘technical criteria for river works and sabo works (draft)’ was first published in 1958 (NILIM et al., 2008) and introduced the seismic load equivalent to the moderate-scale of earthquake ground motions in 1985. This was only for use in design of river structures consisting of reinforced concrete and steel components, but provided a gateway for further thought into the area (Sugita and Tamura, 2007). The technical criteria was revised again in 1997 to include seismic design of earthen levees and since 2007 new structures have been constructed based on the criteria.

### 3.2.1 PERFORMANCE-BASED DESIGN PHILOSOPHY

Initial seismic evaluations were based on experimental relationships between the settlement of levee crests established by historic data and the safety factor derived from the seismic coefficient method as described in Sugita and Tamura (2007). The most recent criteria require seismic performance and design earthquake ground motions to be properly determined and then an appropriate seismic analysis method to be adopted (a shift to a performance-based design). A pseudostatic analysis is generally considered to be sufficient however, in some cases a dynamic response analysis may be required. Earthquake ground motions are subdivided into two categories: Level 1 corresponds to an earthquake ground motion that has a high probability of occurring during its service period, and Level 2 is the maximum credible ground motion that the site may experience (Sugita and Tamura, 2007).

Levees are assigned a required seismic performance level based on an importance classification scheme. The static analysis estimates the settlement of the levee in respect to the extent of soil liquefaction. This can then be used to determine whether the levee will meet the defined criteria for the required seismic performance level.

### 3.2.2 RISK-BASED DESIGN PHILOSOPHY

A risk-based design approach assesses the requirements of levees and prioritises upgrading and maintenance funds, allowing for funds to be allocated in a manner consistent with the potential risk of damage and loss of life. In British Columbia, 'The seismic design guidelines for dikes' (Golder, 2012) uses this approach by providing guidance on:

- seismic ground motions to be considered for the analysis and design of levees along with corresponding performance expectations;
- suitable geotechnical investigation methods to characterise and obtain engineering properties of the site soils;
- commonly used methods for seismic analysis considered appropriate for levees;
- threshold seismic events that should trigger a post-event evaluation of the integrity of the levee system;
- seismic rehabilitation and strengthening measures; and,
- post-earthquake temporary emergency repair and permanent remediation measures.

Once a geotechnical investigation has been undertaken in order to identify soil strata that are susceptible to liquefaction and/or cyclic softening as a result of strong ground shaking, and to determine their in-situ state and engineering properties, performance-based design criteria are established. Design earthquake, performance categories and permissible displacements must be established. These can be used to undertake an assessment of seismic hazards of the levees, involving the following steps:

- i. Evaluate applicable accelerations for ground surface, crest, and at selected locations of the levee;
- ii. Evaluate liquefaction potential of soil and associated consequences;
- iii. Evaluate stability of slopes under seismic loads, including post-earthquake conditions;
- iv. Evaluate seismic deformations; and
- v. Evaluate post-event piping failure potential.

Golder (2012) also suggests guidance on a threshold seismic event for post-event levee integrity inspection and levee remediation methods. Based on past experience, earthquakes of magnitude  $M_w \leq 5.0$  are unlikely to cause liquefaction and significant ground displacements in earth structures of relatively good workmanship.

In summary the critical design issues are:

- i. If there are materials in the structure or foundation that have potential to liquefy as a result of cyclic loading, these should be the primary focus of the evaluation, as they could result in large displacement flow slides.
- ii. Will the structure undergo significant deformations that may jeopardise safety?

The critical components of the seismic displacement analysis are:

- i. Earthquake ground motion. This is the most important input for the calculation of the amount of seismic displacement and is usually defined as an acceleration in terms of Peak Ground Acceleration (PGA) and the magnitude of the energy released in terms of Moment Magnitude Scale ( $M_w$ );
- ii. Liquefaction potential of the subsurface materials;
- iii. Dynamic resistance of the structure, and
- iv. Dynamic response of the potential sliding mass.

Other factors such as topographic effects can be important in some cases. As yield coefficient increases, the probability of “zero” seismic displacement increases and the median estimate of non-zero displacement decreases sharply. A logic tree approach is a frequently used approach to integrate the results of variations assumptions made throughout the design process. Figure 14 shows an example of this methodology..

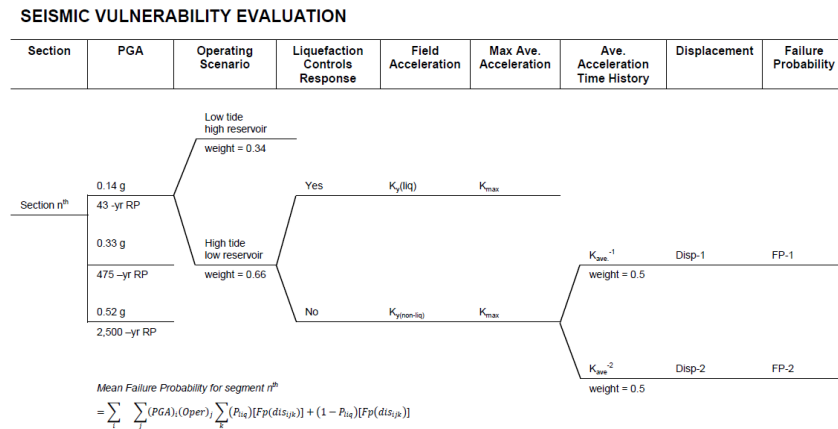


**FIGURE 14: LOGIC TREE APPROACH FOR INTEGRATING THE RESULTS OF VARIOUS ASSUMPTIONS (ROSIDI, 2007).**

### 3.3 REVIEW OF SEISMIC FAILURE MECHANISMS

The basis for common potential foundation failure modes for earthen dams are described by (Veltrop, 1992) and include liquefaction/seismic softening of foundation materials, stability of foundation/reservoir rim materials and

landslide-induced waves. The first of these failure modes is the most relevant to levees constructed on alluvial soils and is described in more detail by Towhata (2008) who illustrates a variety of deformation modes recognized in earth fills during past earthquakes (Figure 15). They are classified as:

Type 1) Shallow surface sliding of slope,

Type 2) Development of slip surface

Type 2'') development of slip surface reaching the soft foundation soil,

Type 3) Slumping

Type 4) Densityfication

Type 5) Lateral Displacement

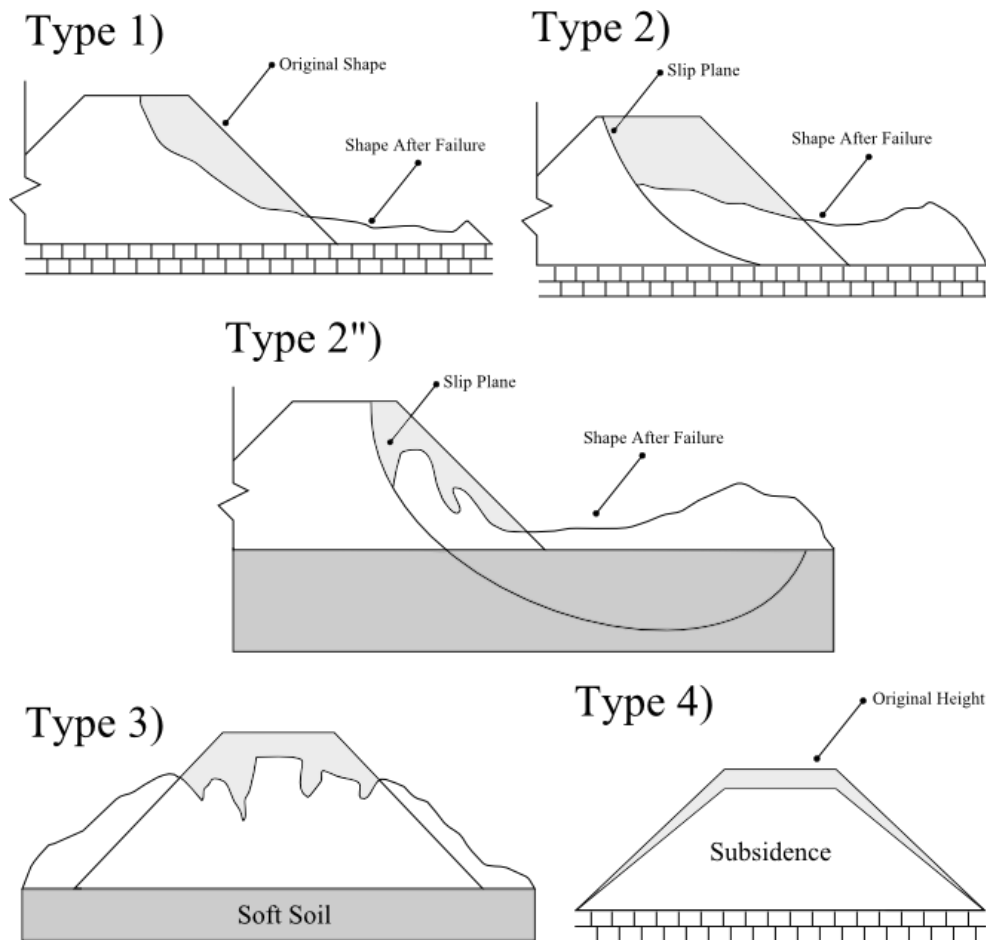


**FIGURE 15: TYPICAL FAILURE MODES (TOWHATA, 2008)**

Liquefaction is the most critical factor affecting instability of earth embankments during earthquakes and may cause large deformation, loss of capacity and even complete failures (Huang et al., 2009).

### 3.3.1 EXPERIMENTAL TESTS

Generally, seismic deformation in levees occurs due to the presence of saturated loose sandy materials in the foundations that are susceptible to liquefaction during earthquake shaking. The basic principle of liquefaction is that pore water pressure increases due to the contractive tendency of liquefiable soils induced by earthquake shaking, which leads to consequent decrease of effective stress. According to the reduction in the effective stress, the soil may undergo progressive degradation of strength and stiffness. Experimental tests have confirmed that liquefaction plays a major role in the process of damage to earth embankments. Most of the seismic failures of levees are attributed to increase in pore water pressure and subsequent liquefaction in foundation materials (Huang et al., 2009; Miller and Roycroft, 2004; Ozutsumi et al., 2002; Sasaki, 2009; Wang, 1984).

An effective stress analysis was undertaken by Ozutsumi et al. (2002) using FLIP software on seven case histories of levee failure. The failure modes were characterized by crest settlement associated with lateral spread of the foundation soil. The effect of pore water pressure on levees was studied and it was concluded that excess pore water pressures were consistent with field evidence of liquefaction. In the fully liquefied zones pore water pressure ratios were higher than 0.9 and pore water pressure was found to be increased beneath the levee and at some distance from the levee. In some cases only partial rises in excess pore water pressures directly beneath the levee were noted. These are due to shear stresses acting on the foundation soils due to overburden pressures and the embankment failures are due to shear failure rather than liquefaction because of the constantly applied shear stresses due to gravity before and during earthquake shaking. As expected, excess pore water pressures in cohesive layers were not significant and helped reduce liquefaction-induced deformation of the levees.

Huang et al. (2009) concluded that severity of deformation was found to be a direct function of the geotechnical conditions within the subsurface soil profile. Particularly, the presence of a layer of cohesive soil within the liquefiable sand layers beneath the levee was found to reduce the liquefaction-induced deformation of the levee. Conversely, if the foundation soils are in a fully liquefied state, shear strength of the soil is very low and large deformations can occur.

### 3.3.2 CASE STUDIES

A review of case studies confirms the failure modes presented by Towhata (2008) and established by experimental tests. Ten cases of levee performance during earthquakes are reviewed in Appendix A, focusing primarily on trapezoidal soil levees, the primary type of flood protection used in Canterbury. A summary of these case studies is presented in Table 4. The purpose of this review is to understand the primary driving mechanisms behind levee failure in order to better understand the failure mechanisms observed in Christchurch.

**TABLE 4: CASE HISTORIES OF PERFORMANCE OF LEVEES DURING EARTHQUAKES**

Case History No.	Earthquake Event	Magnitude	Key References
1	2011 Tohoku, Japan	$M_w = 9.0$	Harder et al. (2011); Lekkas et al. (2011)
2	2011 Tohoku, Japan	$M_w = 9.0$	Harder et al. (2011); Lekkas et al. (2011)
3	1966 Xingtai, China	$M_s = 6.8$ $M_s = 7.2$	Wang (1984)
4	1987 Edgecumbe, New Zealand	$M_w = 6.5$	Pender and Robertson (1987)
5	2001 Gujarat, India	$M_w = 7.7$	Towhata et al. (2002)
6	1993 Hokkaido-nansei-oki, Japan	$M_w = 7.8$	Isoyama (1994)
7	2003 Tokachi-oki, Hokkaido, Japan	$M_w = 8.1$	Sasaki (2009)
8	2003 Tokachi-oki, Hokkaido, Japan	$M_w = 8.1$	(Cubrinovski, 2011); Sasaki (2009)
9	1989 Loma Prieta, San Francisco	$M_w = 6.9$	Miller and Roycroft (2004); Perry (1994); Yegian et al. (1994)
10	1995 Hyogoken-nanbu, Japan	$M_w = 6.9$	Sasaki and Shimada (1997)

Valuable lessons from Japanese earthquakes are the primary contributions to this area of research. However, earthquake prone countries across the world have also begun to identify the importance of performance based design and are documenting the performance of levees during earthquakes in order to improve levee performance in future earthquakes. A prudent example of this is the development in India of a seismic design guideline for earth dams and embankments following the 2001 Gujarat earthquake (Towhata et al., 2002).

Case histories provide an insight in to the modes of failure. Most of the case histories indicate foundation failure although some indicate liquefaction of the levee fill itself. The majority of the historical observations show that the earthquake-induced deformations resulted in severe damage. Typical failure modes included extensive slumping, cracking and differential settlement of the crest, both parallel and perpendicular to the crest, and bulging at the toe. In many cases severe damage occurred throughout the levee, but the landside batter did not suffer much damage.

### 3.4 LOCAL FAILURES OF LEVEES

A limited number of studies have been carried out to explain the phenomenon of periodical appearance of damage in sections of embankment with similar foundation conditions (Ambraseys and Sarma, 1967; Hatanaka, 1952; Kano et al., 2007). They all consider the three-dimensional response of embankments to seismic shaking. Conclusions are that amplitudes are larger at locally-limited spots along the longitudinal axis during shaking and Rayleigh waves are the cause of periodical failure of earth structures. Kano et al. (2007) studied the influence of the three-dimensional response of embankments on local failures where the reason for the local failure was unknown. Model embankments made of gelatin were tested on a shaking table to simulate and ground shaking and were simplified to a cross section of a triangular-shaped prism with a length of 480 mm and height of 40 mm. The conclusions were that there are several reasons why these localised failures occur:

- Variance in input motion
- Partial difference in stiffness of the embankment,
- The influence of the Rayleigh wave,
- Amplified acceleration caused by the three-dimensional response of the embankment.

The response displacement at the crest of an embankment during shaking becomes larger at locally-limited spots. Its amplitude changed periodically along the longitudinal direction like a wave, though the model base was shaken uniformly.

The distance between the anti-nodal point and the nodal point varies with the frequency of input motion and shear wave velocity of the embankment, see Figure 16 for definitions. Amplitude at the nodal points agrees well with the theoretical solution of a two-dimensional response of an embankment. However, amplitudes at the anti-nodal points were about 1.5 to 2.0 times larger than at the nodal point under the condition of the conducted tests. The reason why the amplitude at the anti-nodal point becomes larger is due to the three-dimensional response of the embankment. If the embankment lies on soft ground, its wavelength can be obtained by the same equation by substituting the height of the embankment with the total thickness including the thickness of the soft ground.

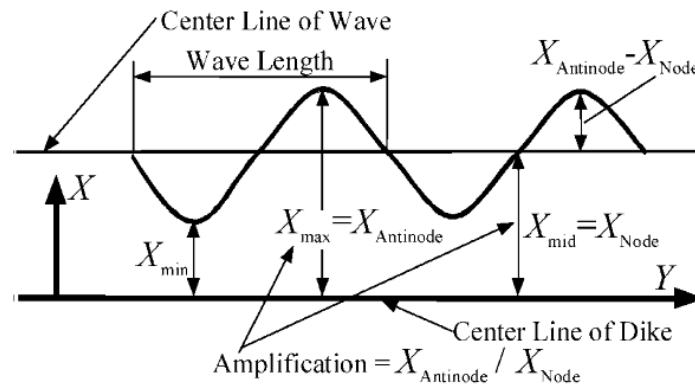


FIGURE 16: DEFINITION OF WAVE AT THE CREST (KANO ET AL., 2007)

### 3.5 SUMMARY

The hypothesis that levee deformation during earthquakes is controlled predominantly by behaviour of the foundation materials has developed through field case histories and experimental tests confirming that liquefaction plays a major role in damage to earth embankments.

The cause of failure for levees and embankments in recent earthquakes may be attributed to the following:

- (i) Foundation movements/failure due to poor local soil conditions.
- (ii) Potential liquefaction/liquefaction severity and consequent settlement, bearing capacity failures and lateral spreading that may undermine the stability of the levee.
- (iii) Horizontal and vertical ground accelerations that result in initial loads and stress variations within the slope, decreasing the stability of the slope in the instants when the dynamic forces act in adverse directions. Note that if the cyclic loading causes loss of soil strength, the effects may be more adverse.
- (iv) Potential deformation of the levee fill material due to liquefaction in the case of saturated non-cohesive soils, or consolidation settlement due to cyclic loading.

Some common causes of damage to levees are inferred from embankment and earth dams for which there is a larger amount of scientific research available. Other factors affecting damage to levees include:

- (i) Geometry of the levee which may influence the slope stability and will affect the stresses acting on the foundation soils.
- (ii) Geomorphology and geometry of the native soils beneath the levee which affect the style of damage to the levee.
- (iii) Groundwater/river levels during the time of the earthquake which will effect whether liquefaction occurs within the levee and the extent of liquefaction beneath the levee.

While the soil is in a fully liquefied state large permanent deformations and even complete failure of earth embankments may occur. Liquefaction of the foundation soils can result in the following general modes of damage to an embankment:

- Shallow surface sliding of slope,
- Development of a slip surface,
- Bearing capacity failure,
- Slumping,
- Settlement associated with densification,
- Lateral Displacement.



## 4.0 OBSERVED DAMAGE PERFORMANCE OF THE FLOOD PROTECTION SYSTEM DURING THE CANTERBURY EARTHQUAKE SEQUENCE

### 4.1 INTRODUCTION

The Canterbury earthquakes which occurred between September 2010 and December 2011, with ongoing aftershock activity at the time of writing, caused substantial damage along the Waimakariri, Kaiapoi and Avon Rivers as well as many other smaller streams and tributaries.

Reinstatement works on stopbanks began almost immediately following the earthquake events and as a result the damage data is sparse and not well documented. This chapter aims to bring together this data in order to summarise the observed and recorded response of the Canterbury Flood Protection System to the 2010 and 2011 earthquake events.

### 4.2 OVERVIEW OF OBSERVED DAMAGE

The 4 September 2010 and 22 February 2011 Earthquakes, as well as the major aftershocks, caused land damage along the natural banks and stopbanks of the Waimakariri River and its tributary the Kaiapoi River, which are under the management of Environment Canterbury, and the Avon and Halswell Rivers, which are managed by the Christchurch City Council (CCC). The majority of the damage to the Waimakariri, Eyre, Cust and Kaiapoi system (WEC system) occurred following the 4 September 2010 earthquake, whereas the majority of the damage to the Avon River occurred during the 22 February 2011 earthquake, although on-going damage occurred incrementally throughout the Canterbury Earthquake Sequence.

The damage to the stopbanks was variable in nature as was the degree of severity; however the damage was mostly restricted to the east of State Highway 1, for the Waimakariri and Kaiapoi Rivers, and bounded by Barbadoes St to the west and South Brighton Bridge to the east for the Avon River. The locations of the rivers are shown in Figure 1 – Chapter 2.

The total damage length for all three rivers (including damage to stopbanks and damage to river banks) resulting from the cumulative effect of all four significant earthquakes was approximately 38 km, with a total of 28 km of damage to the stopbank system, with the total lengths of damage for each of the rivers are summarised in Table 5 and illustrated in Figure 17 and Figure 18.

There was additional damage in other areas that was reported anecdotally. These areas include small localised regions of damage west of the State Highway 1 Bridge on the Waimakariri River and minor damage along the Ashley River approximately 13 km north of the Waimakariri River, however the specific locations were not surveyed and are therefore not clearly known. Aside from this the areas outside of the surveyed zones were not damaged, and hence not surveyed, for example west of Christchurch.

**TABLE 5: APPROXIMATE CUMULATIVE LENGTHS OF DAMAGE FOR THE PRIMARY RIVERS AND STOPBANK SYSTEM**

River	Length of Damage to Natural Banks (km)	Length of Damage to Stopbank Lengths (km)	Total Length of Damage to the River System (km)	Total Surveyed Length of River Banks (km) [Total Surveyed Length of River (km)]
Avon	5.3	19.2	24.5	30.0 [15.0]
Waimakariri and Kaiapoi	0	14.1	14.1	18.7 [9.4]
Total	5.3	33.3	38.6	48.7 [24.4]

#### 4.2.1 AVON RIVER

Damage caused by the September 2010 earthquake to the stopbank system of the Avon River was extensive. The February 2011 earthquake caused additional damage to the lower Avon which was much greater than that of the September 2010 earthquake, most likely due to the higher seismic demand observed locally (PGAs ranging from 0.34 g – 0.62 g) and consequent of severe liquefaction and lateral spreading. This resulted in further damage to the river as well as extensive damage to the initial and temporary restoration works. The June 2011 and December 2011 events also caused damage to the system, however this was mostly limited to additional damage of the emergency and temporary stopbanks.

Damage morphology along the Avon River was highly variable due to the inconsistent nature of the flood protection system and the heterogeneous nature of the underlying soils. A summary of the damage morphology is as follows:

- Trapezoidal soil stopbanks were damaged with several lines of longitudinal cracks.
- In some areas where the stopbank was built immediately adjacent to the river the entire riverside batter slumped into the river.

Slumping was the primary failure mechanism observed along the Avon River; transverse cracks also occurred but were less common. The land damage that occurred indicated that large amounts of deformation have occurred not within the stopbank body itself but within the native ground outside the stopbank.

Engineered features are present along the river and gabion walls are used intermittently along the Lower Avon to either support the stopbank or to maintain the natural river bank. Damage to the gabion was generally a slight

outwards rotation of the basket of less than  $10^\circ$ , or ‘consolidation’ of stopbank fill causing minor crest settlements. In some areas, however, there was complete outwards rotation and failure of the gabion baskets causing the retained materials to slump into the resulting void. Damage morphology is discussed in detail in Chapter 5.

#### 4.2.2 WAIMAKARIRI AND KAIAPOI RIVERS

The northern Canterbury townships of Kaiapoi, Kainga, Brooklands and Kairaki have all suffered repetitive seismic-induced damage to flood protection assets during the 4 September, 22 February, 13 June and 22 December earthquakes. As mentioned earlier the majority of the damage along the Waimakariri River occurred downstream of State Highway 1. Fortunately, due to low water levels in the river during the September event, during which the majority of damage occurred, a secondary disaster due to breaches of embankments did not take place (T&T, 2010). The majority of the damage seen along the Waimakariri and Kaiapoi Rivers occurred during the 4 September 2010 earthquake, however the subsequent major aftershocks caused additional damage to the same areas. This region experienced the highest seismic demand during this event than any of the other events.

#### 4.2.3 COMPARISON OF SEISMIC DEMAND

The seismic demand experienced by the stopbanks during the various seismic events can be compared by scaling the observed PGAs to a  $M_w 7.5$  event, as discussed in Section 2.3.1 and shown in Figure 9. The seismic demands experienced at each study site are given in Table 6.

**TABLE 6: EXPERIENCED  $PGA_{M7.5}$  (COMPARISON OF SEISMIC DEMAND)**

<b>River</b>	<b>PGAs Experienced</b>	
	<b>4<sup>th</sup> September 2010 (<math>M_w 7.1</math>)</b>	<b>22<sup>nd</sup> February 2011 (<math>M_w 6.2</math>)</b>
Avon River	0.14 – 0.20	0.16 – 0.40
Kaiapoi/Waimakariri River	0.16 – 0.21	0.13

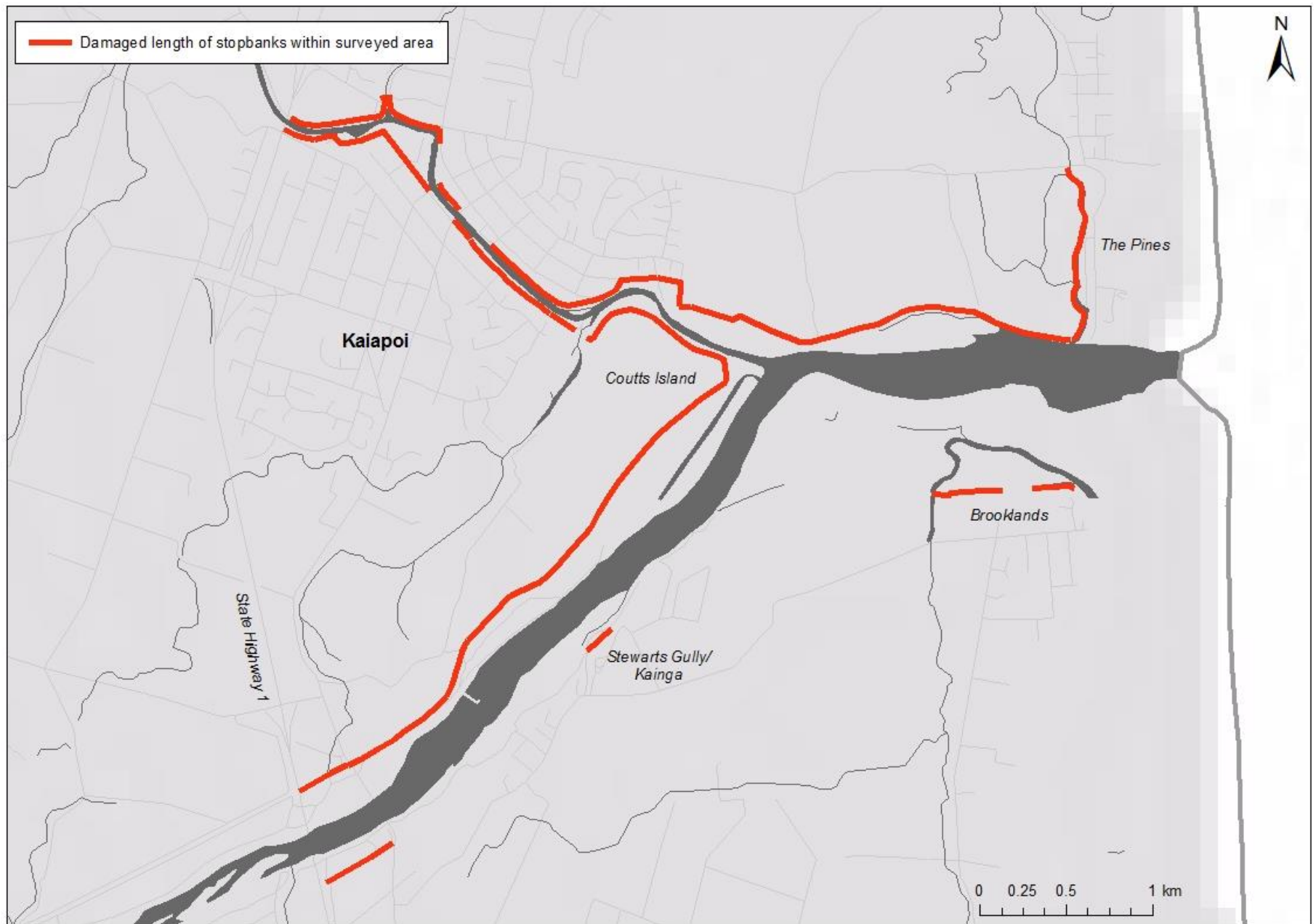


FIGURE 17: DAMAGED LENGTHS OF STOPBANK WITHIN WEC SURVEYED AREA

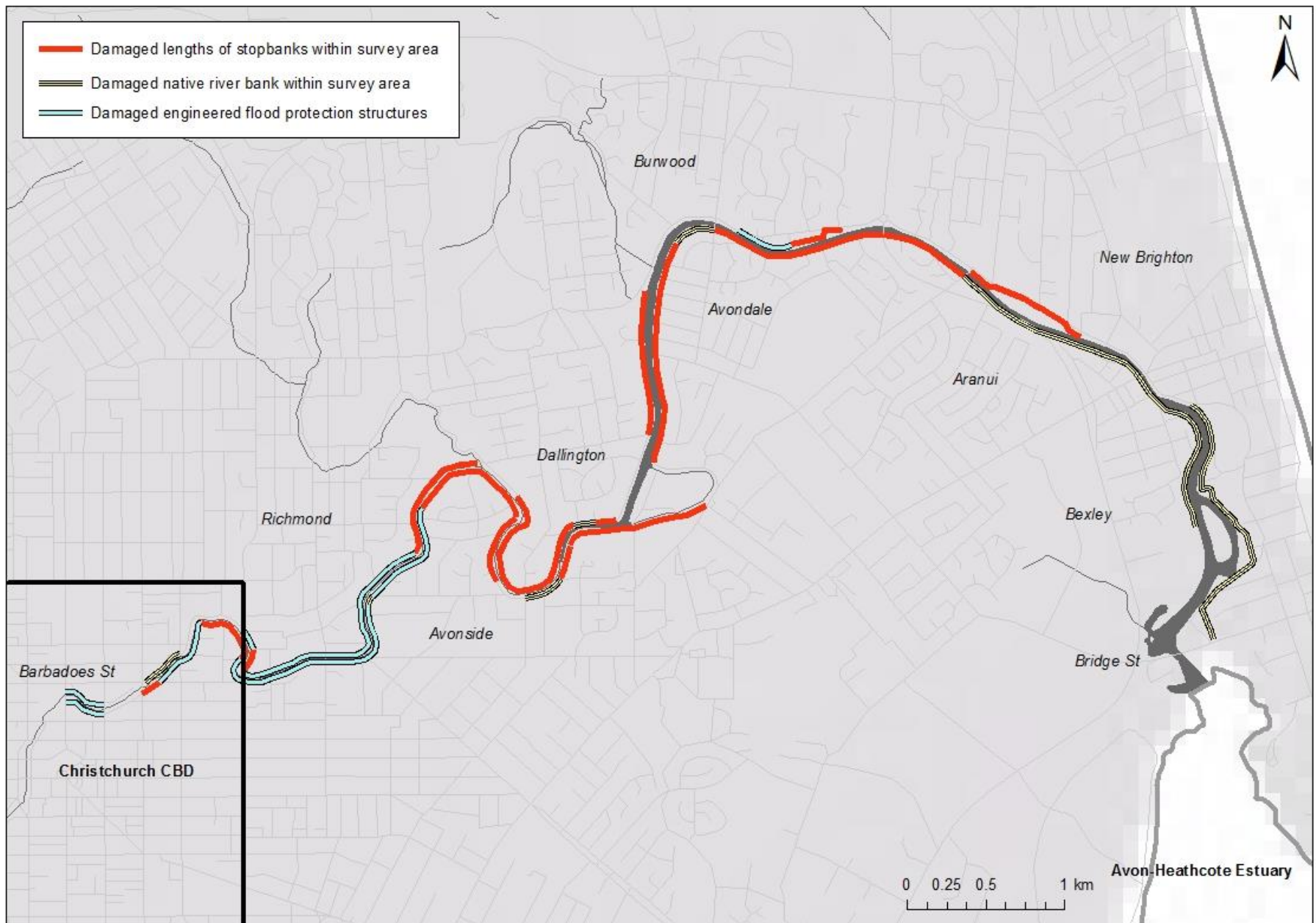


FIGURE 18: DAMAGED LENGTHS OF STOPBANK WITH AVON SURVEYED AREA

### 4.3 DATA COLLECTION

This research project commenced following the 22<sup>nd</sup> February 2011 earthquake and draws from data collected following the 4<sup>th</sup> September 2010 earthquake and subsequent major aftershocks. The key data sets are discussed in detail below and are then introduced where necessary throughout the text.

#### 4.3.1 KAIAPOI AND WAIMAKARIRI RIVER

A local engineering consultancy, Riley Consultants Ltd (RILEY), was engaged by Environment Canterbury to provide an assessment of the condition of the Waimakariri River stopbanks after the September 4<sup>th</sup> 2010 and February 22<sup>nd</sup> 2011 earthquake events (RILEY, 2010b, c, 2011).

A preliminary visual inspection was undertaken over four days, from 15<sup>th</sup> – 20<sup>th</sup> September 2010, in order to identify damage to the stopbank system and to suggest further geotechnical investigations required prior to repair. This was then followed by a subsurface investigation completed by 29<sup>th</sup> October 2010. This comprised:

- Eight shallow test pits to maximum depths of 1.4 - 3 m; and
- Bulk sampling at five of the test pits for Particle Size Distribution (PSD) analysis.

Approximately 19.1 km of the stopbank system was inspected (Appendix B), including:

- The true right hand side of the Waimakariri River from the Northern Motorway (State Highway 1) to the edge of Brooklands Lagoon;
- The true left hand side of the Waimakariri River from the Main North Road overbridge to the mouth of the Kaiapoi River, then along the true right side of the Kaiapoi River up to the railway line crossing; and,
- The true left hand side of the Kaiapoi River from the railway line crossing.

Earthquake damage, including cracking, slumping and liquefaction was documented using a Global Positioning Devices (GPS), and was complimented with detailed soil logs and photographs. Generally damage was variable over reasonably short distances; in order to visually represent the observed damage severity Riley Consultants Ltd. adopted a damage classification scheme Table 7. The system was re-surveyed following the 22 February 2011 earthquake using the same classification scheme.

**TABLE 7: RILEY CLASSIFICATION GUIDE FOR STOPBANK DAMAGE**

<b>Damage Category</b>	<b>Description</b>
None	No damage
Minor	Cracks up to 5 mm wide and/or 300 mm deep. Negligible settlement of crest.
Moderate	Cracks up to 1 m deep. Some settlement of crest.
Major	Cracks greater than 1 m deep. Evidence of deep seated movement and/or settlement.
Severe	Sever damage or collapse. Gross lateral spread and/or settlement, cracks showing deformation of 50 mm or more.

Remediation to the stopbanks along the Kaiapoi and Waimakariri rivers (WEC system) was undertaken following the 4 September 2010 Earthquake and prior to the 22 February 2011 Earthquake, with minor localised repairs undertaken to the areas which suffered additional damage as a result of the subsequent major aftershocks. Stopbanks along the WEC system were repaired based on their RILEY damage category, as follows:

- **Severe Damage** – Repaired on an individual site by site basis based on local site constraints and stopbank materials.
- **Major Damage** – Remove and re-compact a 3 m wide silty zone of the river-side, forming a 1V:3H batter.
- **Moderate Damage** – Removal and replacement of topsoil of the river-side batter and crest and re-compaction of the surface of the bank. If batter is steeper than 1V:2H, reform to 1V:3H.
- **Minor Damage** – Disturb and compaction of surface cracks within the river-side batter and crest.

#### 4.3.2 AVON RIVER

Along the Avon River, reinstatement works began immediately following all major earthquake events in order to restore the river defences initially to a minimum level of RL 10.8 m and then to RL 11.2 m (Christchurch City Council Drainage Datum) with a 10 to 12 year design life (GHD, 2011). Stopbanks were built along the line of the existing stopbanks, with an original design of a well graded sandy gravel (pitrun) core and 4 : 1 soil batters and a 2.5 m crest where width of adjacent land permitted. Sandbags, concrete blocks and steeper batter angles were used where adjacent land widths did not permit standard stopbank morphologies. Furthermore temporary stopbanks were extended upstream of the original stopbank sections.

The emergency stopbank repairs were required to be undertaken rapidly due to imminent risk of high spring tides which could have resulted in stopbank breaches and flooding. This resulted in inadequate construction techniques in order to complete the construction/repairs quickly. Inadequate compaction, materials and/or design, as well as insufficient ground improvement to foundations resulted in the stopbanks being prone to on-going damage, from liquefaction, during major aftershock events. Reinstatement works were ongoing as temporary stopbanks constructed across the Avon were damaged multiple times from substantial aftershocks, as well as experiencing ongoing minor settlement (horizontal and vertical) due to subsequent smaller aftershocks and ground relaxation. A condition survey of the stopbanks was undertaken by GHD (2012) between 18 to 22 July 2011 of the stopbank.

The stopbank reaches were divided into four risk categories, based primarily on flood risk modelling, as follows:

- **No Stopbanks** – 5180 m
- **Low Failure Risk** – 8990 m
- **Medium Failure Risk** – 3180 m
- **High Failure Risk** – 3380 m

No geotechnical investigations of the stopbanks along the Avon River were undertaken prior to rehabilitation works beginning, this meant that the majority of the damage was masked by gravel (from temporary protection/repair measures) before it could be surveyed.

## 4.4 TYPICAL CROSS SECTIONS OF STOPBANKS AND CONSTRUCTION HISTORIES

### 4.4.1 AVON RIVER

The Avon River is a low-energy system that can be divided at Barbadoes Street into two reaches. West of Barbadoes St the Avon has a steeper hydraulic gradient, characterised by a narrower cross section and steeper banks, with flows of approximately  $2\text{m}^3/\text{s}$ . East of Barbadoes St the river has a lower gradient, characterised by a wider cross section and shallower banks, with flows of approximately  $35\text{m}^3/\text{s}$  (GHD, 2012). Figure 19 shows typical river profiles throughout the lower reach of the Avon River. These reaches have a long history of infrequent flood events dating back to 1886 with two significant events occurring in 1925 and 1930 (Scott, 1963). These events prompted the construction of the pre-earthquake stopbank system circa 1983 – 1985.

Prior to the earthquakes most of the stopbank crests were at RL: 11.2 m (CCD Datum) and those along Hulverstone Drive were at RL: 10.9 m, as reported by Harris (2003). The stopbank crest levels are based on storm surge modeling only as CCC modeling has determined that while there is likely to be some cross correlation between storm surge events and heavy rainfall, the levels in the Lower Avon are predominantly determined by storm surge. Table 8 shows the annual exceedance probability for different RL scenarios. Based on this the 11.2 m was adopted, which includes a 0.2 m freeboard.

**TABLE 8: PREDICTED ANNUAL EXCEEDANCE PROBABILITY FOR THE AVON RIVER (GHD, 2012)**

Crest (m) CCD Datum	Annual Exceedance Probability (AEP)
RL 10.75	20%
RL 10.80	10%
RL 10.95	2%
RL 11.00	1%

Prior to the Canterbury Earthquakes there was no asset summary available for the Avon. According to GHD (2012) a sales force damage register refers to 45 stopbank sections, however these are not specified. There is no ‘typical’ stopbank morphology for the Avon River. The flood protection system generally comprises:

- Small (less than 1 m) compacted trapezoidal earth stopbanks which in some cases are retained from the river by a gabion wall, and in some cases retained from the road by a small concrete wall;
- Native sloping ground retained by a gabion wall;
- Modified slopes with no engineered features;
- Native slope supported by rip-rap; and,
- Adjacent to bridges the slope and fill are supported by engineered concrete walls.



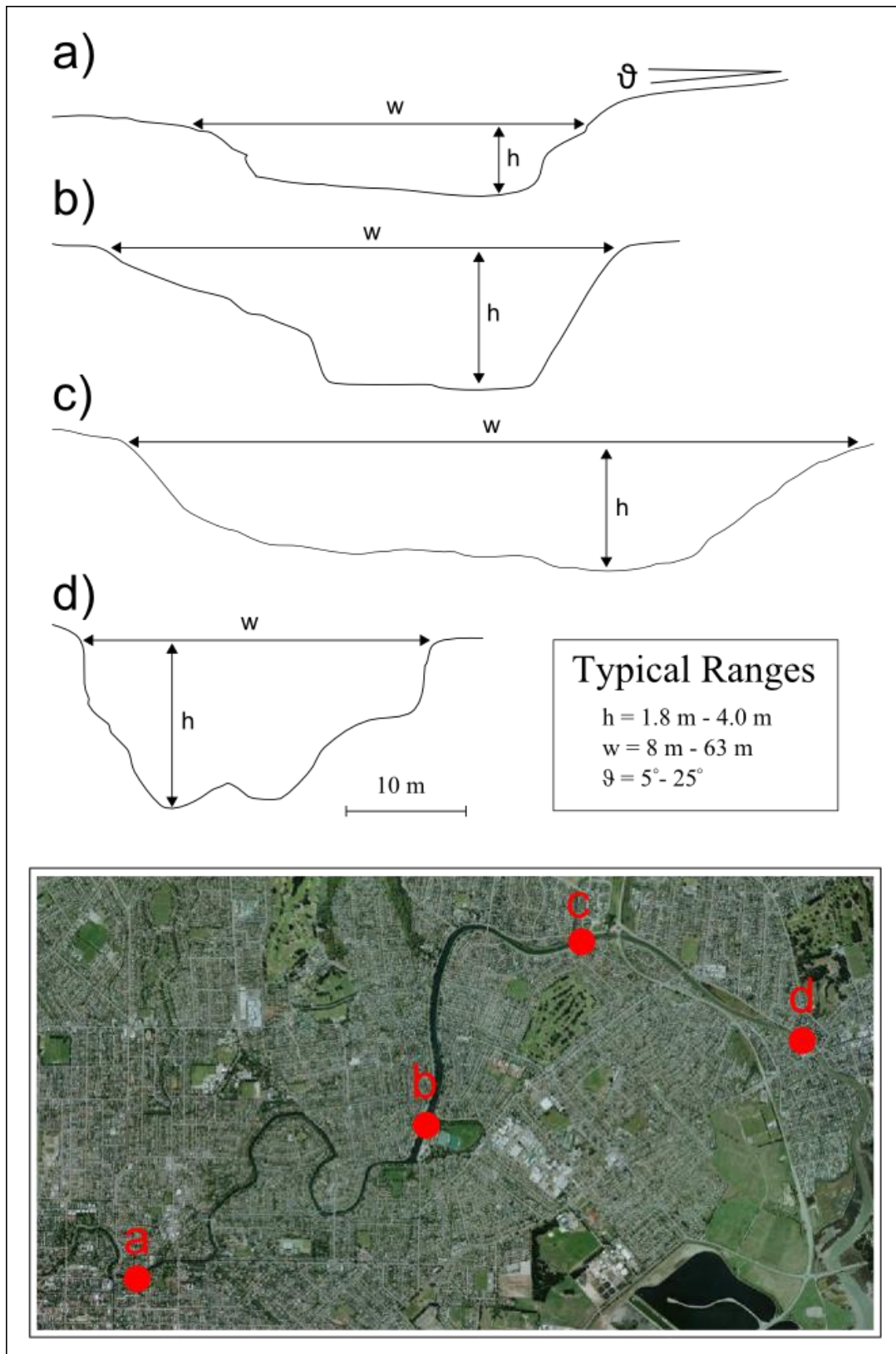


FIGURE 19: TYPICAL AVON RIVER GEOMETRIES.

Figure 20 shows design drawings for typical cross section options for the rehabilitation of the Avon River stopbanks as proposed by GHD (2012), these stopbanks are considered to be similar to the stopbanks that existed prior to the Canterbury Earthquakes. Standard practice, although not always implemented, indicates that the stopbanks were constructed from well graded silty gravelly pit run, approximate fines content of 15% and a compaction of 95% maximum modified dry density, although there are no available grain size curves from the various times of construction. This generates a permeability of no less than  $10^{-6}$  m/s.

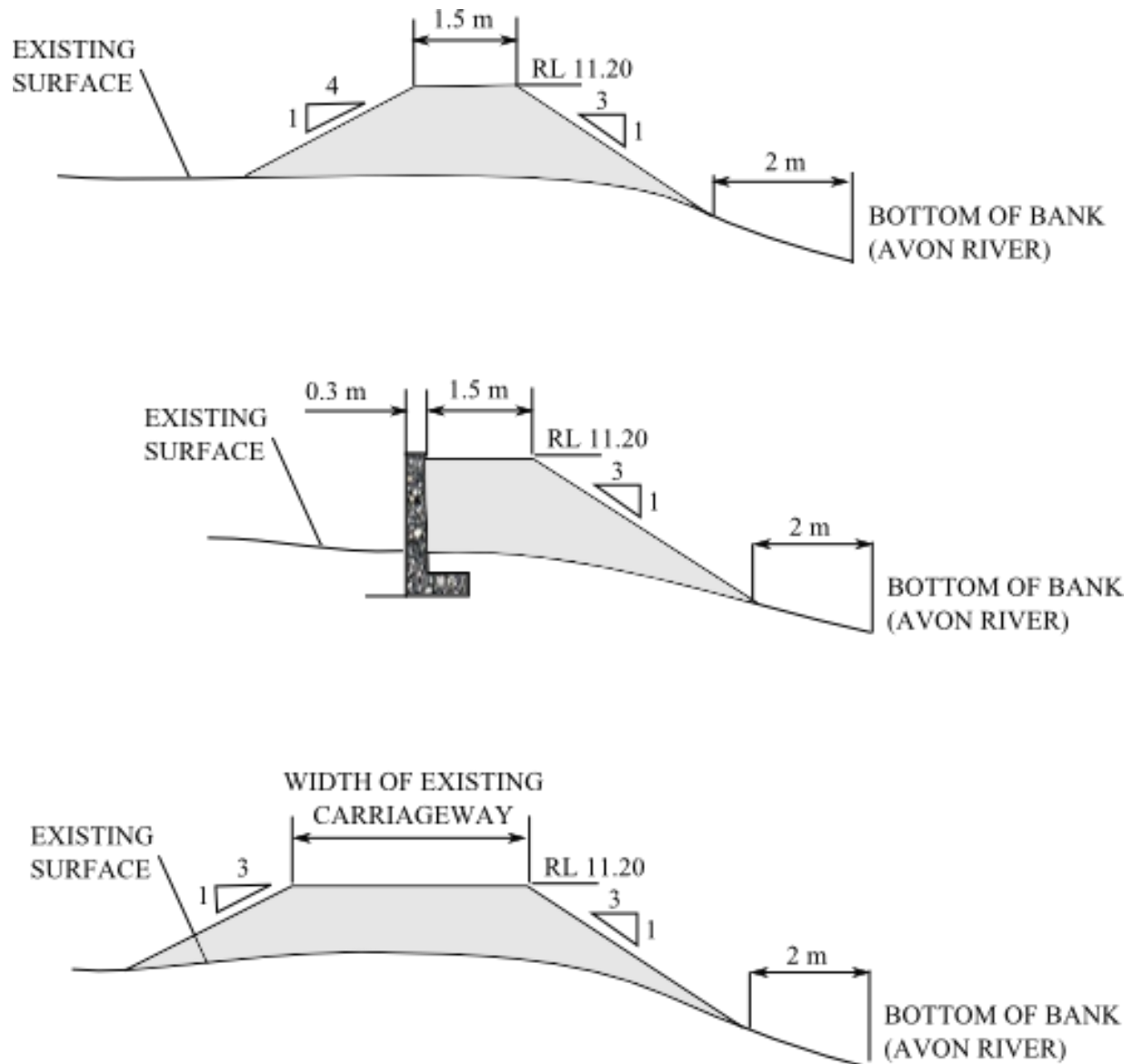


FIGURE 20: PROPOSED TYPICAL AVON RIVER CROSS SECTIONS, ADAPTED FROM GHD, 2012.

#### 4.4.2 KAIAPOI AND WAIMAKARIRI RIVERS

As aforementioned in Chapter 2, the Waimakariri and Kaiapoi Rivers have been extensively anthropogenically modified. The Waimakariri River flood protection system downstream of the lower gorge has the capacity to convey the design flow ( $4,730 \text{ m}^3/\text{s}$ ) to the sea (Heslop, 2011). Throughout this time the morphology of the stopbank system was being constantly changed and subsequently improved. A complete history of the river works from 1859 until 1988 is detailed in Reid and Poynter (1989). The earliest known protection works were constructed in 1859 by the Provincial Government. The Hays No. 2 Scheme, which began construction in 1930, was the first attempt to develop a comprehensive strategy towards the flood threat from the Waimakariri River. The scheme included extensive stopbanks throughout the lower 40 km of the Waimakariri River. However, until the introduction of the Waimakariri River Improvement Scheme in 1960, flood protection works were not adequate to contain large floods. The stopbanks for this scheme were designed to withstand a flood level flow of  $4,730 \text{ m}^3/\text{s}$  plus a freeboard margin of 0.9 m. The stopbanks generally comprise silt and silty sand with minor gravel. Typical stopbank cross sections for the WEC system are shown in Figure 22 and evolution of the geometry is summarised below and in Figure 21:

- Stopbanks built prior to 1960, primarily through the Hays No. 2 Scheme generally had a top width of 1.8 m and 2:1 batters, but in places were narrower and steeper.
- The 1960 Waimakariri River Improvement Scheme proposed strengthening the banks to a 3.6 m top width with 2:1 batters.
- A Scheme review in 1976 resulted in a standard cross section for stopbanks of 4.2 m top width with river and landward batters of 2.5:1 and 3:1, respectively.
- Stopbanks strengthened after 1979 were constructed with 3:1 batters on both sides or with equivalent on base width, and the existing batter on one side and greater crest width.
- The stopbanks range in height from approximately 1.5 m to 4 m in height.

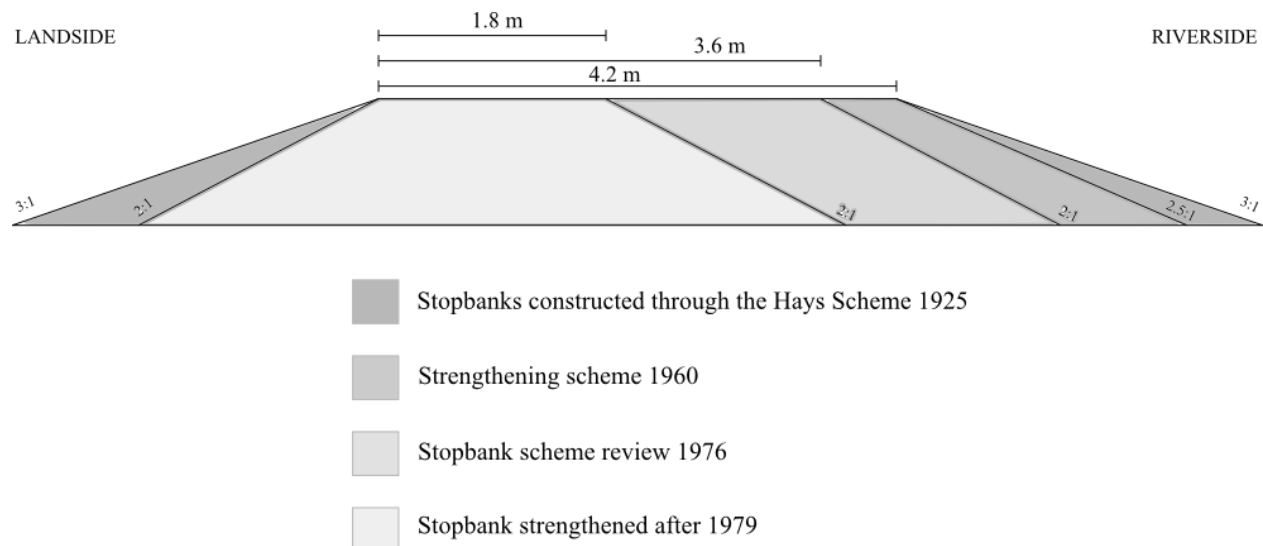


FIGURE 21: EVOLUTION OF STOPBANK MORPHOLOGY ALONG THE WAIMAKARIRI AND KAIAPOI RIVERS

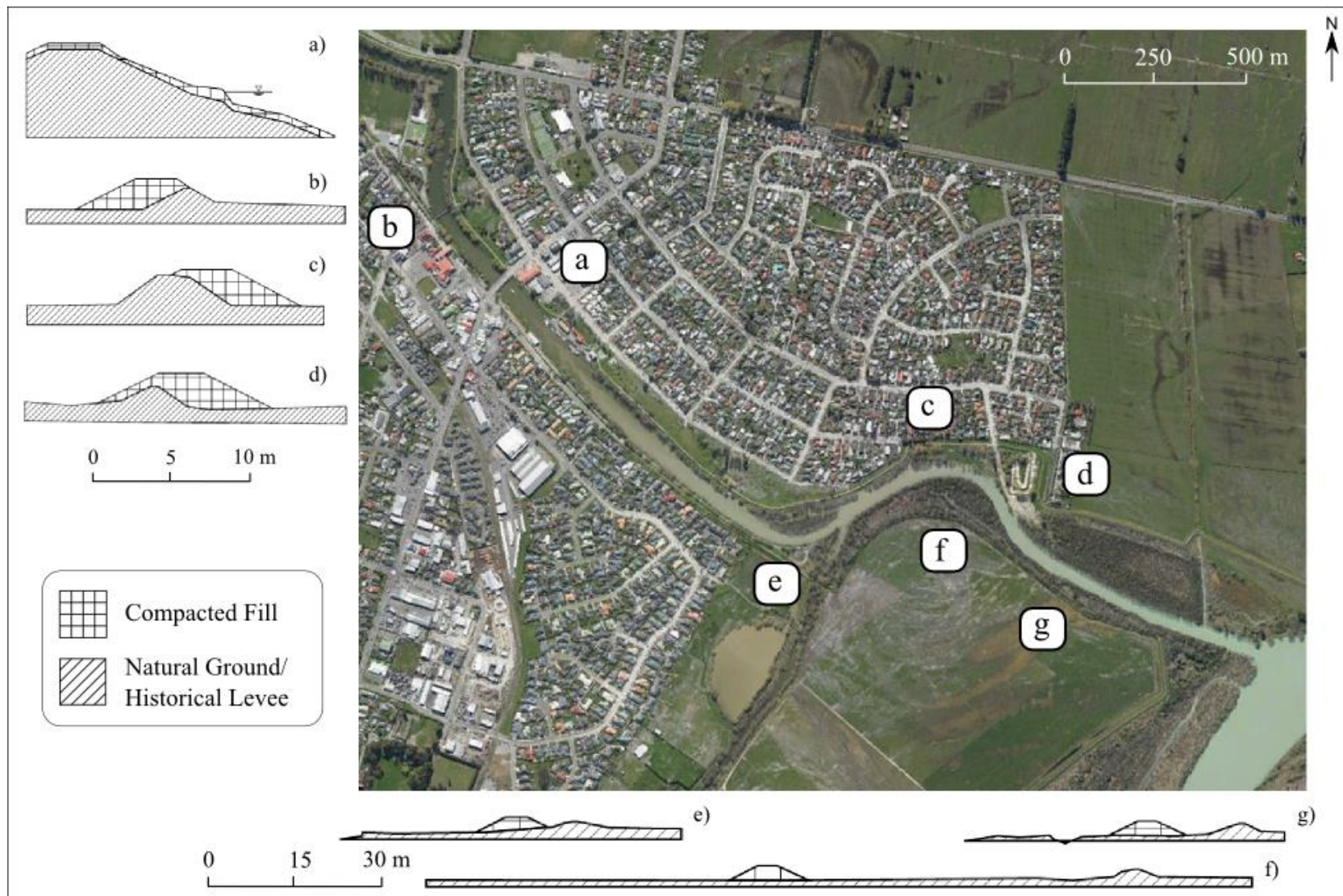


FIGURE 22: TYPICAL KAIAPOI RIVER STOPBANK GEOMETRIES, TAKEN FROM HISOTRICAL ECAN RIVER STOPBANK DESIGN DRAWINGS.

WHERE WATER IS NOT SHOWN THIS IS DUE TO SET BACK OF STOPBANK FROM RIVER, IE. THE STOPBANK DOES NOT PERMANENTLY RETAIN WATER.



## 4.5 DISTRIBUTION OF CREST SETTLEMENT

The residual height of the stopbanks following each significant Earthquake event provides valuable information on the severity of liquefaction effects that have occurred at that particular location. A rudimentary analysis of crest settlement can be undertaken using vertical elevation changes between LiDAR sets that approximate ground movement during significant earthquakes from elevation changes calculated between pairs of Digital Elevation Models (CGD0600). Crest surveys of both stopbanks were also undertaken in order to provide a higher resolution data set, as discussed below.

Along the Kaiapoi and Waimakariri River the LiDAR data set following the 4 September 2010 Earthquake shows a range from no settlement up to -2.0 m settlement. Interestingly, the LiDAR clearly shows in many locations settlement of the stopbank being significantly greater than settlement of the surrounding native ground. This generally occurs in areas where the stopbank is larger in size and therefore heavier and more compressible, for example on Coutts Island, east of Kaiapoi, where the stopbanks along approximately 1.6 km of the river settled by -0.8 m to -2.0 m relative to the surrounding ground that settled by up to -0.4, for stopbanks approximately 2 m high, following the 4 September 2010 Earthquake as shown in Figure 23. LiDAR following the 22 February Earthquake is not as useful as restoration works had begun and in the places where damage occurred multiple times in the WEC system, the stopbank levels had been built up to generally higher than previous levels, showing an apparent rise in elevation of 0.3 to 0.5 m in many places, and the seismic demand was lower.

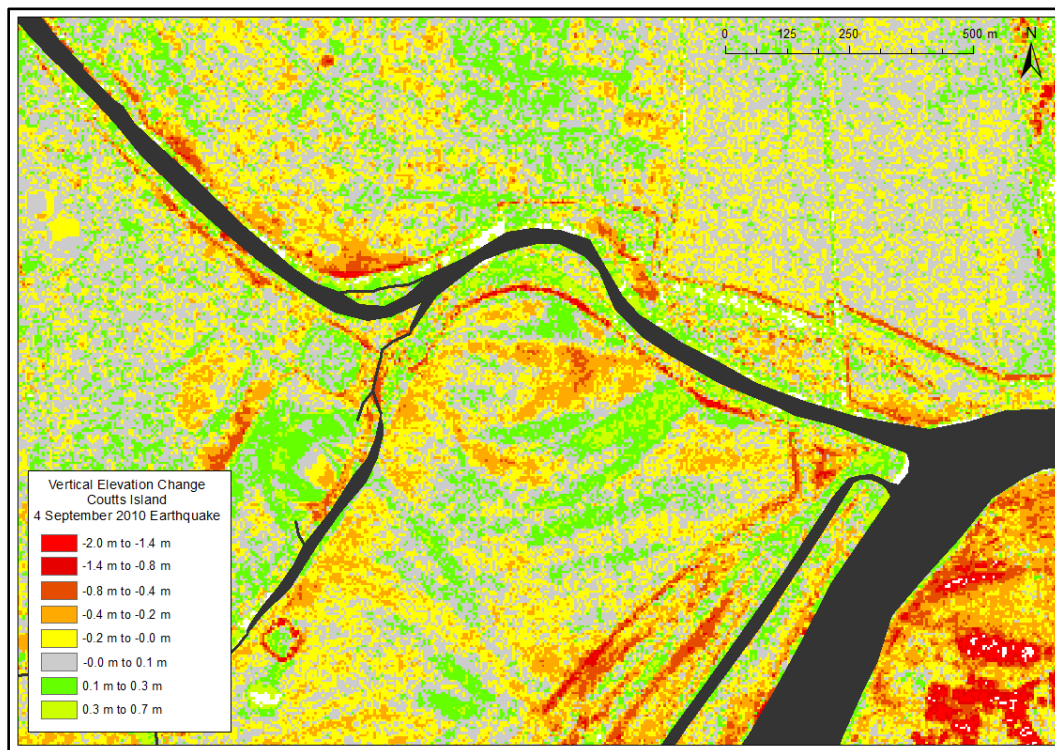


FIGURE 23: COUTTS ISLAND (KAIAPOI) EXAMPLE OF STOPBANK SETTLEMENT BEING SIGNIFICANTLY GREATER THAN THAT OF ADJACENT NATIVE SOILS.

Environment Canterbury also commissioned a survey of crest height following significant earthquakes and repairs using differential GPS and referenced to the Lyttelton Vertical Datum 1937 which is a local mean sea level datum. This detailed information has been used to determine failure modes in Chapter 5. An example of one of the pages of this survey is shown in Figure 26.

Stopbank settlements along the Avon River were reported by GHD in their post 22 February Earthquake report (GHD, 2011) as settling by a cumulative amount of 0.3 to 0.6 m as a result of the September 2010 and February 2011 earthquakes. This is consistent with CGD Map Layer (CGD0600) showing that following the 4 September Earthquake settlement along the Avon was generally in the range of -0.2 to -0.1 m, with some localized places along Hulverstone Drive and New Brighton Road having settlements of up to -1.0 m. The majority of the settlement along the river occurred following the 22 February event where settlements were mostly in the range of -0.4 to -1.5 m. Cumulatively, over the entire earthquake sequence to date the land along the Avon River generally settled by -0.5 m to -1.0 m and up to -1.5, with settlement increasing towards the Avon-Heathcote Estuary in the west, as shown in Figure 26.

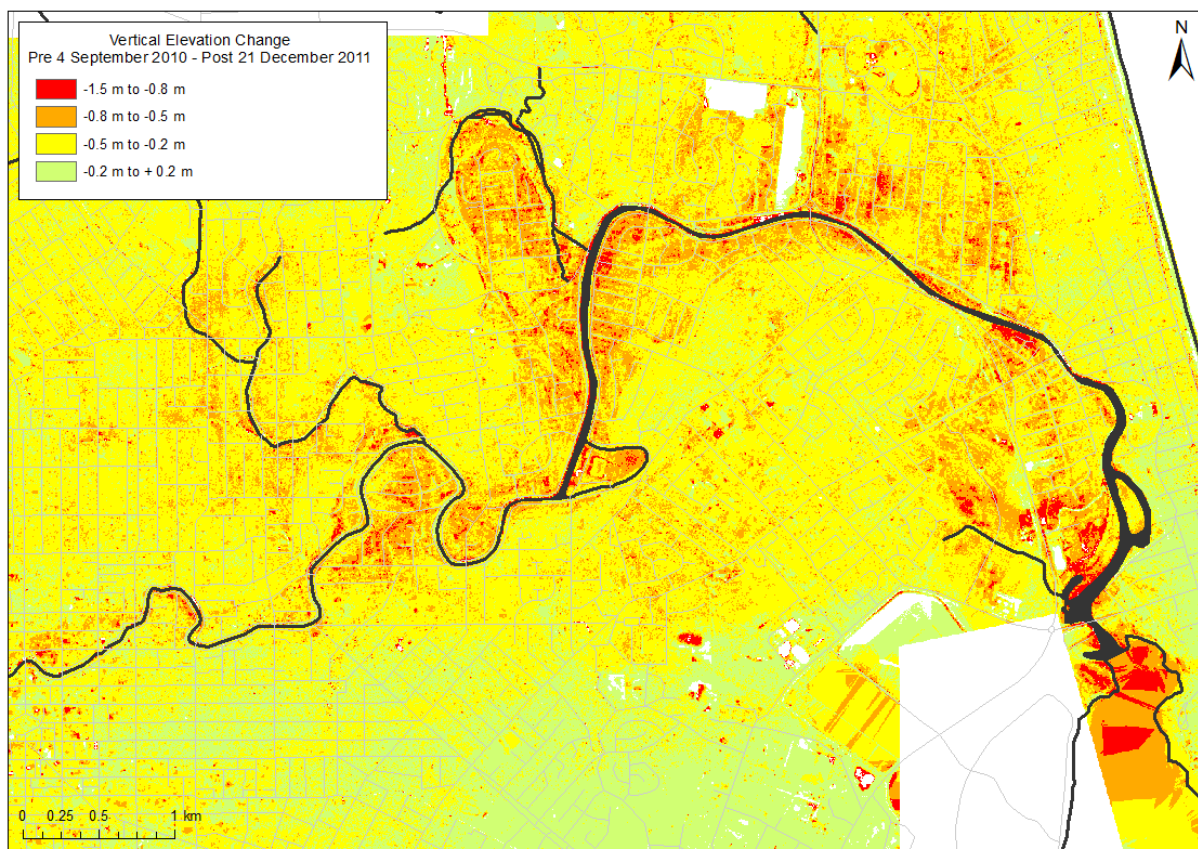
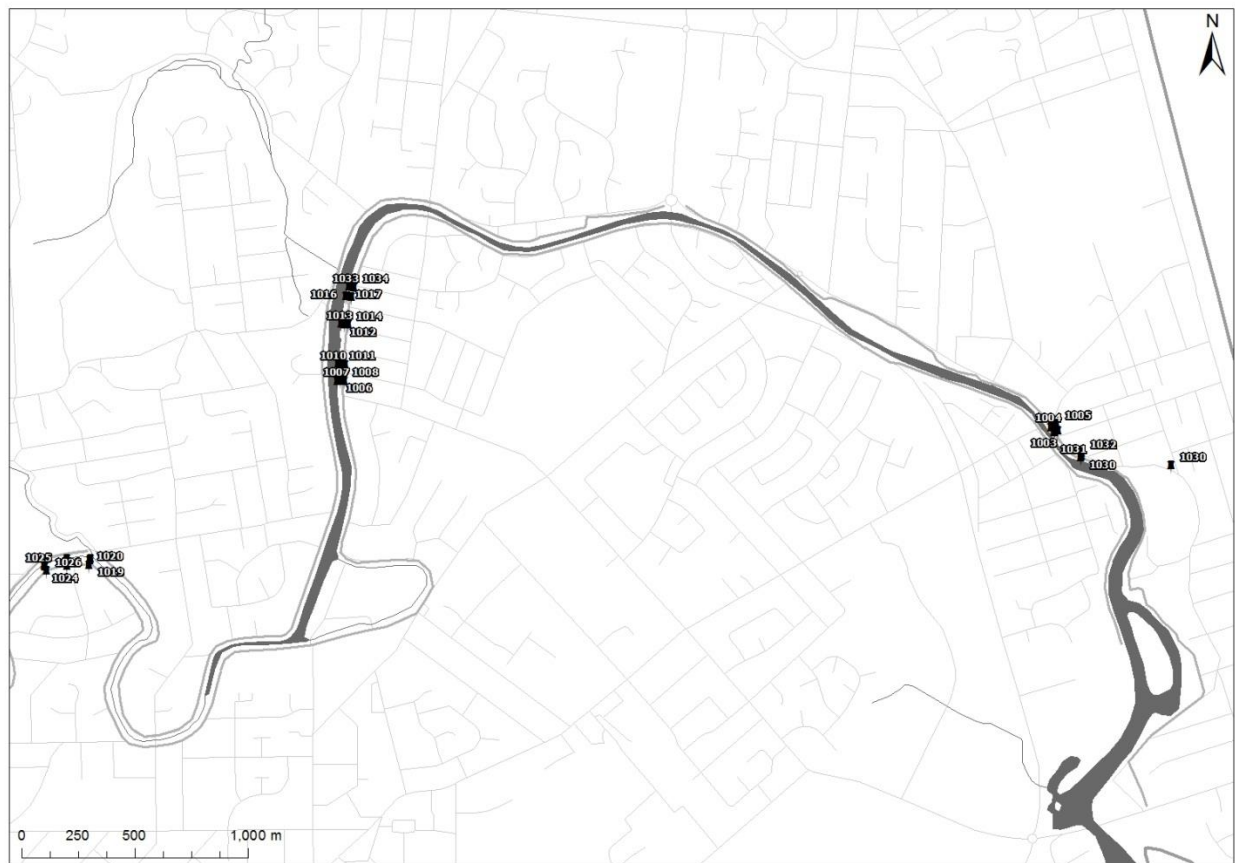


FIGURE 24: VERTICAL ELEVATION CHANGE CANTERBURY EARTHQUAKE SEQUENCE - AVON RIVER

Davie Lovell-Smith Ltd. undertook settlement monitoring from the period between May 2011 and August 2011 of fixed survey points along the Avon River in order to measure ongoing horizontal and vertical movement of the ground. The survey was undertaken on fixed monitoring pegs that were measured using differential GPS at roughly one week intervals, the exact locations of these monitoring pegs are provided in Figure 25. All levels are in terms of the Christchurch Drainage Datum (CDM Datum), which is the reference plane for all drainage purposes in Christchurch. Levels above this plane are stated as ‘reduced level’ or RL in metres. The CDM Datum has been established as 9.043 m below the Lyttelton Vertical Datum 1937.

The results of the settlement monitoring indicate gradual movement, or creep, of previously damaged ground where lateral spreading and/or liquefaction has been severe, as presented in Figure 27. The ongoing creep was occurring, possibly due to consolidation of disturbed material under an increased surcharge, migration of material under exposure to tidal effects, or dissipation of excess pore water pressures and post-liquefaction re-solidification and re-consolidation. This survey data indicates a residual ground level of between approximately RL 10.04 m and RL 11.04 m (CGD Datum).





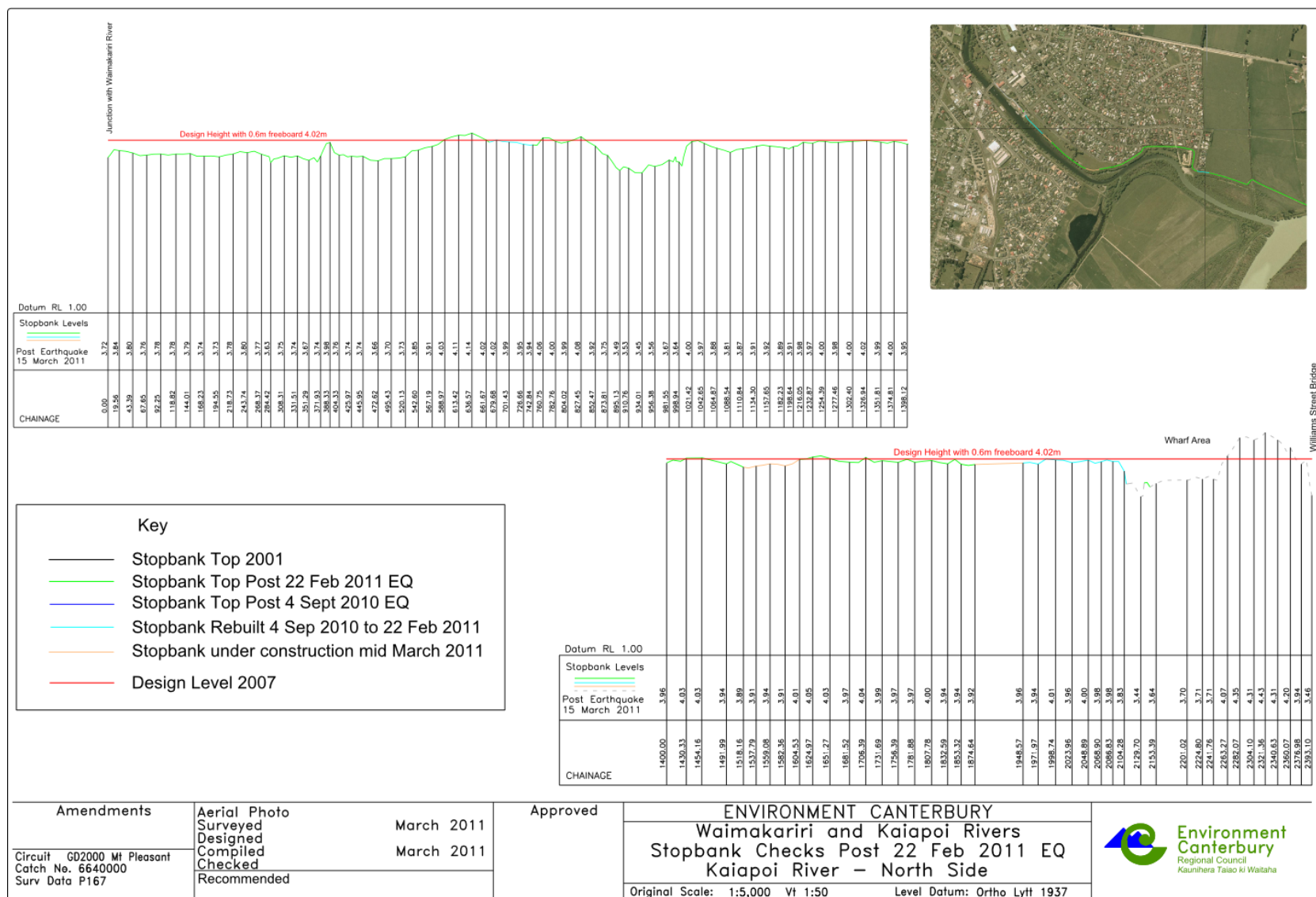


FIGURE 26: NORTH KAIAPOI RIVER CREST SURVEYS (ENVIRONMENT CANTERBURY, 2011).

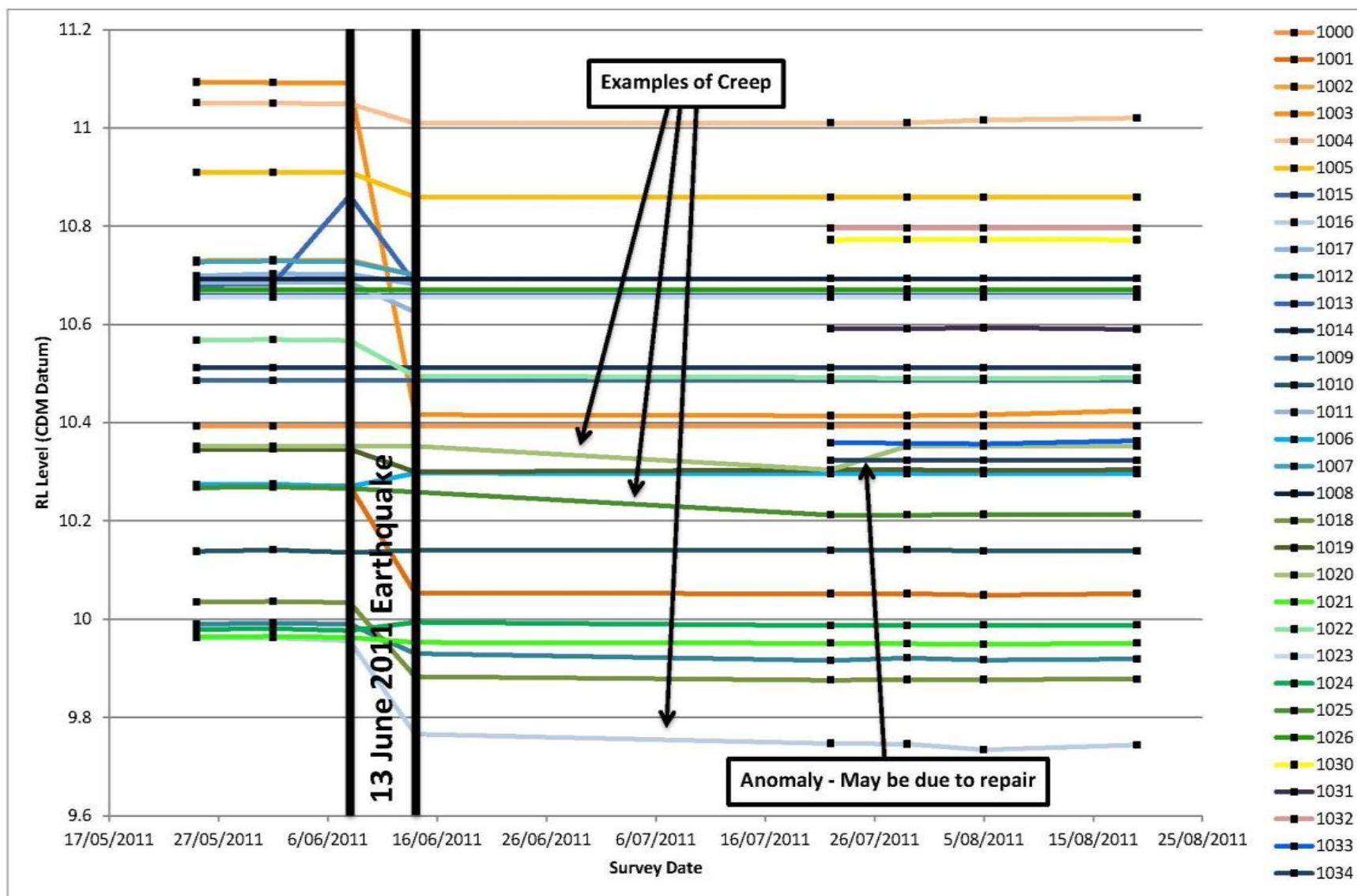


FIGURE 27: HORIZONTAL SETTLEMENT VS. TIME ALONG THE LOWER AVON RIVER

## 4.6 DISTRIBUTION OF GROUND CRACKS

Identifying patterns and widths of various mapped cracks provides insight into the patterns of movement and types of stresses imposed on the native ground beneath the stopbank and the stopbank itself. Multiple cracks parallel to the river can indicate lateral spreading in the downslope direction (commonly towards the river), transverse cracks and closely spaced parallel cracks generally represent complex modes of deformation and slumping, and the distribution of cracks can help identify the general movement of an area of land towards a free face.

Crack mapping was undertaken by geotechnical engineers and engineering geologists commissioned by the Earthquake Commission (EQC) following the 4 September 2010 and 22 February 2011 Earthquakes and is publically available on the Canterbury Geotechnical Database (CGD0400). Field observations of crack locations were recorded using coloured pens on paper copies of aerial photographs. The crack mapping is incomplete and only observations made by the mapping teams are presented. In particular, the mapping following the 4 September 2010 Earthquake was incomplete before the 22 February 2011 Earthquake occurred and subsequent mapping remains incomplete within the residential 'red zone' areas. Also, cracks in roads were often not able to be mapped because many were filled and the roads resealed before a mapping team arrived. For this study the 22 February 2011 crack map data has been used as the 4 September 2010 data provides minimal information adjacent to the rivers.

Maps of the ground crack locations are shown in Figure 28 and Figure 29.

There are cracks adjacent to the river along the majority of the Avon River with the cracks generally being the widest, greater than 200 mm, adjacent to the meandering loops and towards the mouth of the estuary. Cracks along the rest of the river are in the range of 10 to 200 mm wide. Generally, the density of the cracks decreases with distance from the river, with significant cracking still occurring as far back as 150 m from the river. Cracks typically track in a parallel direction to the river, however at sharp bends in the river there are often multiple transverse cracks fanning out, as illustrated on the Dallington Loop in Figure 29.

According to CGD0400 ground cracks were apparent along approximately half of the surveyed length of the Kaiapoi River. Multiple ground cracks greater than 200 mm in width were identified east of Raven Quay, at the end of Hall Street and adjacent to Revell Street. The first of these two locations correlate with significant stopbank damage.

Detailed crack mapping was undertaken along the Kaiapoi, Waimakariri and Kairaki Rivers by RILEY consultants following both the 4 September 2010 and 22 February 2011 Earthquakes (RILEY, 2010c, 2011). The location of each crack was recorded using a hand held global positioning device (GPS) with accuracy to +/- 5 m, however the thickness were not measured. As with the Avon River, the cracks generally ran in a parallel direction to the river, longitudinally along the crest of the stopbank, apart from at sharp bends in the river, where transverse cracks are apparent. The nature of the cracks following the two mapped earthquakes was similar, however, following the 22 February 2011 Earthquake there was significantly less cracking, apart from at the eastern most extent of Coutts Island where there was approximately three times as much cracking reported. This

is consistent with the higher seismic demands experienced in Kaiapoi following the 4 September 2010 Earthquake.

Test pitting was undertaken in 23 locations along Coutts Island, Kairaki and Brooklands to determine the depth and width of the ground cracks on the crests of the stopbanks. The logs show that the cracks extended to a maximum depth of 2.9 m below ground level with the majority of the cracks being less than 1 m deep, before closing. This indicates that while some cracks were going through the stopbank and the foundation materials, most cracks terminated within the stopbank materials. The locations and logs of these test pits are included in Appendix C.



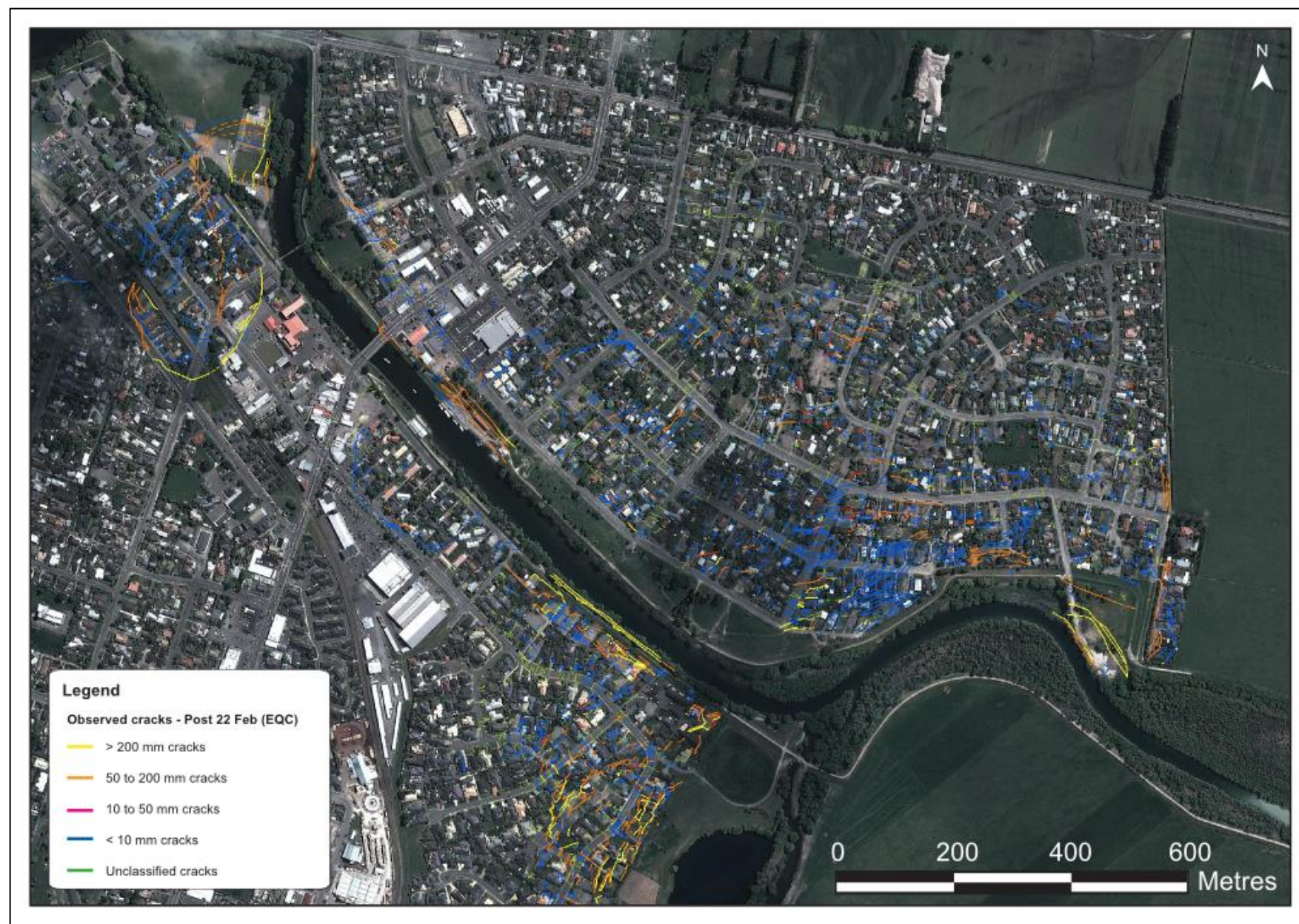


FIGURE 28: KAIAPOI RIVER OBSERVED CRACKS - POST 22 FEBRUARY 2011 (CGD0400).



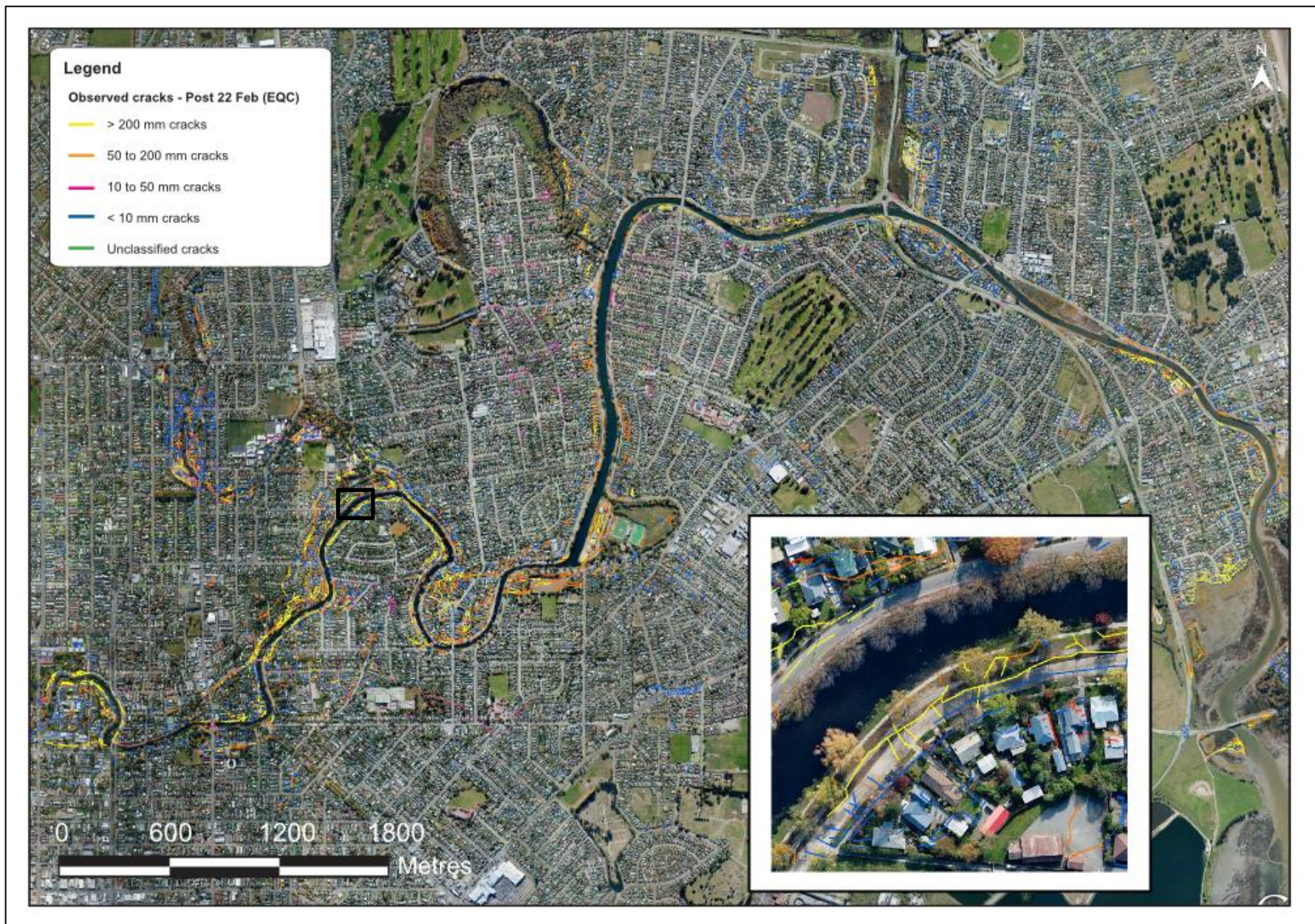


FIGURE 29: AVON RIVER OBSERVED CRACKS, POST 22 FEBRUARY 2011 (CGD0400).



## 4.7 CHANGES IN RIVER CAPACITY

Reduction in river capacity due to the earthquakes is not only a primary risk factor that could contribute to flooding, it also provides valuable indications about the permanent displacement of the natural ground.

### 4.7.1 HALSWELL RIVER

A study undertaken by McCracken and Surman (2012) illustrates how the natural river bank of the Halswell River (Figure 1 – Chapter 2) performed following the Canterbury Earthquake Sequence. The Halswell River does not have an engineered flood protection system, such as stopbanks or gabions. However, for the purposes of this study, the response of the Halswell River to the Canterbury Earthquakes is a useful assessment in to the behaviour of the river bank. The Canterbury Earthquakes caused significant liquefaction damage within the eastern part of the Selwyn District. In general, liquefaction was confined to a strip of 0.5 to 1.5 km wide land along the Halswell River. Damage was generally minor to moderate, with a few locations of major land damage associated with lateral spreading into the Halswell River (Yetton et al., 2011).

The Canterbury Earthquakes caused a reduction in the waterway capacity of the Halswell River in some locations. Initially, this was thought to be due to horizontal movement of the river banks towards the centre of the river, associated with lateral spreading. However, analysis undertaken by McCracken and Surman (2012), concluded that this was not due to large-scale narrowing, but was a result of a combination of horizontal, vertical and rotational movement.

Figure 30 and Figure 31, taken from McCracken and Surman (2012), illustrate the failure mechanism associated with the reduction in waterway capacity. Figure 31 demonstrates how flow into the river from a liquefied sand layer and outwards rotation of the native river bank has caused an increase in the height of the bed of the river. This same manifestation is seen in both the Avon and Kaiapoi Rivers.

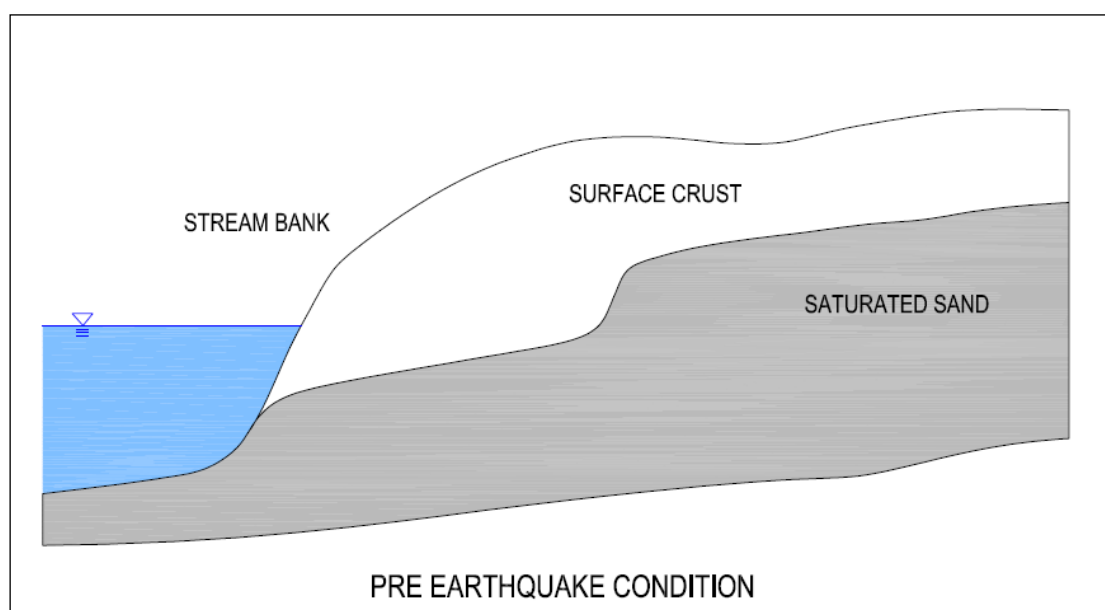


FIGURE 30: TYPICAL HALSWELL RIVER BANK CONDITION PRIOR TO THE SEPTEMBER EARTHQUAKE EVENT (ECAN, 2012)



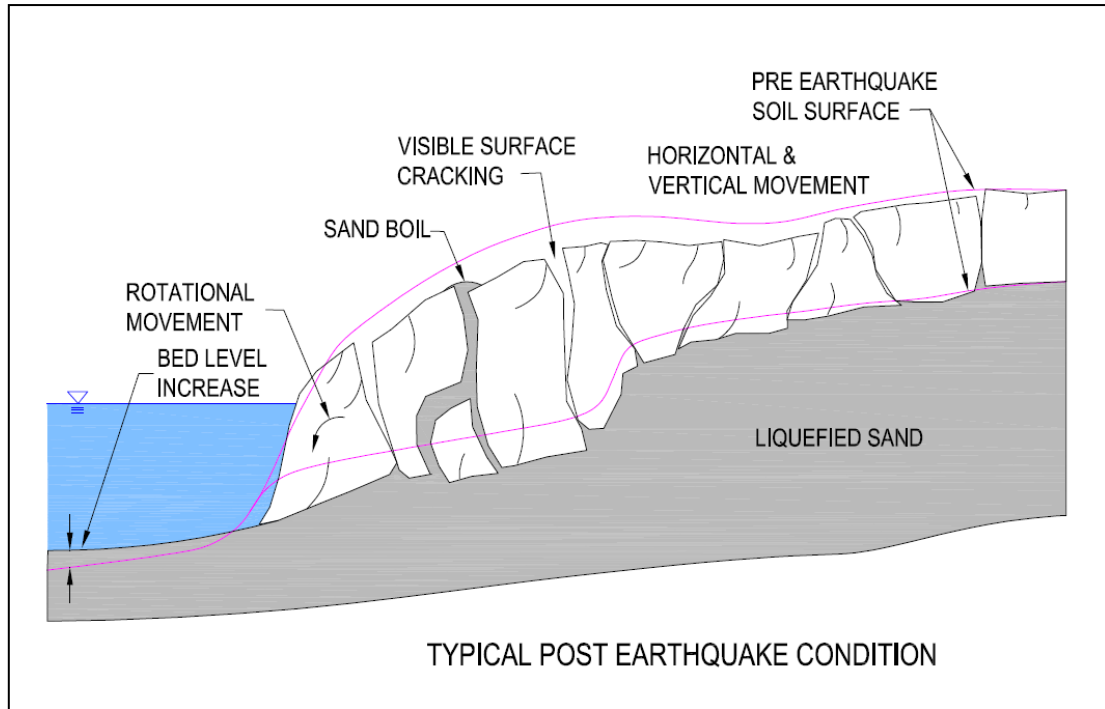


FIGURE 31: TYPICAL HALSWELL RIVER BANK CONDITION AFTER THE SEPTEMBER EARTHQUAKE EVENT (MCCRACKEN AND SURMAN, 2012)

#### 4.7.2 KAIAPOI RIVER

As illustrated in Appendix D the capacity of the Kaiapoi River was reduced to different degrees along the length of the river (Environment Canterbury Kaiapoi River Cross Sections 1964 and 2008 surveys). The width of the river was decreased by up to 8 m (approximately 18% of a 45 m wide stretch of river) at one of the surveyed locations and the height was decreased by a maximum of 1.2 m (approximately 30%). Whilst there are only five surveys along the Kaiapoi River, these indicate similar patterns to that which occurred in Halswell, namely a combination of horizontal, vertical and rotational movement caused a reduction in channel width. No surveys have been provided for the Waimakariri River.

Table 9 shows a summary of the stopbank performance along the eastern reach of the Waimakariri River and Kaiapoi River, as described in detail by (GEER, 2011).

TABLE 9: STOPBANK PERFORMANCE SUMMARY ALONG WAIMAKARIRI AND KAIAPOI RIVERS

	Estimated pre-earthquake flood capacity	Estimated post-earthquake flood capacity	Approximate cost of repairs (NZD)
<b>4 September 2010</b>	450 year event (4730 m <sup>3</sup> /s)	15 year event (1500 m <sup>3</sup> /s)	\$NZ 4 million
<b>22 February 2011</b>	30 year event (3000 m <sup>3</sup> /s)	20 year event (2500 m <sup>3</sup> /s)	\$NZ 2 million
<b>13 June 2011*</b>	100 year event (4000 m <sup>3</sup> /s)	100 year event (4000 m <sup>3</sup> /s)	-

\*Based on status at July 2011, no reduction in flood capacity was noted for the June M<sub>w</sub>6.0 aftershock event.

#### 4.7.3 AVON RIVER

A complete set of cross sections for the Avon River comparing a 2008 survey with post-4 September 2010 and post-22 February 2011 surveys is included in Appendix D (Christchurch City Council ‘Cross Sections of Avon River Bank’). These show that, as with the Kaiapoi River, the degree of variability in river morphology differs significantly between different river locations, generally however, the behaviour shows a similar pattern to that of the Kaiapoi and Halswell Rivers. The unique thing about the Avon River is that where the river widens to 60 m or greater near the mouth of the estuary, and the profile curves and slopes gradually, deformation tends to be significantly less than where the river has steeper slopes and a narrower profile.

## 5.0 GEOTECHNICAL STOPBANK DEFORMATION MODES OBSERVED DURING THE CANTERBURY EARTHQUAKE SEQUENCE

### 5.1 INTRODUCTION

It is not possible to develop a complete list of deformation modes of stopbanks that occurred as a result of the Canterbury Earthquake Sequence. Each stopbank foundation is as different as each stretch of stopbank; different materials, design configurations and construction histories are all variables that contribute to the pattern of mode of deformation. Each foundation is unique, with its own set of geological, geomorphological and geotechnical conditions. However, there are common features to the deformation modes that can be identified. Some of the common deformation modes that occurred under certain seismic conditions as a result of the Canterbury Earthquake Sequence are presented in this chapter.

#### 5.1.1 SCOPE AND OBJECTIVES

This chapter investigates the recorded and observed performance data reviewed in Chapter 4, to define and assign the damaged lengths of stopbank a characteristic deformation mode, and to identify the driving mechanism for each of these. Information on the damaged sections of stopbank which has been obtained from post-earthquake surveys conducted by various consultancies (GHD, 2011, 2012; RILEY, 2010b, c, 2011), are confirmed by a review of photographs and site visits (where possible). The selected deformation modes are compared and correlated with geotechnical and geomorphological data together with post-earthquake ground deformation maps in order to assess the factors affecting deformation. Seven deformation modes are introduced and characterised in this chapter.

## 5.2 OBSERVED STOPBANK DEFORMATION MODES

The seven observed stopbank deformation modes are summarised in Table 10 and the extent of these occurrences have been indicated on the maps in Figure 32 for the Waimakariri, Eyre, Cust (WEC) system and Figure 33 for the Avon River system.

As aforementioned, emergency stopbanks were constructed along the Avon River due to imminent risk of flooding as a result of spring tides. This meant that geotechnical damage data was not collected in this area and the evidence of the deformation modes has been obscured by the temporary repairs to the stopbanks. In this area, damage photographs and aerial photographs were inspected to replace site visits.

**TABLE 10: SUMMARY OF STOPBANK DEFORMATION MODES**

Deformation Mode	Description	Cause of Deformation	Total Length (km)	
			WEC	AVON
LIQUEFACTION-INDUCED DEFORMATION MODES				
DM1-BC	Bearing Capacity Failure	Severe liquefaction impact	1.6	0
DM2-MCCS	Minor Central Crest Settlement	Low liquefaction impact	1.4	0
DM3-S	Slumping	Partial loss of stability adjacent to a free face	4.3	1.5
DM4-LS	Lateral Stretch / Foundation Extension	Lateral stretch of foundation soils	2.9	6.3
DM5-DS	Differential Settlement	Low liquefaction impact	3.6	3.0
SLOPE STABILITY DEFORMATION MODES				
DM6-RD	Rotational Deformation	Sliding along defined deformation plane	0.3	0.0
ENGINEERED STRUCTURES				
Damage to Engineered Structures				
DM7-EF	a) Outwards rotation of the gabion basket, b) Collapse of the gabion basket, c) Settlement or spread of materials behind the gabion with no evidence of gabion damage, d) Damage to the reinforced concrete wall, e) Damage to the rock gravity wall.		0.1	5.4
TOTAL LENGTH OF DAMAGE			14.2	16.2
TOTAL SURVEYED LENGTH			18.7	30.0

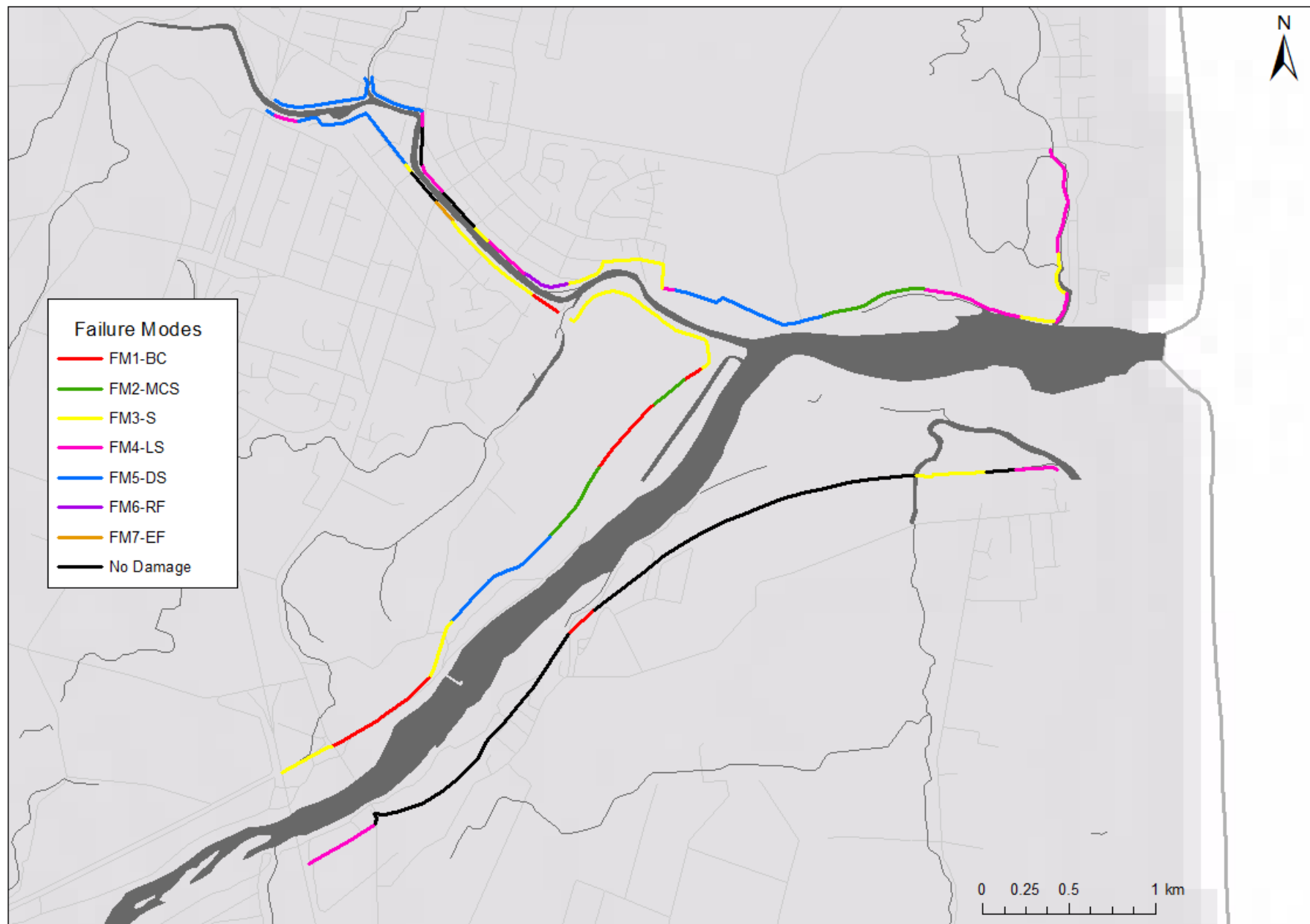


FIGURE 32: WEC SYSTEM STOPBANK DEFORMATION MODES

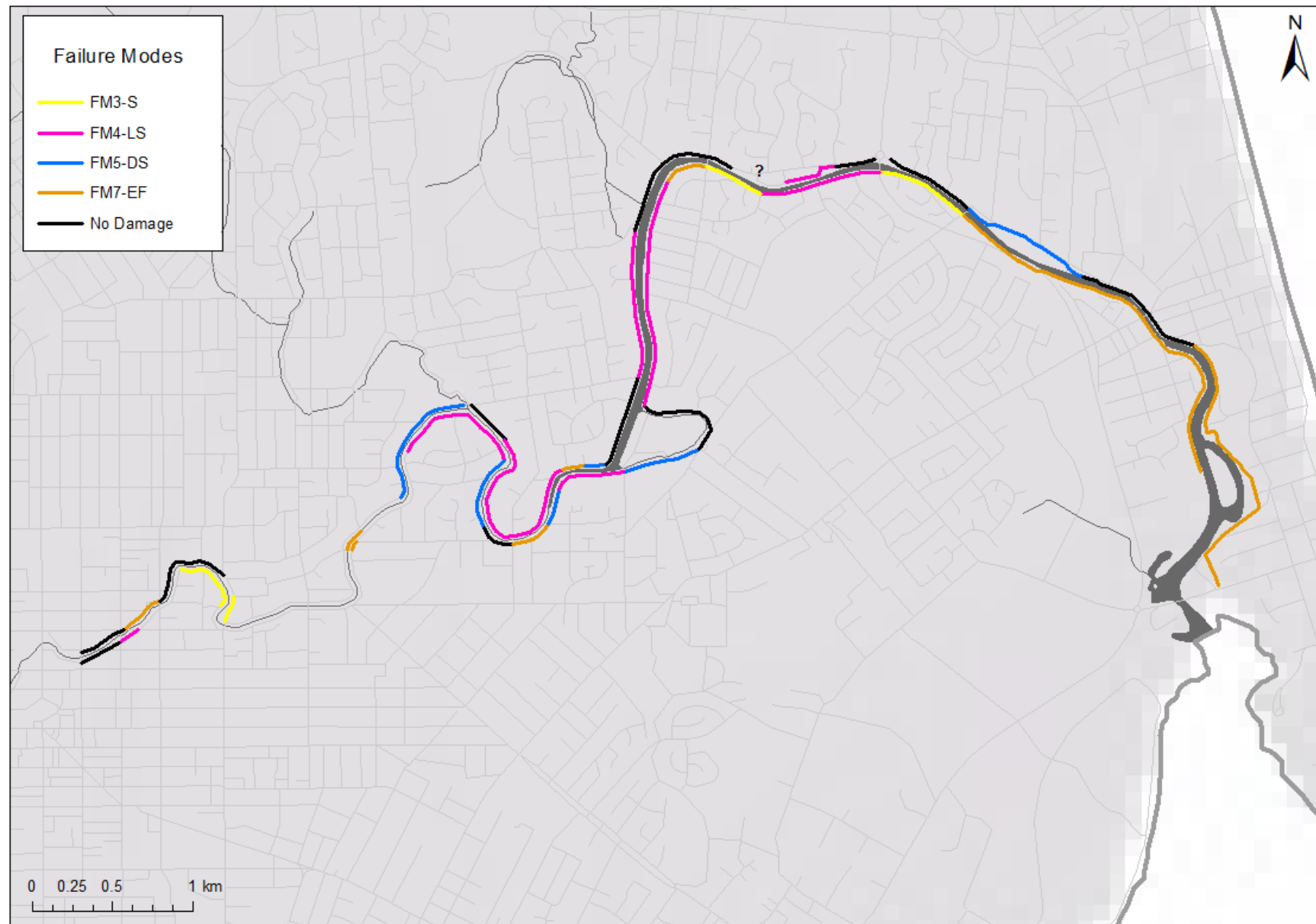


FIGURE 33: AVON RIVER STOPBANK DEFORMATION MODES

## 5.3 LIQUEFACTION-INDUCED DEFORMATION OF STOPBANKS

### 5.3.1 LIQUEFACTION AND LATERAL SPREADING

Earthquake liquefaction is the process by which saturated, unconsolidated soil suddenly loses its strength as a result of ground shaking during an earthquake. When cohesionless soils are saturated, and rapid loading (ie. Seismic) occurs under undrained conditions, the tendency for densification causes excess pore water pressures to increase and effective stresses to decrease. As a consequence, the soil essentially loses its strength, which can result in high volumetric strains and associated ground deformation. These ground deformations take various forms and are often excessive, non-uniform and result in large permanent vertical displacements (settlement), substantial ground distortion and liquefaction ejecta comprising sand, silt and/or water covering the ground surface.

Soil liquefaction occurs in granular soils such as sands, gravels and non-plastic silts. Looser soils are more susceptible to liquefaction as they have more voids in their inherent structure. When shaken they show large tendency for densification (contraction), which in turn leads to rapid excess pore water pressure and eventual liquefaction. Conversely, very dense soils show a lower tendency to densify and hence produce low excess pore water pressures; therefore they are less susceptible to liquefaction.

Lateral spreading involves lateral movement and extension of a soil mass combined with a general subsidence of the fractured mass into softer underlying materials. It is the result of liquefaction and typically occurs in sloping ground or where a free face is present (ie. Waterways). If no free face is present, liquefaction can still occur if there is a slope in the ground will create a bias in the cyclic loads acting on the soil mass during earthquakes which will drive the soil to move in the down-slope direction. Lateral spreading commonly results in large cracks and fissures in the ground.

In areas of Christchurch and Kaiapoi affected by lateral spreading as a result of the 2010 – 2011 Canterbury earthquakes, the residual slope of the land affected by spreading was often only about 2 – 3 degrees indicating very low residual strength of the liquefied soils (Cubrinovski and McCahon, 2011). A simplified analogy of liquefied soil is that it behaves like a viscous liquid (Towhata et al., 1991); liquid flowing down a sloping surface will not stop until the head is equilibrated.

During earthquakes, soil layers are subjected to seismic loading consisting of cyclic motion caused by numerous shear (S) waves, dilatational or pressure (P) waves, and surface (Rayleigh and Love) waves, which result in ground motion. The ground motion at the site will depend on the characteristics of the soil layers. Liquefaction and in some cases lateral spreading occurs when the shear stress required for static equilibrium (the static shear stress) is greater than the shear strength of the soil in its liquefied state. As the seismic waves arrive in the sub-surface soil (including the stopbank material), the soil layers may deform, either due to liquefaction and/or liquefaction-induced lateral spreading, or due to strain softening of materials with a low shear strength.

Figure 34 depicts examples of liquefaction-induced lateral spreading as defined by Seed et al. (2003). These illustrate the typical manifestation of lateral spreading in different ground geometries.



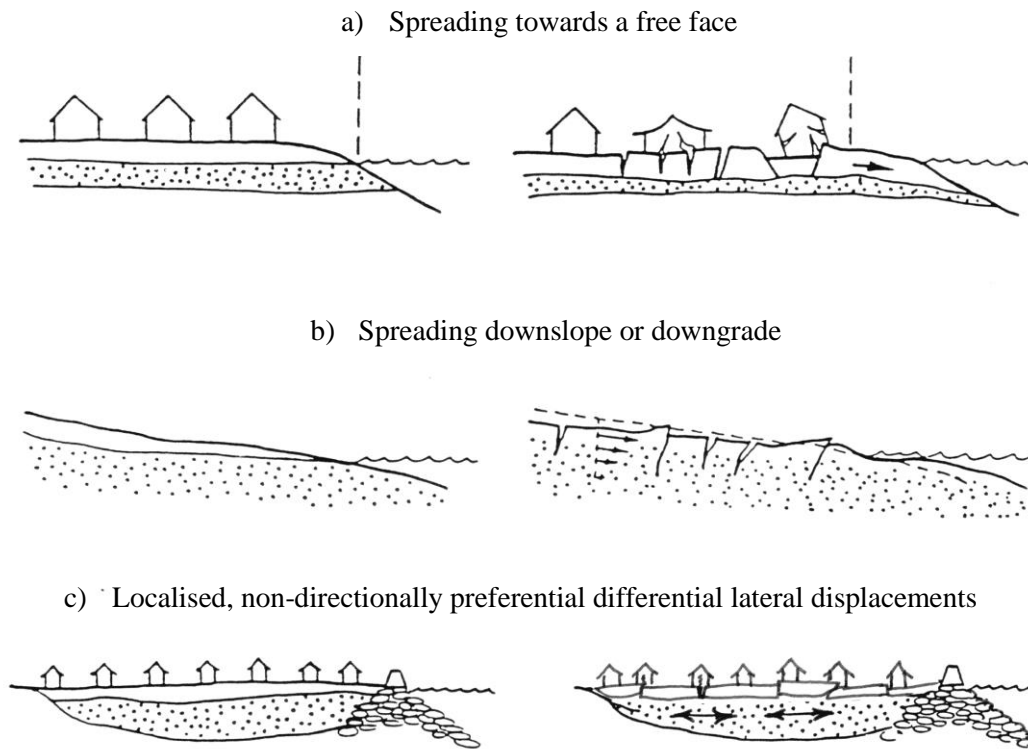


FIGURE 34: SCHEMATIC EXAMPLES OF DEFORMATION MODES OF 'LIMITED' LIQUEFACTION-INDUCED LATERAL SPREADING

The process of spreading within backfill behind retaining walls is similar, whereby large ground shaking displaces the retaining structure outwards (e.g. towards a waterway), which is then followed by lateral spreading within the backfill.

### 5.3.2 INITIAL STRESS STATE OF THE STOPBANK AND NATIVE SOILS

The distribution of principal stresses beneath a stopbank prior to ground shaking are illustrated in Figure 35 (Huang et al., 2008). Higher principal stresses occur below the stopbank with maximum stresses near the center directly beneath the stopbank due to the added stopbank weight. An example assessment of stresses beneath a stopbank and their effects on pore water pressure development and consequent deformation was undertaken by Huang et al. (2009). They showed that the shear stresses significantly increase below the toe of the stopbank, which is associated with the rotation of the principal stresses. During shaking, the level ground free field (at some distance from the stopbank) exhibits simple shear mode deformation with zero lateral strain. In many “real-life” situations there is also the influence of the natural geometry of the slope towards the river. The foundation soils beneath the stopbank and adjacent to it do not have such lateral constraints in the deformation. The three conditions that distinctly influence the dynamic response of the ground and consequent ground deformation are:

1. Initial shear stresses,
2. Laterally unconfined deformation, and
3. Gravity loads imposed by the stopbank.

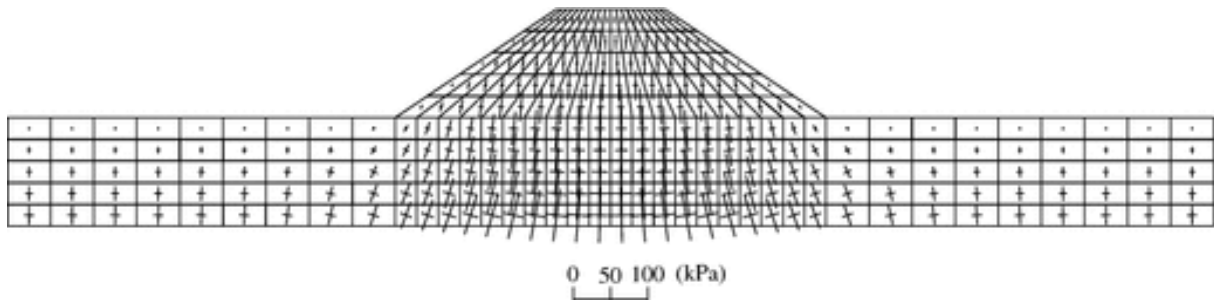


FIGURE 35: DISTRIBUTION OF PRINCIPAL STRESSES WITHIN THE STOPBANK AND UNDERLYING FOUNDATION SOILS PRIOR TO EARTHQUAKE LOADING (HUANG ET AL., 2008)

### 5.3.3 PORE WATER PRESSURE

The large pore water pressures created within the soil mass during liquefaction are in excess of equilibrium pressures, thus triggering flow of water towards the ground surface. These high pore water pressures will carry soil particles towards the ground surface and form liquefaction ejecta on the ground surface.

Pore water pressure distribution is a primary factor in the final deformation pattern of the stopbank. An example of this is shown in Figure 36 with results from numerical analysis based on the effective stress (Huang et al., 2009). The seismic loading induces a typical pattern of liquefaction response of the foundation soil, with excess pore pressure ratios directly beneath the embankment approaching 1.0 resulting in no effective stress after about 30 seconds, and remaining at this level thereafter. Fully liquefied zones are characterised by an excess pore water pressure ratio higher than 0.9 (Ozutsumi et al., 2002). According to analysis undertaken by (Huang et al., 2008), depicted in Figure 37, it can take 2 to 6 seconds for the excess pore water pressure to reach its maximum value, and therefore liquefaction and its resulting damage does not occur immediately after the earthquake starts. The liquefaction caused by the increase in pore pressure may cause lateral spreading towards the free field, with larger displacements in soils higher in the soil column compared to soils at depth. The migration of the liquefied soils combined with the deformation of the stopbank itself causes settlement of the stopbank crest, which continues to deform until the full dissipation of the excess pore water pressure.

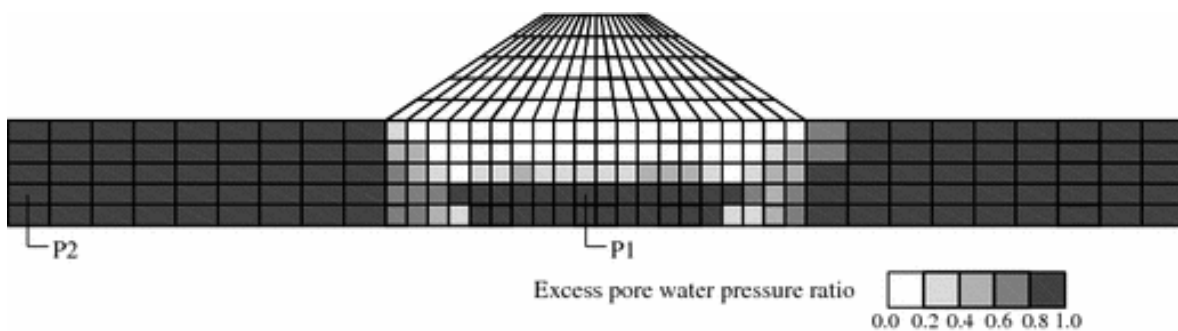
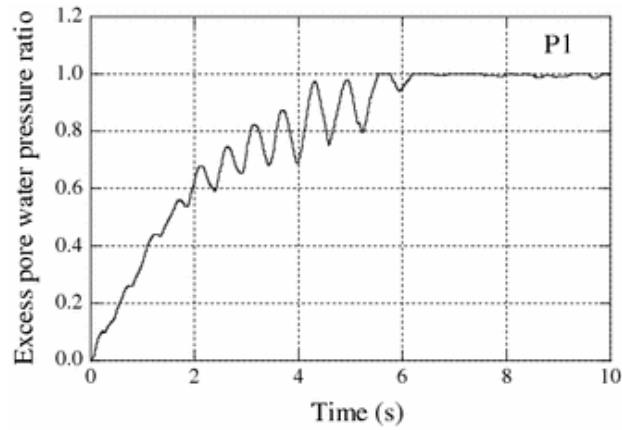
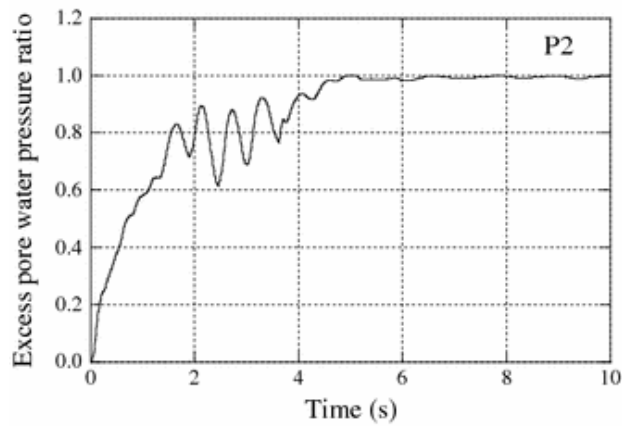


FIGURE 36: EXCESS PORE WATER PRESSURE RATIO OF A STOPBANK AT THE END OF AN EARTHQUAKE (HUANG ET AL., 2008)



**(a) P1, below the embankment centre.**



**(b) P2, in the free field.**

**FIGURE 37: EXCESS PORE WATER PRESSURE VS. TIME DURING AN EARTHQUAKE A) BELOW AN EMBANKMENT AND B) WITHIN THE FREE FIELD (HUANG ET AL., 2008)**

#### 5.3.4 EFFECT OF SOIL PROFILE ON STOPBANK DEFORMATION

The deformation of a stopbank is sensitive to soil parameters governing the dynamic response of the subsurface and stopbank soils including the development of excess pore water pressures, and the resulting liquefaction together with cyclic softening of cohesive soils. Detailed experimental analysis undertaken by (Ozutsumi et al., 2002) indicates that cohesive soil layers interbedded with liquefiable sand layers beneath a stopbank can be a primary factor for reducing the liquefaction-induced deformation of the stopbank. This is consistent with a study suggesting a non-liquefiable surface layer (crust) at the surface may prevent the expression of liquefaction occurring at depth (Ishihara, 1985b). Figure 38 shows the required thickness of surface crust required to prevent surface expression of liquefaction for various liquefiable layer thicknesses. A thicker crust will result in less liquefaction damage at the surface.

In some cases, crest settlement is caused by bearing capacity deformation of the liquefied foundation soils, as the stopbank ‘sinks’ into the liquefied soils beneath. This large downward movement of the stopbank into the underlying liquefied soils displaces the foundation soils laterally but not necessarily symmetrically as deformation will preferentially occur in a down slope direction towards an open face (or point of lesser lateral resistance). This adds another degree of variability to the final deformation pattern of the stopbank.

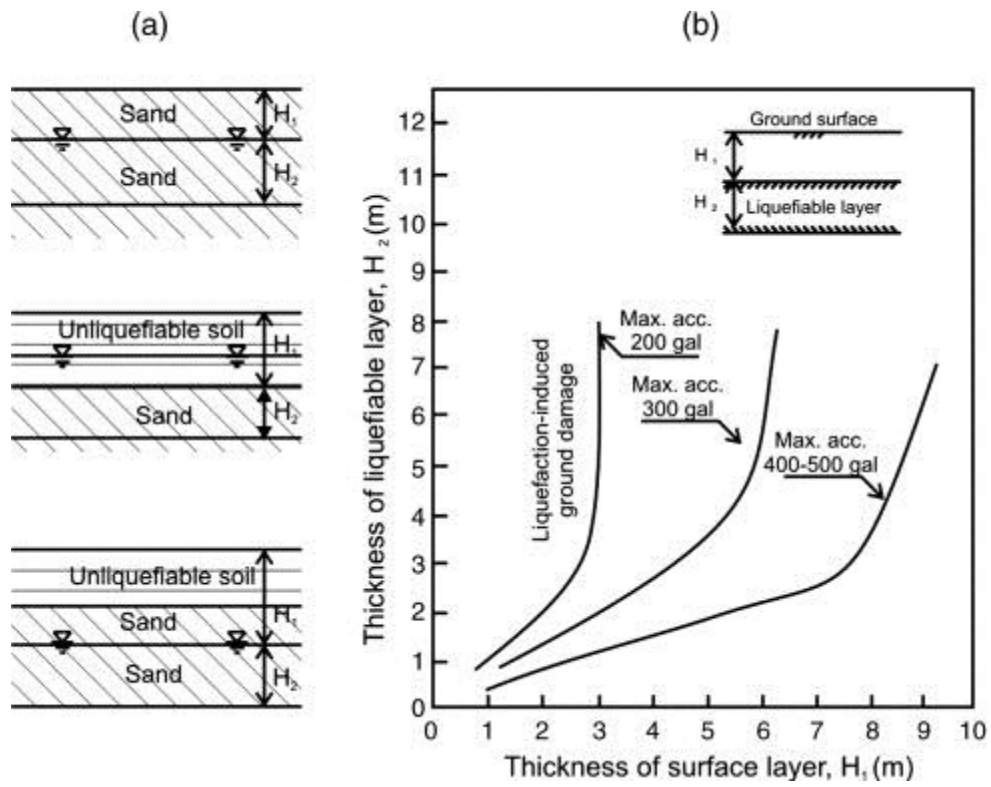


FIGURE 38: BOUNDARY CURVES RELATING THICKNESS OF A NONLIQUEFIABLE SURFACE LAYER TO THICKNESS OF THE LIQUEFIED ZONE, AS A FUNCTION OF PEAK EARTHQUAKE ACCELERATIONS REQUIRED TO INDUCE VENTING OR GROUND RUPTURING AT THE SURFACE (ISHIHARA, 1985).

### 5.3.5 DEFORMATION MODE 1 – BEARING CAPACITY DEFORMATION

Figure 39 depicts a deformation pattern where slumping of the stopbank has occurred as a result of both settlement and downslope lateral movement. Large cracks and fissures are present due to the loss of bearing capacity due to liquefaction within the foundation soils. An example of this is shown in Figure 40. This deformation mode has occurred along approximately 1.6 km of the WEC system, but did not occur along the Avon River, which is discussed further below.

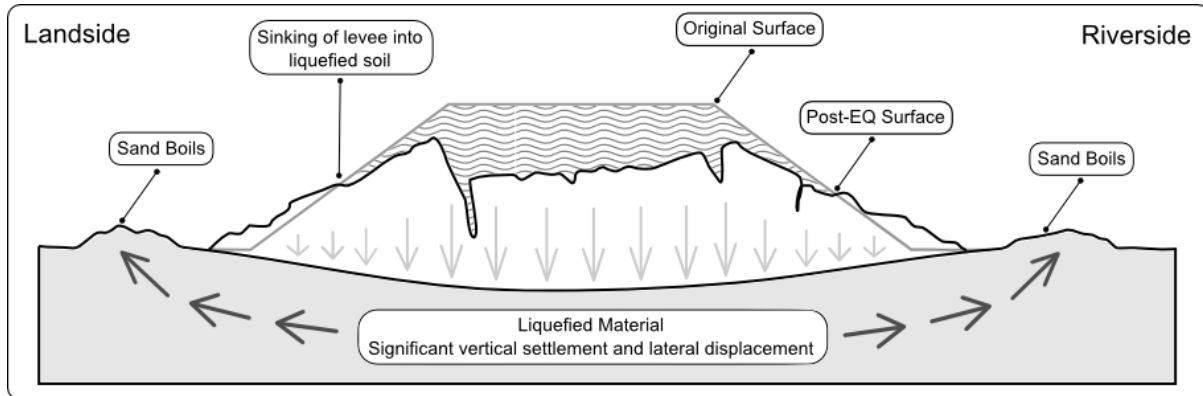


FIGURE 39: DEFORMATION MODE 1 - BEARING CAPACITY DEFORMATION



FIGURE 40: EXAMPLE OF BEARING CAPACITY DEFORMATION (DM1-BC). PHOTO PROVIDED BY ENVIRONMENT CANTERBURY, 2011.

### ***CHARACTERISTICS OF DEFORMATION***

Common characteristics of this deformation mode are the nearly complete loss of the original shape of the stopbank, significant loss of height, large fissures, cracks and ground deformation and extensive sand boils on either side of the stopbank are expressed at the surface in the foundation soils. Lateral spreading, settling and cracking of the stopbank batters results in an overall shape where the central portion of the stopbank (ie. the crest) has sunk more than the batters.

This particular deformation mode was arguably one of the most dramatic in terms of visual damage and extent of cracking, and repair works were undertaken almost immediately following the 4 September 2010 earthquake event. Therefore, the crest surveys undertaken to estimate the post-earthquake deformation cannot be used to determine the extent of damage as the surveys were undertaken post remediation. Photographs provided by Environment Canterbury following the 4 September 2010 earthquake indicate settlement greater than 1.5 m in places and vertical LiDAR suggest 0.5 m to greater than 1.5 m vertical settlement.

### ***DEFORMATION MECHANISM***

The mechanism for this deformation mode is bearing capacity failure that results in significant settlement and loss of integrity of the entire stopbank. The vertical settlement in the liquefied foundation soils are the principal cause for deformation and lateral spreading displacements are of secondary importance. Adachi and Oka (1997) summarise the processes involved with deformation due to liquefaction of the foundation soil. The deformation of the stopbank is caused by a loss of strength at the base of the stopbank, and the lateral and vertical deformations are caused by distribution of the excess pore water pressures of the liquefied layer. The crest of the stopbank often settles more than the adjacent batters as the vertical loads are higher beneath the crest. Once the shear resistance of the ground is lost due to liquefaction, the tangential stress between the boundary of the stopbank base and the liquefied soil layer becomes zero. As the excess pore water pressure dissipates in the liquefied layer, the stopbank settles relative to the magnitude of vertical principal stress at that point (ie. The stresses reduce towards the stopbank toe).

### ***FACTORS AFFECTING DEFORMATION***

At each of the damaged stopbank locations surface expressions of liquefaction (in the form of ejecta) were present adjacent to the stopbanks in the foundation soils. From this, one can conclude that the primary factor affecting the deformation at these locations is the severity of liquefaction of the foundation soil. This theory is supported by the following information:

- Aerial photographs following the 4 September 2010 and 22 February 2011 earthquakes (CGD0100) indicate that the adjacent ground suffered from extensive liquefaction ejecta.
- Historical maps indicated that two of the locations are underlain by the 1985 Waimakariri River Channel. According to Wotherspoon et al. (2011) the areas underlain by old river channels in the Kaiapoi area were subject to some form of liquefaction, and in most areas liquefaction and/or lateral spreading were significant.
- Subsurface geotechnical investigation (CPT-KGA-01) from CGD, located immediately adjacent to the damaged stopbank at Stewarts Gully, indicated liquefiable materials throughout the majority of the top 6.5 m of the soil column, beneath the water table (Figure 41). These materials are:

- Predominantly free draining, compressible soils, with  $I_c$  values of 2 to 3 and a very low cyclic resistance ratio, correlating to inferred soil behaviour types of interbedded silty sand, sandy silt and silt.
- Very soft to soft and very loose to loose materials, becoming medium dense below 6.5 m.
- Young alluvial river channel deposits.
- Liquefaction resistance of foundation soils calculated from this CPT is low ( $FOS < 0.7$ ) directly beneath the water table, in the bearing stratum of the stopbank. Depending on the depth of the water table this provides the ideal conditions for the stopbank to punch through the thin crust into the weak liquefiable materials below (ie. bearing capacity deformation).
- LiDAR mapping (CGD0600) indicates a vertical crest displacement between 1 m and 1.5 m for the 2010-2011 Canterbury earthquakes. The majority of this settlement occurred following the 4 September 2010 earthquake, where the stopbank settled by 0.5 m to 1.5 m.

The secondary factors affecting deformation at these sites are:

- Stopbank geometry; at the three locations where this deformation mode has occurred the stopbank was large, with a crest width of 5 to 6 m.
- Setback from the river; in all locations the stopbank is setback from the river by a minimum of 80 m, excluding one location where the levee is setback by 10 m. If the stopbank is too close to the river the behavior may become more like FM3-S (Slumping).

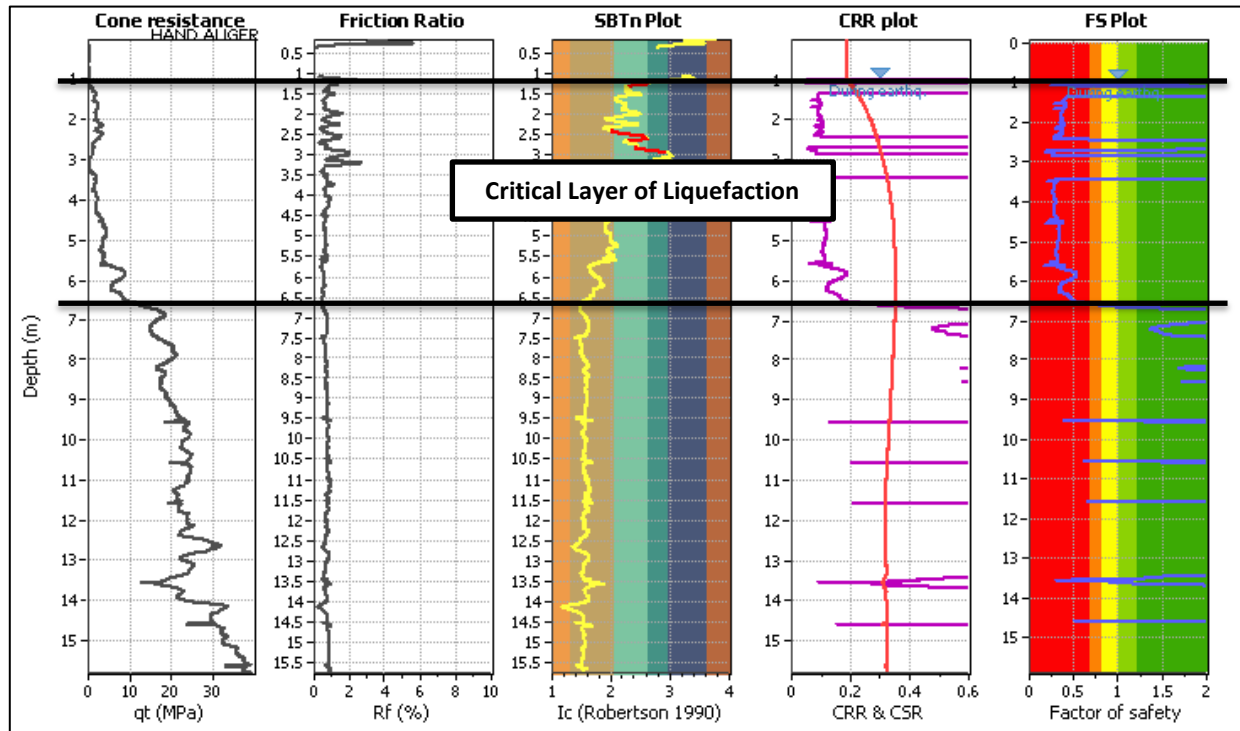


FIGURE 41: CPT PLOTS FOR CPT-KGA-01 (CGD, 2012)

### 5.3.6 DEFORMATION MODE 2 – MINOR CENTRAL CREST SETTLEMENT

In some locations the stopbank has behaved in a similar fashion to Deformation Mode 1, except that the crest settlement is minor (Figure 42). This deformation mode has been characterised as deformation Mode 2, minor crest settlement, and affected approximately 1.4 km of the WEC system. Deformation mode 2 was not observed along the Avon River.

#### ***CHARACTERISTICS OF DEFORMATION***

This deformation mode is characterised by minor (less than 20 mm wide) cracks at the shoulder of the stopbank and negligible loss of crest. The cracks do not arc and run parallel with the crest as depicted in Figure 43. This may or may not be associated with liquefaction ejecta at the surface. According to LiDAR this deformation mode occurred for settlements in the range of 0.4 m to 1 m. It is expected that a large amount of this settlement is total rather than differential. The differential settlement is more likely to translate to surface deformations. This is broadly consistent with crest surveys undertaken along the Kaiapoi River, which indicate up to 0.5 m of differential settlement along the length of this deformation mode.

#### ***DEFORMATION MECHANISM***

Adachi and Oka (1997) discuss the interaction between stopbank deformation and liquefaction of underlying foundations based on occurrence of cracks in the stopbank. The deformation of the stopbank, caused by soil liquefaction is induced by the loss of tangential stress at its base. As the results of the change of boundary condition, active Rankine state is developed in the stopbank which causes cracks in the stopbank even when no deformation occurs within the liquefied layer. The first crack will appear at the point where the active Rankine triangle state reaches the stopbank slope surface. This location of the crack will change its position with stopbank material properties and geometry. The location of the moves towards the stopbank toe as the slope angle increases.

#### ***FACTORS AFFECTING DEFORMATION***

This stopbank deformation is related to liquefaction and generally occurs where the stopbank is setback from the river and lateral spreading is less. Deformation Mode 1 cannot develop into bearing capacity deformation because this is a low liquefaction-impact mode. In order for the bearing capacity deformation mode to develop a sufficient thickness of liquefiable materials is required. The stopbank also needs to be large enough so that the effective stresses below the stopbank cause the stopbank to break through the crust into the liquefiable materials.



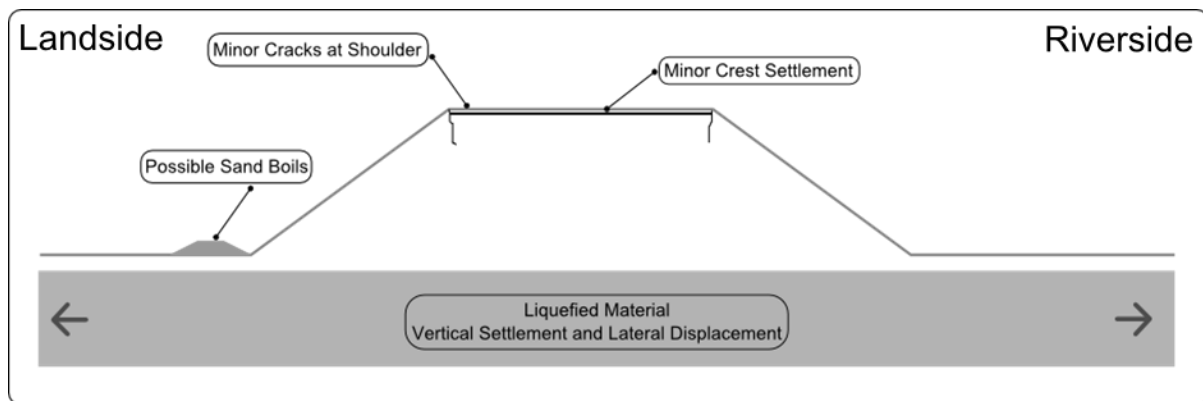


FIGURE 42: DEFORMATION MODE 2 - MINOR CENTRAL CREST SETTLEMENT



FIGURE 43: EXAMPLE OF MINOR CREST SETTLEMENT (DM2-MCCS). PHOTO PROVIDED BY ENVIRONMENT CANTERBURY.

### 5.3.7 DEFORMATION MODE 3 – SLUMPING

An example of slumping deformation that occurred as a result of liquefaction of the foundation soils adjacent to a free face is depicted in Figure 44. This deformation mode occurred along approximately 5.8 km of stopbank in total, 4.3 km along the WEC system and 1.5 km along the Avon River.

#### ***CHARACTERISTICS OF DEFORMATION***

The characteristics of this deformation mode are the movement of materials laterally and settled vertically (slump). This is accompanied by the rotation of the crest if the slump extends a significant distance into the stopbank, then cracking throughout the stopbank of varying widths and bulging at the toe will be apparent as shown in Figure 45. The degree of damage is highly variable but in some cases the cracks are up to 1 m deep (RILEY, 2010a). LiDAR maps indicate that the settlement of the crest associated with this mechanism ranges between approximately 0.5 m and 1.0 m. The majority of the cases involve multiple local failures and slumps of the river side slope, which is most likely due to weaker soils and a steeper river gradient. The density of geotechnical information is not enough to confirm the strength of the soil. In some cases, there has been no significant deformation due to settlement of the crest, but the riverside batter has behaved like a rotational deformation causing large arc structures.

#### ***DEFORMATION MECHANISM***

This deformation is due to the materials moving and settling horizontally and vertically (slump), due to liquefaction and lateral flow of the foundation ground. This process may not necessarily result in ground cracking but can result in large deformation of the foundations and at least a partial loss of bearing capacity causing biased movement and permanent displacement towards the free face. This may be due to removal of the toe or sliding along multiple deformation planes.

#### ***FACTORS AFFECTING DEFORMATION***

Slumping generally occurs in stopbanks adjacent to the river, or a marshland, as the mechanism generally requires large lateral movements of the liquefied foundation towards a free face or loss of soil volume and potential bearing support in the foundation soils. This deformation mechanism is associated with liquefaction of the foundation and in the majority of cases occurs where liquefaction ejecta is present, with significant thickness of liquefiable materials from the water table to depths of 6.5 m to 10 m.

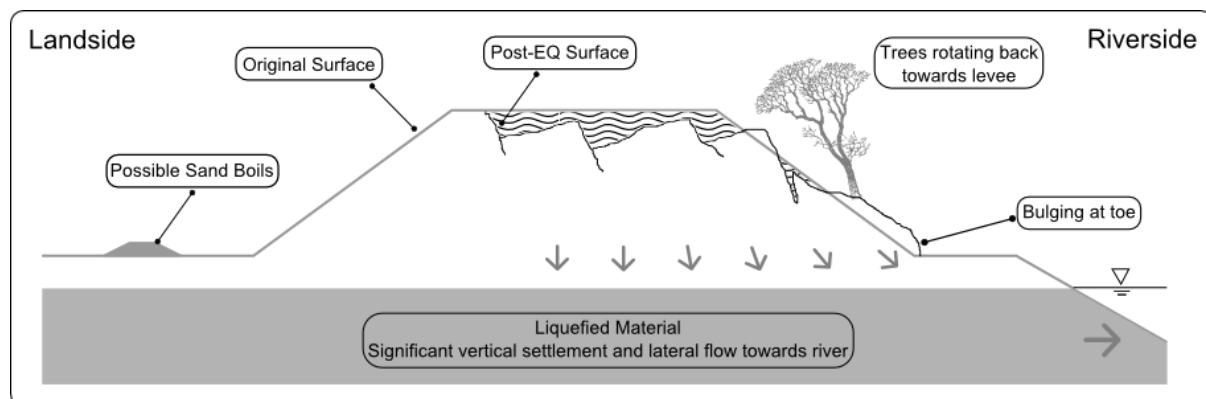


FIGURE 44: DEFORMATION MODE 3 - SLUMPING





**FIGURE 45: EXAMPLES OF SLUMPING DEFORMATION (DM3-S). PHOTO 1 (KAIAPOI SOUTH BANK) PROVIDED BY ENVIRONMENT CANTERBURY; PHOTO 2 (AVON RIVER SOUTH BANK) PROVIDED BY GHD.**



### ***VARIATION IN FOUNDATION MATERIAL TYPES***

In one location, the foundation of the stopbank has split longitudinally in to two different material types, as a result of narrowing of waterways along Raven Quay, with part of the stopbank constructed on the old river bank and part on the old river. This area is outlined in Figure 46 and the damaged length of river is shown in Figure 45 – Photo 1. The part of the stopbank constructed on the reclaimed or narrowed channel has slumped into the old river. The other half of the crest and the landside batter that have been built on the old riverbank have performed well. This differential performance illustrates the wide variety in foundation conditions adjacent to the rivers that may not necessarily be picked up through geotechnical investigations due to a lack of density of geotechnical investigations, but are understood due to the nature of reclaiming land along river edges.



**FIGURE 46: AERIAL PHOTO INDICATING 1865 KAIAPOI RIVER BANKS, RED BOX INDICATES ZONE OF PARTIAL SLUMPING.**

#### **5.3.7.1. CORNER SLUMPING**

Occurring only on bends in the stopbank, both gentle and sharp, corner slumping has occurred along approximately 370 m and 590 m of the WEC system and the Avon River, respectively. Corner slumping is caused by slumping and has similar deformation mechanisms and characteristics of deformation to slumping. These corner slumps produce transverse cracks reflecting the particular geometry and the associated deformational displacement pattern can be a high risk for medium to long term stopbank performance due to an increased vulnerability of seepage.

### ***CHARACTERISTICS OF DEFORMATION***

A rotational arc structure, which is more evident in plan view, occurs at the bend in the stopbank and is accompanied by radiating cracks throughout the stopbank and in some cases through the natural soils (Figure 47). The termination of the arc deformation is often bounded by transverse cracks through the stopbank. The degree to which the slide displaces varies considerably. A similar pattern occurred in the native ground following the 2010-2011 Canterbury earthquakes along the Avon River (across from Admirals Way), where the lateral spreading cracks not only behaved like an arc in the stopbank but also were reflected in the pattern of the lateral spreading cracks in the ground behind the stopbank.

### ***DEFORMATION MECHANISM***

The forces driving this mechanism can be compared to that of an arch dam. An arch dam is supported by the hydrostatic pressure pressing against the arch, which compresses and strengthens the structure and at the same time pushes it into its foundations. The hydrostatic pressure of the water pressing against the earth performs the same function as the mass of earth between the river and the stopbank, or, the water in the river, if levels are high enough. When the earthquake occurs and the foundation soil loses its strength the active forces pushing the stopbank outwards are greater than the resistive forces, which cause the stopbank to fail. Even a small outward movement toward the river will relax the stresses in the ground and cause cracking near the surface which will gradually migrate landward in subsequent angles from the river.

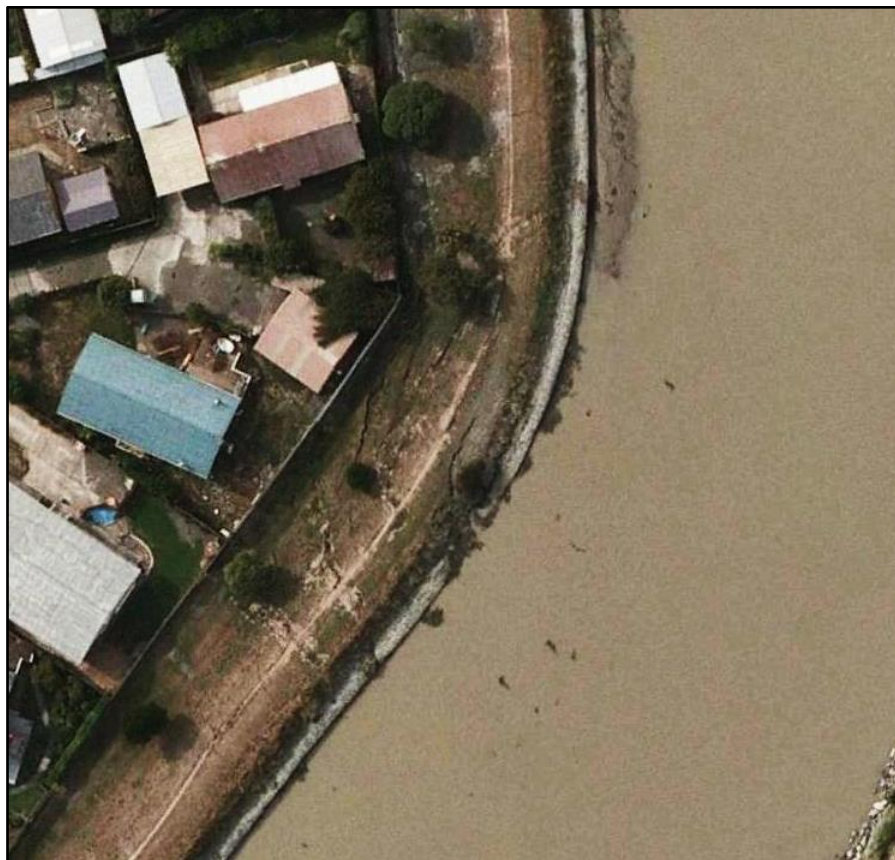


**FIGURE 47: PLAN VIEW OF CORNER SLUMPING DEFORMATION ON THE AVON RIVER, APPROXIMATELY 1.3 KM NORTH OF AVON-HEATHCOTE ESTUARY MOUTH (CGD 0100)**

### 5.3.8 DEFORMATION MODE 4 – LATERAL STRETCH / FOUNDATION EXTENSION

Stopbank deformation associated with lateral stretch, which does not result in Deformation Mode 3 is generally characterized by longitudinal cracks throughout the stopbank profile (crest and batters). Lateral stretch (foundation extension) is a deformation mode that varies significantly in severity and nature and results in longitudinal cracking through the stopbank, typically mirroring the degree of lateral stretch in the native soil. A typical lateral stretch pattern is illustrated in Figure 48. This deformation mode was quite common affecting 2.9 km of the WEC system and 6.3 km of the Avon River.

#### ***CHARACTERISTICS OF DEFORMATION***

Lateral stretch is predominantly characterised by longitudinal cracking throughout the crest, batters and adjacent ground of the stopbanks, as shown in Figure 49. The width of the cracks varies significantly although the largest cracks are generally at the toe of the stopbank, which indicates lateral stretch in the native soil adjacent to the stopbanks. The cracks on the stopbank can range in width from minor hairline cracks to significant parallel cracks up to 200 mm wide (RILEY, 2010a), with larger cracks in the native soils adjacent (CGD0100).

There are a variety of ways the ground cracks manifest themselves in the stopbank. The cracks can widen and narrow with depth. They do not form a rotational arc surface and run parallel with the crest of the stopbank for their entirety. The cracks occur on both the riverside and landside batter. This deformation mode may or may not be accompanied by a loss of crest, although any loss of crest is minor. In some areas very small scale slumps occur within the stopbank due to cracks being close together and the stopbank losing its structural integrity. In general where lateral spreading is the primary mechanism for deformation, the integrity of the stopbank is preserved and the cracks are not too deep.

#### ***DEFORMATION MECHANISM***

As previously described, lateral spread is an extension of a soil mass, combined with a general subsidence of the fractured mass into softer underlying materials. Once sufficient pore water pressures are generated due to earthquake shaking, flow of the liquefied materials begins to occur downslope towards a free face. The lateral spread causes deformation including ground cracking, which in some cases migrates up through the stopbank to be expressed at the surface.

Test pitting undertaken by Riley Consultants (RILEY, 2010a) indicates that cracks as large as 100 mm wide at the surface generally reduced to zero by 2.5 m depth, however some cracks remained as wide as 50 mm down to a minimum depth of 3 m, indicating that the cracks continued into the subsurface ‘natural’ soils. Personal communications with Ian Heslop indicate that these cracks would often widen with depth, whilst appearing quite small at the surface. This indicates that the stopbank stretches more at the base while the crest stays reasonably intact. The majority of the cracks, as recorded in test pits undertaken by RILEY, indicate that the cracks either generally stay the same width or decrease in width towards the base; the decreasing width may be due to some external rotation of the separate blocks between the cracks. It is expected that at the water table the cracks will terminate.



This stopbank deformation must be underlain by liquefiable materials for lateral stretch to occur. This deformation mode does not result in slumping as the stopbank is generally setback sufficiently from the river. Bearing capacity deformation and minor crest settlement have not occurred for the following reasons:

- 
- Diagram illustrating the effects of liquefaction on a riverbank. The diagram shows a cross-section of a riverbank with a crest. Labels include 'Landside' on the left, 'Riverside' on the right, 'Original Surface' (the top line), 'Post-EQ Surface' (the lower line after settlement), 'Minor Crest Settlement' (the difference between the two lines at the crest), 'Possible Sand Boils' (indicated by downward arrows from the original surface), and 'Liquefied Material Vertical Settlement and Lateral Displacement' (the area below the original surface). Arrows at the bottom indicate lateral displacement of the liquefied material.

A photograph of a coastal landscape. In the foreground, a dirt path with visible tire tracks runs diagonally across a grassy dune area. The ground is uneven, with patches of green grass and exposed brown soil. To the left, a calm body of water stretches towards the horizon. A line of trees, including tall pines, is visible on the right side of the path. The sky is filled with soft, white clouds.

88

### 5.3.9 DEFORMATION MODE 5 – DIFFERENTIAL SETTLEMENT (DUE TO LIQUEFACTION)

Differential settlement of the stopbank crest is a common deformation mode that occurs both independently and with all of the other deformation modes (Figure 50). This is the most prevalent deformation mode affecting approximately 3.6 km and 3.0 km of the WEC system and the Avon River, respectively.

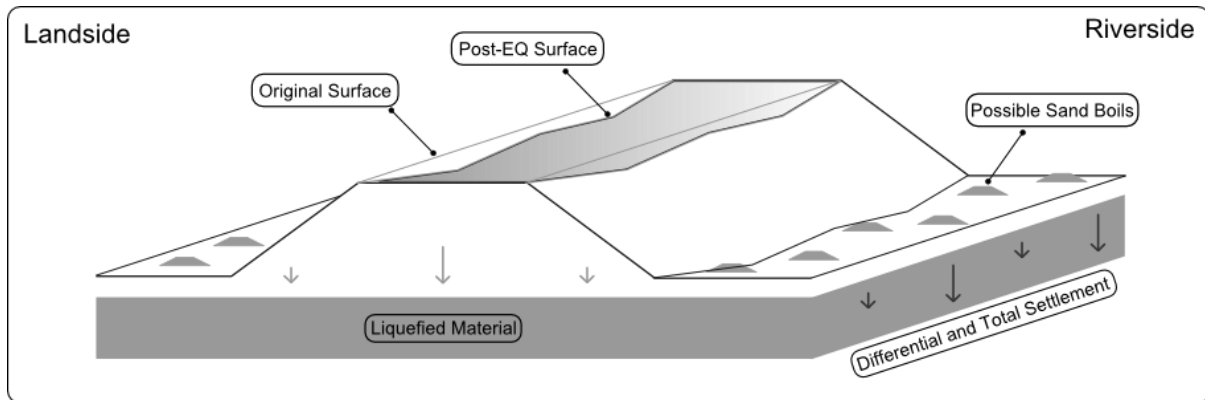


FIGURE 50: DEFORMATION MODE 5 - DIFFERENTIAL SETTLEMENT OF THE STOPBANK



FIGURE 51: EXAMPLE OF DIFFERENTIAL SETTLEMENT (DM5-DS). PHOTO PROVIDED BY ENVIRONMENT CANTERBURY.



### ***CHARACTERISTICS OF DEFORMATION***

Differential settlement along the crest is characterised by a visibly hummocky surface with minor offsets in construction joints of concrete walkways. This deformation mode may not always be visible to the naked eye but can be picked up by topographic surveys. It may or may not be accompanied by sand boils at the toe and in its simplest form is not accompanied by any cracking. According to stopbank crest survey data and LiDAR data (CGD0600) in locations where differential settlement occurred along the WEC system the stopbank crest had suffered total settlement of up to 800 mm and differential settlement of up to 600 mm (for stopbanks approximately 4 m high). Along the Avon River the stopbank system has suffered total settlement and differential settlement of up to 1000 mm and 600 mm respectively (for stopbanks up to 1.5 m high). This shows that the stopbank is mirroring the settlement of the adjacent native soils. The stopbank settlement equals the settlement of the native soils.

### ***DEFORMATION MECHANISM***

This deformation mode has occurred along large portions of the stopbank system as a result of liquefaction of the subsurface soils (shallow and/or deep). Differential settlement commonly refers to the variation in settlement across a single structure, the difference between the highest and lowest point on an initially planar structure post deformation. In this case, the differential settlement refers to the change in vertical elevation between two points along the centerline of the stopbank.

### ***FACTORS AFFECTING DEFORMATION***

Where a non-liquefiable surface layer (crust) is present the surface expression of liquefaction occurring at depth may be reduced or not present at all. The reason that this deformation mode has not developed into DM1-BC, DM2-MCS or DM4-LS is explained by examples depicted in Figure 52 and Figure 53. Figure 52 shows a liquefaction calculation where the majority of the soils in the tested soil column are relatively poorly draining dilative soils. Liquefaction and post-earthquake strength loss are unlikely and no significant observations of settlement occurred. The minor settlements that occurred are due to the thin layers of relatively free draining contractive soils (ie. sands). There may also be an influence of some relatively poorly drained contractive soils where cyclic liquefaction and strength loss depend on soil plasticity, sensitivity and peak strain. Cyclic liquefaction and strength loss likely depends on soil plasticity, sensitivity, peak strain and ground geometry.

Figure 53 is an example where the crust is thick enough to provide some protection against differential settlement caused by liquefaction at depth. Based on the chart by Ishihara (1985b) shown in (Figure 38), the 1.8 m crust would be sufficient to provide protection against the 1.2 m liquefiable layer in an event with a PGA less than or equal to 0.3 g. At this location a PGA of 0.23 g during the M7.1 4 September 2010 earthquake was recorded and hence it is assumed that differential settlement was reduced due to the ability of the capping layer to mitigate most of the effects of the liquefaction, ie. liquefaction has occurred ‘at depth’ resulting in total settlement and some minor differential settlement, but no liquefaction ejecta.

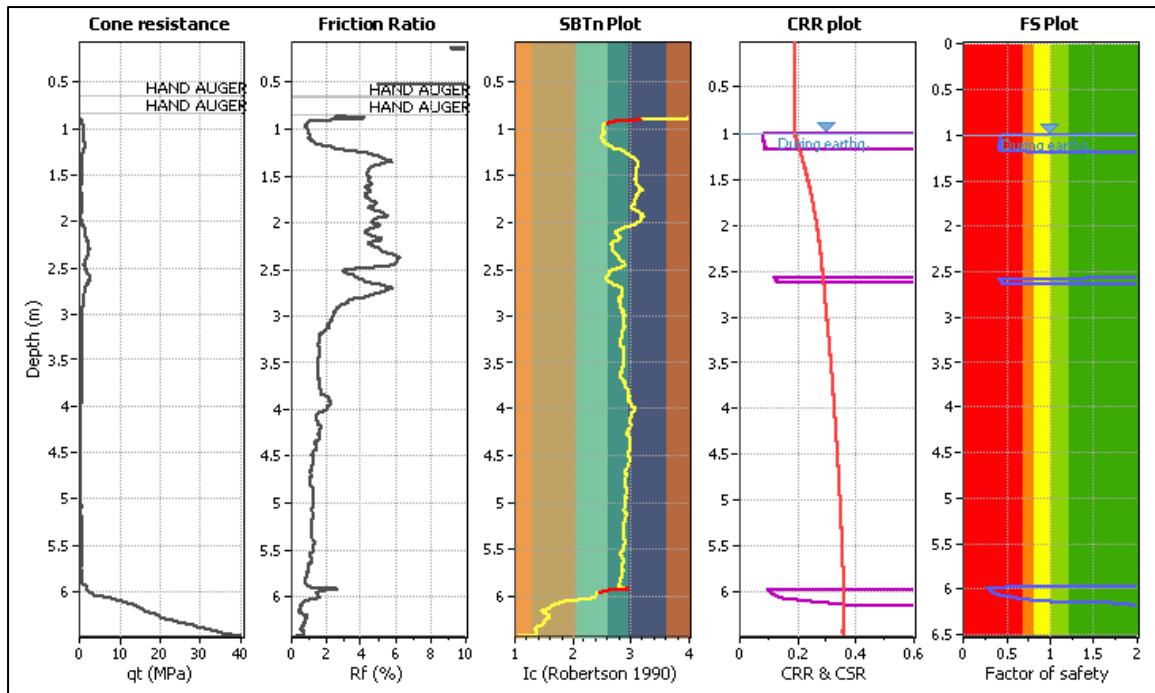


FIGURE 52: CPT\_1337 CLIQ ANALYSIS DEPICTING LIQUEFACTION BEHAVIOUR OF PREDOMINANTLY FINE GRAINED SOILS

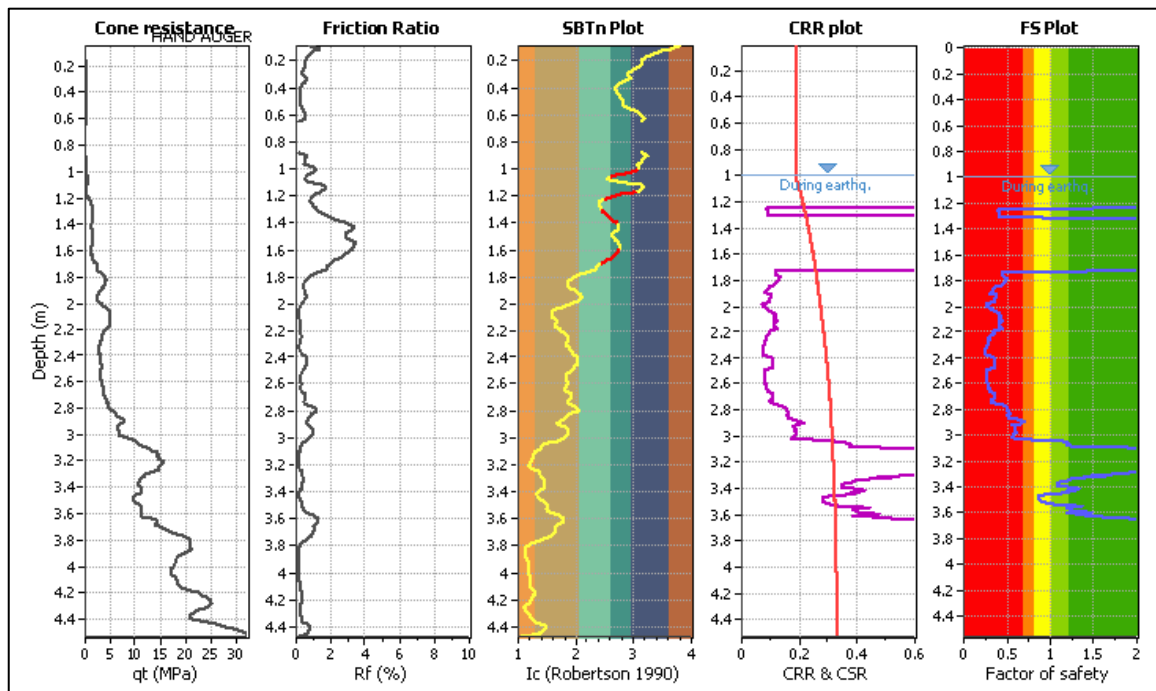


FIGURE 53: CPT\_1341 CLIQ ANALYSIS DEPICTING BEHAVIOUR OF LIQUEFIABLE SOILS WITH A CRUST

## 5.4 DEFORMATION MODE 6 – ROTATIONAL DEFORMATION

Rotational deformation and sliding deformations in general were not significant deformation modes during the 2010 – 2011 Canterbury earthquakes. This is due to the following reasons:

- The majority of post-earthquake deformation was controlled by liquefaction and liquefaction-induced lateral spread.
- There is a lack of soft materials, such as clays, in the Christchurch subsurface stratigraphy that could act as a preferential sliding plane.
- The stopbanks generally are small and / or have shallow batter angles.

This deformation mode occurred in one location (0.3 km) where the effects of the earthquake on the ground were not conclusive. Cubrinovski et al. (2012) indicate that the land beneath this length of the stopbank has been underlain by fill, which is consistent with old river channels in the area, and the stopbanks influenced the lateral spread that occurred at this site.

### ***DEFORMATION MECHANISM***

Rotational failures may occur where cyclic loading due to an earthquake triggers slope instability in the stopbank batter. There are a number of potential mechanisms for triggering a slope deformation in an earthquake and these can vary significantly. Most slope deformations that occur during earthquakes are caused by reductions in the shear strength of the soil that lead to a reduced ability of the soil to resist the driving forces of the soil. In addition, the stability of the slope is reduced for those brief instants when the dynamic forces act in adverse directions. If the cyclic loading causes reduction in soil strength, the effects are even more severe.

In rotational slips the shape of the deformation surface may be a circular arc or a non-circular curve. Circular slips are generally associated with homogeneous, isotropic soil conditions (such as those found in stopbank fill) and non-circular slips are associated with non-homogeneous conditions (such as those found in foundation materials) (Craig, 2004). In this case the deformation is a circular deformation, which is consistent with the description of fill underlying the stopbank.

## 5.5 DEFORMATION MODE 7 – DAMAGE TO ENGINEERED STRUCTURES

Gabion baskets and reinforced concrete flood protection walls are two common flood protection structures along the Avon River. These engineered structures have deformed due to the earthquakes in two key ways: outward rotation and complete collapse, as shown in Figure 54 through Figure 57. Approximately 100 m of the WEC system and 5400 m of the Avon River were affected by this mechanism.

### *CHARACTERISTICS OF DEFORMATION*

Damage to Engineered Structures fall into five categories, including:

- a) Outwards rotation of the gabion baskets,
- b) Collapse of the gabion basket due to the basket breaking,
- c) Settlement or spread of materials behind the gabion baskets with no evidence of gabion damage,
- d) Damage to the reinforced concrete wall in the form of vertical cracks, or
- e) Damage to the rock gravity wall in the form of collapse

In the case of a gabion basket deformation, observation showed that the gabion has either rotated outwards by a maximum of approximately  $10^0$ , has been laterally pushed forwards in to the river by the retained ground, or has collapsed completely in to the river. Where outwards rotation or lateral movement of the gabion basket has occurred, the retained ground showed signs of cracking and slumping into the accommodation space. Where the gabion has suffered minor rotation, the pattern of deformation is similar to the lateral stretch deformation mode (DM4-LS). As accommodation space increases the deformation mode becomes more similar to the slumping deformation mode (DM3-S). Where complete collapse of the gabion has occurred, the retained ground slumped in to the accommodation space.

In the case of an engineered concrete wall, the characteristics of deformation included outwards rotation (by a maximum of approximately  $10^0$ ) and vertical cracks apparent in the retaining wall. The retained ground behaved in the same way as the gabion basket deformation.

### *DEFORMATION MECHANISM*

The outward movement of retaining walls due to liquefaction in the backfill or foundation soils results in ground deformation behind the wall that is often described as “lateral spreading” (Ishihara, 1996). However, the deformations are more correctly associated with lateral earth pressures and performance of the wall. The process of spreading in backfills behind retaining walls is similar to lateral spreading, with large ground shaking first displacing the retaining structure outwards (e.g. towards the waterway), which is then followed by lateral spreading in the backfills. There are two possible causes of deformation for the gabion basket deformation:

- 1) Acceleration induced deformation, caused by high horizontal ground accelerations forcing the basket in to the free face. This is thought to occur where the gabion basket has completely collapsed.
- 2) Liquefaction induced deformation, where the gabion basket foundations and tie backs fail due to loss of strength in the supporting soils. This is thought to occur where the gabions baskets have rotated outwards

### ***FACTORS AFFECTING DEFORMATION***

This deformation mechanism occurs where there are engineered flood protection systems in place. According to the Liquefaction Map (CGD0200) this deformation mode occurred in areas that underwent liquefaction ranging from minor to severe during the 4 September 2010 and 22 February 2011 earthquakes. The Observed Ground Crack Map (CGD0400) indicates that these areas were also subjected to extensive lateral spread adjacent to the river following these two earthquakes.



**FIGURE 54: SETTLEMENT OF GABION BASKET AND SLUMPING OF RETAINED LAND**



**FIGURE 55: SLUMPING OF LAND BEHIND REINFORCED CONCRETE RETAINING WALL, WALL HAS BULGED OUT SLIGHTLY AND THERE ARE MINOR CRACKS**





**FIGURE 56: OUTWARD ROTATION OF GABION BASKET AND ASSOCIATED SLUMPING OF RETAINED LAND**



**FIGURE 57: COLLAPSE OF GABION BASKET AND SUBSEQUENT SLUMPING OF LAND INTO ACCOMMODATION SPACE**



## 5.6 SUMMARY AND CONCLUSIONS

The seven principal stopbank deformation modes that caused damage to the stopbank system during the 2010 – 2011 Canterbury Earthquake Sequence are summarized in Table 11.

Each of these deformation modes incorporates various damage patterns to create its own set of unique characteristics that ultimately indicate the deformation mechanism. The identified damage to the stopbank system shows trends in the damage sustained including longitudinal cracks, settlement of the crest, sand boils at the toe and minor transverse cracking.

**TABLE 11: SUMMARY OF STOPBANK DEFORMATION MODES / MECHANISMS**

Deformation Mode	Principal Mechanism	Typical Location/Geometry
DM1-BC	Loss of bearing capacity due to liquefaction in loose foundation soils.	Stopbank size is larger and generally set back from river, therefore no slumping develops.
DM2-MCS	Liquefaction where the crust is too thick or the soil layers are too thin to cause a loss of bearing capacity.	Generally occurs where the stopbank is setback from the river and the effects of lateral spreading are less.
DM3-S	Liquefaction of the foundation soils adjacent to a free face, may also occur on corners causing radial patterns.	Immediately adjacent to a free face, or on the bend of a stopbank.
DM4-LS	Liquefaction of the foundation soil resulting in significant lateral stretch at the stopbank location.	In close proximity to a free face, sloping topography and/or abandoned river channel.
DM5-DS	Liquefaction of the foundation soil resulting in differential settlement, where lateral spreading is minor and there has been no loss of bearing capacity or surface expressions of cracking.	Controlled by susceptibility of foundation soils to liquefaction and occurs across a range of stopbank geometries and locations.
DM6-RF	Rotational failure in fill along a preferred sliding plane due to earthquake shaking.	Occurred in one location where foundation soils and stopbank had been backfilled with homogenous fill material.
DM7-EF	Acceleration-induced or liquefaction-induced deformation causing damage to the stopbank system.	Occurred in locations where engineered features had been used as the primary source of flood protection.

## 6.0 ANALYSIS OF GEOTECHNICAL FACTORS INFLUENCING STOPBANK DEFORMATION

### 6.1 INTRODUCTION

In order to further understand the factors that influence the type and the severity of the damage to stopbanks a regional assessment needs to be undertaken in order to correlate the factors on a larger scale. The assessment presented in this chapter is based on a detailed study comparing deformation modes and deformation severity with land damage parameters, geomorphological parameters, and geotechnical parameters calculated from the analysis of Cone Penetration Tests (CPTs). The calculated parameters are based on the groundwater levels at the time of each earthquake and the location specific shaking intensity experienced. From this comparison conclusions on the likely key triggers and mechanisms responsible for driving the damage type and severity can be made.

### 6.2 SCOPE AND OBJECTIVES

One of the objectives of this study are to determine parameters that are key in predicting stopbank damage severity and/or vulnerability. The framework for this study is based on the observed deformation modes presented in Chapter 5 and a severity classification index derived from the deformation modes. Analysis has been undertaken on approximately 178 Cone Penetration Tests (CPTs) which were undertaken in response to the Canterbury Earthquakes to collect additional data to aid in stopbank repair and rebuild.

## 6.3 SAMPLING PROCEDURE

This study incorporates the earthquake response of the stopbank at 178 different locations along the Kaiapoi River and Avon River during the 4 September 2010 and 22 February 2011 earthquakes. Sites were selected based on their proximity to a Cone Penetration Test (CPT), within 5 m to 50 m of the stopbank and whether there was sufficient recorded data at the location to determine a deformation mode as presented in Chapter 5. The distribution of the 187 sample sites is outlined in Table 12 and the locations are shown in Figure 58.

**TABLE 12: DISTRIBUTION OF CONE PENETRATION TESTS**

<b>River Bank</b>	<b>Sample Size</b>
Northern bank of Avon	73
Southern bank of Avon	84
Northern bank of Kaiapoi	13
Southern bank of Kaiapoi	17

The majority of the data at each of these locations was obtained from the Canterbury Geotechnical Database (CGD) a database available to professional engineering companies involved with Canterbury Recovery, the Government, scientific and academic institutions, the Earthquake Commission, councils and insurers (<https://canterburygeotechnicaldatabase.projectorbit.com/>). The CGD was developed for professional geotechnical engineers and researchers to access geotechnical data shared by other engineers and researchers. At the time of undertaking the analyses presented in the report, the CGD contained approximately 7,500 CPT investigations at discrete locations around Canterbury.

The specific data that has been collected for analysis from the CGD is summarised in Table 13.

**TABLE 13: CANTERBURY GEOTECHNICAL DATABASE DATA USED IN ANALYSIS**

<b>Geotechnical data</b>	<b>Field-collected land damage data</b>
Cone Penetration Tests (CPTs)	Observed ground cracks
Peak Ground Accelerations (PGAs)	Global lateral movement
Event specific depth to groundwater	Vertical elevation change
	EQC observed land damage

Additional data that has been collected for analysis that was not taken from the CGD is summarised in Table 14.

**TABLE 14: ADDITIONAL DATA USED IN ANALYSIS**

<b>Stopbank damage data</b>	<b>Geomorphology</b>
Deformation mode	Height of channel
Damage/No damage index	Angle of slope
Repair/No repair index	Stopbank distance to river



## 6.4 CALCULATED PARAMETERS

Calculated parameters are derived from analysis of data obtained from Cone Penetration Testing (CPT). CPT is a method by which a probe consisting of a cylindrical penetrometer and a cone is pushed into the ground at a constant rate of 2 cm/s. During the penetration, the forces on the cone tip and along the friction sleeve are measured, and in some cases the pore water pressure is also measured. Through empirical correlations the results of a cone penetration test can be used to evaluate a soil behaviour type, and liquefaction triggering based on simplified liquefaction evaluation procedures. The test provides a continuous record of penetration resistance throughout the depth of the soil profile.

The CPT results have been combined with groundwater data and models of earthquake shaking distribution to allow the calculation of Liquefaction Potential Index (LPI) and settlement. Key geotechnical factors have been derived from the CPT data including the non-liquefiable crust thickness, depth and thickness to and of the critical liquefiable layer, and average cone resistance ( $q_c$ ), soil behaviour type index ( $I_c$ ) and Factor of Safety (FoS) of the critical layer.

The overarching CPT analysis methodology is outlined below followed by a discussion of the LPI and settlement calculated parameters. The key inputs in the liquefaction analysis are Peak Ground Acceleration (PGA) and depth to groundwater, a summary of these inputs is also included. A description of the key geotechnical factors is also presented.

### 6.4.1 CPT ANALYSIS METHODOLOGY

This section presents a summary of the methods and assumptions used in the liquefaction triggering assessment. The parameters used in this analysis were calculated using the procedures given in “*Soil Liquefaction during Earthquakes*” (Idriss and Boulanger, 2008).

Modifications for fines content were applied according to the methodology outlined by Robertson and Wride (1998). For this analysis, we have assumed that no liquefaction occurs where the calculated soil behaviour index  $I_c$  exceeds 2.6. The potential for soils to liquefy is related to the amount of fine and plasticity of the fines in particular, present. A higher  $I_c$  represents soils that behave more like fine grained materials and may experience strain softening rather than liquefaction, a phenomenon not evaluated in this analysis.

Modifications were also applied for the calculation of post-liquefaction induced settlements, according to the methodology outlined by Zhang et al. (2002). The Zhang et al. (2002) method predicts strain in layers where the liquefaction factor of safety is less than 2.0. The calculated settlement indicator increases as the factor of safety drops and the material approaches a liquefied state. Therefore, some settlement is calculated when FoS is more than 1 even though liquefaction triggering has not occurred.

Of the 178 CPTs used for this analysis 34 terminated at less than 10 m and 5 of these were less than 5 m deep. This termination was due to effective refusal. For the shorter CPTs the liquefaction contribution from the soil profile beneath the depth at which the CPT test was terminated would not be included in the calculation. This means that the actual value for settlement or LPI would be underestimated. As the CPTs ranged in depth from 3 m to 40 m, calculations were limited to the upper 10 m of the soil profile. Ground

deformations resulting from soil liquefaction at depths greater than 10 m do contribute to total ground settlements, which can be important in areas of high flood hazard. However, it does not produce the same amount of damage as the differential settlement caused by layers in the top 10 m.

#### 6.4.2 PEAK GROUND ACCELERATIONS

The key input to determine for liquefaction analysis is the Peak Ground Acceleration (PGA) representative of what was observed at the site during each of the earthquakes. The assessment considers the response of the site to the ‘primary *earthquake* event’ and the ‘secondary *earthquake* event’. The primary event is the Canterbury Earthquake event that provided the highest  $M_w 7.5$  corrected PGAs for each particular location, and the secondary event in the Canterbury Earthquake that provided the next highest  $M_w 7.5$  corrected PGAs for the site. The primary and secondary events for the two river systems are shown in Table 15.

TABLE 15: DEFINITION OF PRIMARY AND SECONDARY EARTHQUAKE EVENTS

River	Primary Event	Recorded PGA Range	PGA <sub>M7.5</sub>	Secondary Event	Recorded PGA Range	PGA <sub>M7.5</sub>
Avon River (CBD and to the east of the CBD)	22 <sup>nd</sup> February 2011	0.28 – 0.60	0.20 – 0.43	4 <sup>th</sup> September 2010	0.16 – 0.22	0.14 – 0.20
Kaiapoi/Waimakariri River	4 <sup>th</sup> September 2010	0.18 – 0.19	0.13	22 <sup>nd</sup> February 2011	0.21 – 0.23	0.19 – 0.21

Based on the recorded accelerations at strong motions sites and magnitude of the two earthquake events considered, the PGA at each site was estimated. These PGA values were obtained from the conditional PGA (median and standard deviation) values reported according to the probabilistic model presented by Bradley and Hughes (2012), shown in Figure 59, and obtained from the Canterbury Geotechnical Database (<https://canterburygeotechnicaldatabase.projectorbit.com/>).

In order to provide a comparison between the two events corrected M7.5 PGA values were determined from these PGAs using a MSF of 1.11 and 1.41 for the 4 September 2010 and 22 February 2011 Earthquakes respectively. The Magnitude Scaling Factor (MSF) corrects the analysis for earthquake magnitudes other than 7.5, allowing for direct comparison of PGAs observed at different earthquakes magnitudes. The MSF was determined using the equation (Idriss & Boulanger, 2008):

$$MSF = 6.9 \exp\left(-\frac{M}{4}\right) - 0.058$$

Site specific event PGAs were corrected to a M7.5 event using the equation:

$$PGA_{7.5} = PGA/MSF$$



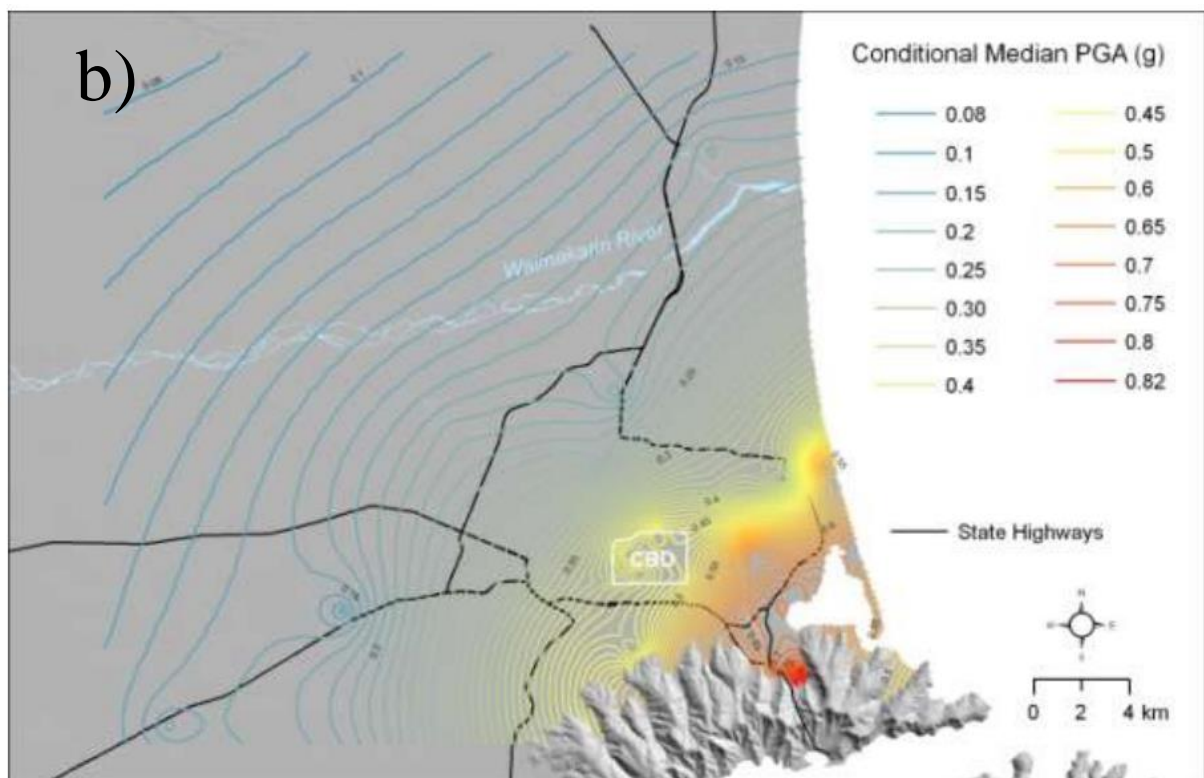
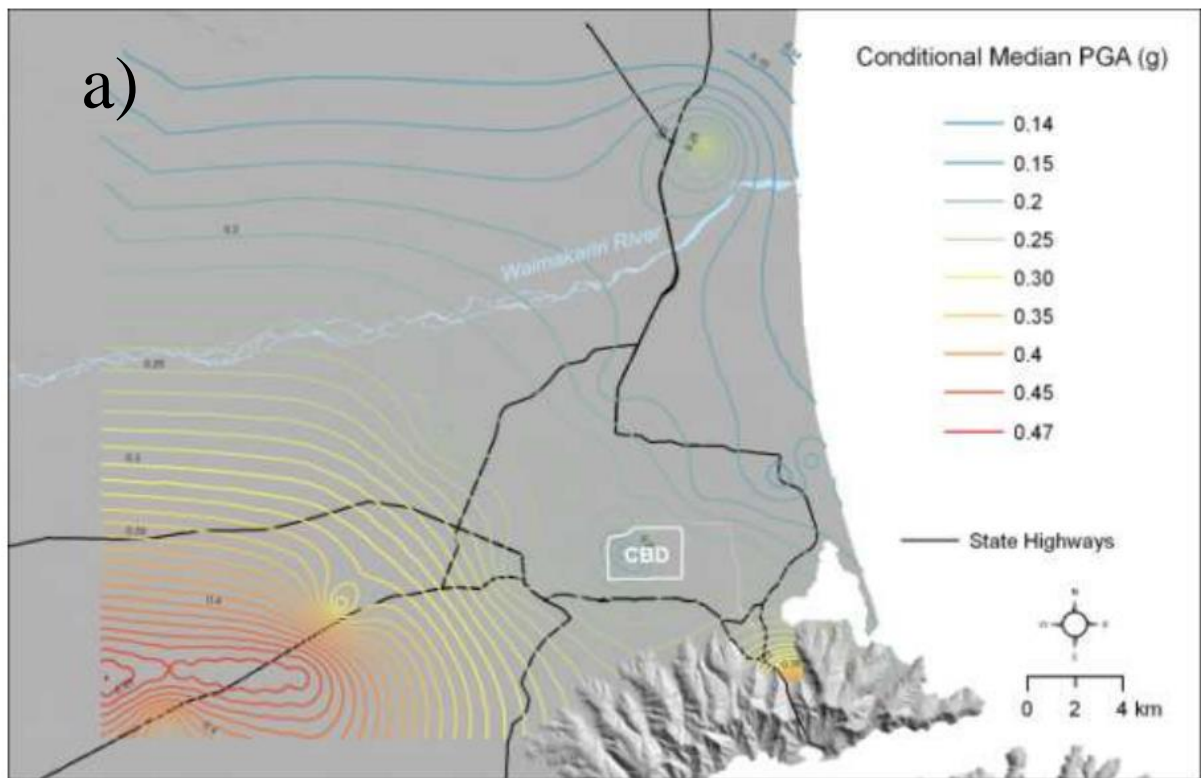


FIGURE 59: CONDITIONAL MEDIAN PGA PREDICTED IN CANTERBURY FROM A) THE 4 SEPTEMBER 2010 EARTHQUAKE AND B) THE 22 FEBRUARY 2011 EARTHQUAKE (BRADLEY AND HUGHES, 2012)

### 6.4.3 EVENT SPECIFIC DEPTH TO GROUNDWATER

Event specific groundwater depths for the individual earthquakes were obtained from the Canterbury Geotechnical Database (CGD0800). A regional groundwater model has been developed to provide a basis for geotechnical liquefaction modelling around Christchurch at the time of the earthquakes. The model created was based on groundwater level data from over 800 monitoring wells across Christchurch. Four earthquake-specific groundwater surfaces were developed based on the median water table surface which was created for greater Christchurch, as summarised in van Ballegooy et al., (2013).

Groundwater depths were derived from free surface elevations prior to each earthquake by subtracting the elevations from the most appropriate LiDAR-derived digital surface elevation model for that particular earthquake. An example of the depth to groundwater map is included in Chapter 2 (Section 2.2.1 ).

### 6.4.4 LIQUEFACTION POTENTIAL INDEX (LPI)

LPI for the critical layer was calculated based on the Idriss & Boulanger (2008) triggering method. The LPI presents the risk of liquefaction damage as a single value and was developed by Iwasaki et al. (1984; 1978). Iwasaki's LPI is presented as a measure of the vulnerability of sites to liquefaction effects. The LPI is defined as:

$$LPI = \int_0^{20} F_1 W(z) dz$$

Where  $W(z) = 10 - 0.5z$ ,  $F_1 = 1 - \text{FoS}$  for  $\text{FoS} < 1.0$ ,  $F_1 = 0$  for  $\text{FoS} > 1.0$  and  $z$  is the depth below the ground surface in metres.

### 6.4.5 CALCULATED SETTLEMENT

This methodology is based on published methods to estimate volumetric shear strain consistent with that recommended in Section C3.5.1 DBH 2012, the accepted peer-reviewed guidelines for use in the Christchurch rebuild that have been adopted by the geotechnical community as the current state of practice for liquefaction assessments. The liquefaction assessment has been undertaken using proprietary software CLiq (GeoLogismiki 2006). It should be noted the settlement the CLiq software calculates is the overall global settlement of the tested soil, and should not be confused with differential settlement. Generally the differential settlement is less than the global settlement. Due to the limitations and assumptions inherent in analytical models such as CLiq. Settlements are reported to the nearest 5 mm.

### 6.4.6 NON-LIQUEFIABLE CRUST THICKNESS

The crust thickness, as depicted in Figure 60, is defined by the thickness of the surficial non-liquefiable soil layer at the site, defined by a Cyclic Stress Ratio (CSR) less than the Cyclic Resistance Ratio (CRR), an  $I_c$  of greater than 2.6. In many cases where liquefiable soils are present throughout the soil column the crust thickness is the thickness of soil above the water table.

The crust quality is related to its soil properties (particle size distribution, plasticity, packing arrangement), consistency and number of penetrations (such as service trenches, power poles, foundations). As discussed in Section 5.3 having an upper layer of non-liquefying material has a beneficial effect in mitigating the

occurrence of sand ejecta and differential settlement and therefore the damaging effects of liquefaction at the ground surface (Ishihara, 1985a).

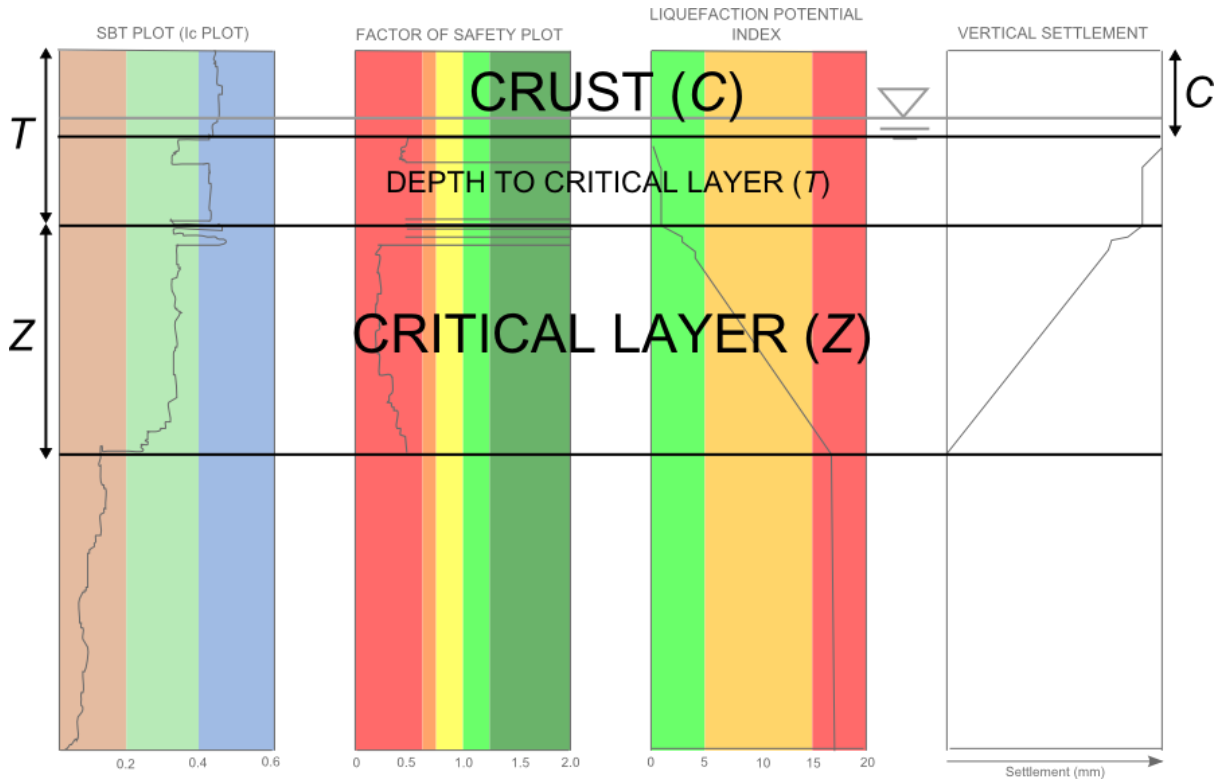


FIGURE 60: VISUAL EXPLANATION OF CRUST THICKNESS (C), DEPTH TO CRITICAL LAYER (T) AND THICKNESS OF CRITICAL LAYER (Z)

#### 6.4.7 DEPTH AND THICKNESS TO AND OF THE CRITICAL LIQUEFIABLE LAYER

The critical layer is defined as where the FoS has the lowest value, based on potential to liquefy defined where Cyclic Stress Ratio (CSR) is greater than the Cyclic Resistance Ratio (CRR). In some cases the critical layer for liquefaction is very clear, and is overlain and underlain by a non-liquefiable crust. However, many soils in Christchurch are highly interbedded and the soil materials do not divide into two discrete units of liquefying and non-liquefying materials. Therefore, the thickness of the critical layer is reported as the cumulative thickness of the key liquefying materials in the soil profile, with a maximum interbedded non-liquefiable layer thickness of 0.5 m.

#### 6.4.8 CONE RESISTANCE (QC)

When the cone is pushed into the ground the pressure exerted on the end of the cone (cone end resistance '  $q_c$  ') is an indirect indication of the strength and stiffness of the soil, i.e. it is more difficult to push a cone into dense sand than loose sand or soft clay. As the CPT provides a continuous soil profile the  $q_c$  value can vary significantly within a few centimetres and it is difficult to summarise the typical  $q_c$  value as a single value that can be used in analysis. The average  $q_c$  value for the Critical Layer (Z) at each site is reported in the analysis; the  $q_c$  range for the tested CPTs is illustrated in the individual CPTs in Appendix E.

#### 6.4.9 SOIL BEHAVIOUR TYPE ( $I_c$ )

The Soil Behaviour Type ( $I_c$ ) is derived from the CPT and is a useful tool for soil profiling and classification. The  $I_c$  is a value calculated from the CPT data for each soil layer using the corrected total cone resistance  $q_t$  and the friction ratio  $F_r$  which is determined from the CPT sleeve friction  $f_s$ . The average  $I_c$  value for the critical layer is reported for each of the individual CPTs.

#### 6.4.10 FACTOR OF SAFETY (FoS)

The factor of safety for level ground liquefaction resistance has been defined as  $FoS = CRR / CSR$  where CSR is the cyclic stress ratio generated by the anticipated earthquake ground motions at the site, and CRR is the cyclic resistance ratio required to be exceeded to generate liquefaction (Seed and Idriss, 1982).

A FoS of 1.0 or more indicates no liquefaction (i.e. capacity exceeds demand) and a FoS less than 1.0 indicates liquefaction is likely (i.e. demand exceeds capacity). However, the liquefaction triggering processes are not presented as 'bright line' distinctions between sites affected or not affected by liquefaction. Moss et al. (2006) noted that a calculated factor of safety of 1.0 generally indicated a 15% chance of liquefaction affecting that soil layer. The average FoS for the critical layer is reported in the analysis.

### 6.5 LAND DAMAGE PARAMETERS AND DAMAGE INDEX

The land damage parameters presented here within are considered to be the most reliable damage attribute for the purposes of correlation with the calculated parameters, stopbank damage and geomorphological parameters considered. The key parameters considered are outlined below and are combined into a damage index that can be used for further analysis by assigning quantitative levels to qualitative observations and ranges of damage.

#### 6.5.1 OBSERVED GROUND CRACKS (A)

Following the 2010 – 2011 Canterbury earthquake sequence the EQC commissioned field observations of crack locations to be recorded using coloured pens on paper copies of aerial photographs. The marked-up photographs were later scanned and the coordinates of the coloured lines were manually digitized. The resulting crack location maps provide a visual observation of the amount of manifested lateral stretch observed at the individual locations. (CGD0400).

The crack mapping is incomplete and only observations made by the mapping teams are presented. In particular, the mapping following the 4 Sept 2010 Earthquake was incomplete before the 22 Feb 2011 Earthquake occurred and subsequent mapping remains incomplete within the residential 'red zone' areas. Also, cracks in roads were often not able to be mapped because many were filled and the roads resealed before a mapping team arrived.

### 6.5.2 GLOBAL LATERAL GROUND MOVEMENT (B)

Global lateral ground movement; due to lateral spreading, is the amount of uniform translation of the ground surface at a site. Such movement is usually the result of a site that has experienced liquefaction being in close proximity to a stream or on sloping ground. Global lateral movement may not necessarily result in observed ground cracks, rather it is the gross scale movement of material in a horizontal direction.

The horizontal ground surface movements provide the approximate movements during significant earthquakes (CGD0700) and were also commissioned by the EQC. The horizontal movements were calculated by Imagin' Labs Corporation and California Institute of Technology for each earthquake using a sub-pixel correlation method. The movements were calculated on 4 m grids (8 m for the pre-earthquake LiDAR sets) from both ground and non-ground LiDAR points and averaged to provide Cartesian movements in a 56 m grid. The averaging distance was tailored to the noise in the two LiDAR sets.

### 6.5.3 VERTICAL ELEVATION CHANGE

Vertical ground movement, or land settlement, has occurred due to a combination of tectonic effects, and liquefaction-induced ground deformation. The vertical ground movement map was generated by EQC, and is based on LiDAR topographic surveys. LiDAR is an aerial imaging technique that generates digital topographic surfaces. Comparing surveys before and after each earthquake indicates how much vertical ground movement has occurred. The data shows local ground settlements from pre-earthquake (prior to September 2010) to post-earthquake (after June 2011). The tectonic component of the movement, which represents the deformation due to the fault movement that generated each earthquake, has been subtracted from the surface elevation changes to create this layer. The remaining movement reflects liquefaction-induced settlement of the ground. The accuracy of data is +/- 40 mm for the 4 September 2010 earthquake and +/- 30 mm for the 22 February 2011 earthquake.

### 6.5.4 EQC LAND DAMAGE CATEGORY

The Earthquake Commission (EQC) Land Damage maps are based on rapid visual assessments of individual residential properties conducted by geotechnical engineers for EQC following the 4 September 2010; 22 February 2011; and 13 June 2011 earthquakes. The quantities of material ejected due to liquefaction and observations of lateral spreading were collated from on-foot rapid inspection following each significant earthquake. The observations were categorized according to the quantity of ejected material observed on the ground surface and according to the presence or absence of evidence of lateral spreading.

The observations were collected for the Earthquake Commission and were only made in residential areas. The mapping only identified liquefaction and lateral spreading that was visible at the surface at the time of inspection.

It should be noted that the assessments conducted following the 4 September 2010 and 22 February 2011 earthquakes were done by inspecting each individual property, while the 13 June 2011 assessment was done by taking observations from the road only.

### 6.5.5 DAMAGE INDEX

In order to correlate the various observed and recorded land damage indicators from the earthquake with stopbank damage, a damage index has been created. This assigns a damage index value to different types of and severities of damage, as summarised in Table 16. The weighting for the scores are non-linear as they are based on the influence of that particular damage indicator to performance. As shown, Category C (vertical elevation change) has been weighted with slightly lower damage index values, this is because part of this settlement is assumed to be global settlement, which is not as damaging as the differential settlement.

**TABLE 16: DAMAGE INDEX**

Observed Widths of Ground Cracks (A) <sup>1</sup>	Description	Damage Index
None	No ground cracks	0
Minor	Less than 100 mm of cumulative ground cracks within 30 m of the stopbank	1
Moderate	Between 100 mm and 200 mm of cumulative ground cracks within 30 m of the stopbank	2
Major	Between 200 mm and 500 mm of cumulative ground cracks within 30 m of the stopbank	5
Severe	Between 500 mm and 1000 mm of cumulative ground cracks within 30 m of the stopbank	8
Very severe	Greater than 1000 mm of cumulative ground cracks within 30 m of the stopbank	10
Global Ground Movement (B) <sup>2</sup>	Description	Damage Index
Minor	0.0 m to 0.1m of horizontal movement	1
Moderate	0.1 m to 0.2 m of horizontal movement	2
Major	0.2 m to 0.5 m of horizontal movement	5
Severe	0.5 m to 1.0 m of horizontal movement	8
Very Severe	Greater than 1.0 m of horizontal movement	10
Vertical Elevation Change (C) <sup>3</sup>	Description	Damage Index
None	> 0.1 m	0
Minor	-0.1 to 0.1 m	1
Moderate	-0.2 to -0.1 m	2
Major	-0.3 to -0.2 m	3
Severe	-0.5 to -0.3 m	5
Very Severe	> -0.5 m	10
EQC Land Damage Category <sup>4</sup>	Description	Damage Index
None	No observed ground cracking or ejected liquefied material	0
Minor	Minor ground cracking but no observed ejected liquefied material	5
Moderate	No lateral spreading but minor to moderate quantities of ejected material	8
Major	No lateral spreading but large quantities of ejected material	8
Severe	Moderate to major lateral spreading or large quantities of ejected material	10
Very severe	Severe lateral spreading; ejected material often observed	10

<sup>1</sup> Canterbury Geotechnical Database (2012) "Observed Ground Crack Locations", Map Layer CGD0400 - 23 July 2012, retrieved 26/05/13 from <https://canterburygeotechnicaldatabase.projectorbit.com/>

<sup>2</sup> Canterbury Geotechnical Database (2012) "Horizontal Ground Surface Movements", Map Layer CGD0700 - 23 July 2012, retrieved 26/05/13 from <https://canterburygeotechnicaldatabase.projectorbit.com/>

<sup>3</sup> Canterbury Geotechnical Database (2012) "Vertical Ground Surface Movements", Map Layer CGD0600 - 23 July 2012, retrieved 26/05/13 from <https://canterburygeotechnicaldatabase.projectorbit.com/>

<sup>4</sup> Canterbury Geotechnical Database (2012) "Liquefaction and Lateral Spreading Observations", Map Layer CGD0300 - 11 Feb 2013, retrieved 26/05/13 from <https://canterburygeotechnicaldatabase.projectorbit.com/>



## 6.6 STOPBANK DAMAGE PARAMETERS AND SEVERITY CLASSIFICATION

Stopbank damage has been covered in detail in Chapter 4 and from this specific deformation modes have been derived in Chapter 5. This data is used to create a damage severity classification that has been used as the primary tool for analysis of the key factors resulting in deformation of the stopbank.

### 6.6.1 STOPBANK DEFORMATION MODE

Stopbank deformation modes are based on the maps presented in Chapter 5. Each stopbank locations has been assigned a deformation mode, and this information provides the basis of the damage severity classification.

### 6.6.2 REPAIR INDEX

The repair index has been developed to capture damage to the stopbank during the secondary earthquake event for that site. Due to a lack of data mostly due to immediate repair works following these earthquakes, aerial photographs and site visits were used to determine if there had been any repairs undertaken following the secondary earthquake at the 178 sites. Sites that have not had any repair work undertaken are assumed to have experienced no damage, sites that have had repair work undertaken are assumed to have experienced some form of damage although what type and severity this damage is, is not well documented.

### 6.6.3 SEVERITY CLASSIFICATION

The deformation mode observations outlined in Chapter 5 have been used to classify the stopbank systems in terms of damage severity. This has been done in order to segregate the areas that have suffered no to low damage against the areas that have suffered major to severe damage to delineate factors that differentiate between the level of severity that will occur at any given site. The criteria for dividing up these areas are described in Table 17. The distribution of the severity classification for the Avon River is illustrated in Figure 61 and for the WEC system in Figure 62.

It should be noted that in creating the severity classification system there are limitations involved with the assigning of categories based around the aforementioned limitations on the initial data set. Namely, there are gaps in the data set where assumptions have been made on the level and type of damage based on aerial and nearby damage photographs.

**TABLE 17: DAMAGE SEVERITY CLASSIFICATION**

Damage Classification	Severity	Description	Deformation Modes Included in this Category (as defined in Chapter 5)
No Damage	to Low	Stopbank suffered no damage, or minor damage that did not result in repairs and did not impact the ability of the stopbank to protect against the design flood. Cracks on the stopbank are generally non-continuous and less than 50 mm wide. Differential settlement is less than 0.2 m.	DM2-MCCS DM4-LS <sup>1</sup> DM5-DS
Major Damage	to Severe	Stopbank suffered extensive damage that generally required repairs as the ability of the stopbank to protect against the design flood was compromised. Extensive cracking, slumping and settlement were often observed. Differential settlements are large and in many cases exceed 0.5 m.	DM1-BC DM3-S DM4-LS <sup>1</sup> DM6-RF
Engineered Features		Engineered features have been generally excluded from the analysis as there is a lack of construction data, and therefore there is a need for site specific / structure specific analysis to be undertaken.	DM7-EF
<b>Notes</b>			
<sup>1</sup> DM4-LS (Lateral Stretch/Foundation Extension) deformation styles have been divided depending on the severity of the failure mode at each individual location.			

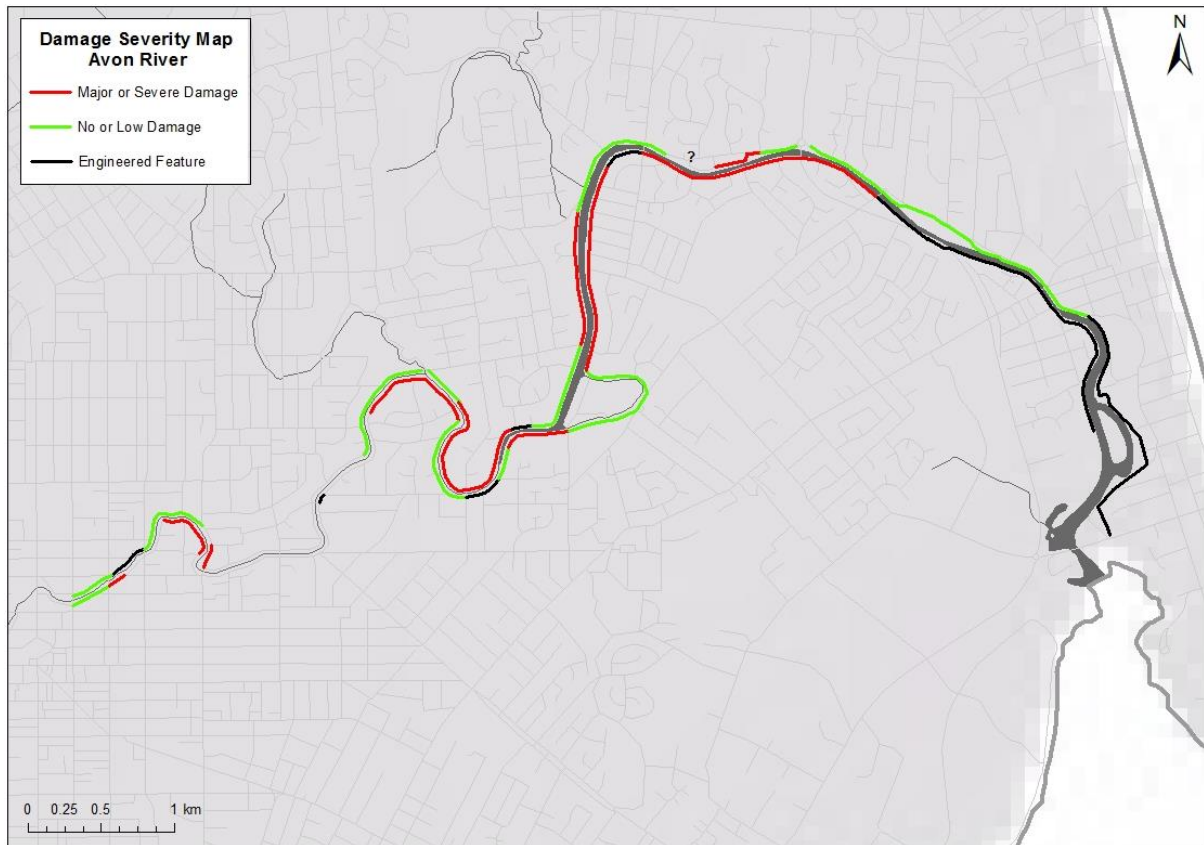


FIGURE 61: DAMAGE SEVERITY MAP - AVON RIVER

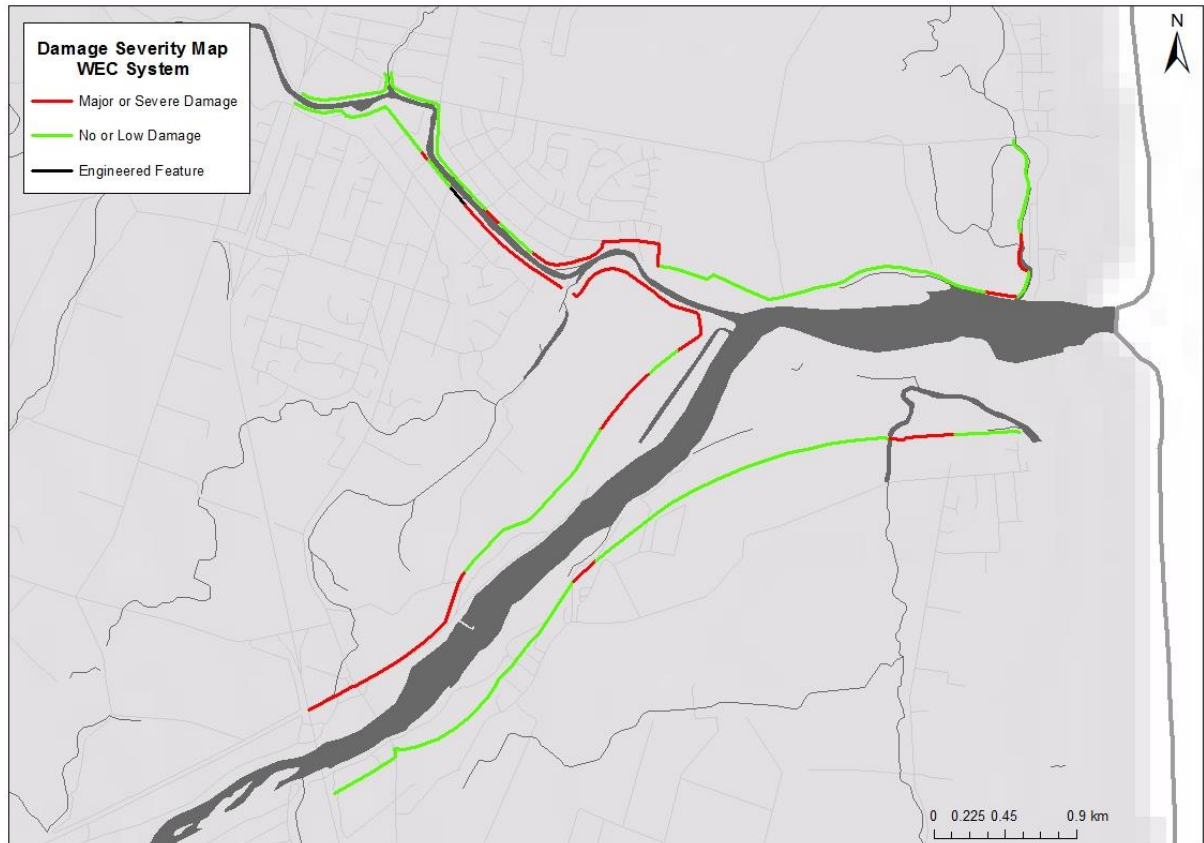


FIGURE 62: DAMAGE SEVERITY MAP - WEC SYSTEM

## 6.7 GEOMORPHOLOGY PARAMETERS

Geomorphological parameters are crucial to understanding how the stopbanks performed. From a geological perspective this is because the geomorphology can indicate depositional processes that provide useful information on the nature of the deposits, ie. abandoned / old river channels indicate loose, potentially liquefiable soils. The natural slope and height of the free face play a significant role in determining the severity of lateral spreading at a site.

### 6.7.1 HEIGHT OF CHANNEL

The height of the free face of the adjacent river channel ( $H_{FF}$ ) has been derived from the cross sections presented in Appendix D and discussed in more detail in Chapter 2 and illustrated in Figure 64. The deepest part of the channel at the site of interest has been taken for the analysis, this is considered to be accurate to approximately 1 m.  $2 \times H_{FF}$  is considered to be the depth at which the lateral spreading influence becomes insignificant, therefore this value has also been considered in the analysis.

### 6.7.2 ANGLE OF SLOPE

The angle of the slope was derived from digital elevation models and incorporated the 30 m closest to the river in the angle, as shown in Figure 64. Where the overall angle is not accurate due to the stopbank then a shorter distance is used and this distance is written in brackets next to the angle in Appendix F.

### 6.7.3 STOPBANK DISTANCE TO RIVER

The stopbank distance to river is measured from the bottom of the riverside batter to the edge of the river, this measurement was undertaken using aerial photographs and is accurate to the nearest 5 m.

### 6.7.4 LOCATION ON THE RIVER

The location on the river of the point has been documented in terms of whether the CPT falls on the cut bank, point bar or straight part of the river, as shown in Figure 63. As will be covered later in the chapter the location is a crucial indicator in performance of the stopbank.

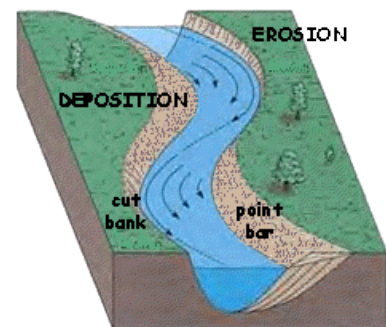


FIGURE 63: DEFINITION OF CUT BANK AND POINT BAR DEPOSIT

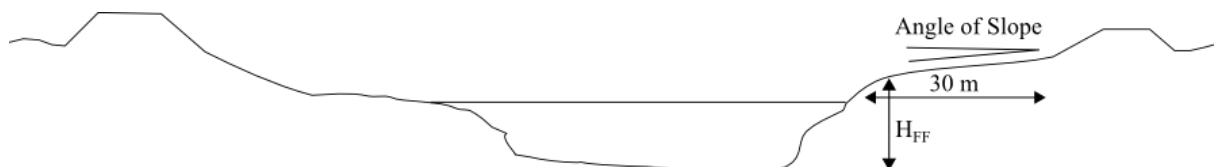


FIGURE 64: LOCATION OF ANGLE OF SLOPE AND  $H_{FF}$

## 6.8 ANALYSED DATASET AND CPT SAMPLES

The resultant dataset produced by combining all of these parameters is the basis for all the analysis here within. The CPT analysis plots are included in Appendix E and the complete dataset has been included in Appendix F. Based on the calculated, land damage, stopbank damage and the geomorphological parameters presented, Table 18 shows an example of the typical response of two CPTs that have been chosen based on their location within different severity modes (no to low damage and major to severe damage).

**TABLE 18: SAMPLE CPTS**

CPT Number		CPT_543	CPT_40
Stopbank Damage Observations	Deformation Mode	DM5-DS	FM4-LS
	Damage vs No damage	Damage has occurred	Damage has occurred
	Damage Severity Classification	Low Damage	Major or Severe Damage
	Repair/No Repair Secondary Event	No Repair	Repair
Penetration Depth		27.38 m	9.46 m
Seismic Parameters	Primary Event Magnitude	M <sub>w</sub> 6.2	M <sub>w</sub> 6.2
	Primary Event PGA	0.42 g	0.40 g
	Primary Event PGA M7.5	0.30 g	0.28 g
	Secondary Event Magnitude	M <sub>w</sub> 7.1	M <sub>w</sub> 7.1
	Secondary Event PGA	0.20 g	0.19 g
	Secondary Event PGA M7.5	0.18 g	0.17 g
Depth to Groundwater		1.0 m	1.0 m
Geomorphology Parameters	Angle of Slope	3°	1°
	Height of Channel (H <sub>FF</sub> )	1.5 m	4 m
	2 x H <sub>FF</sub>	3 m	8 m
	Cut Bank/Point Bar/Straight	Cut Bank	Straight
	Stopbank distance to river	2 m	7 m
	CPT distance to river	5 m	40 m
CPT Analysis Results	Crust Thickness	1.1 m	1.0 m
	Depth to Critical Layer	1.6 m	1.0 m
	Thickness of Critical Layer	4.7 m	7.0 m
	Average q <sub>c</sub> Critical Layer	7.0	5.5

	Average I <sub>C</sub> Critical Layer	1.75	1.86
	FoS Critical Layer	0.64	0.48
	Settlement Critical Layer	50 mm	195 mm
	Settlement Top 10 m	165 mm	195 mm
	DLPI Critical Layer	17	20
	LPI Top 10 m	20	20
Observed and Recorded Damage from Canterbury Geotechnical Database and Damage Weighting	Ground Cracks (A)	Minor	Moderate
	Ground Cracks (A) Weighting	1	2
	Horizontal Movement (B)	0.3 m	0.5 m
	Horizontal Movement (B) Weighting	5	8
	Settlement (C)	+0.1 to +0.2 m	-0.5 to -1.0 m
	Settlement (C) Weighting	0	10
	Visual Damage Observation (EQC)	No lateral spreading but minor to moderate quantities of ejected material	Moderate to major lateral spreading; ejected material often observed
	Visual Damage Observation (EQC) Weighting	5	10
Calculated Damage Indices	Damage Index (A + C)	1	12
	Damage Index (B + C)	5	18
	Damage Index (EQC)	5	10



## 6.9 PRIMARY DATASET RESULTS

This section provides an introduction to the data analysis that has been undertaken whilst providing some selected results. The results presented in this section are based on the calculated land damage, stopbank and geomorphology parameters covered in this chapter. The data set is included as Appendix F.

A summary of the case studies is presented in Section 3.3 and the deformation modes presented in Chapter 5 indicate that liquefaction and lateral spreading of the stopbank foundation soils are the two primary factors that determine the extent and severity of stopbank deformation. Liquefaction is the key aspect which determines whether there will be damage or no damage, and lateral spreading is the aspect that will determine if this damage is negligible to minor or if it is major to severe.

The damage index provides the opportunity to make an initial correlation between land damage and the presence of stopbank damage, although not the degree or severity of the damage. In order to do this both vertical settlement due to liquefaction and horizontal movement due to lateral spreading are combined. Independently, the effects of ground cracking, determined by the cumulative widths of ground cracks within 30 m of the stopbank (A) and global horizontal movement, interpreted from LiDAR (B) have been combined with vertical settlement. This creates an A + C damage index value and a B + C damage index value.

The correlation between damage index and observed stopbank damage for A + C is shown in Figure 65. This shows the general trend of lower damage index scores correlating with no observed stopbank damage, while higher damage index score correlate with observed stopbank damage. However, the overlap of damage index for undamaged and damaged stopbanks can also be clearly seen.

The correlation between damage index and observed stopbank damage for B + C is shown in Figure 66. The trend for this is not as convincing as A + C as there is an even distribution of damaged and non-damaged sites across the different damage scales. This is not surprising as global horizontal movement does not necessarily result in ground deformation and it is not uncommon to see a large amount of horizontal translation where there has not been any significant ground cracking as the land has moved as one unit.

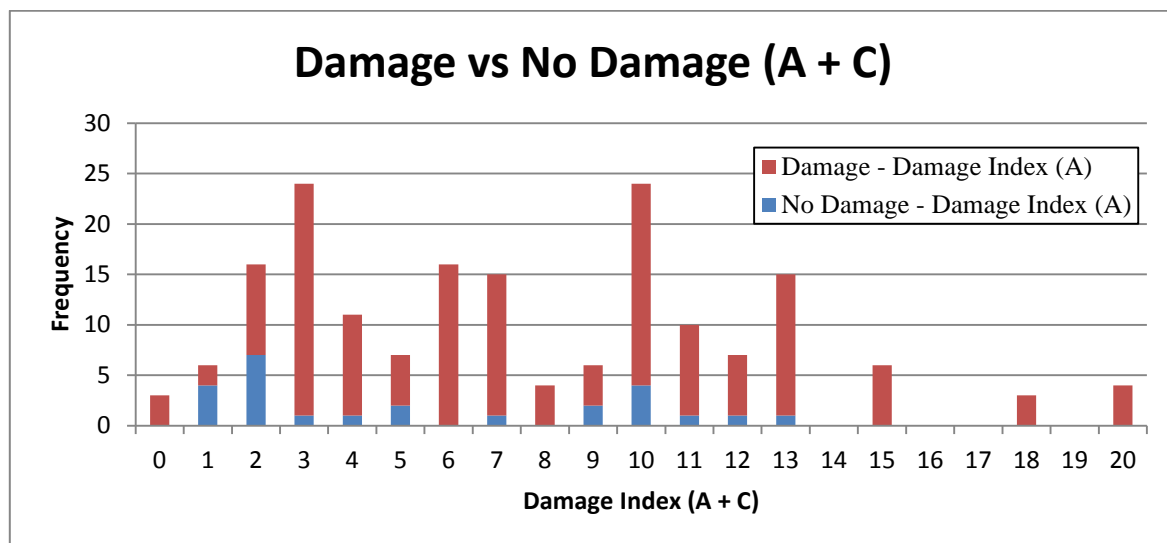


FIGURE 65: DAMAGE INDEX FOR DAMAGED AND NON-DAMAGED SITES (A + C).

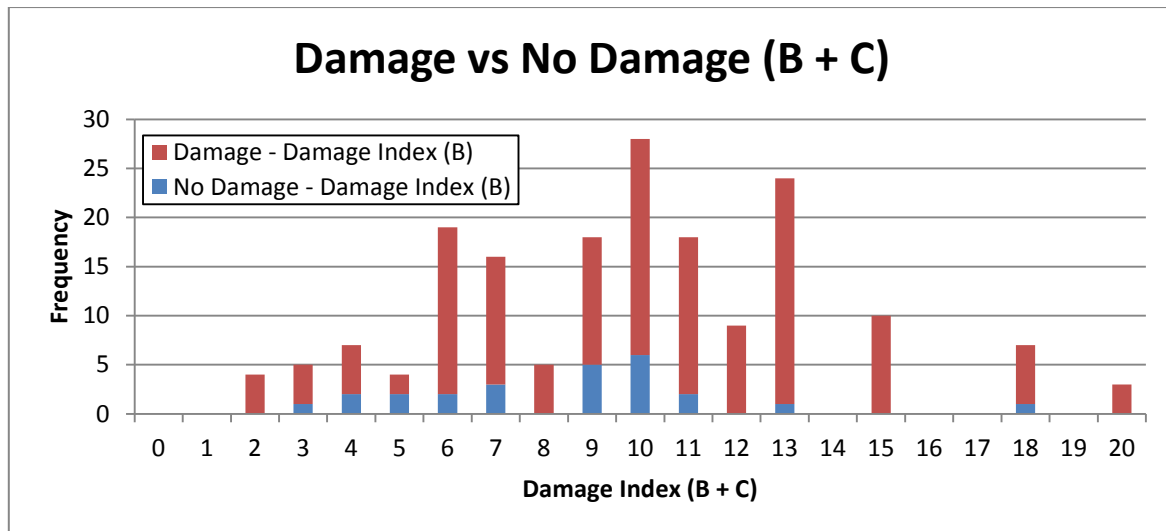


FIGURE 66: DAMAGE INDEX FOR DAMAGED AND NON-DAMAGED SITES (B + C).

The key results of both of these graphs are that there was damage to stopbanks exposed to low land damage, and that there was no damage to stopbanks that were exposed to major to land damage.

#### 6.9.1 LIQUEFACTION

Following a review of the liquefaction maps it is evident that the presence of liquefaction within the ground materials beneath the stopbanks is a key factor influencing the occurrence of damage to the stopbank. It has been shown that where there has been no liquefaction of the stopbank foundation materials, as seen to the west of Christchurch, stopbank damage is not present.

However it is apparent that the presence of liquefaction in the ground materials beneath the stopbanks is not critical in determining the type or severity of damage, instead it is merely the triggering mechanism. It appears that type and severity is instead governed by a complex assortment of other factors such as location, geometry, position along the river, etc.

#### LIQUEFACTION TRIGGERING

The distribution of PGAs for the damaged vs non-damaged stopbank for the primary earthquake events and repair vs no-repair for the secondary earthquake events is shown in Figure 67. The Primary Event PGA refers to the event where the stopbank system experienced the highest recorded PGA7.5 values, while the Secondary Event PGA refers to the event where the stopbank system experienced the second highest recorded PGA7.5 values. For the Kaiapoi system the primary event was 4 September 2010 and the secondary event was 22 February 2011. For the Avon System the primary event was 22 February 2011 and the secondary event was 4 September 2010.

Whilst there is sufficient data to classify the damaged vs non-damaged stopbanks for the primary event, there were less resources (ie. Damage data) available for the secondary events, hence the damage has been classified as areas that have been repaired vs areas that weren't. Generally areas that were repaired are assumed to have suffered some damage although this is of varying degrees. Also, some areas that may not

have been repaired following the secondary earthquake, due to time between earthquakes may have suffered some minor damage.

As discussed above, liquefaction is significant in determining the presence of damage to stopbanks. It would be suitable to assume that with increasing PGA one would observe an increasing degree of damage. This however is not the case and it is apparent that an increased PGA does not correlate to increased damage. This is lent credibility by the data presented in Figure 67 where between the PGA ranges of 0.13 g and 0.43 g damage has occurred or repairs have been required. It would be reasonable to assume that at lower PGAs (that were experienced by the flood protection system during smaller aftershocks) liquefaction would not be triggered and damage/repairs would not be seen or required. It is clear that there are a variety of other factors which are more prevalent in determining damage type and severity.

This also indicates that for particular ground conditions there exists a threshold PGA for triggering damage. The threshold PGA appears to be relatively low along the Avon River and Kaiapoi River. This may be a  $PGA_{M7.5}$  of approximately 0.13 g.

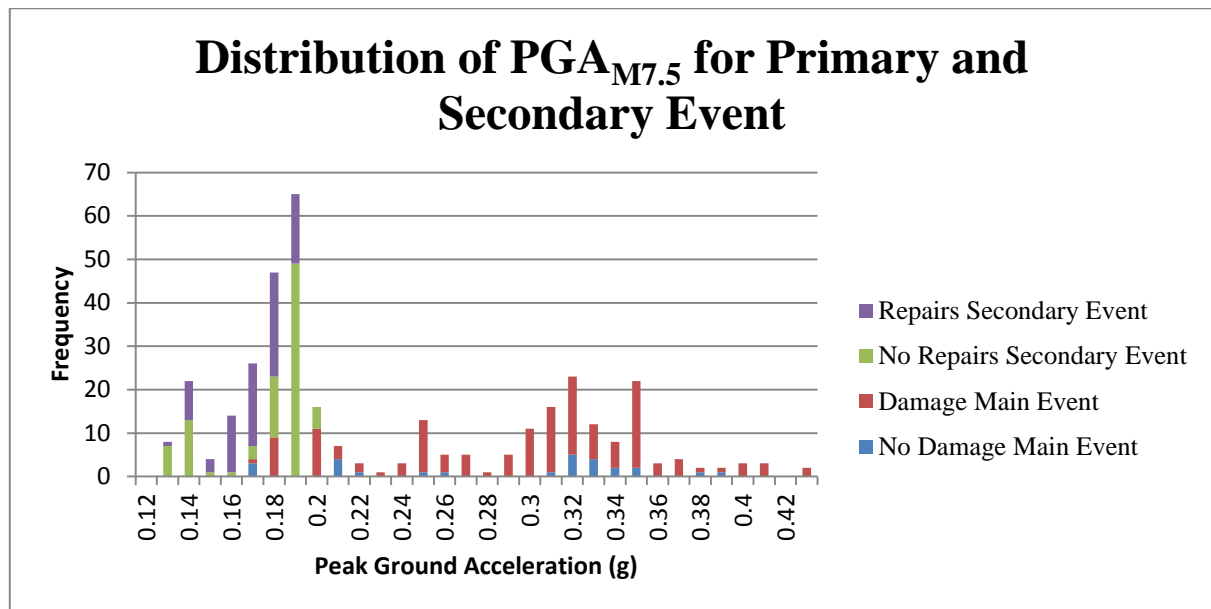


FIGURE 67: DISTRIBUTION OF  $PGA_{M7.5}$  FOR PRIMARY AND SECONDARY EVENTS

#### PROPERTIES OF THE CRITICAL LAYER

A critical layer was present in every CPT regardless of the severity of the damage, some layers were as thin as 0.2 m. As these layers were all liquefiable, when compared, the geotechnical parameters were found to be broadly consistent.

Average  $q_c$  values ranged from between 0.27 to 16.06 MPa, although these values are the extremes, as shown in the graph presented in Figure 68, 66% of the distribution fell between 3.3 MPa and 8.0 MPa. These values are typical of liquefiable soils and represent loose soil conditions with high liquefaction potential. Only 8% of the QC values for damaged stopbanks are above 10 MPa, a threshold above which damage is

considered to be unlikely. Of these critical layers exceeding a 10 MPa average, 40% were in areas affected by engineered failure damage, as shown in Figure 69. The reason for this is uncertain by may be due to a number of factors including large scale gross lateral spreading, poor engineering design and/or construction or that damage to engineered structures is more obvious as deformations are easier to pick up in a structure. Of the remaining 60%, the majority were within highly interbedded stratigraphy with the interbedded nature of the soil bringing the average QC of the layer to greater than 10 MPa, which is more representative of data scatter rather than an actual observation.

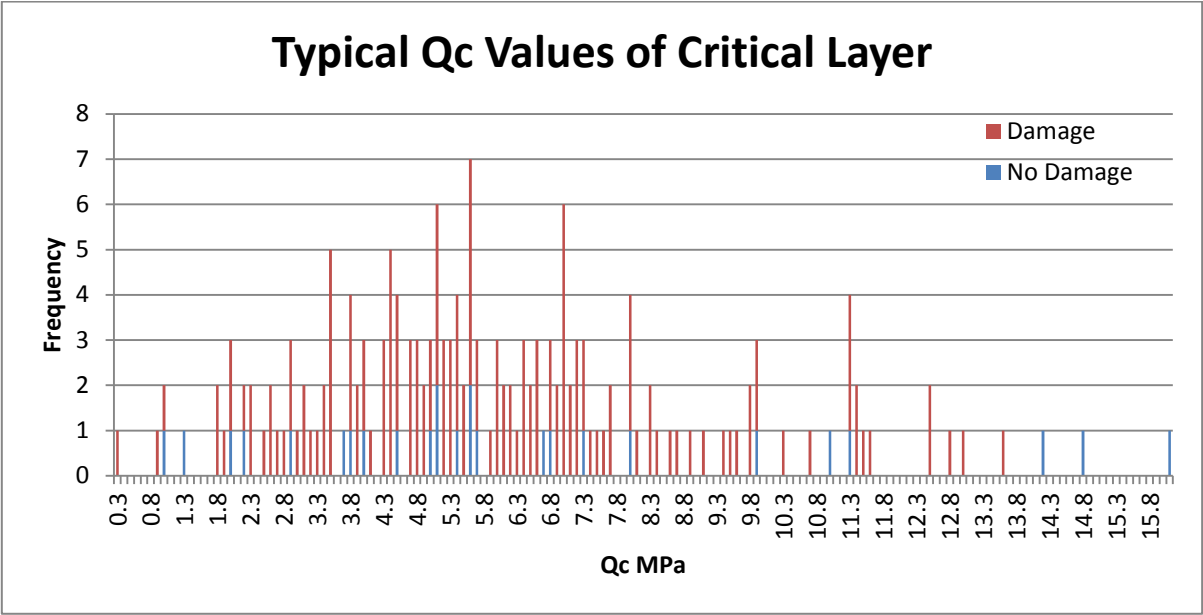


FIGURE 68: TYPICAL QC VALUES OF THE CRITICAL LAYER

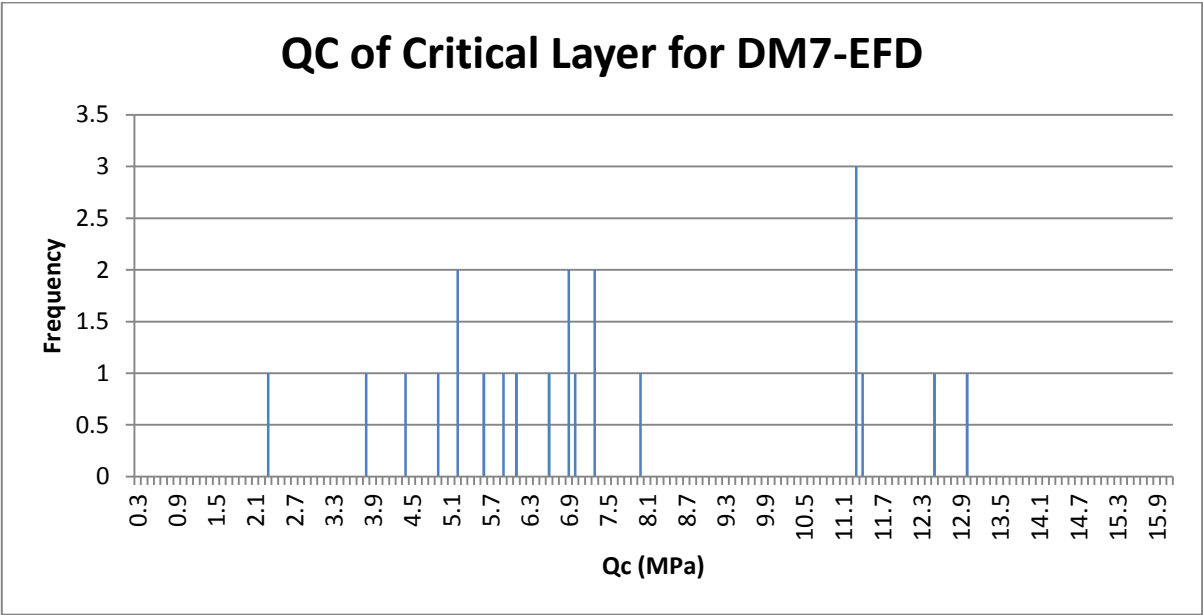


FIGURE 69: TYPICAL QC VALUES OF THE CRITICAL LAYER FOR DM7-EFD

As previously discussed  $I_C$  is a measure of the distance (the radius) from a point above and to the left of the plot of normalized tip resistance ( $q_{c,1}$ ) and normalized Friction Ratio ( $F$ ).  $I_C$  cut-off value between cohesionless (sand-like) and cohesive (clay-like) soils is 2.67 for the Robertson and Wride's expression (Robertson and Wride, 1998). On the other hand,  $I_C = 2.58$  was found to be the most suitable cut-off value by Been and Jefferies (1985). As shown in Figure 70, an  $I_C$  of greater than 2.4 is the threshold above which no damage is higher than damage, indicating that a lower  $I_C$  cut-off could be more appropriate for Christchurch soils. As an  $I_C$  cut off of 2.6 has been used in the analysis as a boundary between triggering liquefaction versus not triggering liquefaction, we cannot say if there has been any damage to sites with an  $I_C$  of greater than 2.6. This would be an interesting detail to research further based on the available data.

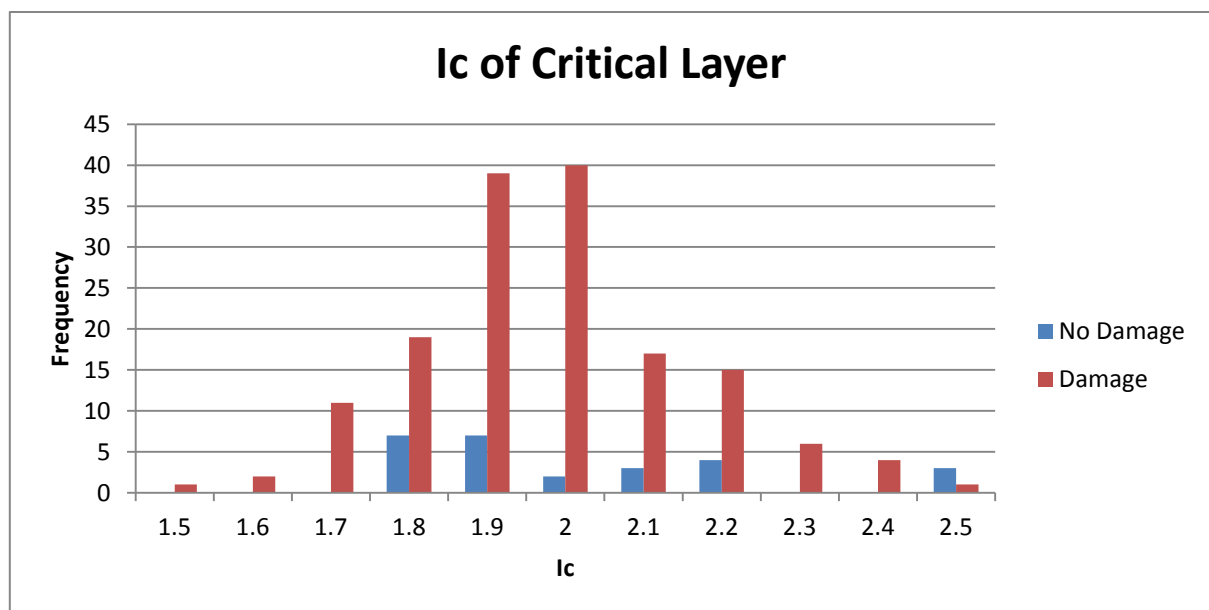


FIGURE 70: AVERAGE  $I_C$  OF THE CRITICAL LAYER

The Factor of Safety (FoS) of the critical layer shows a normal distribution as shown in Figure 71 and ranges between 0.14 and 1.02. Therefore, the method predicts that all of the critical layers liquefied. With the exception of eight cases (out of 178) the critical layer occurred within  $2 \times H_{FF}$ , meaning that in these cases the impact of the 'critical layer' causing deformation is greatly reduced, as the likelihood of deformation occurring at that depth is low. Of the remaining eight critical layers not within  $2 \times H_{FF}$ , four suffered no or low damage, one was an engineered feature deformation and the remaining three may be explained by data scatter due to limitations on the data set.

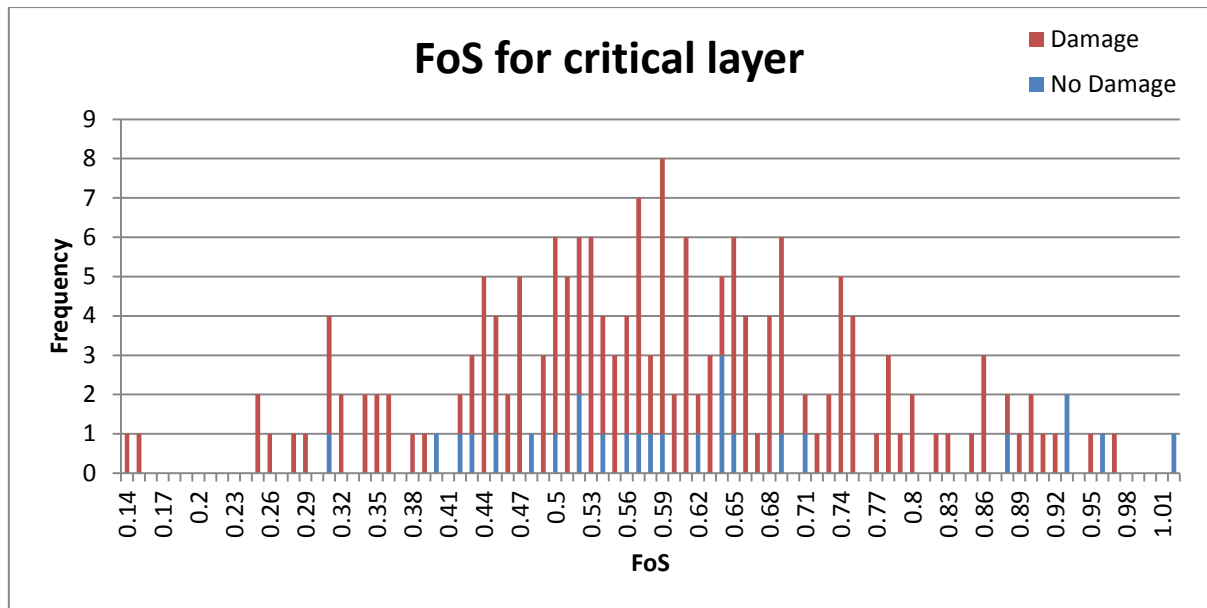


FIGURE 71: AVERAGE FOS OF THE CRITICAL LAYER

### 6.9.2 LATERAL SPREADING

Lateral spreading is difficult to predict as it involves a complex interplay of various factors including topography, soil profile, development and dissipation of pore pressures generated over the time history of an earthquake, residual strength and stiffness of liquefied soils and characteristics of ground motion. Slope angle does not appear to play a contributing factor in the influence of lateral spreading although this is not surprising as the minimum angle for lateral spreading to occur is low and the range of angles along the Avon and Kaiapoi Rivers is primarily between  $1^\circ$  and  $3.5^\circ$ . The height of channel must also be sufficiently high. Along the Avon River the channel ranges in height from 1.5 m to 3.5 m, and is slightly deeper in localised places up to 5m; along the Kaiapoi River the channel ranges in height from 2.5 m to 3.5 m. In all of these cases there is a sufficient free face and slope for lateral spreading to occur.

Most of the major to severe damage occurred in areas affected by lateral spreading, which tends to be more severe in the following circumstances:

- Within abandoned/old river channels
- Within fills/recent backfills (often found within old river channels that have been recently backfilled due to anthropogenic modification)
- Within the point bar deposit on a meandering river

Lateral stretch and spread was commonly associated with major to severe stopbank damage. As shown in Figure 72 cracks with width of greater than 200 mm are commonly associated with the major or severe damage zones, whereas there are generally fewer and narrower cracks adjacent to the no or low damage zones.



Property based EQC observations indicating areas which suffered lateral spreading induced damage verses areas that suffered only liquefaction induced damage can be compared with stopbank severity to demonstrate that the severity is often due to lateral spreading rather than just liquefaction alone. This is preliminary as the observations are property based, and therefore not directly adjacent to the river. They show that areas which suffered no or low damage there was a 57% likelihood of suffering some form of ground cracking as defined by the EQC, compared to an 83% likelihood in the areas that are classed as major or severe damage, as shown in Figure 73. This indicates that there are areas where the native ground suffered extensive damage that was not reflected in the stopbank system.

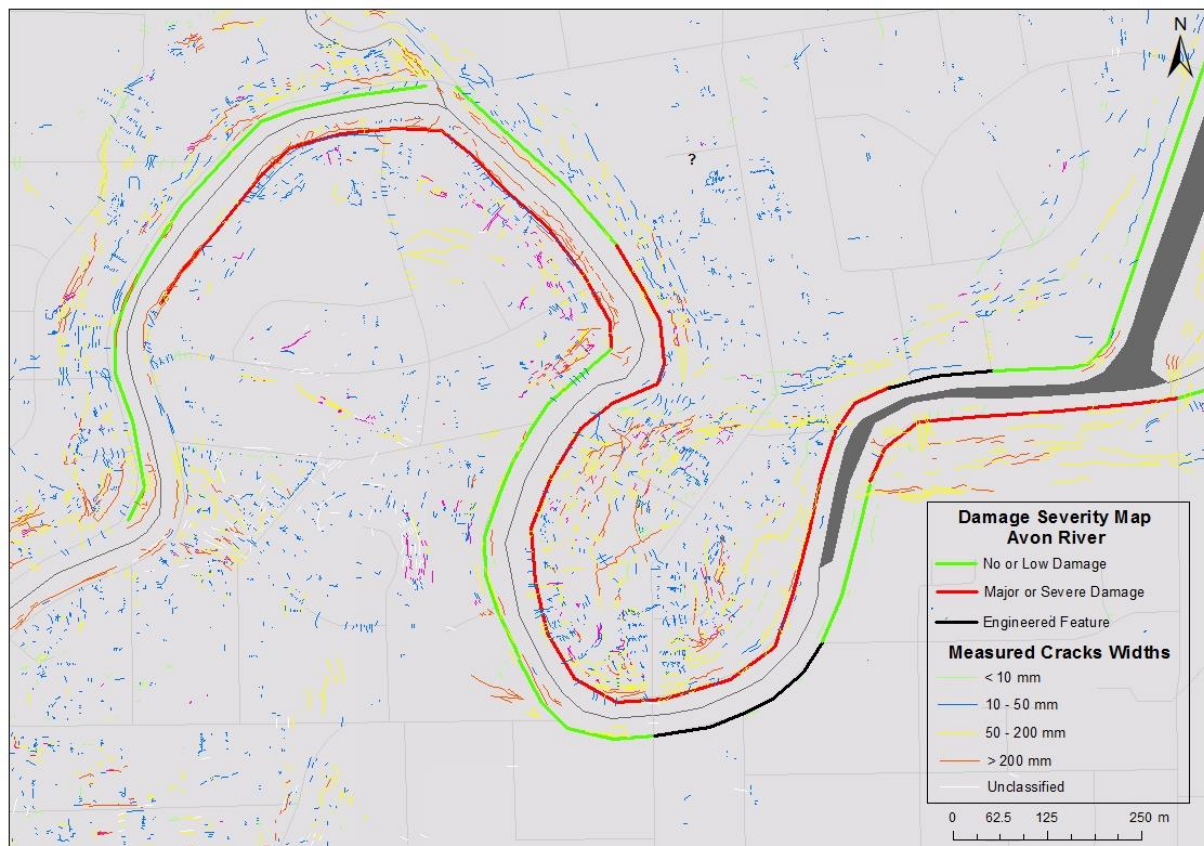
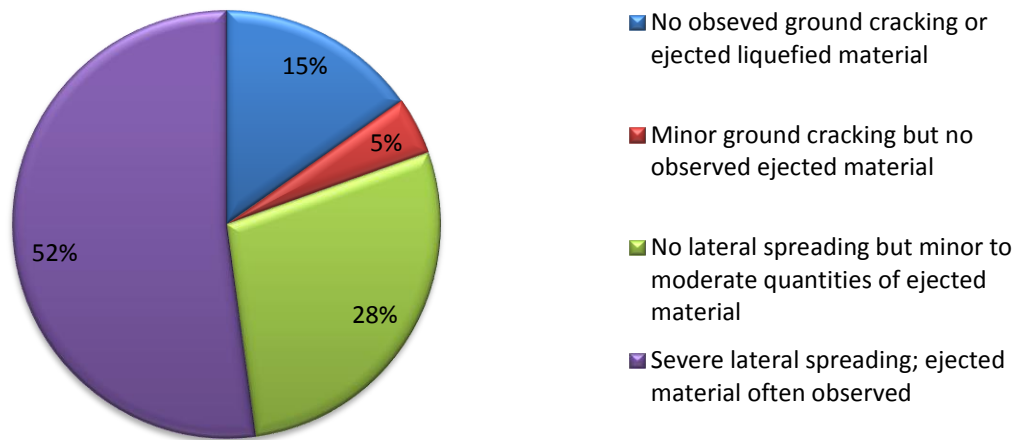


FIGURE 72: LOCATION OF CRACKS IN RELATION TO DAMAGE SEVERITY

### a) No or Low Damage



### b) Major or Severe Damage

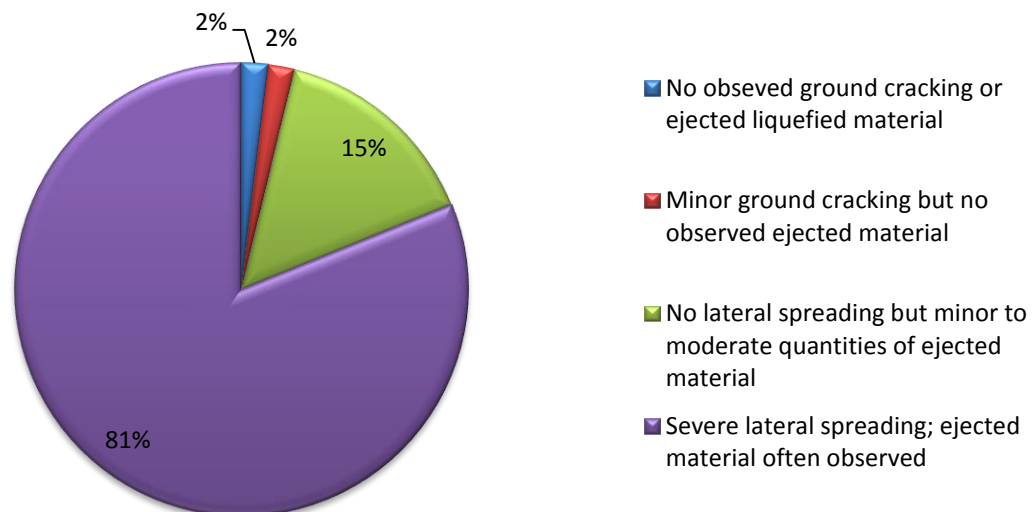
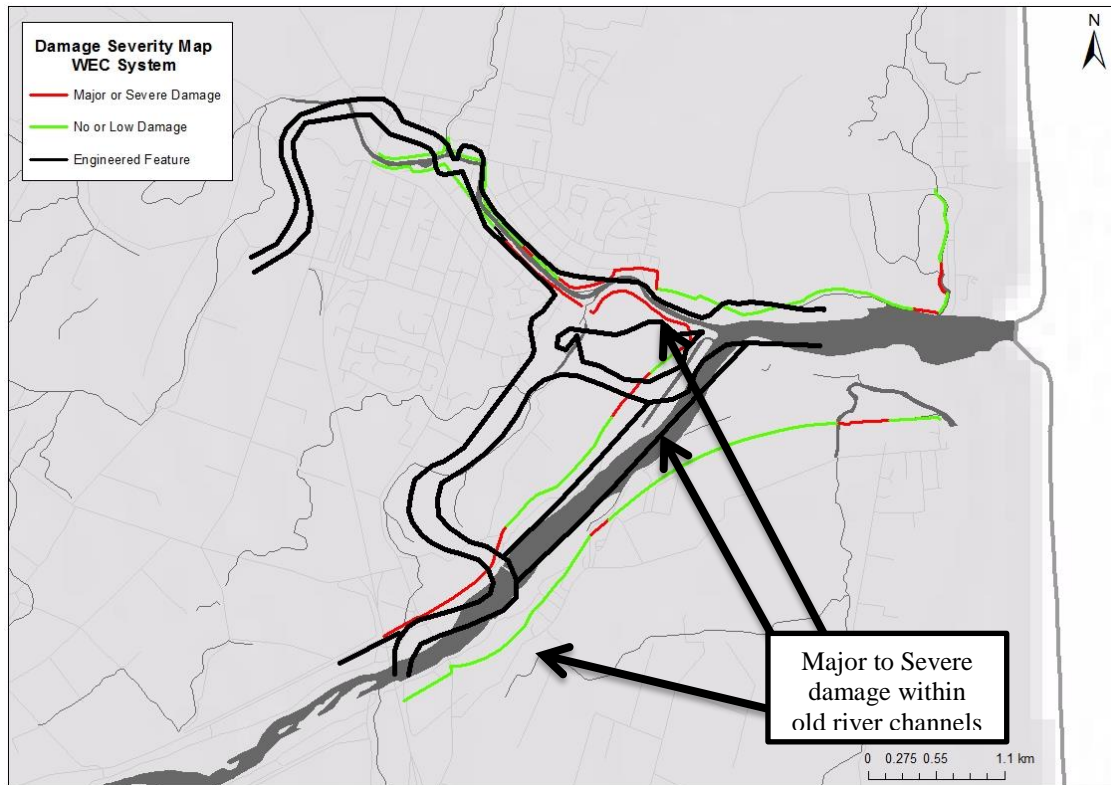


FIGURE 73: EQC LIQUEFACTION AND LATERAL SPREADING OBSERVATIONS IN AREAS OF A) NO OR LOW DAMAGE AND B) MAJOR OR SEVERE DAMAGE OF STOPBANKS

#### ABANDONED RIVER CHANNELS

The presence of abandoned river channels beneath the stopbank is a key indicator for damage along the WEC system where there has been extensive anthropogenic modification of the river system. As shown in Figure 74 major or severe damage correlates well with the presence of abandoned/old river channels. As mentioned previously, according to Wotherspoon et al. (2011) the areas underlain by old river channels in the Kaiapoi area were subject to some form of liquefaction, and in most areas however liquefaction and/or lateral spreading were significant.



**FIGURE 74: DAMAGE SEVERITY MAP FOR THE WEC SYSTEM SHOWING LOCATION OF ABANDONED RIVER CHANNELS**

A review has been undertaken of relevant geomorphological digital elevation models, for example the one presented in Figure 5 of Chapter 2, which may provide more information into smaller paleochannels that existed around the Kaiapoi and Waimakariri River. The review indicates that as well as the locations of the abandoned river channels shown in Figure 74 there are many other smaller channels which coincided with the other locations that have suffered major to severe damage. Therefore, it is reasonable to conclude that all of the major to severe damage observed to the stopbank system in Kaiapoi and Waimakariri was within or directly adjacent to an abandoned river channel. Furthermore, a small portion of areas with no to low damage occurred within the abandoned river channels.

Paleochannels are a failure point because they were deposited in different depositional settings that mean that the soils are looser than those in the surrounding areas and therefore are more susceptible to losses in shear strength (Lekkas et al., 2011). Stopbanks which experienced significant damage due to liquefaction generally reflected the geomorphic conditions beneath the stopbank, and had reasonably short failure lengths of 100 m to 300 m.

This is a useful conclusion to indicate the worth of a digital elevation model and old map review prior to stopbank design and as a measure of potential severity. However, Kaiapoi has a unique set of circumstance in that large areas have been backfilled with undocumented heterogeneous fill due to the anthropogenic changes in the river, which means that the deformation modes may not be representative of what would normally occur, if the river channels had been abandoned naturally through geological processes. It is

entirely likely that these recent deposits, created by the potentially uncontrolled backfilling of the abandoned river channels, contributed to the increased vulnerability to liquefaction and observed damage of the stopbanks at Kaiapoi.

#### POINT BAR/CUT BANK

The role of lateral spreading in the case of the Avon River is directly relevant to river morphology. As shown in Figure 61 the majority of the major to severe damage occurred within the meandering loops (the point bar) whereas the low or no damage zones are often located on the outside of the loops (the cut bar). The distribution for each of these locations is shown in Figure 75 for areas where no damage was observed and areas where damage was observed. These pie charts show that at every test location, within the point bar deposit on the river there was some observed damage, and where there was no observed damage the stopbank was constructed on either the cut bank slope or on a straight edge of the river.

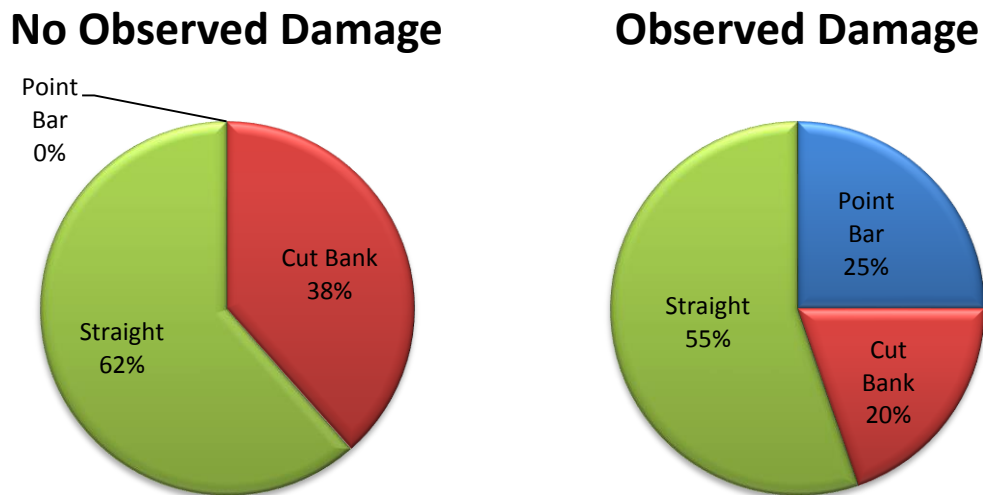


FIGURE 75: LOCATION ON RIVER COMPARING DISTRIBUTION OF CUT-BANK, POINT BAR OR STRAIGHT LENGTHS OF THE RIVER.

Robinson et al. (2012) explored this phenomenon further by computing maximum lateral displacements from transects within the point bar area and cut bank area of the Dallington/Avonside loop. As shown in Figure 76 the point bar data indicates a maximum horizontal displacement of about 1.8 m and an average of approximately 1.0 m; while the cut bank data shows a maximum of about 1 m and an average of only 0.3 m. The differences in the observed horizontal displacements can be attributed to the contrast in soil conditions characteristic of the depositional setting. As the river meanders downslope the point bar is deposited as the water cuts into the opposite bank due to its higher velocity at this point. Point bars are composed of sediment that is well sorted, loose and fine grained. They also have a very gentle slope and an elevation very close to water level meaning that the sediments are saturated closer to the water surface.

Although not statistically significant, the CPT results don't show any clear patterns of this depositional history, however there appears to be a greater total thickness of loose ( $Q_c < \sim 10$  MPa) liquefiable material

within the upper 6 meters associated with CPTs located along the point bar. It is expected that the influence of the channel would not be deeper than this as the Avon River is relatively young and the deeper sediments may have been deposited through different mechanisms.

Lateral continuation of the deposit may also influence the damage, within the meander loop it is reasonable to assume that there is a horizontally continuous deposit that may stretch for 10 s of metres of loose, well sorted materials that will all liquefy in a similar manner. However on the cutbank side of the river there may not be the horizontal continuity as the stratigraphy here is defined by an older depositional environment, therefore the materials may liquefy but there will be a complex interplay of factors that may cause the damage to not be as severe.

The other key factor that influences lateral spreading at these locations is the stresses acting on the soil due to the geometry. Within the meander the soil movement toward the river produces tensile stresses that create ground cracking. Conversely, at the cut bank the movement towards the river causes compressional stresses.

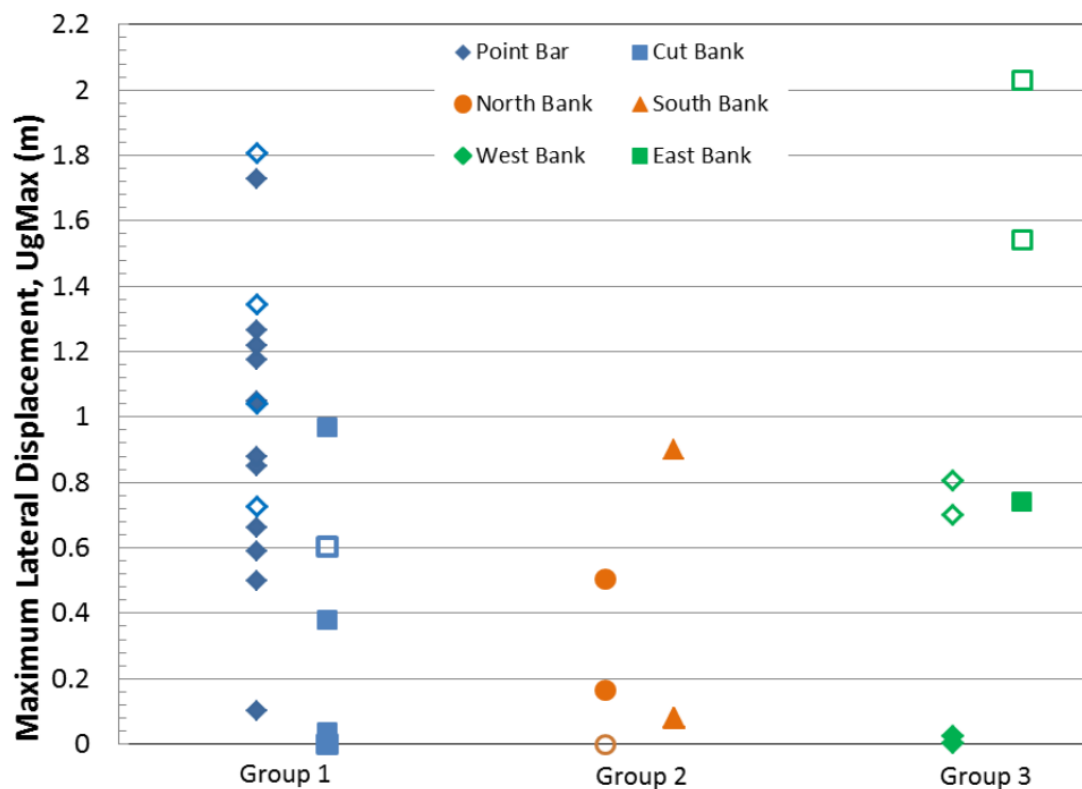


FIGURE 76: COMPARISON OF LATERAL SPREADING MEASUREMENTS WITHIN SPECIFIC AREAS ALONG THE AVON RIVER (SOLID SYMBOLS CORRESPOND TO 4 SEPTEMBER 2010 DATA, HOLLOW SYMBOLS CORRESPOND TO 22 FEBRUARY 2011 DATA); TAKEN FROM ROBINSON ET AL., 2012.

## 6.10 SUMMARY

This section has identified that the presence of liquefaction was the key trigger causing damage of stopbanks, and without liquefaction there was no damage. Furthermore increases in PGA did not result in increases in damage. Liquefaction, however, is not the only factor governing damage type and severity. Indeed there were stopbanks which suffered no damage even where liquefaction has occurred. This indicates a reliance of other factors which must be driving the type and severity of damage, such as ground conditions, depositional history (natural or manmade) and location along the river.

A number of calculated, land damage, stopbank damage and geomorphological parameters have been compared for 178 individual locations along the stopbank system. These locations were selected based on their proximity to a Cone Penetration Test (CPT) that has been used to infer the geological profile at each site and has been analysed to provide geotechnical parameters of the soil column.

Calculated parameters based on the geotechnical investigation data, event specific PGA and groundwater levels have been derived for each CPT location and comprise:

- i) Liquefaction Potential Index (LPI) for the critical layer and the top 10 m
- ii) Calculated settlement based on procedures defined in I & B (2008)
- iii) Non-liquefiable crust thickness
- iv) Depth and thickness of the critical liquefiable layer
- v) Cone resistance (QC) of the critical layer
- vi) Soil behaviour type ( $I_c$ ) of the critical layer
- vii) Factor of Safety (FoS) of the critical layer

A land damage index has been calculated using the following attributes that have been collected represent liquefaction effects on the native soils and comprise:

- i) Observed mapped ground cracks
- ii) Global lateral ground movement (derived from LiDAR flown surveys)
- iii) Vertical elevation change (derived from LiDAR flown surveys)
- iv) Mapped land damage category (derived from on foot surveys undertaken by the EQC)

These attributes have been quantified using a non-linear weighting system that represents the land damage influence of liquefaction and lateral spreading at an individual location.

The stopbank damage attributes that have been collected represent damage to the stopbanks and comprise:

- i) Stopbank deformation mode (from Chapter 5)
- ii) Damage/No Damage index
- iii) Repair/No Repair index for the secondary earthquake event at each location

These parameters have been used to create a severity index for each site which characterises the observed stopbank damage at each location in terms of 'no or low damage' and 'major or severe damage'.



Geomorphological parameters have been collected in an attempt to quantify the site specific geomorphology variables and depositional setting at each location. These comprise:

- i) Height of the channel (river)
- ii) Angle of the slope within 30 m of the river
- iii) Stopbank distance to the river (setback)
- iv) Location on the river (point bar/cut bank/straight)

The comparison of these results indicates that there is a critical liquefiable layer present at every location and the geotechnical parameters of this layer are relatively consistent across the study site.

Average QC values ranged from between 0.27 to 16.06 MPa, although these values are the extremes, with 66% of the distribution falling between 3.3 MPa and 8.0 MPa. Approximately 8% of the QC values for damaged stopbanks fall above 10 MPa, a threshold above which damage is considered to be unlikely. Of these critical layers exceeding a 10 MPa average, 40% were in areas affected by engineered failure damage.

$I_C$  of the critical layer showed a distribution of 1.5 to 2.5, above 2.4 there is a higher frequency of no damage than damage, indicating that a lower  $I_C$  cut-off could be more appropriate for Christchurch soils. As an  $I_C$  cut off of 2.6 has been used in the analysis as a boundary between triggering liquefaction verses not triggering liquefaction, we cannot say if there has been any damage to sites with an  $I_C$  of greater than 2.6.

The Factor of Safety (FoS) of the critical layer shows a normal distribution and ranges between 0.14 and 1.02, with the majority of the damaged stopbanks having a FoS of less than 0.8. Therefore, the data suggests that all of the critical layers liquefied. With the exception of eight cases the critical layer occurred within  $2 \times H_{FF}$ , meaning that shallow layers within  $2 \times H_{FF}$  are the most likely contributors / factors of damage.

Depositional setting appears to be the key aspect in determining severity and type of deformation. Specifically the presence or absence of abandoned / old river channels and the location on the river of the stopbank on a point bar / cut bank / straight part of the river. To investigate this further Kaiapoi was used as a case study to indicate the influence of the presence of abandoned river channels and the Avon River was used as case study into the location on the river of the stopbank.

Kaiapoi has a unique set of circumstance in that large areas have been backfilled with undocumented heterogeneous fill due to the anthropogenic changes in the river, which means that the deformation modes may not be representative of what would normally occur, if the river channels had been abandoned naturally through geological processes. A review of old maps and digital elevation models indicates that all of the major to severe damage observed to the stopbank system in Kaiapoi was within or directly adjacent to an abandoned river channel.

The distribution of damage verses no damage along the Avon River was compared with the location of the river. The results show that at every test location within the point bar deposit on the river there was some observed damage, and where there was no observed damage the stopbank was constructed on either the cut bank slope or on a straight edge of the river. This indicates that the point bar deposit is extremely vulnerable to earthquake-induced damage.

## 7.0 DISCUSSION, CONCLUSIONS AND RECOMMENDATIONS

### 7.1 CONCLUSIONS

This section presents a summary of key findings related to this study.

- The 4 September 2010 and 22 February 2011 Canterbury Earthquakes, as well as the major aftershocks, caused land damage along the natural banks and levees of the Waimakariri River and its tributary the Kaiapoi River and the Avon and Halswell Rivers.
- The majority of the damage to the Waimakariri, Eyre, Cust and Kaiapoi system (WEC system) occurred following the 4 September 2010 earthquake, whereas the majority of the damage to the Avon River occurred during the 22 February 2011 earthquake, although some additional damage occurred incrementally throughout the Canterbury earthquake sequence.
- The total damage length for all three rivers (including damage to stopbanks and damage to river banks) resulting from the cumulative effect of all four significant earthquakes was approximately 38 km, with a total of 28 km of damage to the stopbank system. The total surveyed length of the river was 48.7 km.
- The stopbank system along the Kaiapoi River comprises trapezoidal stopbanks ranging in height from 1.5 m to 4 m high, with 3:1 batters on both sides. The stopbanks for this scheme were designed to withstand a flood level flow of 4,730 m<sup>3</sup>/s plus a freeboard margin of 0.9 m and generally comprise silt and silty sand with minor gravel.
- There is not typical stopbank morphology for the Avon River, the flood protection system comprises small (less than 1 m high) compacted trapezoidal earth stopbanks which in some cases are retained from the river by a gabion wall. Standard practice for construction indicates a fill of well graded silty gravelly pit run, approximate fines content of 15% and a compaction of 95% maximum modified dry density.
- The damage at each location along the 28 km of damaged stopbank has been summarised into seven characteristic deformation modes based on post-earthquake surveys conducted by various consultancies and confirmed by a review of photographs. The following deformation modes have been identified:
  - a. DM1 – Bearing Capacity Failure; caused by loss of bearing capacity due to liquefaction in loose foundation soils.
  - b. DM2 – Minor Central Crest Settlement; caused by liquefaction where the crust is too thick or the soil layers are too thin to cause a loss of bearing capacity.
  - c. DM3 – Slumping; where liquefaction of the foundation soils has occurred directly adjacent to a free face, and the material has slumped in to the adjacent free face.

- d. DM4 – Lateral Stretch / Foundation Extension; caused by liquefaction of the foundation soil resulting in significant lateral stretch at the stopbank location.
  - e. DM5 – Differential Settlement; this is caused by liquefaction of the foundation soil where lateral spreading is minor and there has been no loss of bearing capacity or surface expressions of cracking.
  - f. DM6 – Rotational Deformation; this has occurred in fill materials in one location in Kaiapoi where the stopbank has failed along a preferred sliding plane due to earthquake shaking.
  - g. DM7 – Deformation to Engineered Feature; this occurred in locations where engineered features had been used as the primary source of flood protection, due to acceleration-induced or liquefaction-induced deformation.
- These deformation modes have been used to create a severity classification for the whole stopbank system, and have been used to classify the damage in to two categories; ‘no or low damage’ (DM2-MCCS, DM4-LS and DM5-DS) and ‘major or severe damage’ (DM1-BC, DM3-S, DM4-LS and DM6-RD).
  - The deformation modes and severity classification have been evaluated, analysed and compared with various geotechnical factors in order to come up with correlations that determine stopbank damage severity. A number of calculated, land damage, stopbank damage and geomorphological parameters have been compared for 178 individual locations along the stopbank system. These locations were selected based on their proximity to a Cone Penetration Test (CPT) that has been used to infer the geological profile at each site and has been analysed to provide geotechnical parameters of the soil column.
  - Calculated parameters based on the CPTs, event specific PGA and groundwater levels have been derived for each CPT location and comprise:
    - a. Factor of Safety (FoS) of the critical layer
    - b. Liquefaction Potential Index (LPI) for the critical layer and the top 10 m
    - c. Calculated settlement based on procedures defined in I & B (2008)
    - d. Non-liquefiable crust thickness
    - e. Depth and thickness of the critical liquefiable layer
    - f. Cone resistance ( $Q_C$ ) of the critical layer
    - g. Soil behaviour type ( $I_C$ ) of the critical layer
  - A non-linear weighting system that represents the land damage influence of liquefaction and lateral spreading at an individual location has been calculated using the following attributes that have been collected to represent liquefaction effects on the native soils and comprise:
    - a. Observed mapped ground cracks
    - b. Global lateral ground movement (derived from LiDAR flown surveys)
    - c. Vertical elevation change (derived from LiDAR flown surveys)
    - d. Mapped land damage category (derived from on foot surveys undertaken by the EQC)
  - The stopbank damage attributes that have been collected represent damage to the stopbanks and comprise:

- a. Stopbank deformation mode (from Chapter 5)
  - b. Damage/No Damage index
  - c. Repair/No Repair index for the secondary earthquake event at each location
- Geomorphological parameters have been collected in an attempt to quantify the site specific geomorphology variables and depositional setting at each location comprise:
  - a. Height of the channel (river)
  - b. Angle of the slope within 30 m of the river
  - c. Stopbank distance to the river (setback)
  - d. Location on the river (point bar/cut bank/straight)
- The analysis of the CPTs shows that there is a critical liquefiable layer present at every location and the geotechnical parameters of this layer are relatively consistent across the study site. With the exception of eight cases the critical layer occurred within  $2 \times (\text{Height of the Free Face}) H_{FF}$ , a depth below which deformation is not likely to occur.
- The majority of the  $q_c$  values of the critical layer (66%) ranged between 3.3 MPa and 8.0 MPa. Approximately 8% of the  $Q_C$  values for damaged stopbanks fall above 10 MPa, a threshold above which damage is considered to be unlikely. Of these critical layers exceeding a 10 MPa average, 40% were in areas affected by engineered failure damage. This may be due to the engineered structures reflecting damage more obviously than the stopbanks.
- An  $I_c$  cut off of 2.6 has been used in the analysis as a boundary between triggering liquefaction versus not triggering liquefaction, hence we cannot say if there has been any damage to stopbanks with an  $I_c$  of greater than 2.6. However,  $I_c$  of the critical layer showed a distribution of 1.5 to 2.5, above 2.4 there is a higher frequency of no damage than damage, indicating that a lower  $I_c$  cut-off could be more appropriate for Christchurch soils.
- The Factor of Safety (FoS) of the critical layer shows a normal distribution and ranges between 0.14 and 1.02, with the majority less than 0.8. Therefore, we can assume that all of the critical layers liquefied and of these 95% of the critical layers occurred within  $2 \times H_{FF}$ , meaning they could contribute to lateral spreading.
- The analysis has indicated that the presence of liquefaction was the key trigger causing damage of stopbanks, and without liquefaction there was no damage. The role of Peak Ground Acceleration (PGA) in triggering liquefaction was crucial to causing damage; however there was no correlation between increased PGA and increased damage. The threshold for damage is considered to be 0.13 g.
- Once liquefaction triggering has occurred severity of damage appears to be significantly influenced by the depositional history (natural or manmade) and location along the river, specifically the presence or absence of abandoned / old river channels and the location on the river of the stopbank on the point bar deposit of the river. This is due to these areas having a high susceptibility to lateral spreading as well as liquefaction.
- The Kaiapoi River was used as a case study to investigate the correlations between old river channels and stopbank damage. A review of digital elevation models and old maps found that all of the major to severe damage observed occurred within or directly adjacent to an abandoned river

channel. Furthermore, a small portion of areas with no to low damage occurred within the abandoned river channels.

- The Avon River was used as a case study to investigate the effects of a meandering river on the stopbank. The results of the analysis showed that every location within a point bar flood deposit suffered some form of damage. This is due to the depositional environment creating a flood deposit highly susceptible to liquefaction that has a high lateral continuity and has tensile stresses acting on it that create ground cracking.

## 7.2 DISCUSSION

This thesis has considered the mechanisms of failure behind liquefaction-induced stopbank damage and factors that have influenced the nature and severity of stopbank deformation during the 2010 – 2011 Canterbury Earthquakes. The observed and recorded response of the stopbank system along the Kaiapoi, Waimakariri and Avon Rivers has been summarised into seven key deformation modes and two damage severity classifications. The deformation modes and damage severity have been compared with land damage parameters, geomorphological parameters, and geotechnical parameters calculated from the analysis of Cone Penetration Tests (CPTs). These deformation modes and comparisons are discussed below and conclude that liquefaction is the key driving mechanism behind stopbank damage, and lateral spreading is the mechanism that defines the severity of damage.

The majority of research work that has been carried out relating to liquefaction-induced stopbank damage confirms that when the foundation soils beneath a stopbank liquefy large permanent deformations and even complete failure of earth embankments may occur. Valuable lessons have been learnt primarily from Japanese earthquake including the 2011 Tohoku, 1993 Hokkaido-nansei-oki and 1995 Hyogoken-nanbu earthquakes. These case histories provide an insight into typical failure modes of stopbanks including extensive slumping, cracking and differential settlement of the crest, both parallel and perpendicular to the crest, and bulging at the toe. Most of the case histories indicate foundation failure although some indicate liquefaction of the levee fill itself.

The Canterbury earthquakes have provided a unique opportunity to undertake a regional assessment of the effects of liquefaction on a stopbank system. The study is unique in that the research area encompasses two significantly different river morphologies with different stopbank systems and requirements. The analysis carried out was only possible due to the relatively high level of information relating to:

- a) The ground acceleration distribution through the earthquake series based on numerous strong ground motions stations
- b) The frequency of CPT data allowing a thorough understanding of the geological profile
- c) A well-developed groundwater model showing the water table during the main earthquake events
- d) Mapping of the stopbank damage after each of the main earthquakes
- e) LiDAR data showing vertical and horizontal ground settlements
- f) A comprehensive map showing the location of observed ground cracks following the main earthquakes

Assigning a characteristic deformation mode to each damaged length of stopbank based on this information provides an opportunity to summarise the key deformation characteristics are contributing factors to different deformation modes. As there is inherent variability in the foundation soils and stopbanks at each location it is not possible to develop a complete list of deformation modes that occurred as a result of the Canterbury Earthquake Sequence. These deformation modes have been eventually used as the basis for defining a severity classification on which the majority of the analysis within this thesis is based, discriminating between ‘no or low damage’ and ‘major or severe damage’.

This data can then be combined into large datasets and used to extract trends in the data. Upon undertaking this analysis it became immediately apparent that there would be no statistically significant trends extracted from the data population between deformation modes and any of the analysed factors. Each individual deformation mode involves a complex interplay of factors that are difficult to represent through correlative analysis. In order to do this, the variability in the generated datasets would need to be reduced. This could be reduced if there were a significantly greater number of subsurface geotechnical investigations and a higher resolution damage data set of the stopbanks following the major earthquakes.

Whilst the data set may not be satisfactory to draw conclusions about the individual deformation modes one can derive the key factors that have affected severity of deformation. Specifically that the presence of liquefaction was the key trigger causing damage of stopbanks, and without liquefaction there was no damage. Furthermore, there were stopbanks which suffered no damage even where liquefaction has occurred. This indicates a reliance of other factors which must be driving the type and severity of damage, such as ground conditions, depositional history (natural or manmade) and location along the river.

### 7.2.1 LIQUEFACTION TRIGGERING

It has been shown that stopbank damage is directly related to the presence of liquefaction in the ground materials beneath the stopbanks, but is not critical in determining the type or severity of damage, instead it is merely the triggering mechanism. From this one may assume that with increasing Peak Ground Acceleration (PGA) you would observe an increasing degree of damage. This however is not the case and it is apparent that an increased PGA does not correlate to increased damage, ie. Once liquefaction is triggered it is the gravity-induced deformation that causes the damage in addition to the damage induced during shaking. However, it should also be noted that the Canterbury earthquakes have only tested the stopbank system with short durations of shaking, and a longer duration earthquake (such as the Alpine Fault) could produce larger number of significant load cycles that may result in more damage.

It would be reasonable to assume that at lower PGAs (that were experienced by the flood protection system during smaller aftershocks) liquefaction would not be triggered and damage/repairs would not be seen or required. Hence, the importance of a threshold  $PGA_{M7.5}$  required for triggering of damaging liquefaction.

### 7.2.2 GEOTECHNICAL PROPERTIES OF THE CRITICAL LAYER

The analysis of the 178 CPTs indicates that there is a critical liquefiable layer present at every location and the geotechnical parameters of this layer are relatively consistent across the study site. With the exception of eight cases the critical layer occurred within  $2 \times (\text{Height of the Free Face}) H_{FF}$ , a depth below which



deformation is not likely to occur. The critical layers all show representative geotechnical parameters of a liquefiable layer, with anomalies generally due to data scatter or engineered features where poor construction may also play a significant role in deformation. The key limitation in identifying the data set is the influence of interbedded materials within the critical layer. Logically, having interbedded layers throughout a critical layer would play a role in reducing the severity of the impact of liquefaction at the surface. This, however, is difficult to quantify and therefore remains a significant limitation in understanding the performance of the critical layer.

### 7.2.3 LATERAL SPREADING

Old paleochannels were identified as a key failure point because they were deposited in different depositional settings that mean that the soils are looser than those in the surrounding areas and therefore are more susceptible to liquefaction loss and shear strength. This is a useful conclusion to indicate the worth of a simple and cost-effective geomorphology review of digital elevation models and old maps prior to stopbank design, which can then be used to locate potential areas of severe risk.

The results of the analysis showed that every location within a point bar flood deposit suffered some form of damage. Although these results aren't well confirmed by the CPT analysis it is reasonable to assume that depositional setting has resulted in shallow deposits composed of sediment that is well sorted, loose and fine grained. They also have a very gentle slope and an elevation very close to water level meaning that the sediments are saturated closer to the water surface.

Lateral continuation of the deposit may also influence the damage, within the meander loop it is reasonable to assume that there is a horizontally continuous deposit that may stretch for 10 s of metres of loose, well sorted materials that will all liquefy in a similar manner. However on the cutbank side of the river there may not be the horizontal continuity as the stratigraphy here is defined by an older and different depositional environment, therefore the materials may liquefy but there will be a complex interplay of factors that may cause the damage to not be as severe.

The other key factor that influences lateral spreading at these locations is the stresses acting on the soil due to the geometry. Within the meander the soil movement toward the river produces tensile stresses that create ground cracking. Conversely, at the cut bank the movement towards the river geometry promotes compressional stresses within the soil mass.

### 7.3 RECOMMENDATIONS

Advances in modern technology, specifically GIS, have provided a means of documenting lifeline networks and linear networks such as stopbanks and plays an important role in collating the associated data. Upon beginning this project it became apparent that there was not a detailed inventory of stopbanks along the Avon prior to the earthquakes. As well as having a detailed register of stopbanks, it is also important to make use of rapid response teams to survey damage following an earthquake event to try and document as much damage as possible before remediation works can commence. These two tools aligned can ensure that remediation is targeted to the critical areas which are at most immediate risk of other factors, such as flooding breaches, which can have a benefit from a cost perspective by ensuring that funding is targeted at the areas which need it the most. This documentation process is crucial as, as we have found, the rapid response and repair can mask any evidence of damage and potential learning's are lost.

From these findings it has been deduced that the key issue that needs to be considered in designing stopbanks in the Canterbury region is liquefaction. In order to determine if liquefaction would be an issue one would need to determine the seismic hazard at the site and whether the foundation soils have liquefaction potential. The threshold for  $PGA_{M7.5}$  as determined by this study is considered to be around 0.13 g, so we can infer that once this threshold is met and liquefaction triggered the severity of damage will be determined by geomorphology rather than increased shaking duration or energy.

The presence, or lack of presence of liquefaction in the foundation soils can be inferred through subsurface investigations, geomorphology and historic events. Once this is established it can be used to help estimate the severity of the liquefaction at the site, which can then be used to establish how severe the deformation may be at that site.

This case study, the key deformation modes and key factors determining severity of deformation can be used to better understand the mechanisms of failure behind liquefaction-induced stopbank damage and factors that influence the nature and severity of stopbank deformation during an earthquake in New Zealand and around the world.

## 8.0 REFERENCES

- Adachi, T., and Oka, F., 1997, Deformation and progressive failure in geomechanics, Pergamon Pr.
- Ambraseys, N., and Sarma, S., 1967, The response of earth dams to strong earthquakes: *Geotechnique*, v. 17, no. 3, p. 181-213.
- Been, K., and Jefferies, M., State parameter for sands, in *Proceedings International Journal of Rock Mechanics and Mining Sciences and Geomechanics Abstracts* 1985, Volume 22, Elsevier Science, p. 198-198.
- Bradley, B., and Hughes, M., 2012, Conditional Peak Ground Accelerations in the Canterbury Earthquakes for Conventional Liquefaction Assessment – Technical Report for the Ministry of Business, Innovation and Employment Department of Building and Housing Te Tari Kaupapa Whare.
- Brown, L., and Weeber, J., 1992, Geology of the Christchurch urban area: Institute of Geological and Nuclear Sciences Geological Map 1: Institute of Geological and Nuclear Sciences Limited, Lower Hutt, New Zealand, scale, v. 1, no. 25,000, p. 1.
- Browne, G. H., and Naish, T. R., 2003, Facies development and sequence architecture of a late Quaternary fluvial-marine transition, Canterbury Plains and shelf, New Zealand: implications for forced regressive deposits: *Sedimentary Geology*, v. 158, no. 1, p. 57-86.
- Canterbury Geotechnical Database, <https://canterburyrecovery.projectorbit.com/SitePages/Home.aspx> accessed via Google Earth.
- Canterbury Geotechnical Database, "Vertical Ground Surface Movements", Map Layer CGD0600 - 23 July 2012, retrieved 27 April 2013.
- Canterbury Geotechnical Database, "Horizontal Ground Surface Movements", Map Layer CGD0700 - 23 July 2012, retrieved 27 April 2013.
- Canterbury Geotechnical Database. "Aerial Photography", Map Layer CGD0100 - 1 June 2012, retrieved 27 April 2013.
- Canterbury Geotechnical Database, "Liquefaction and Lateral Spreading Observations", Map Layer CGD0300 - 23 July 2012, retrieved 27 April 2013.
- Canterbury Geotechnical Database, "Liquefaction Interpreted from Aerial Photography", Map Layer CGD0200 - 23 July 2012, retrieved 27 April 2013.
- Canterbury Geotechnical Database, "Observed Ground Crack Locations", Map Layer CGD0400 - 23 July 2012, retrieved 27 April 2013.
- Canterbury Geotechnical Database, "Conditional PGA for Liquefaction Assessment", Map Layer CGD5110 - 27 September 2012, retrieved 27 April 2013.
- California Department of Water Resources (CDWR), 2012, Urban Levee Design Criteria, Floodsafe California and Department of Water Resources.

California Department of Water Resources (CDWR) and California Business District Association (CBDA), 2005, Preliminary Seismic Risk Analysis Associated with Levee Failures in the Sacramento – San Joaquin Delta.

Craig, R. F., 2004, *Craig's soil mechanics*, Taylor & Francis.

Cubrinovski, M., 2011, *Seismic effective stress analysis: modelling and application*.

Cubrinovski, M., Bradley, B., Wotherspoon, L., Green, R., Bray, J., Wood, C., Pender, M., Allen, J., Bradshaw, A., and Rix, G., 2011a, Geotechnical aspects of the 22 February 2011 Christchurch earthquake.

Cubrinovski, M., Bray, J. D., Taylor, M., Giorgini, S., Bradley, B., Wotherspoon, L., and Zupan, J., 2011b, Soil liquefaction effects in the central business district during the February 2011 Christchurch earthquake: *Seismological Research Letters*, v. 82, no. 6, p. 893-904.

Cubrinovski, M., Green, R., Allen, J., Ashford, S., Bowman, E., Bradley, B., Cox, B., Hutchinson, T., Kavazanjian, E., and Orense, R., 2010, Geotechnical reconnaissance of the 2010 Darfield (New Zealand) earthquake: University of Canterbury. Civil and Natural Resources Engineering.

Cubrinovski, M., and McCahon, I., 2011, *Foundations on deep alluvial soils: University of Canterbury, Christchurch*, v. 40.

Cubrinovski, M., Robinson, K., Taylor, M., Hughes, M., and Orense, R., 2012, Lateral spreading and its impacts in urban areas in the 2010–2011 Christchurch earthquakes: *New Zealand Journal of Geology and Geophysics*, v. 55, no. 3, p. 255-269.

De Mets, C., Gordon, R., Argus, D., and Stein, S., 1990, Current plate motions: *Geophysical journal international*, v. 101, no. 2, p. 425-478.

Department of Public Works and Highways (DPWH), 2002, *Japanese Technical Standard and Guidelines for Planning and Design - Project for the Enhancement of Capabilities in Flood Control and Sabo Engineering of DPWH*.

Environment Canterbury, 2011, *WRRP Management Plan - Kaiapoi Island Chapter 2*, in Park, W. R. R., and Canterbury, E., eds.

Federal Emergency Management Agency (FEMA), 2008, *Proposed interim design criteria for urban and urbanizing state-federal project levees*.

Fifield, R. L., 2011, *Integrated stormwater management in the Avon River catchment*.

Forsyth, P. J., Jongens, R., and Barrell, D. J. A., 2008, *Geology of the Christchurch area*, GNS Science Lower Hutt, New Zealand.

Fry, B., and Gerstenberger, M. C., 2011, Large Apparent Stresses from the Canterbury Earthquakes of 2010 and 2011: *Seismological Research Letters*, v. 82, no. 6, p. 833-838.

Institute of Geological and Nuclear Sciences (GNS), N., Brown, L. J., Reay, M., and Weeber, J. H., 1992, *Geology of the Christchurch urban area*, Institute of Geological and Nuclear Sciences.

GHD, 2011, *Work Package Concept Report: Lower Avon River Stopbanks - Engineering Review*, v. 3, no. IRWP/001.

-, 2012, *Investigation into the river and tidal flood protection needs in Christchurch - Avon River Stage 1 Report*.

- Gledhill, K., Ristau, J., Reyners, M., Fry, B., and Holden, C., 2011, The Darfield (Canterbury, New Zealand) Mw 7.1 earthquake of September 2010: A preliminary seismological report: *Seismological Research Letters*, v. 82, no. 3, p. 378-386.
- Golder, 2003, *Dike Design and Construction Guide - Best Management Practices for British Columbia*, Ministry of Water, Land and Air Protection, Golder Associates Ltd. and Associated Engineering (B.C.) Ltd.
- , 2012, *The Seismic Design Guidelines for Dikes - Ministry of Forests, Lands and Natural Resource Operations Flood Safety Section*.
- Harder, L., Kelson, K., and Kishida, T., 2011, Preliminary Observations of Levee Performance and Damage following the March 11, 2011 Tohoku Offshore Earthquake, Japan: *Geotechnical Extreme Events Reconnaissance (GEER)*.
- Harris, 2003, *Climate Change Case Study: Assessment of the impacts of sea level rise on floodplain management planning for the Avon River*: Harris Consulting.
- Hatanaka, M., 1952, Three-dimensional considerations on vibrations of earth dam.: *Journal of the Japan Society of Civil Engineers, JSCE*, v. 37(10), p. 1-6.
- Hawkins, D. N., 1957, *Beyond the Waimakariri: a regional history*, Whitcombe and Tombs.
- Heslop, I., *Effect of Canterbury Earthquakes on Waimakariri, Kaiapoi & Halswell Rivers - Flooding & Drainage Perspectives*, in *Proceedings Symposium 2011: IPENZ and Rivers Group* 2011.
- Huang, Y., Yashima, A., Sawada, K., and Zhang, F., 2008, Numerical assessment of the seismic response of an earth embankment on liquefiable soils: *Bulletin of Engineering Geology and the Environment*, v. 67, no. 1, p. 31-39.
- , 2009, A case study of seismic response of earth embankment foundation on liquefiable soils: *Journal of central south university of technology*, v. 16, no. 6, p. 994-1000.
- Idriss, I., and Boulanger, R. W., 2008, *Soil liquefaction during earthquakes*, Earthquake Engineering Research Institute.
- Ishihara, K., *Stability of natural deposits during earthquakes*, in *Proceedings Proc., 11th Int. Conf. on Soil Mechanics and Foundation Engineering 1985a*, Volume 2, Balkema Rotterdam, The Netherlands, p. 321-376.
- Ishihara, K., 1985b, *Stability of Natural Deposits during earthquakes*. *Proceedings of the Eleventh International Conference on Soil Mechanics and Foundation Engineering*, San Francisco, 12-16 August 1985: Publication of: Balkema (AA).
- , 1996, *Soil behaviour in earthquake geotechnics*: Oxford : Clarendon Press ; New York : Oxford University Press, 1996, p. 350.
- Isoyama, R., *Liquefaction-induced Ground Failures and Displacements along the Shiribeshi-toshibetsu River Caused by the 1993 Hokkaido-nansei-oki Earthquake*, in *Proceedings Proceedings of the 5th US Japan Workshop on Earthquake Resistant Design of Lifeline Facilities and Countermeasures for Soil Liquefaction 1994*, p. 1-26.
- Iwasaki, T., Arakawa, T., and Tokida, K.-I., 1984, Simplified procedures for assessing soil liquefaction during earthquakes: *International Journal of Soil Dynamics and Earthquake Engineering*, v. 3, no. 1, p. 49-58.

- Iwasaki, T., Tatsuoka, F., Tokida, K.-i., and Yasuda, S., A practical method for assessing soil liquefaction potential based on case studies at various sites in Japan, in *Proceedings Proc., 2nd Int. Conf. on Microzonation* 1978, p. 885-896.
- Kano, S., Sasaki, Y., and Hata, Y., 2007, Local failures of embankments during earthquakes: Soils and foundations, v. 47, no. 6, p. 1003-1015.
- Lekkas, E., Andreadakis, E., Alexoudi, V., Kapourani, E., and Kostaki, I., The Mw= 9.0 Tohoku Japan earthquake (March 11, 2011) tsunami impact on structures and infrastructure, in *Proceedings Environmental Geosciences and Engineering Survey for Territory Protection and Population Safety (EngeoPro)* International conference, Moscow 2011, p. 97-103.
- MBIE (Ministry of Business, Innovation and Employment), December 2012, *Repairing and rebuilding houses affected by the Canterbury earthquakes*, Version 3, available from: [www.dbh.govt.nz](http://www.dbh.govt.nz)
- McCracken, S., and Surman, M., 2012, Halswell Drainage District Revised Earthquake Reinstatement Plan: Environment Canterbury, R12/10.
- Miller, E. A., and Roycroft, G. A., 2004, Seismic performance and deformation of levees: four case studies: *Journal of Geotechnical and Geoenvironmental Engineering*, v. 130, no. 4, p. 344-354.
- Moss, R., Seed, R. B., Kayen, R. E., Stewart, J. P., Der Kiureghian, A., and Cetin, K. O., 2006, CPT-based probabilistic and deterministic assessment of in situ seismic soil liquefaction potential: *Journal of Geotechnical and Geoenvironmental Engineering*, v. 132, no. 8, p. 1032-1051.
- Murashev, A., Davey, R., Brabhakaran, P., and Curley, B., 2006, Earthquake Risk Assessment of Flood Protection Assets in the Wellington Region, NZSEE Conference.
- National Institute for Land and Infrastructure Management (NILIM), International Centre for Water Hazard (ICHARM), and Public Works Research Institute (PWRI), 2008, The Japanese Ministry of Land, Infrastructure, Transport and Tourism's Technical Criteria for River Works: Practical Guide for Planning.
- NZS1170.5:2004, Structural Design Actions Part 5: Earthquake actions - New Zealand: New Zealand Standard.
- Ozutsumi, O., Sawada, S., Iai, S., Takeshima, Y., Sugiyama, W., and Shimazu, T., 2002, Effective stress analyses of liquefaction-induced deformation in river dikes: *Soil Dynamics and Earthquake Engineering*, v. 22, no. 9-12, p. 1075-1082.
- Pender, M., and Robertson, T., 1987, Edgecumbe earthquake: reconnaissance report, Earthquake Engineering Research Institute.
- Perry, E. B., 1994, Proceedings of the Repair, Evaluation, Maintenance, and Rehabilitation Research Program Workshop on Levee Rehabilitation Held at Vicksburg, Mississippi on 17 March 1992: DTIC Document.
- Pettinga, J. R., Yetton, M. D., Van Dissen, R. J., and Downes, G., 2001, Earthquake source identification and characterisation for the Canterbury region, South Island, New Zealand: *Bulletin of the New Zealand National Society for Earthquake Engineering*, v. 34, no. 4, p. 282-317.
- Reid, R. E., and Poynter, R. H., 1989, Waimakariri River Floodplain Management Plan.
- Reinfelds, I., and Nanson, G., 1993, Formation of braided river floodplains, Waimakariri River, New Zealand: *Sedimentology*, v. 40, no. 6, p. 1113-1127.



- , 2010b, Waimakariri and Kaiapoi River Stopbanks Preliminary Findings of Post-Earthquake Condition Assessment, 10820-A.
- , 2010c, Waimakariri and Kaiapoi River Stopbanks: Post Earthquake Condition Assessment.
- , 2011, Waimakariri and Kaiapoi River Stopbanks Findings of Condition Assessment post 22 February 2011 Earthquake.
- Robertson, P., and Wride, C., 1998, Evaluating cyclic liquefaction potential using the cone penetration test: Canadian Geotechnical Journal, v. 35, no. 3, p. 442-459.
- Robinson, K., Bradley, B., and Cubrinovski, M., 2012, Comparison of Actual and Predicted Measurements of Liquefaction-Induced Lateral Displacements during 2010 Darfield and 2011 Christchurch Earthquakes.
- Robinson, K., Cubrinovski, M., Kailey, P., and Orense, R., Field measurements of lateral spreading following the 2010 Darfield earthquake, in Proceedings Proceedings of the Ninth Pacific Conference on Earthquake Engineering 2011, p. 14-16.
- Rosidi, D., 2007, Seismic Risk Assessment of Levees: Civil Engineering Dimension, v. 9, no. 2, p. pp. 57-63.
- Sasaki, Y., 2009, River dike failures during the 1993 Kushiro-oki earthquake and the 2003 Tokachi-oki earthquake, Earthquake Geotechnical Case Histories for Performance-Based Design, CRC Press, p. 131-157.
- Sasaki, Y., and Shimada, K., 1997, Yodo River dike damage by the Hyogoken-nanbu earthquake. Seismic Behavior of Ground and Geotechnical Structures: Proc. of Discussion Special Technical Session on Earthquake Geotechnical Engineering during 14th International Conference on Soil Mechanics and Foundation Engineering., v. Hamburg/Germany: A. A. Balkema, 307-316.
- Scott, E. F., 1963, Notes and Comments on the Christchurch Drainage and Sewerage Systems: Christchurch Drainage Board.
- Seed, H. B., and Idriss, I., 1982, Ground motions and soil liquefaction during earthquakes, Earthquake Engineering Research Institute Berkeley eCA CA.
- Seed, R. B., Cetin, K. O., Moss, R. E., Kammerer, A. M., Wu, J., Pestana, J. M., Riemer, M. F., Sancio, R. B., Bray, J. D., and Kayen, R. E., Recent advances in soil liquefaction engineering: a unified and consistent framework, in Proceedings Proceedings of the 26th Annual ASCE Los Angeles Geotechnical Spring Seminar: Long Beach, CA2003.
- Stirling, M., McVerry, G., Gerstenberger, M., Litchfield, N., Van Dissen, R., Berryman, K., Barnes, P., Wallace, L., Villamor, P., and Langridge, R., 2012, National seismic hazard model for New Zealand: 2010 update: Bulletin of the Seismological Society of America, v. 102, no. 4, p. 1514-1542.
- Sugita, H., and Tamura, K., 2007, Development of Seismic Design Criteria for River Facilities against Large Earthquakes: Public Works Research Institute (PWRI), Tsukuba, Japan.
- T&T, 2010, Darfield Earthquake 4 September 2010 Geotechnical Land Damage Assessment & Reinstatement Report.
- Towhata, I., 2008, Geotechnical earthquake engineering, Springer.
- Towhata, I., Prasad, S., Honda, T., and Chandradhara, G., 2002, Geotechnical reconnaissance study on damage caused by 2001 Gujarat earthquake, India: Soils and foundations, v. 42, no. 4, p. 77-88.
- Towhata, I., Tokida, K., Tamari, Y., Matsumoto, H., and Yamada, K., Prediction of permanent lateral displacement of liquefied ground by means of variational principle, in Proceedings Proc., 3rd Japan-US

Workshop on Earthquake Resistant Design of Lifeline Facilities and Countermeasures for Soil Liquefaction, Technical Report NCEER-91-0001, NCEER1991, p. 237-251.

U.S. Army Corps of Engineers (USACE), 2003, United States Army Corps of Engineers Manual EM 1110-2-1913.

van Ballegooy, S., Malan, P., Jacka, M., Lacrosse, V., Leeves, J., Lyth, J., and Cowan, H., Methods for characterising effects of liquefaction in terms of damage severity.

Veltrop, J. A., 1992, The role of dams in the 21st century, US Committee on Large Dams.

Wang, W., Earthquake damage to earth and Levees in relation to soil liquefaction, in Proceedings Proc. of the Int. Conf. on Case Histories on Geotech. Engrg1984, Volume 1, p. 511-521.

Wotherspoon, L. M., Pender, M. J., and Orense, R. P., 2011, Relationship between observed liquefaction at Kaiapoi following the 2010 Darfield earthquake and former channels of the Waimakariri River: Engineering Geology.

Yegian, M., Ghahraman, V., and Gazetas, G., 1994, Ground-motion and soil-response analyses for Leninakan, 1988 Armenia earthquake: Journal of geotechnical engineering, v. 120, no. 2, p. 330-348.

Yetton, M., Traylen, N., and McCahon, I., 2011, 2010 Canterbury Earthquake: Liquefaction Report Selwyn District Council: Geotech Consulting Ltd., Reference 3680 Version 05.6.

Zealand, S. A. N., NZS 4203:1984, Coed of Practice for General Structural Design and Deisng Loadings for Buildings.

Zhang, G., Robertson, P., and Brachman, R. W., 2002, Estimating liquefaction-induced ground settlements from CPT for level ground: Canadian Geotechnical Journal, v. 39, no. 5, p. 1168-1180.

## APPENDIX A: CASE STUDIES

### INTRODUCTION

Ten cases of stopbank performance are reviewed focussing on trapezoidal soil stopbanks, and to cover various geological and geomorphological settings and stopbank characteristics. The case studies are also selected to represent stopbanks both with and without seismic design provisions. The case studies used for this study cover a range of variation in characteristics to help in deriving some generally applicable conclusions. Where available, for each case study, the seismic conditions during the earthquake, geometrical properties, material strengths, subsurface geology and any seismic provisions are presented. This appendix accompanies the literature review in Chapter 3 and the conclusions drawn are used as a basis for the Deformation Modes developed in Chapter 5.

### STRUCTURE

Each case study is broadly subdivided into subsections as follows:

- Introduction and earthquake details
- Characteristics of performance
- Mechanism(s) of failure
- Author's conclusions

Table 1 summarises the ten case studies examined.

**TABLE 1: CASE STUDIES OF PERFORMANCE OF STOPBANKS DURING EARTHQUAKES**

Case History No.	Earthquake Event	Magnitude	Key References
1	2011 Tohoku, Japan	$M_w = 9.0$	Harder et al. (2011); Lekkas et al. (2011)
2	2011 Tohoku, Japan	$M_w = 9.0$	Harder et al. (2011); Lekkas et al. (2011)
3	1966 Xingtai, China	$M_s = 6.8$ $M_s = 7.2$	Wang (1984)
4	1987 Edgecumbe, New Zealand	$M_w = 6.5$	Pender and Robertson (1987)
5	2001 Gujarat, India	$M_w = 7.7$	Towhata et al. (2002)
6	1993 Hokkaido-nansei-oki, Japan	$M_w = 7.8$	Isoyama (1994)
7	1993 Kushiro-oki, Hokkaido, Japan	$M_w = 7.6$	Sasaki (2009)
8	2003 Miyagiken-Hokubu, Tokachi-oki, Hokkaido, Japan	$M_w = 8.1$	Cubrinovski (2011); Sasaki (2009)
9	1989 Loma Prieta, San Francisco	$M_w = 6.9$	Miller and Roycroft (2004); Perry (1994); Yegian et al. (1994)
10	1995 Hyogoken-nanbu (Kobe), Japan	$M_w = 6.9$	Sasaki and Shimada (1997)

## CASE STUDY 1 – PERFORMANCE OF STOPBANK FOUNDATIONS IMPROVED WITH MIX-IN-PLACE SOIL COLUMNS DURING THE MW 9.0 TOHUKU EARTHQUAKE

This case study describes the damage of stopbanks constructed on liquefiable soils and dredged fill/reclaimed land as a result of the  $M_w$  9.0 Tohoku earthquake in Japan in March 2011.

### CHARACTERISTICS OF PERFORMANCE

Performance of stopbanks in the Miyagi Prefecture are summarised in Table 2. Generally this region suffered PGAs ranging from 0.27g to 0.66g with max PGAs of 0.94g recorded at the coast near the town of Oshika.

The stopbanks in the area are generally large with crest widths of up to 40 m and heights of up to 8 m. Settlements of 20 cm to 40 cm were recorded in areas where liquefaction had occurred (some isolated observations were greater than 40cm). In most areas, the general settlement of non-distressed stopbanks appeared to be about 7 cm to 15 cm (Harder et al., 2011).

**TABLE 2: TYPE AND NUMBER OF STOPBANK DAMAGE SITES REPORTED (TAKEN FROM GEER (2011))**

River System	Type and Number of Levee Damage Sites Reported							
	Failure	Settlement	Slope Slumping	Levee Cracking	Revetment /Wall Damage	Gate Damage	Other	Total
Mabuchi	0	1	1	1	5	1	5	13
Kitakami	13	62	47	278	121	67	58	646
Naruse	9	27	25	183	56	26	37	363
Natori	1	2	1	26	2	2	1	35
Abukuma	2	26	16	73	2	10	3	132
<b>TOTAL</b>	<b>25</b>	<b>118</b>	<b>90</b>	<b>561</b>	<b>186</b>	<b>106</b>	<b>104</b>	<b>1190</b>

In the Ibaraki Prefecture where the Hinuma River is located PGAs were generally lower at between 0.2 g and 0.5 g. Geotechnical reconnaissance following the earthquake indicated that the stopbank of the western bank of the Hinuma River suffered extensive damage from foundation liquefaction (Figure 1). The stopbank cracked and slumped continuously for over 2.5 km along the western margin of the shallow, near coastal lake (Harder et al., 2011).

The foundations of the stopbanks along the Hinuma River were understood to include man-made fills (dredged fill/reclaimed land). This was confirmed by sand boils generated in the liquefaction cracks that showed clean, fine to medium-grained sands. The stopbank itself was generally constructed from clayey sands and gravels. In some lengths along this stopbank the water level was about 1 m higher than on the land side of the stopbank (Lekkas et al., 2011).



**FIGURE 1: VIEW OF SLUMPED HINUMA RIVER LEFT STOPBANK INDUCED BY LIQUEFACTION (N36.2861, E140.5238., APRIL 24, 2011).**

#### MECHANISM OF FAILURE

Major damage can be ascribed mostly to foundation liquefaction. Paleochannels are also a failure point because they contain different soils than those in the surrounding areas and therefore may be more susceptible to losses in shear strength (Lekkas et al., 2011). Stopbanks which experienced significant damage due to liquefaction generally reflected the geomorphic conditions beneath the stopbank, and had reasonably short failure lengths of 100 m to 300 m.

The Hinuma River left stopbank was founded on dredged/reclaimed land and suffered extensive damage along its whole length. The conclusions drawn from the extent of the damage at this site (compared to other lengths of the river) was that damage appeared to reflect the presence of man-made foundation materials and/or lake water that was high enough to saturate both the foundation and the lower portions on the embankment. The length of liquefaction damage is thought to have significant implications for saturated stopbanks constructed of or on dredged fill or reclaimed land (man-made fill) rather than natural ground.

## CASE STUDY 2 – PERFORMANCE OF STOPBANK FOUNDATIONS IMPROVED WITH MIX-IN-PLACE SOIL COLUMNS DURING THE Mw 9.0 TOHUKU EARTHQUAKE

This case study compares treated and untreated stopbank foundations along the Naruse River, Japan, in order to gain an insight into the effectiveness of ground improvement on stopbanks. The stopbanks in the area are also large with crest widths of up to 40 m and height of up to 8 m. Several lengths along the Naruse River had major liquefaction damage during the 2003 Miyagi North Continuation earthquake ( $M_w$  6.2) and were repaired by removing the damaged stopbanks and using a mix-in-place soil cement foundation ground improvement technique to treat the foundation to the depth of liquefaction. The mix-in-place soil cement columns were constructed almost edge to edge along the entire stopbank footprint. After the Mw 9.0 Tohoku earthquake, four of the remediated sites were inspected (Harder et al., 2011) and it appeared that all four sites performed well.

Severe stopbank damage was recorded at multiple sites along the Naruse River in response to the Tohoku earthquake. Two of the treated sites had moderate liquefaction related stopbank damage directly beyond the limits of the ground treatment. In some cases, this resulted in transverse cracking at the interface between treated and non-treated sections of the stopbank. Takahashi & Sugita note that although the cost of these treatments was probably significant, it was successful in preventing major liquefaction-related damage.



Figure 2: (a) Aerial view of treatment area (adapted from Google Earth, 2011), (b) Longitudinal cracking and clumping of waterside stopbank slope downstream of treatment area, and (c) transverse cracking on stopbank crown at downstream edge of treatment area on Naruse River right stopbank (GEER Association Report No. GEER-025b)



### CASE STUDY 3 – DAMAGE TO STOPBANKS DUE TO LIQUEFACTION AND SLIPPAGE IN SOFT CLAYS DURING THE 1966 XINGTAI EARTHQUAKES

The 1966 Xingtai earthquakes of magnitude 6.8 on March 8 and magnitude 7.2 on March 22 caused serious damage to stopbanks and banks along the Fuyang River System due to liquefaction of saturated sands or due to slippage in weak layers of soft clays in the river banks and foundations of stopbanks.

#### CHARACTERISTICS OF PERFORMANCE

The first earthquake (March 8) had an intensity of VIII MM, caused no liquefaction-related slumping of the stopbank system. However when the intensity at the site increased to X MM during the second earthquake (March 22) significant damage was observed. The stopbanks along the left side of the river, underlain by loose soils of old river channels, suffered serious cracking and slumping towards the river. Whereas the stopbanks along the right side of the river, underlain by firm clayey soils, remained almost entirely intact. Two examples of damage due to liquefaction of young sand deposits in an abandoned river channel below the elevation of the current river bed are presented in Figure 3.

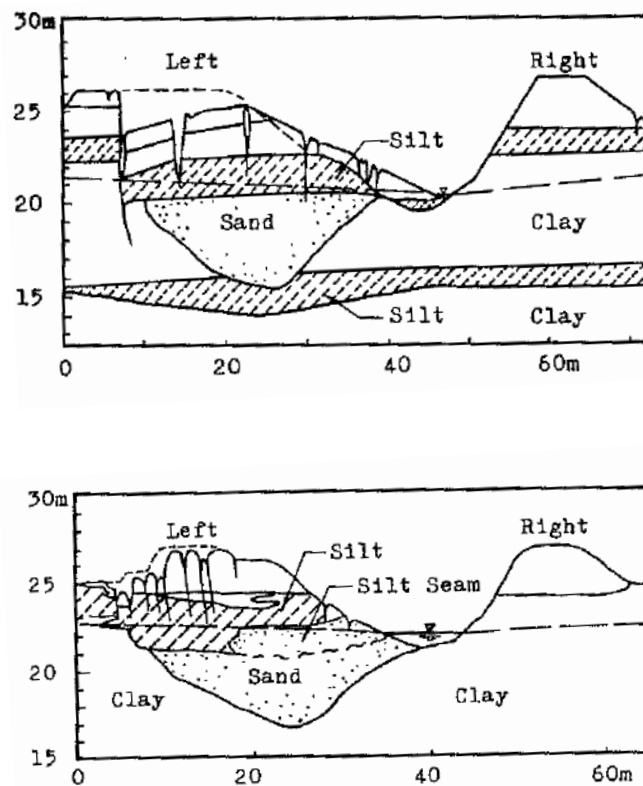


FIGURE 3: DAMAGE OF FUYANG RIVER BANK AND STOPBANK DUE TO LIQUEFACTION OF SATURATED SAND POCKETS

## MECHANISMS OF FAILURE

Slope failure due to weakness in soft clayey soils interbedded with thin layers of sands and silts occurred during the March 8 earthquake. The slope failures presented in Figure 4 are due to slippage on ‘weak materials’, namely materials with very low undrained shear strength (parameters as low as  $\phi = 6.5^\circ$  and  $c = 5$  kPa). Of note is that the foundation soils did not liquefy in the case of slope failure, rather the failure occurred in the weak soft clay layers.

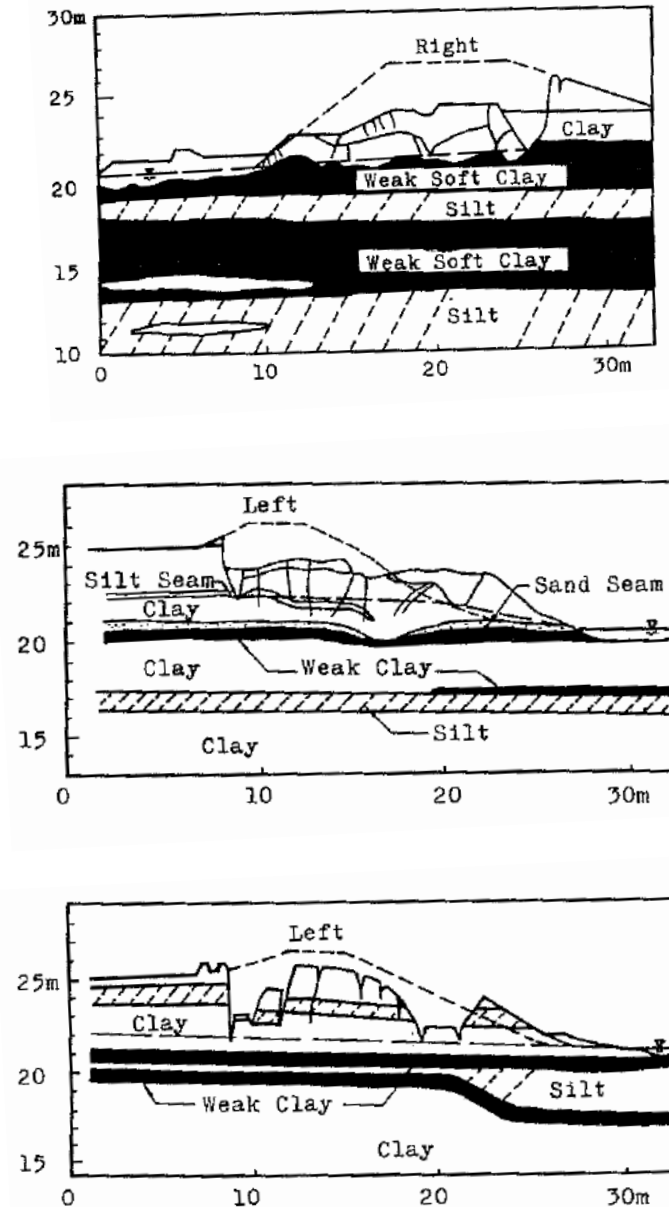


FIGURE 4: SLOPE FAILURE OF BANK AND STOPBANK IN FUYANG RIVER DUE TO SLIPPAGE ON (A) A THICK SOFT CLAY LAYER; (B) A THIN WEAK CLAY LAYER JUST BELOW A THIN SAND SEAM, AND (C) THIN WEAK CLAY LAYERS ADJACENT TO A THIN SILTY SEAM

## CASE STUDY 4 – FAILURE MECHANISMS OBSERVED DURING THE 1987 M6.3 EDGECUMBE EARTHQUAKE, NEW ZEALAND

The M6.3, Edgcumbe earthquake occurred on 2 March 1987 in the Bay of Plenty, New Zealand and caused extensive damage to the flood protection works on the river plains. All 26 km of stopbanks associated with major schemes in the area (the Rangitaiki, Tarawera and Whakatane Rivers) sustained some damage (Pender and Robertson, 1987).

### CHARACTERISTICS OF PERFORMANCE

Following the Edgcumbe earthquake, 1 to 2m of ground settlement was recorded, extending from where the fault crosses the river to downstream of Edgcumbe. The settlement occurred gradually (not instantaneous) after the earthquake and at some locations was measured to be up to 7 mm a day. Following the earthquake, all the stopbanks along the river were inspected for damage and the following types of damage were observed (Pender and Robertson, 1987):

- Cracking of river berm areas,
- Slumping of the stopbanks or movement/damage to floodwalls,
- Transverse and longitudinal cracking of stopbanks,
- Foundation failure of concrete walls, concrete wall failure,
- Cracking of the ground on the landward side of the stopbanks,
- Major failures of stopbanks in areas where the main fault line rupture crossed the river,
- Existing protection works slumped into the river.

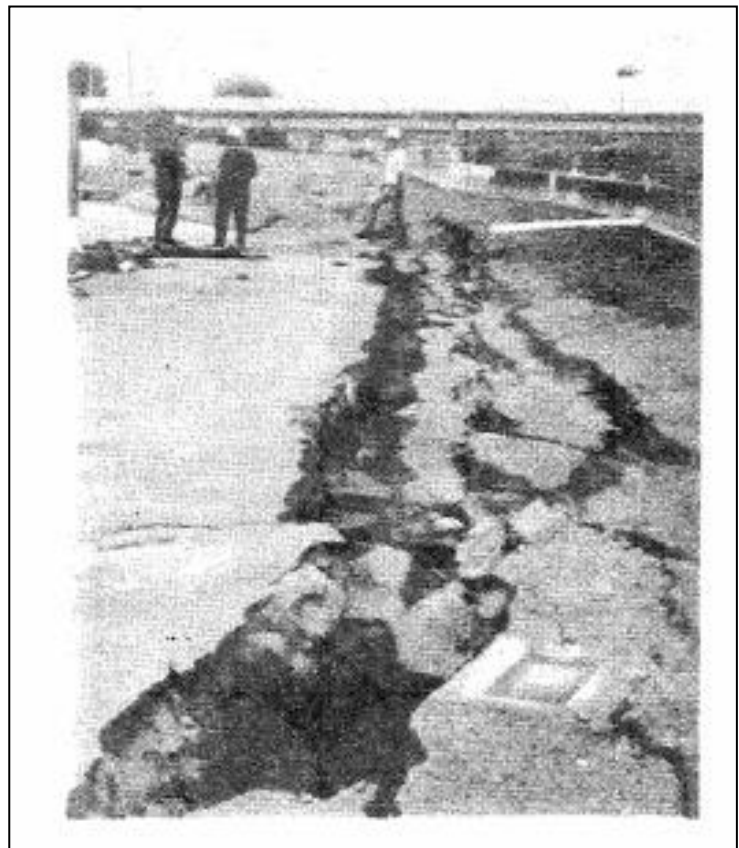


**FIGURE 5: THE TRUE RIGHT STOPBANK OF THE RANGITAIKI RIVER IN EDGECUMBE AFTER THE 1987 EARTHQUAKE**

### MECHANISM OF FAILURE

These failures were associated with liquefaction of young alluvial deposits within the plains. This is evident from sand boils and lateral spreading which were observed. The three main rivers within the damage zone all suffered similar styles of deformation, predominantly relating to lateral spreading (Pender and Robertson, 1987).

## CASE STUDY 5 – BEHAVIOUR OF EARTH DAMS FOUNDED ON SOFT NATURAL SOILS DURING THE 2001 GUJARAT, INDIA EARTHQUAKE

This case study describes the damage sustained to stopbanks resting on soft natural soils during seismic loading of the January 26<sup>th</sup>, 2001 Gujarat earthquake in India ( $M_w$  7.7). The learnings from this earthquake are focused on geotechnical aspects of damage related to earthfill dams. In this case, these are similar to the trapezoidal soil stopbanks focused on in this report, as construction of these dams occurred during elementary stages of soil mechanics understanding in India. A typical earthen dam in the Gujarat region generally extended a few km and was constructed of homogenous coarse materials with an impervious masonry wall, a filter and a longitudinal drain alongside the core wall.

### CHARACTERISTICS OF PERFORMANCE

Geotechnical reconnaissance of four of these dams following the earthquake resulted in the following findings:

- Longitudinal cracking at the crest, predominantly where the stopbank was founded on an old river bed,
- A lack of damage where the dam was founded on basalt bedrock, and;
- Subsidence, cracking and lateral spreading in overlying artificial fills occurred commonly in very soft ground with no frictional resistance during Swedish Sound Testing (where the material is too fine grained to expect liquefaction, ie.  $I_c$  is greater than 2.6).

### MECHANISM OF FAILURE

The presence of loose liquefiable materials through old river beds was associated with damage of longitudinal cracking in the dam. The solid bedrock foundation was attributed for the lack of damage. Although liquefaction and sand boiling was found at many places, these observations did not always accompany damaged fills. This indicates that some localised failures were not due to liquefaction of underlying foundation materials, but due to softening of the clay and silt layers and preferential sliding planes within these layers.

Subsidence, cracking and lateral spreading in overlying artificial fills is inferred to have been caused by a reduction of shear strength in the materials beneath the dam triggering a slope movement of soil and lateral spreading (including cracking of the dam body). Towhata et al. (2002) concluded that large distortions of the fills are associated with soft natural subsoils: *‘The amplification of seismic motion upon the soft subsoil as well as possibly the cyclic and residual deformation of this soft soil induced the damage to the dam body.’* It is suggested that subsoil improvement is key to avoiding repetition of similar damage during future earthquakes.

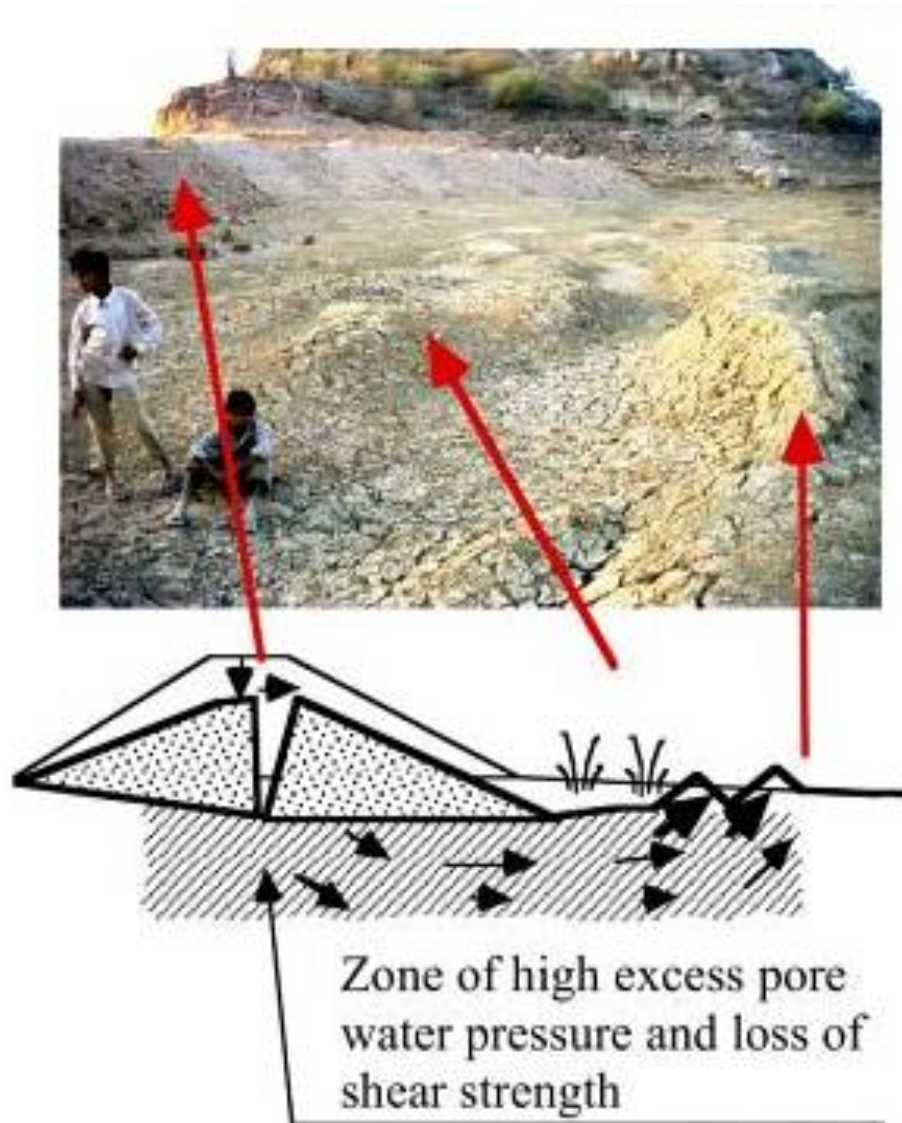


FIGURE 6: GROUND DEFORMATION IN SOFT FOUNDATION SOILS OF THE CHANG DAM (TOWHATA ET AL., 2002)

## CASE STUDY 6 – LIQUEFACTION-INDUCED GROUND FAILURES AND DISPLACEMENTS ALONG THE SHIRIBESHI-TOSHIBETSU RIVER CAUSED BY THE 1993 HOKKAIDO-NANSEI-OKI EARTHQUAKE

This case study summarises the effects of large-scale ground failures due to liquefaction and lateral spreading on the stopbank system of the Shiribeshi-toshibetsu River during the 1993 ( $M_w$  7.6) Hokkaido-nansei-oki earthquake. The earthquake caused damage to the substrate of five rivers, with the majority of the damage occurring along the Tokachi and Kushiro Rivers.

### CHARACTERISTICS OF PERFORMANCE

Lateral spreading was a significant factor in stopbank damage with horizontal displacements ranging from 1 to 3m through the area that liquefied. Vertical settlements due to liquefaction ranged from 0.5 to 1 m. The stopbanks mirrored this with vertical and horizontal settlements apparent along the river. The following observations were made from aerial photo surveys and interpretation of the ground deformations:

- The horizontal ground displacements, as mentioned above, are generally directed toward the extant crescent lakes on the old riverbed or waterways.
- The areas where ground deformation or sand boils occurred can be clearly distinguished from the areas without them. These borderlines often correspond to the topographical change points thought to be the old riverbeds.
- As for the points along the stopbank, the ground displaced mostly outward of the stopbank. The displacements apparently show the spreading or flattening of stopbanks.

The native soils adjacent to the stopbank suffered large-scale ground liquefaction in the alluvial lowlands.

### MECHANISM OF FAILURE

Soil investigations comprising boreholes with SPTs indicate a liquefiable layer comprising loose sands beneath the damage zone approximately 2 to 4 m thick. Soils beneath this depth were also found to have  $N$ -values = 7 and therefore may have potential to liquefy. The results show that severe liquefaction occurred inside the meandering of old river beds.

It is interesting to note that ground cracking related to lateral spreading, sand boils and associated settlement and ground displacements both horizontal and vertical were measured by comparing pre- and post- earthquake photos. As makeshift repairs and remediation generally begins almost immediately, it can be difficult to record in detail the geotechnical damage sustained at a site. Aerial photography immediately following a large earthquake would be extremely beneficial in dealing with this issue.

## CASE STUDY 7 – KUSHIRO RIVER STOPBANK FAILURES DUE TO LIQUEFACTION OF SUBMERGED FILL DURING THE 1993 KUSHIRO-OKI EARTHQUAKE

During the 1993 Kushiro-oki earthquake it was found that stopbank failures were induced by liquefaction of submerged fill. This condition was brought on by consolidation of a peat layer beneath the stopbanks. Stopbank failures in this case showed the importance of drainage to prevent the infiltrated rainwater from accumulating within a stopbank body.

### CHARACTERISTICS OF PERFORMANCE

Over 26 km of stopbanks were damaged along various rivers due to the  $M_w 7.8$  earthquake. Damage was varied along this length with both vertical and horizontal settlements apparent along the river that mirrored ground deformation (Sasaki, 2009). Figure 7 illustrates the typical view of the failed stopbank along the Kushiro River, with typical cross sections shown in Figure 8.

In this case, observed slip planes emanated diagonally within the stopbank from around the shoulder to its base.

### MECHANISM OF FAILURE

The stopbank was constructed directly on highly compressible peat deposits, which resulted in consolidation settlement (2 – 3 m) under the weight.

This settlement had two important effects. First it brought the lower part of the sand fill below the water table that existed at the time of the earthquake. This created the potential for liquefaction in the fill. Secondly, the large settlement caused a redistribution of stresses in the lower part of the stopbank. The stretching and arching of the stopbank reduced the confining stresses in the saturated region of the fill. It is considered that the saturated base of the stopbank was liquefied and this triggered the stopbank failure. This is supported by the observed fact that the amounts of subsidence at the stopbank crest during the earthquake increased with the amounts of consolidation of the peat deposits. Similar failure modes were seen following the  $M_w 9.0$  Tohoku earthquake in March 2011 (Harder et al., 2011).

Dynamic analysis on the stopbank showed the time history of porewater pressure analysed against the input motion of the Kushiro-oki earthquake. This revealed that the pore water pressure in the saturated sandy soil in the stopbank was built up showing complete liquefaction within ten seconds from the start of the shaking. The analysis results

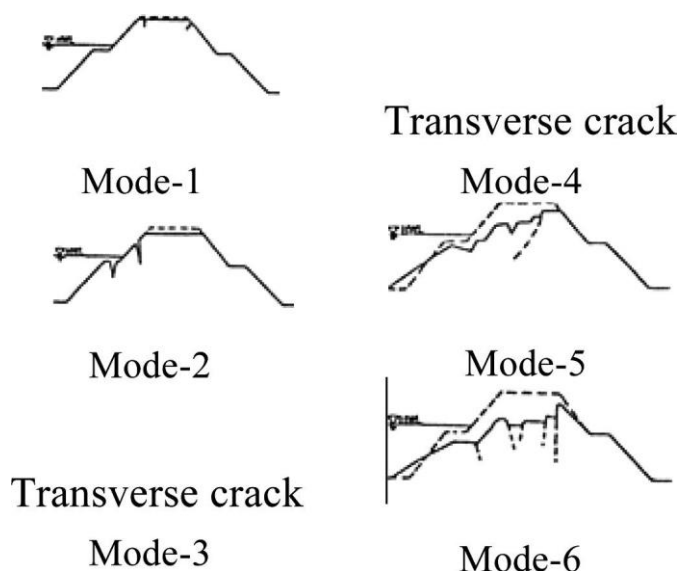


FIGURE 7: STOPBANK FAILURE MODES ALONG THE TOKACHI AND KUSHIRO RIVERS (SASAKI, 2009)



also showed the increase of the pore water pressure ratio in the alluvial sand layer beneath the peat layer of up to 40 %.

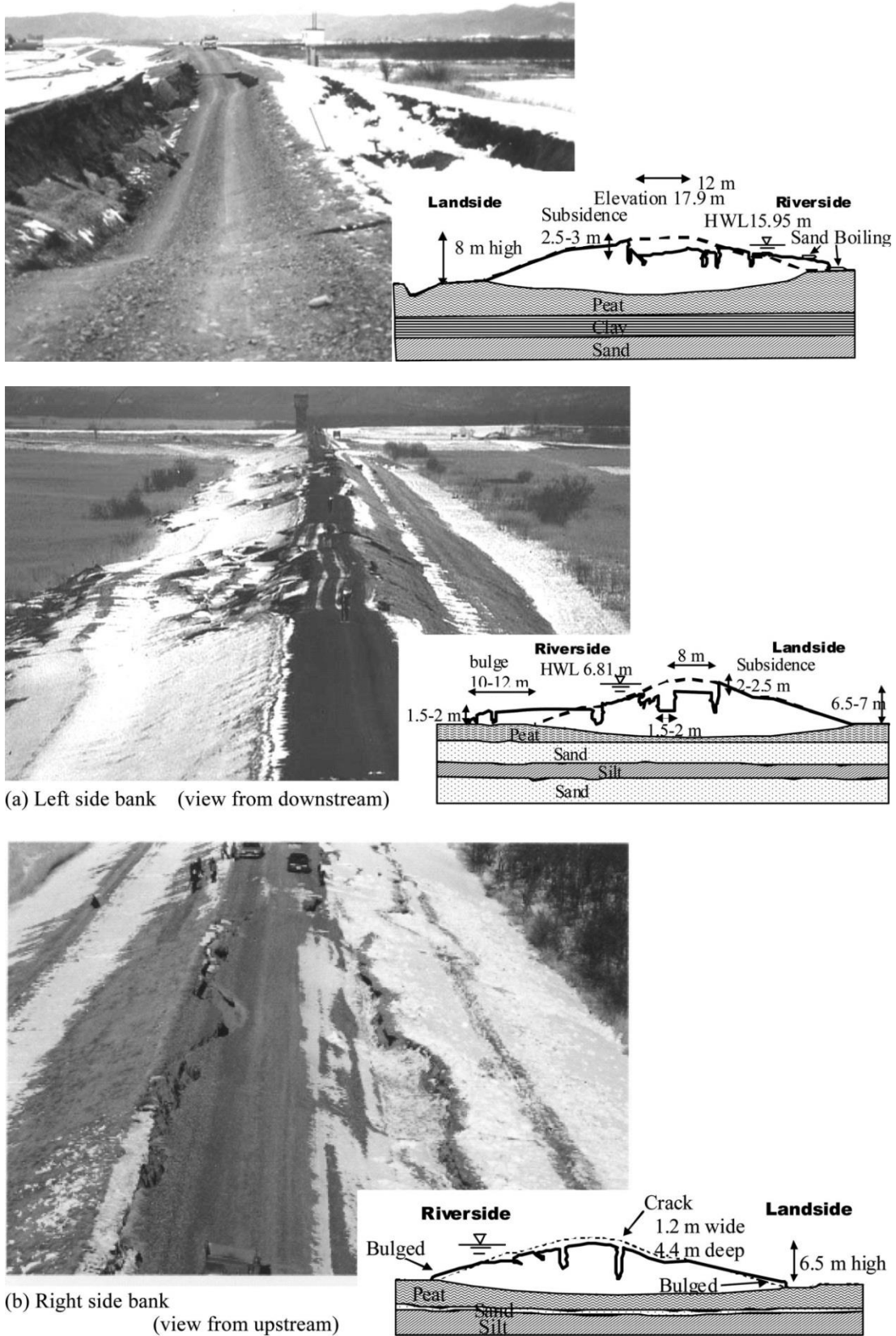


FIGURE 8: TYPICAL VIEW OF THE FAILED STOPBANK OF THE KUSHIRO RIVER. (SASAKI, 2009)

## Case Study 8 – Behaviour of Sand Compaction Pile (SCP) improved stopbanks during the 2003 Miyagiken-Hokubu earthquake

This case study reviews the effectiveness of densification of sandy soils using the Sand Compaction Pile (SCP) as a method of liquefaction remediation based on observations following the July 26, 2003 Miyagiken-Hokubu earthquake, Japan.

To mitigate liquefaction-induced stopbank damage, densification of sandy soils along 350 m of the Naruse River, Miyagi Prefecture at the stopbank berm was undertaken in 1996. Four rows of piles were installed in the direction normal to the stopbank axis, with a 700 mm SCP diameter casing. The spacing between the piles in the stopbank axis direction is 2.2 m and in the direction normal to the stopbank axis is 1.7 m. The improvements resulted in a decrease of void ratio and an increase in SPT-N values of the sandy soil layers at the berm (Takahasi & Sugita, 2009).

Liquefaction arrays, along with seismometer arrays were installed after the 1995 Kobe earthquake along the Naruse River, providing an opportunity to study the effectiveness of densification of sandy soils (via liquefaction remediation) by comparing excess pore water pressure (the amount by which the pore water pressure exceeds the equilibrium pore pressure). On 26 July 2003 these were tested by a series of major inland earthquakes, with the main shock having a JMA magnitude ( $M_j$ ) of 6.2. The earthquakes caused damage to stopbanks of the Naruse River from 8 to 17 km distant from the river mouth and where the stopbanks had been constructed on old river channels or marshes.

Excess pore water pressure changes during the main shock were recorded. The results indicated that ground which had been treated with SCPs had excess pore pressure ratios of approximately 0.4, compared with approximately 0.8 for untreated ground. These records suggest a marked increase in liquefaction resistance of the sandy soil when densified with SCPs (even if the increase of SPT N-values by piling is insignificant).

A more detailed seismic effective stress analysis was undertaken by Cubrinovski (2011) to accurately simulate excess pore water pressures and their effects on the response of the earth structure and soil-structure systems. And effective stress analysis was conducted using the finite element model shown in Figure 9, with the recorded acceleration time history at the location used as the base input motion. Figure 10 and Figure 11 show the analysis and recorded response of excess pore water pressure for both the unimproved and SCP improved zones of the stopbank. This confirms the excess pore pressure ratios of 0.4 (treated), compared with 0.8 (untreated) and illustrates the potential and accuracy of the seismic affective stress analysis as a countermeasure against liquefaction.

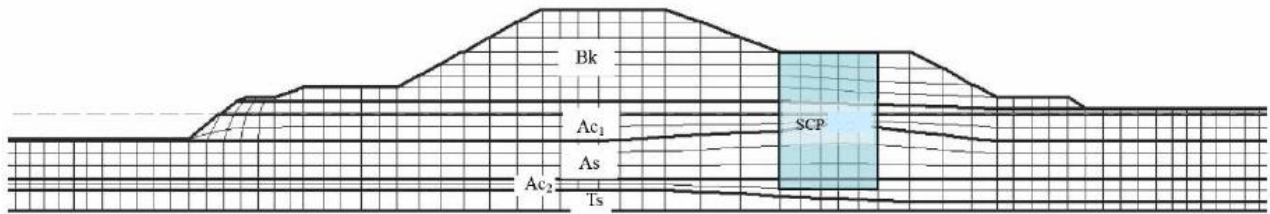


FIGURE 9: NUMERICAL MODEL USED IN THE EFFECTIVE STRESS ANALYSIS OF NARUSE RIVER STOPBANKS

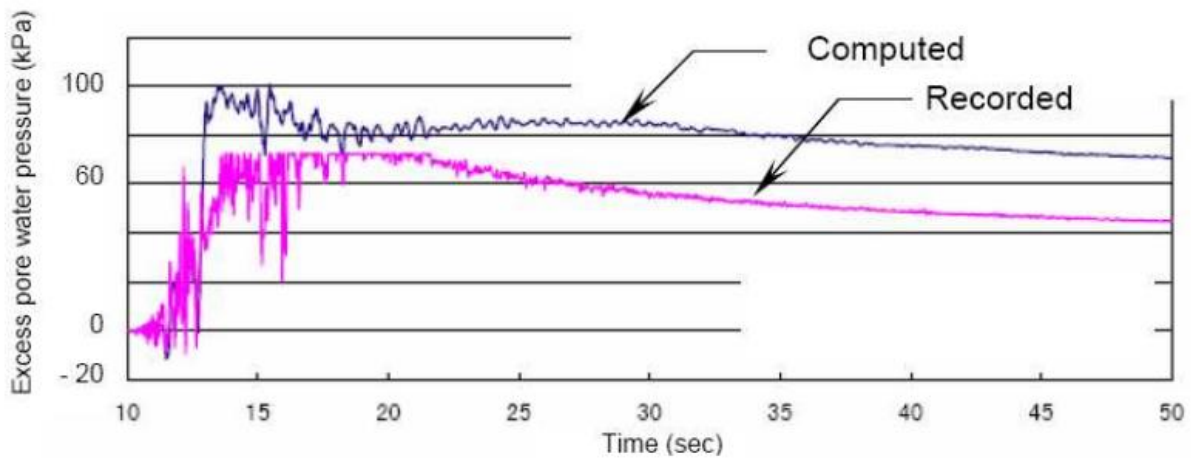


FIGURE 10: EXCESS PORE WATER PRESSURES IN THE UNIMPROVED ZONE (WITHIN THE SHOULDER)

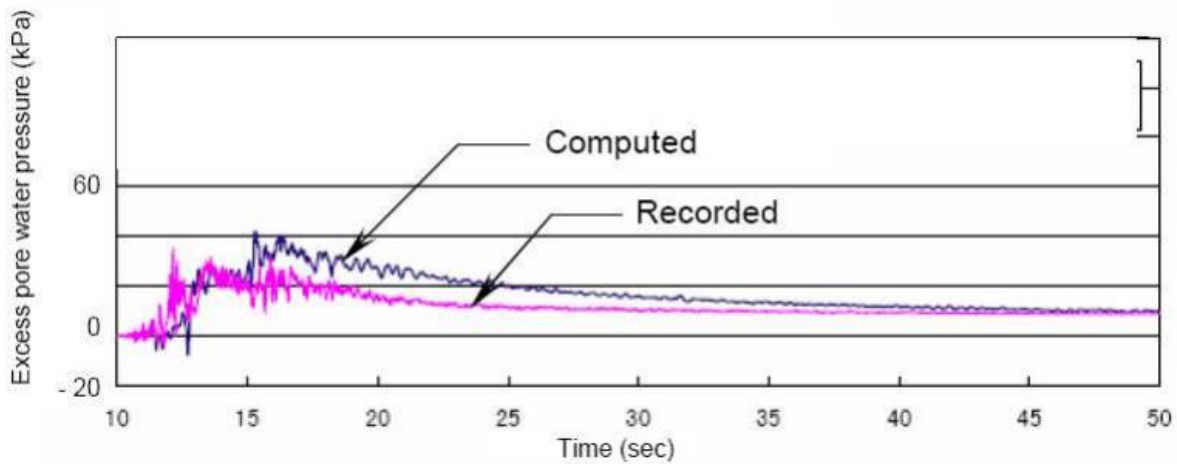


FIGURE 11: EXCESS PORE WATER PRESSURES IN THE SCP ZONE (WITHIN THE BERM)

## CASE STUDY 9 - SEISMIC PERFORMANCE OF STOPBANKS OBSERVED FOLLOWING THE LOMA PRIETA EARTHQUAKE

The  $M_w$ 7.1 Loma Prieta earthquake occurred on 17 October 1989 and caused major damage to the San Lorenzo River stopbank system and Pajaro River stopbank system.

### CHARACTERISTICS OF PERFORMANCE

The earthquake caused approximately 0.9 to 1.2 m of crest settlement and large cracks up to 15 cm wide along the slope and crest of the stopbanks. Damage predominantly occurred near the river mouths. Some areas also showed signs of lateral movement where visible cracks up to 30 cm wide, 2 m deep and 30 m long were recorded. In these areas, there were no visible signs of subsidence (Miller and Roycroft, 2004; Perry, 1994).

### MECHANISM OF FAILURE

Three of the damaged sections were analysed by Yegian et al. (1994). One of the important findings of this research is that the liquefied sand had a very high (40 – 50%) gravel component with field SPT N-values of between 12 and 42 (meaning that the gravelly sands/sandy gravels had liquefied). This is thought to have occurred due to the presence of a low permeability crust (as thin as 30 cm) that did not allow the dissipation of the generated excess pore water pressures. The liquefaction that occurred triggered flow slides leading to permanent deformation and settlement of the overlying embankment. Stability analysis undertaken by Miller & Roycroft (2004) indicates that because of the horizontal soil stratigraphy and the stopbank geometry, the critical failure surface emerges at the middle or rear of the stopbank crest both in static and earthquake conditions.

The liquefaction potential of the San Lorenzo River stopbank foundation materials was assessed using the SPT N-values derived from boreholes on four reaches of the river that sustained major damage and identified that in all areas that suffered major damage the site were underlain by liquefiable materials (Perry, 1994).

Regions that suffered extensive cracking due to lateral movement were not thought to be underlain by liquefiable materials, but a weak cohesive layer of saturated material comprising very soft to soft clays.

## CASE STUDY 10 - YODO RIVER STOPBANK DAMAGE DURING THE HYOGOKEN-NANBU EARTHQUAKE

In the Hyogoken-nanbu district most of the stopbanks have been channelised. During the 17 January 1995 earthquake most of the stopbanks performed well, except for a 1.5 to 2 km length of the Yodo River stopbank where significant damage was reported.

### CHARACTERISTICS OF PERFORMANCE

Failure along this stretch of stopbank was predominantly in the form of cracking and slumping, and settlements of up to half the height of the original stopbank. It was summarized that the embankment broke into blocks and sunk into (and spread out) over a liquefied foundation. At the time of the earthquake, the river level was relatively low, with approximately 1 to 2 m of the bottom of the embankment being saturated. In order to establish a relationship between foundation damage and stopbank damage, a reconnaissance was undertaken on a stopbank system approximately 1 km east of Yodo. It was found that the stopbanks here generally performed well with only minor isolated pockets of moderate damage in the form of cracking and settlements of up to 1 m (these areas were generally associated with sand boils). At this stopbank location the foundation soils are slightly higher than the river level and are exposed on the water side. Sasaki and Shimada (1997) concluded that the improvement in foundation performance was probably due to denser foundation materials and/or relatively lower water levels. The foundation and/or bottom of the stopbank were also considered to have liquefied.

### MECHANISM OF FAILURE

The failure process of the damaged stopbank at the Torishima section as described by Sasaki and Shimada (1997) and depicted in Figure 12 is summarised below:

- 1) Alluvial sandy soil beneath the stopbank was liquefied by earthquake shaking.
- 2) With the raised pore water pressure in the underlying layer, the stress state in the stopbank became active (Rankine state) and a crack developed around the shoulder.
- 3) High pore water pressure continued in the shallower parts of the liquefied layer nearby bottom boundary of the stopbank, and the central portion of the embankment subsided into the liquefied layer by thrusting the side part of the embankment beneath its slope.
- 4) Because the ground surface was lower and there was a non-liquefied surface layer, and the parapet provided additional weight, the water side portion of the stopbank subsided and the rest of the stopbank was sheared towards the water side.
- 5) Sand boils intruded into cracks while subsidence proceeded and thrusting was continued.
- 6) With the lessening of the raised pore pressure, movement of the soil blocks ceased although deformation of the stopbank remained.

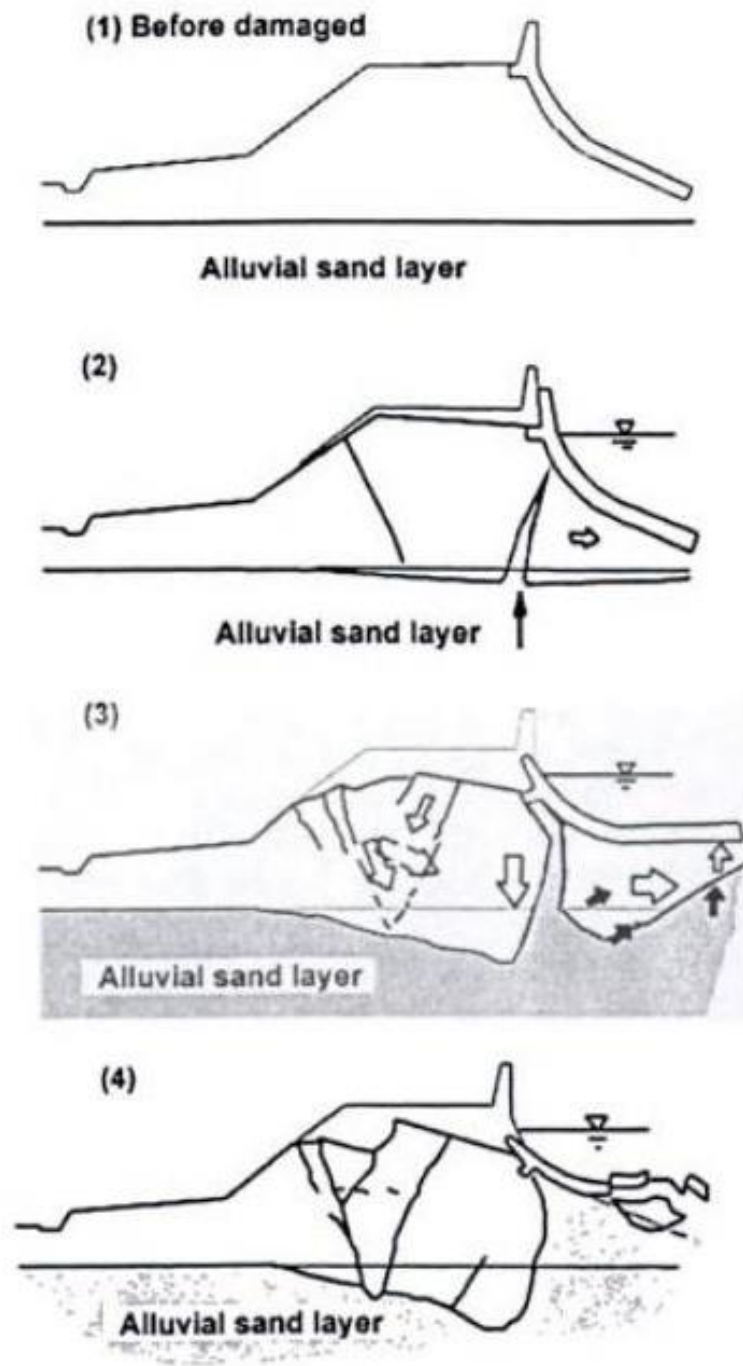


FIGURE 12: FAILURE PROCESS AT THE DAMAGED TORISHIMA STOPBANK (SASAKI AND SHIMADA, 1997)



- Cubrinovski, M., 2011, Seismic effective stress analysis: modelling and application.
- GEER, 2011, Geotechnical Reconnaissance of the 2011 Christchurch, New Zealand Earthquake: GEER Association Report No. GEER-027, v. 1.
- Harder, L., Kelson, K., and Kishida, T., 2011, Preliminary Observations of Stopbank Performance and Damage following the March 11, 2011 Tohoku Offshore Earthquake, Japan: Geotechnical Extreme Events Reconnaissance (GEER).
- Isoyama, R., Liquefaction-induced Ground Failures and Displacements along the Shiribeshi-toshibetsu River Caused by the 1993 Hokkaido-nansei-oki Earthquake, *in* Proceedings Proceedings of the 5th US Japan Workshop on Earthquake Resistant Design of Lifeline Facilities and Countermeasures for Soil Liquefaction 1994, p. 1-26.
- Lekkas, E., Andreadakis, E., Alexoudi, V., Kapourani, E., and Kostaki, I., The Mw= 9.0 Tohoku Japan earthquake (March 11, 2011) tsunami impact on structures and infrastructure, *in* Proceedings Environmental Geosciences and Engineering Survey for Territory Protection and Population Safety (EngeoPro) International conference, Moscow 2011, p. 97-103.
- Miller, E. A., and Roycroft, G. A., 2004, Seismic performance and deformation of stopbanks: four case studies: *Journal of Geotechnical and Geoenvironmental Engineering*, v. 130, no. 4, p. 344-354.
- Pender, M., and Robertson, T., 1987, Edgecumbe earthquake: reconnaissance report, Earthquake Engineering Research Institute.
- Perry, E. B., 1994, Proceedings of the Repair, Evaluation, Maintenance, and Rehabilitation Research Program Workshop on Stopbank Rehabilitation Held at Vicksburg, Mississippi on 17 March 1992: DTIC Document.
- Sasaki, Y., 2009, River dike failures during the 1993 Kushiro-oki earthquake and the 2003 Tokachi-oki earthquake, *Earthquake Geotechnical Case Histories for Performance-Based Design*, CRC Press, p. 131-157.
- Sasaki, Y., and Shimada, K., 1997, Yodo River dike damage by the Hyogoken-nanbu earthquake. Seismic Behavior of Ground and Geotechnical Structures: Proc. of Discussion Special Technical Session on Earthquake Geotechnical Engineering during 14th International Conference on Soil Mechanics and Foundation Engineering., v. Hamburg/Germany: A. A. Balkema, : 307–316.
- Towhata, I., Prasad, S., Honda, T., and Chandradhara, G., 2002, Geotechnical reconnaissance study on damage caused by 2001 Gujarat earthquake, India: *Soils and foundations*, v. 42, no. 4, p. 77-88.
- Wang, W., Earthquake damage to earth and Stopbanks in relation to soil liquefaction, *in* Proceedings Proc. of the Int. Conf. on Case Histories on Geotech. Engrg 1984, Volume 1, p. 511-521.
- Yegian, M., Ghahraman, V., and Gazetas, G., 1994, Ground-motion and soil-response analyses for Leninakan, 1988 Armenia earthquake: *Journal of geotechnical engineering*, v. 120, no. 2, p. 330-348.

## **APPENDIX B:**

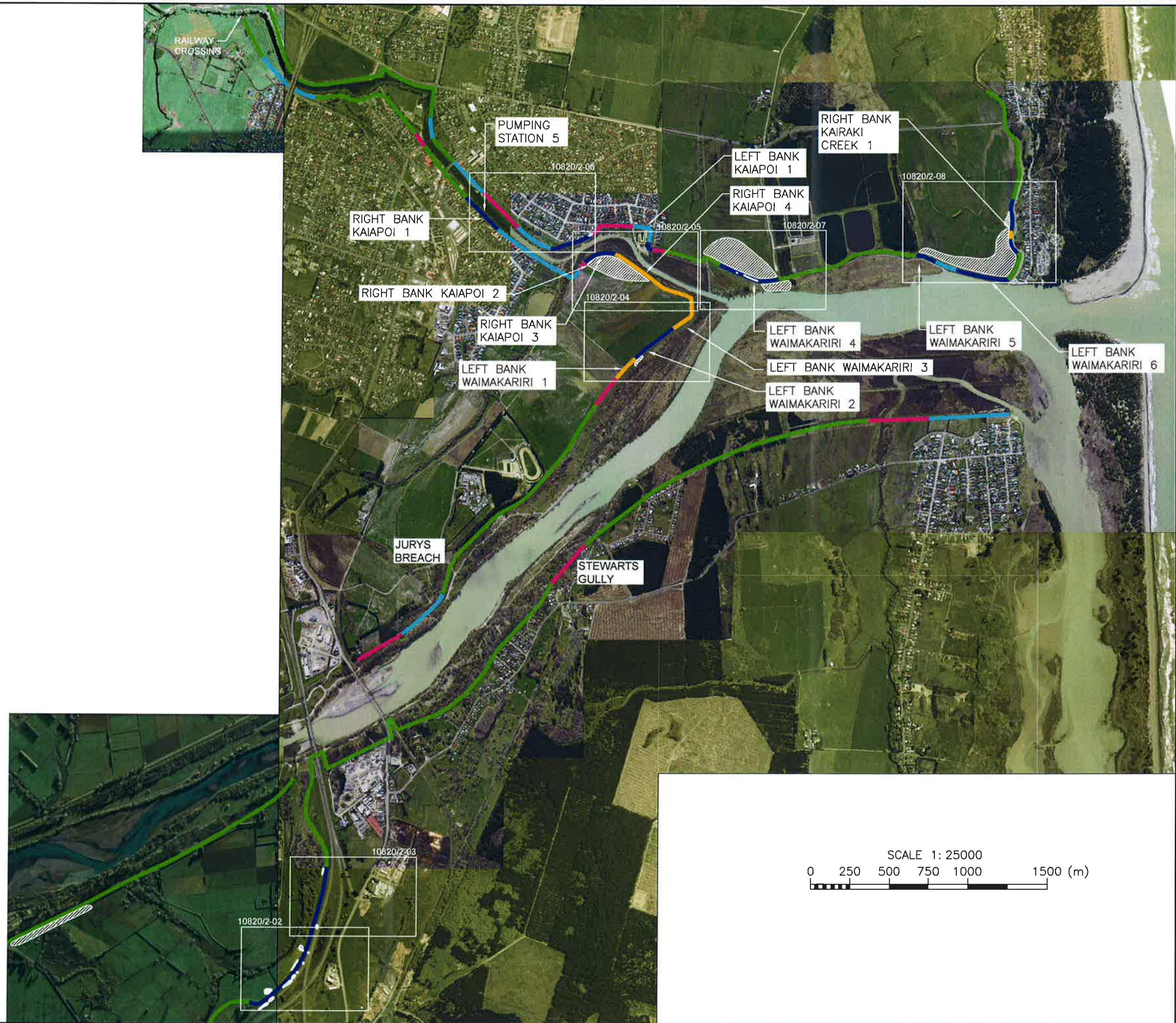
### **RILEY STOPBANK DAMAGE MAPS**





# KEY

- ZONE 1: NO DAMAGE
- ZONE 2: MINOR:  
CRACKS <5mm WIDE,  
30-140mm DEEP WITH  
NEGLECTIBLE SETTLEMENT
- ZONE 3: MODERATE:  
CRACKS 400mm-1m DEEP  
WITH SOME SETTLEMENT
- ZONE 4: MAJOR:  
CRACKS >1m DEEP. DEEP  
SEATED MOVEMENT &  
SETTLEMENT
- ZONE 5: SEVERE:  
LARGE SCALE INSTABILITY,  
SPREADING & GROSS  
SETTLEMENT >500mm
- ZONE 6: AREAS OF RECENT  
OR CURRENT REPAIRS
- AREAS OF MAJOR  
LIQUEFACTION



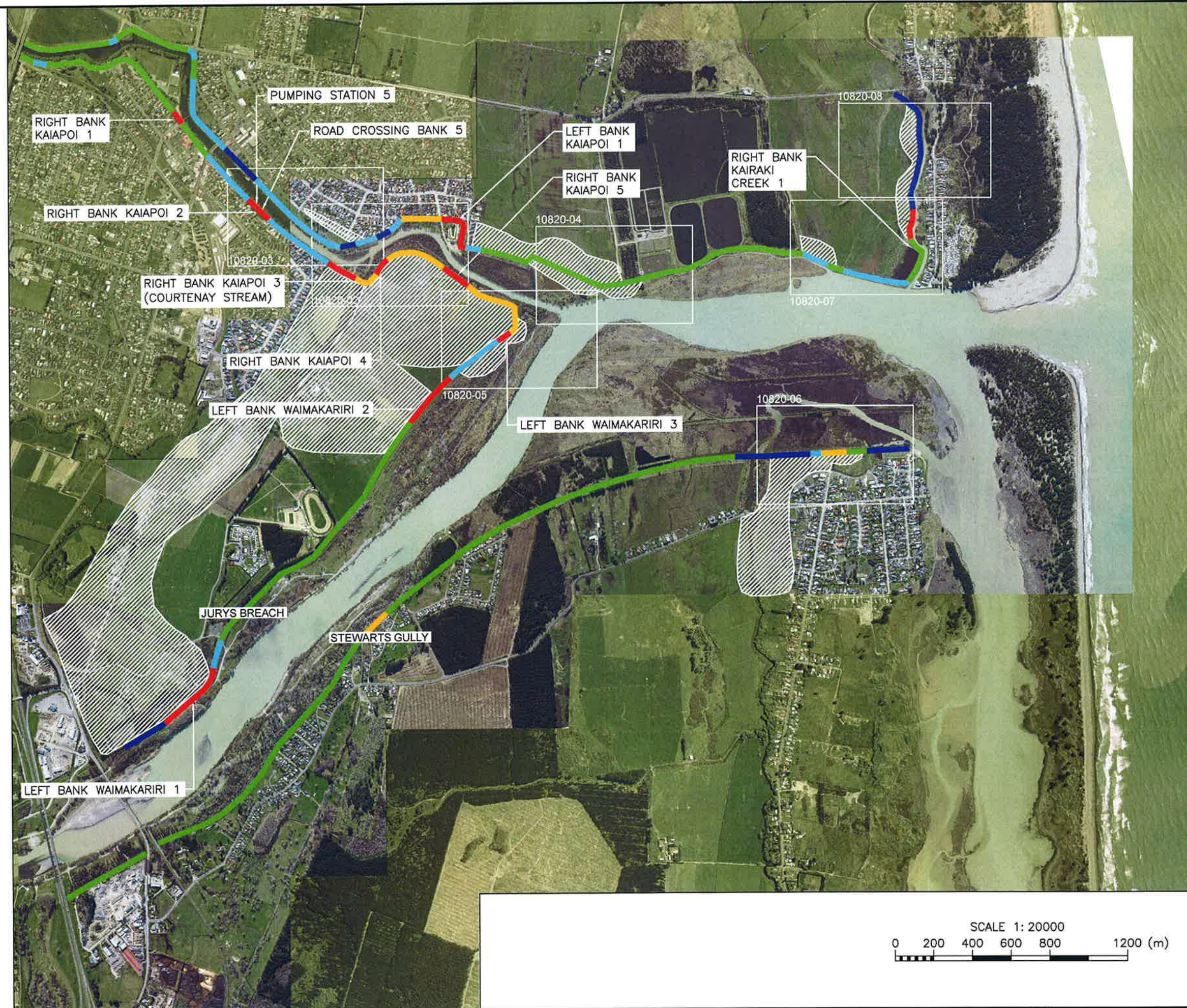
DESIGN		CHECKED		APPROVED FOR ISSUE:		TITLE		CADFILE	
EP		HN		DATE		ECAN		10820_2-01	
DRAWN		CHECKED		DATE		WAIMAKARIRI RIVER STOPBANK CONDITION ASSESSMENT		SCALES (A3)	
HN		DATE		DATE		OVERALL SITE PLAN		AS SHOWN	
0		FIRST ISSUE		05/04/11		RILEY CONSULTANTS		DRAWING No.	
REV		DESCRIPTION		BY		P.O.BOX 4355 CHRISTCHURCH		10820/2-01	
						TEL. 03-3794402 FAX. 03-3794403		REV.	
								0	





# KEY

- ZONE 1: NO DAMAGE
- ZONE 2: MINOR:  
CRACKS <5mm WIDE, 30-140mm  
DEEP WITH NEGLIGIBLE  
SETTLEMENT
- ZONE 3: MODERATE:  
CRACKS 400mm-1m DEEP WITH  
SOME SETTLEMENT
- ZONE 4: MAJOR:  
CRACKS >1m DEEP, DEEP SEATED  
MOVEMENT & SETTLEMENT
- ZONE 5: SEVERE:  
LARGE SCALE INSTABILITY,  
SPREADING & GROSS SETTLEMENT  
>500mm
- AREAS OF MAJOR LIQUEFACTION



1	ZONES AMENDED	HN	27.10.10
0	FIRST ISSUE	DATE DRAWN	SEPT.2010
REV	DESCRIPTION	BY	DATE

DESIGN CHECKED  
EP  
DRAWN CHECKED  
MP  
DATE: / /

**RILEY**  
CONSULTANTS  
P.O.BOX 4355  
CHRISTCHURCH  
TEL. 03-3794402  
FAX. 03-3794403

TITLE

ECAN  
WAIMAKARIRI RIVER STOPBANK CONDITION ASSESSMENT  
OVERALL SITE PLAN

CADFILE  
10820-01  
SCALES (A3)  
1:20000  
DRAWING No.  
10820-01  
REV.  
1



## **APPENDIX C:**

### **RILEY TEST PIT LOGS**



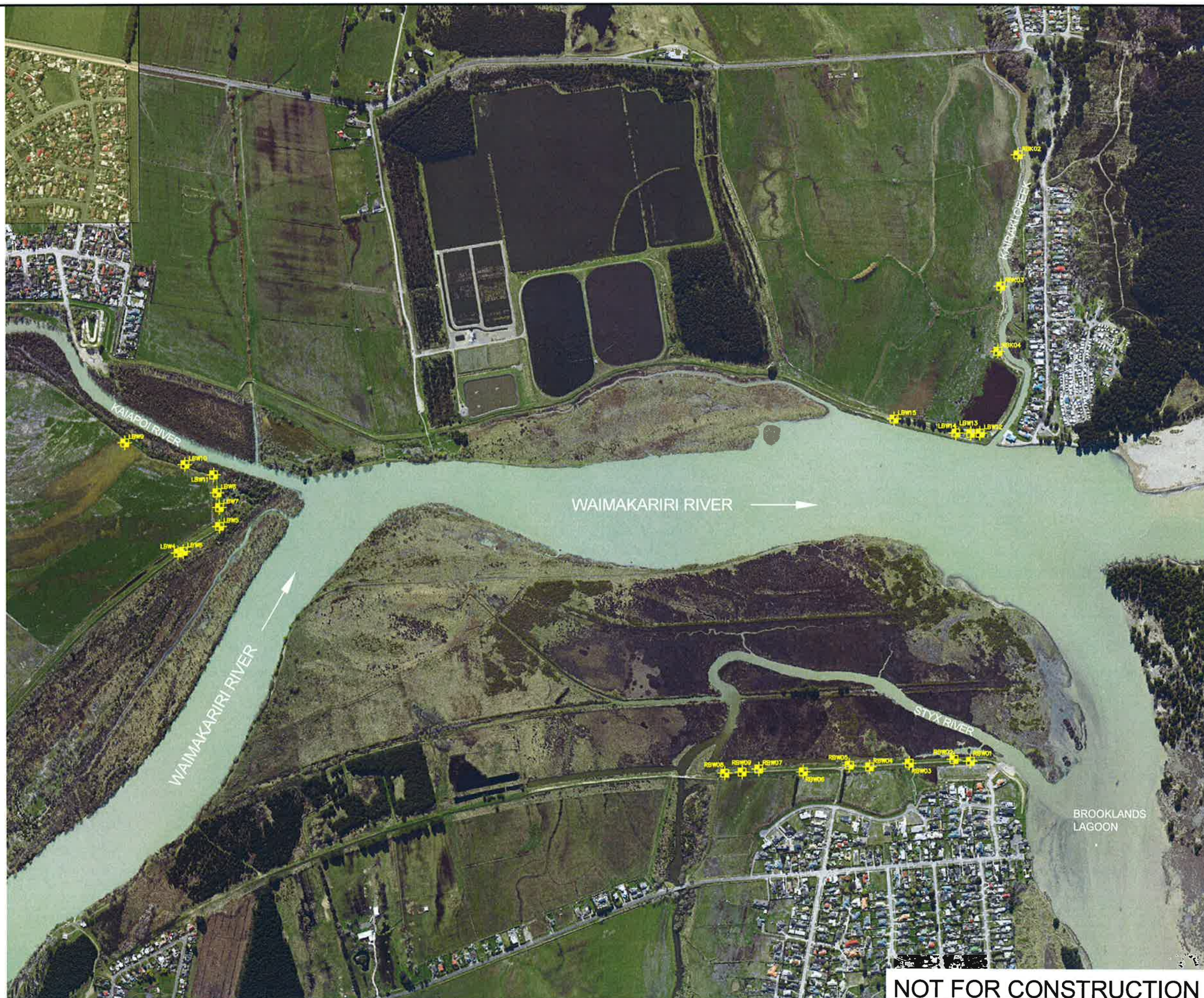


**KEY**



TEST PIT LOCATION

SCALE 1: 10000  
0 100 200 300 400 600 (m)



**NOT FOR CONSTRUCTION**

0	FIRST ISSUE	BY	DATE
REV	DESCRIPTION	BY	DATE

DESIGN	CHECKED
EP	
DRAWN	CHECKED
HN	
DATE DRAWN	OCT 2010

APPROVED FOR ISSUE:
<b>DRAFT</b>
DATE: / /

**RILEY** CONSULTANTS  
P.O. BOX 4355 CHRISTCHURCH  
TEL. 03-3794402  
FAX. 03-3794403

TITLE	ECAN
WAIMAKARIRI RIVER STOPBANK CONDITION ASSESSEMENT	
TEST PIT LOCATION SITE PLAN	

CADFILE	10820-100to103
SCALES (A3)	AS SHOWN
DRAWING No.	10820-100
REV.	0





# KEY

LBW1 TEST PIT LOCATION LBW  
(LEFT BANK WAIMAKARIRI)

SCALE 1: 5000  
0 50 100 150 200 300 (m)



NOT FOR CONSTRUCTION

0	FIRST ISSUE		
REV	DESCRIPTION	BY	DATE

DESIGN	CHECKED
EP	
DRAWN	CHECKED
HN	
DATE DRAWN	OCT 2010
DATE:	/ /

APPROVED FOR ISSUE:

**DRAFT**

**RILEY** CONSULTANTS

P.O. BOX 4355  
CHRISTCHURCH

TEL. 03-3794402  
FAX. 03-3794403

TITLE

ECAN

WAIMAKARIRI RIVER STOPBANK CONDITION ASSESSEMENT

TEST PIT LOCATIONS

CADFILE	10820-100to103
SCALES (A3)	AS SHOWN
DRAWING No.	10820-101
REV.	0





### KEY

RBW1 TEST PIT LOCATION RBW  
(RIGHT BANK WAIMAKARIRI)

WAIMAKARIRI RIVER →

STYX RIVER

BROOKLANDS  
LAGOON

RBW08 RBW09 RBW07 RBW06 RBW05 RBW04 RBW03 RBW02 RBW01

SCALE 1: 5000

0 50 100 150 200 300 (m)

NOT FOR CONSTRUCTION

DESIGN	CHECKED
EP	
DRAWN	CHECKED
HN	

APPROVED FOR ISSUE:  
**DRAFT**

**RILEY**  
CONSULTANTS

P.O. BOX 4355  
CHRISTCHURCH  
TEL. 03-3794402  
FAX. 03-3794403

TITLE

ECAN

WAIMAKARIRI RIVER STOPBANK CONDITION ASSESSEMENT

TEST PIT LOCATIONS

CADFILE  
10820-100to103  
SCALES (A3)  
AS SHOWN

DRAWING No.	REV.
10820-102	0

0	FIRST ISSUE	BY	DATE
REV	DESCRIPTION		

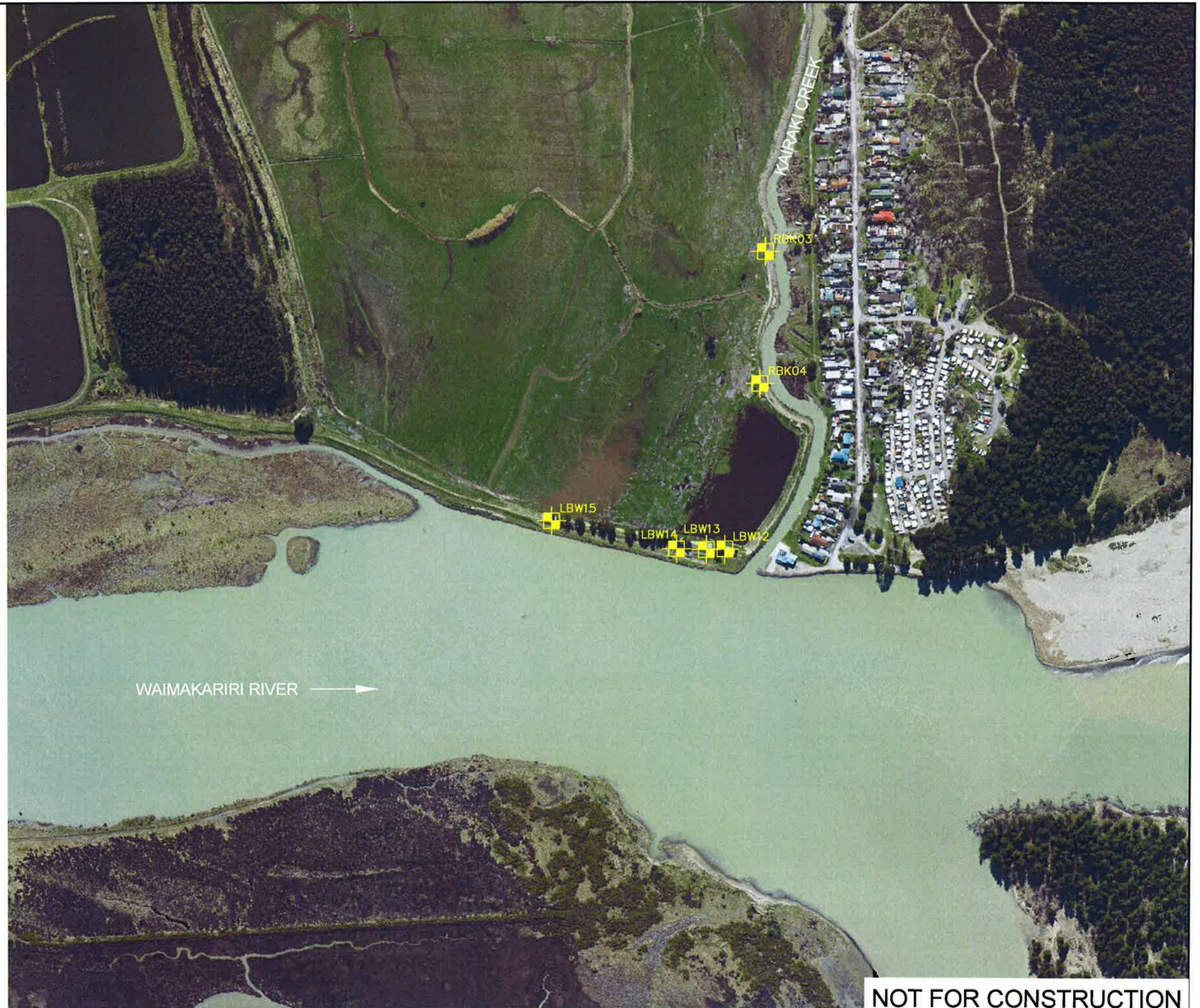




**KEY**

RBK1 TEST PIT LOCATION  
RBK (RIGHT BANK KAIRAKI)  
LBW (LEFT BANK WAIMAKARIRI)

SCALE 1: 5000  
0 50 100 150 200 300 (m)



**NOT FOR CONSTRUCTION**

0	FIRST ISSUE	BY	DATE	DESIGN	CHECKED	EP
REV	DESCRIPTION			DRAWN	CHECKED	HN
				DATE DRAWN		
				OCT 2010		

APPROVED FOR ISSUE:  
**DRAFT**  
DATE: / /

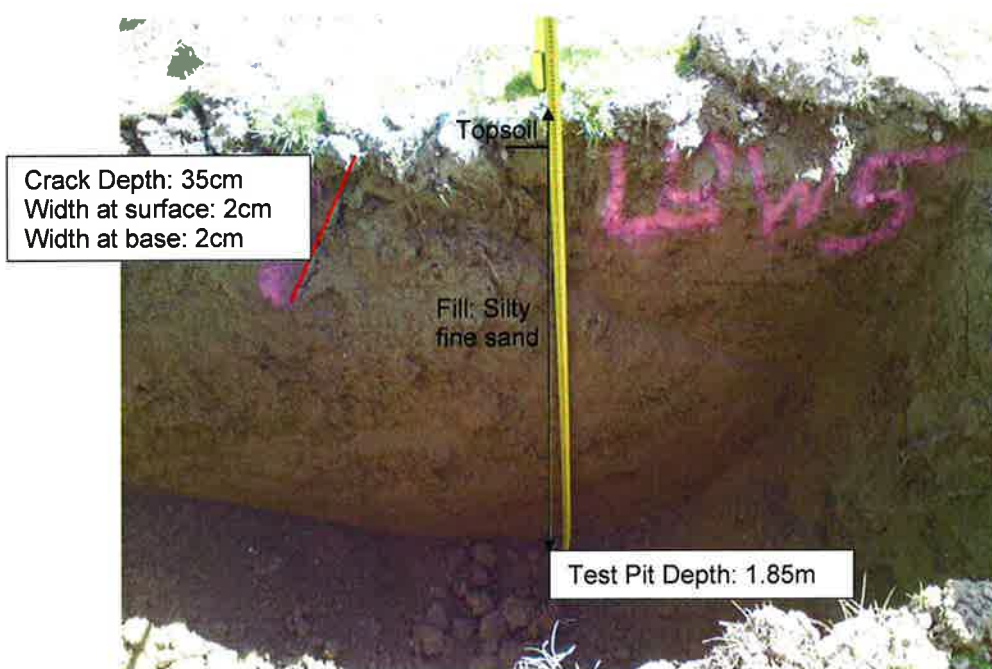
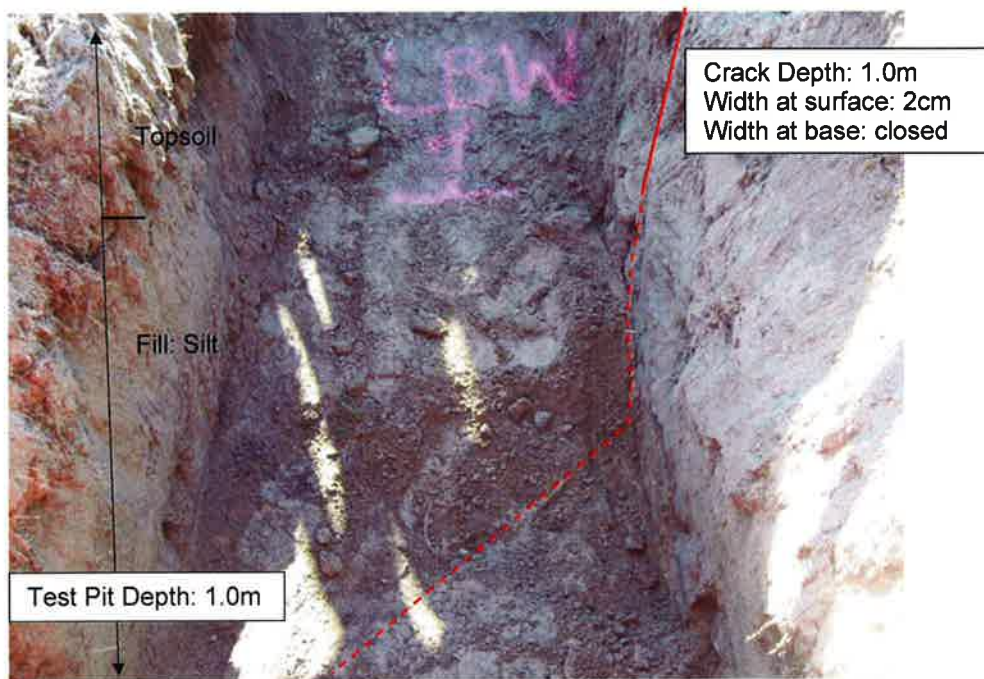
**RILEY** CONSULTANTS  
P.O. BOX 4355 CHRISTCHURCH  
TEL. 03-3794402  
FAX. 03-3794403

TITLE

ECAN  
WAIMAKARIRI RIVER STOPBANK CONDITION ASSESSEMENT  
TEST PIT LOCATIONS

CADFILE 10820-100to103	DRAWING No.	REV.
SCALES (A3) AS SHOWN	10820-103	0
ACENZ		





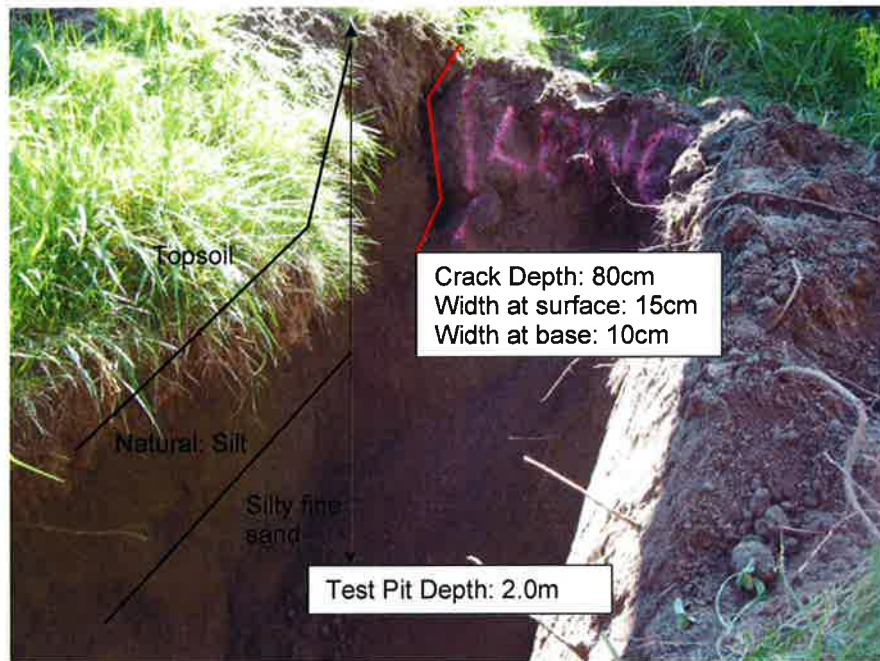
Ground Floor, 395 Madras Street,  
PO Box 4355, Christchurch  
Ph: 03 379 4402 Fax: 03 379 4403  
Email: [riley@riley.co.nz](mailto:riley@riley.co.nz)

### Test Pit Photos Left Bank Waimakariri (LBW) 4 and 5

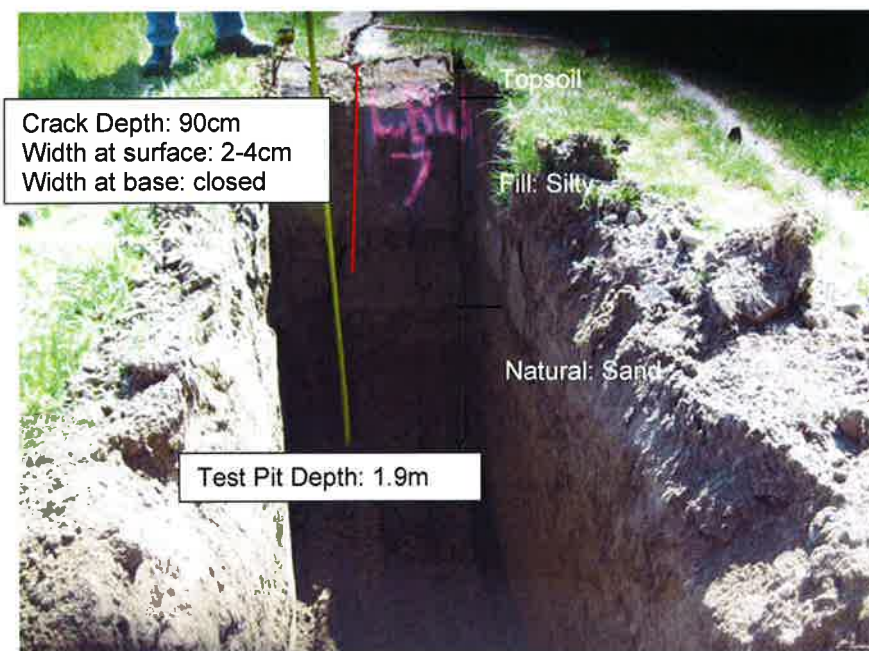
Scale: NTS

Date: 12/10/2010

Dwg / Fig No.:



Note: 2 Excavated on river side slope of LBW



Ground Floor, 395 Madras Street,  
PO Box 4355, Christchurch  
Ph: 03 379 4402 Fax: 03 379 4403  
Email: [riley@riley.co.nz](mailto:riley@riley.co.nz)

### Test Pit Photos Left Bank Waimakariri (LBW) 6 and 7

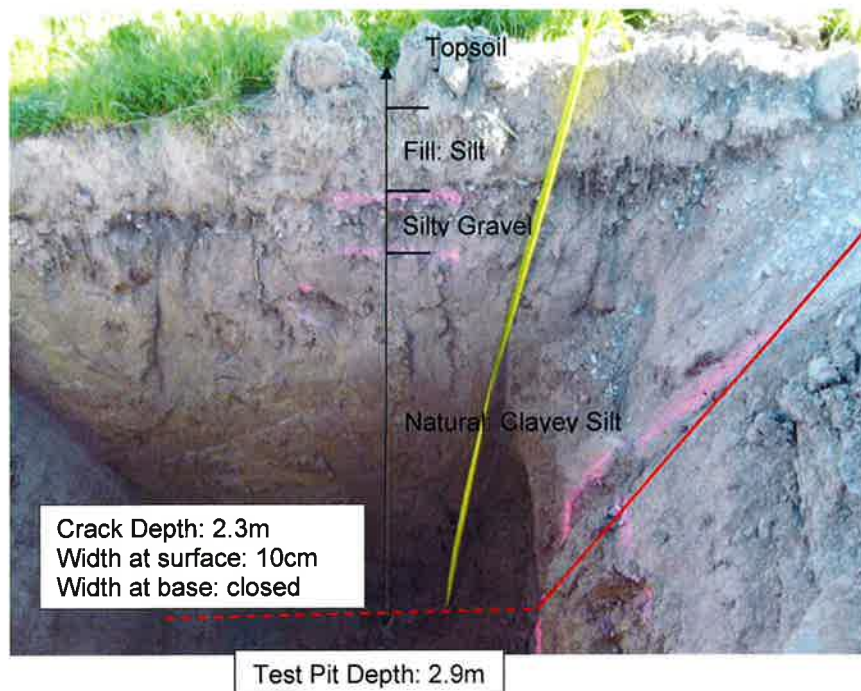
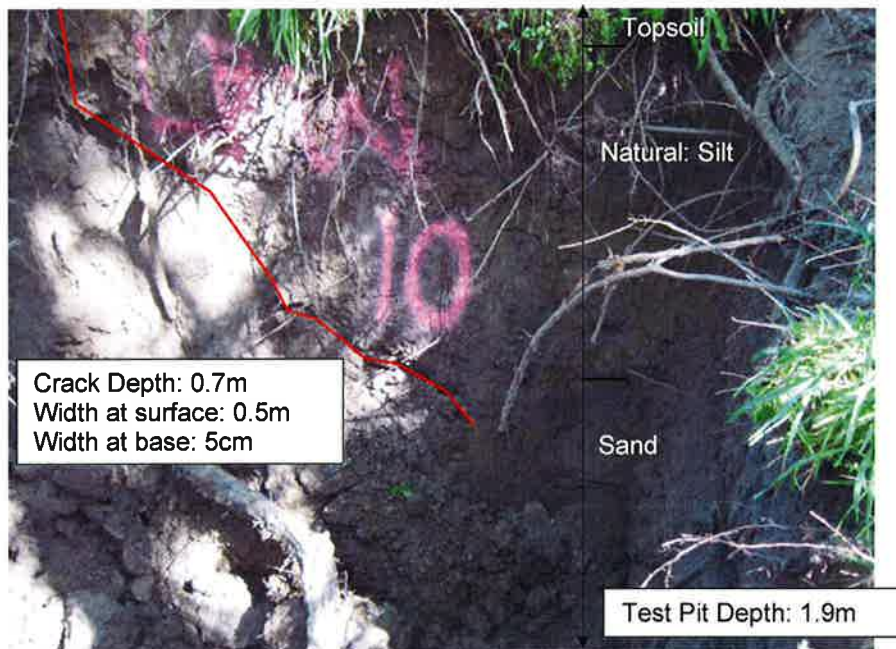
Scale: NTS

Date: 12/10/2010



<div data-bbox="266 506 593 613" data-label="Text"><p>Crack Depth: 1.5m Width at surface: 10cm Width at base: 2-5cm</p></div>	<div data-bbox="494 257 1318 1122" data-label="Image"><p>Topsoil</p><p>Fill: Silt</p><p>Clayey silt</p><p>Natural: Sand</p><p>Silty sand</p><p>Test Pit Depth: 1.5m</p></div>	
	<div data-bbox="389 1180 1256 1830" data-label="Image"><p>Topsoil</p><p>Fill: Silty</p><p>Natural: Sand</p><p>Crack Depth: 60cm Width at surface: 10cm Width at base: closed</p><p>Test Pit Depth: 1.6m</p></div>	
<div data-bbox="352 1861 533 1928" data-label="Image"></div> <div data-bbox="314 1928 545 1991" data-label="Text"><p>Ground Floor, 395 Madras Street, PO Box 4355, Christchurch Ph: 03 379 4402 Fax: 03 379 4403 Email: riley@riley.co.nz</p></div>	<div data-bbox="652 1877 1013 1968" data-label="Section-Header"><p><b>Test Pit Photos Left Bank Waimakariri (LBW) 8 and 9</b></p></div>	<div data-bbox="1056 1863 1227 1924" data-label="Text"><p>Scale: NTS Date: 12/10/2010</p></div>



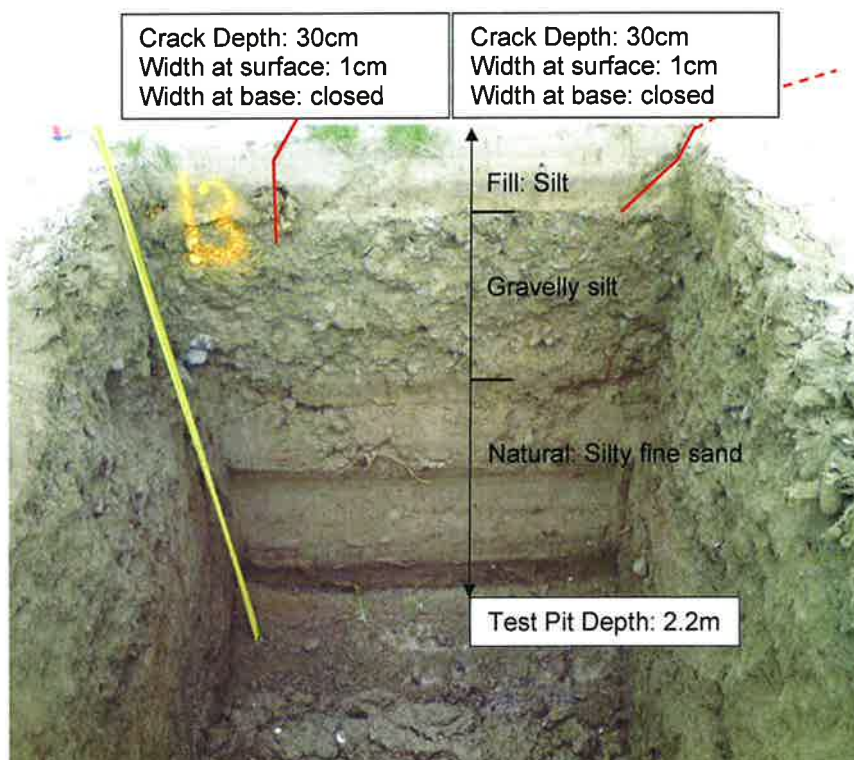
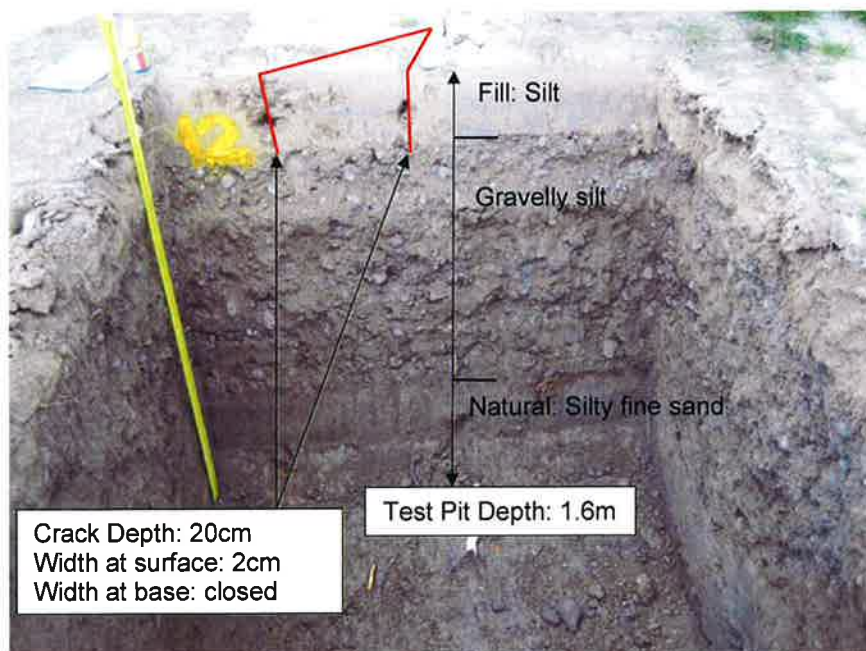


Ground Floor, 395 Madras Street,  
PO Box 4355, Christchurch  
Ph: 03 379 4402 Fax: 03 379 4403  
Email: riley@riley.co.nz

### Test Pit Photos Left Bank Waimakariri (LBW) 10 and 11

Scale: NTS

Date: 12/10/2010



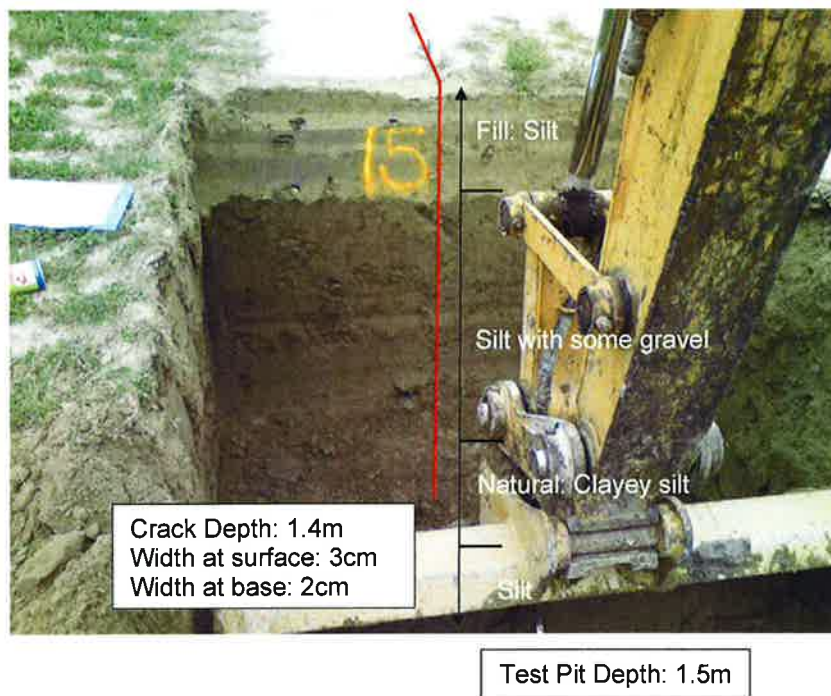
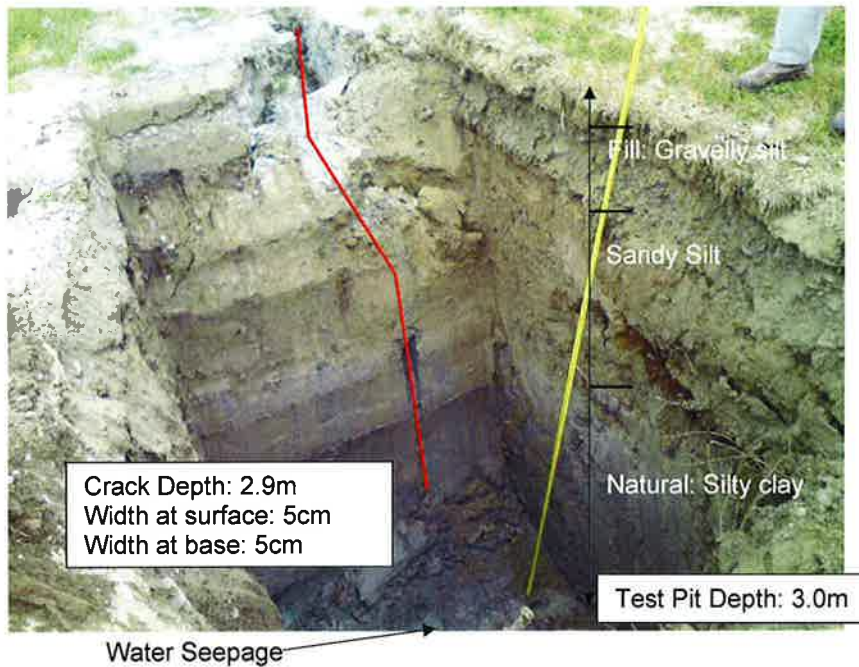
Ground Floor, 395 Madras Street,  
PO Box 4355, Christchurch  
Ph: 03 379 4402 Fax: 03 379 4403  
Email: [riley@riley.co.nz](mailto:riley@riley.co.nz)

### Test Pit Photos Left Bank Waimakariri (LBW) 12 and 13

Scale: NTS

Date: 12/10/2010



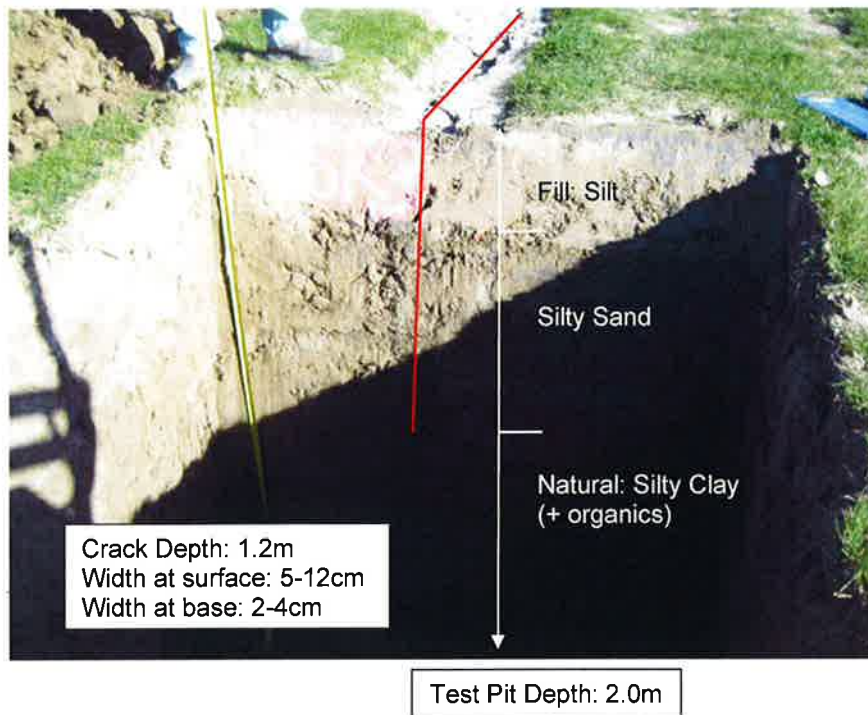
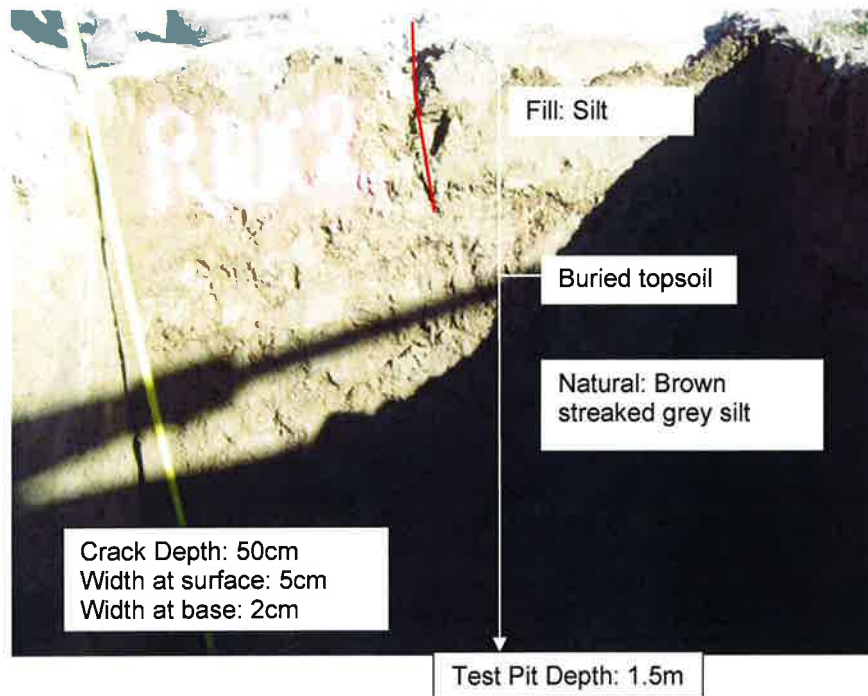


Ground Floor, 395 Madras Street,  
PO Box 4355, Christchurch  
Ph: 03 379 4402 Fax: 03 379 4403  
Email: riley@riley.co.nz

### Test Pit Photos Left Bank Waimakariri (LBW) 14 and 15

Scale: NTS

Date: 12/10/2010

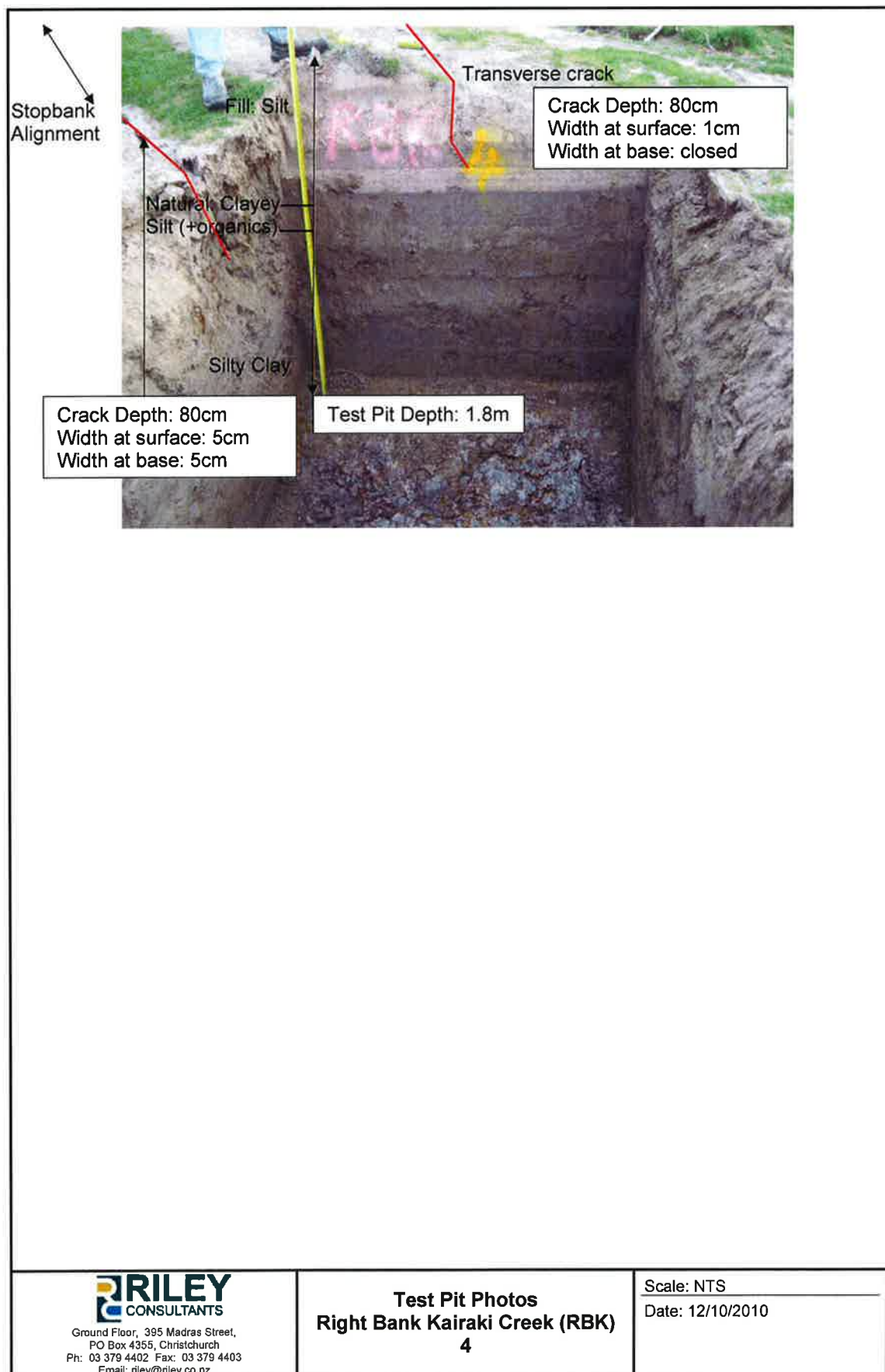


Ground Floor, 395 Madras Street,  
PO Box 4355, Christchurch  
Ph: 03 379 4402 Fax: 03 379 4403  
Email: riley@riley.co.nz

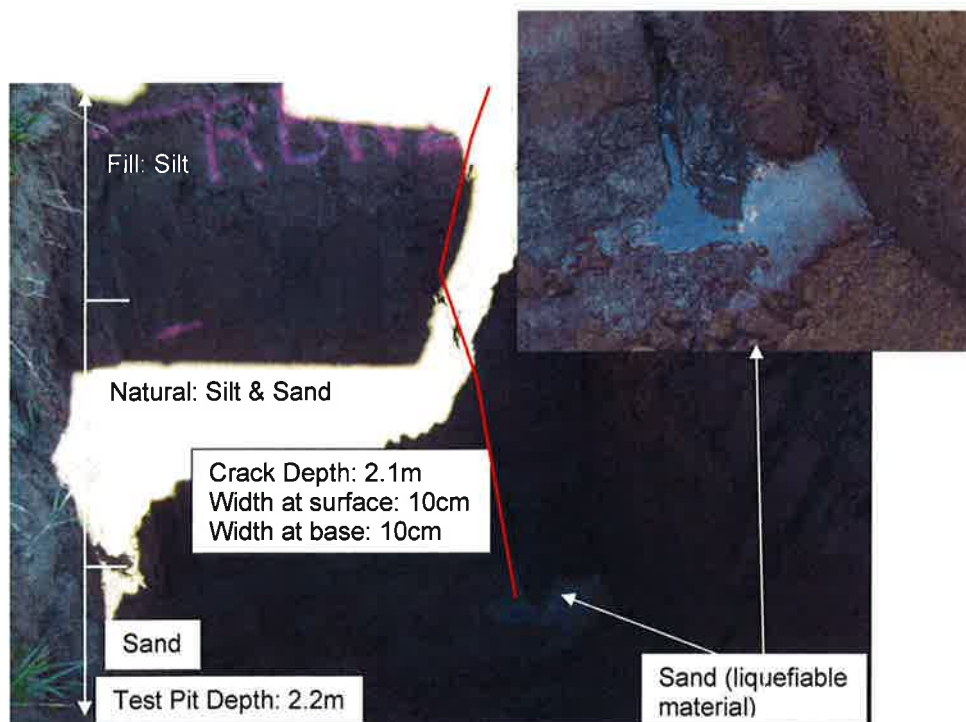
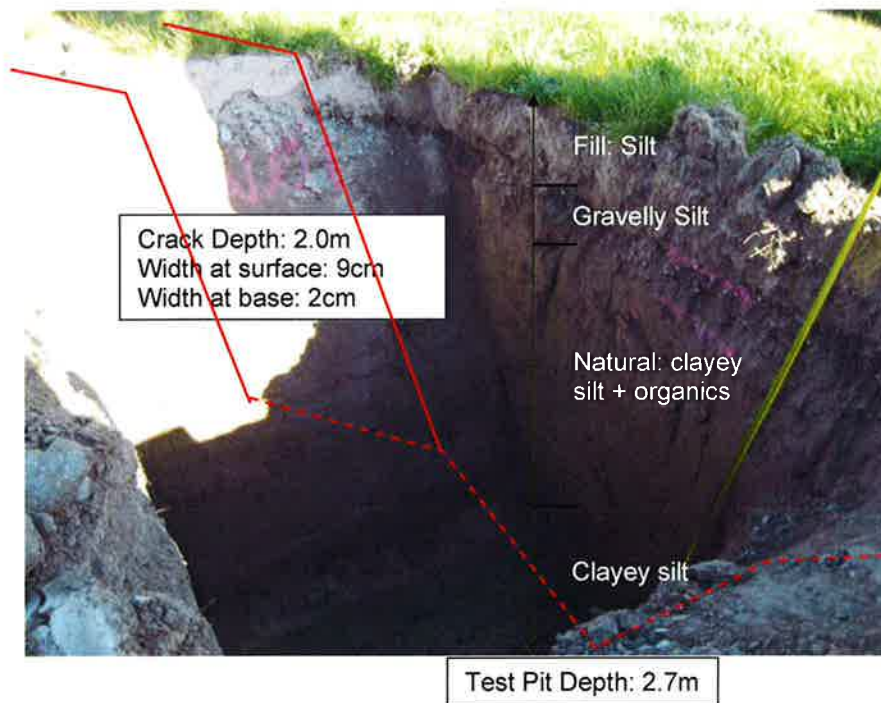
### Test Pit Photos Right Bank Kairaki Creek (RBK) 2 and 3

Scale: NTS

Date: 12/10/2010





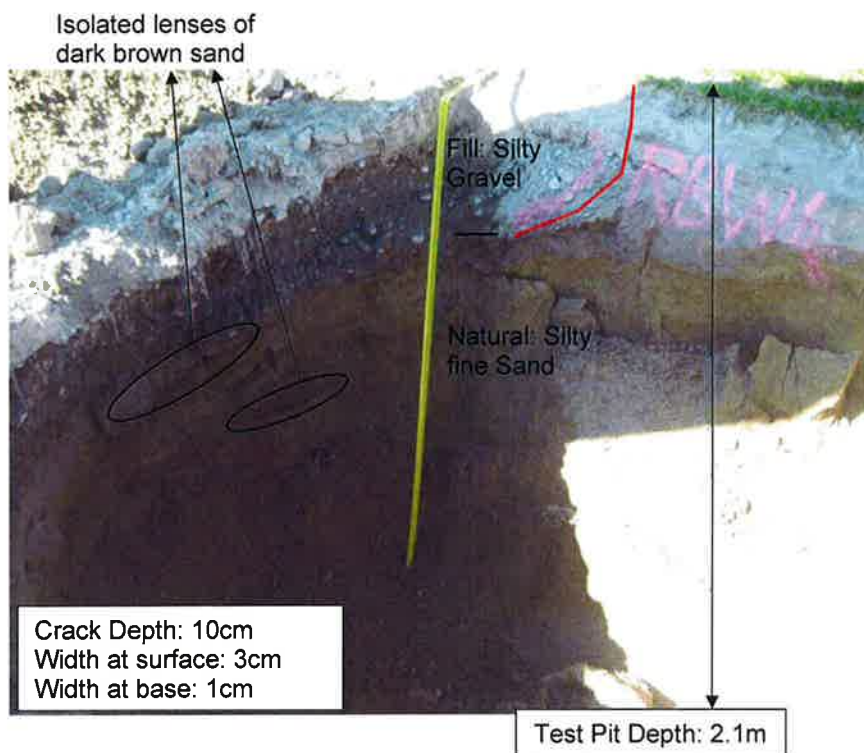
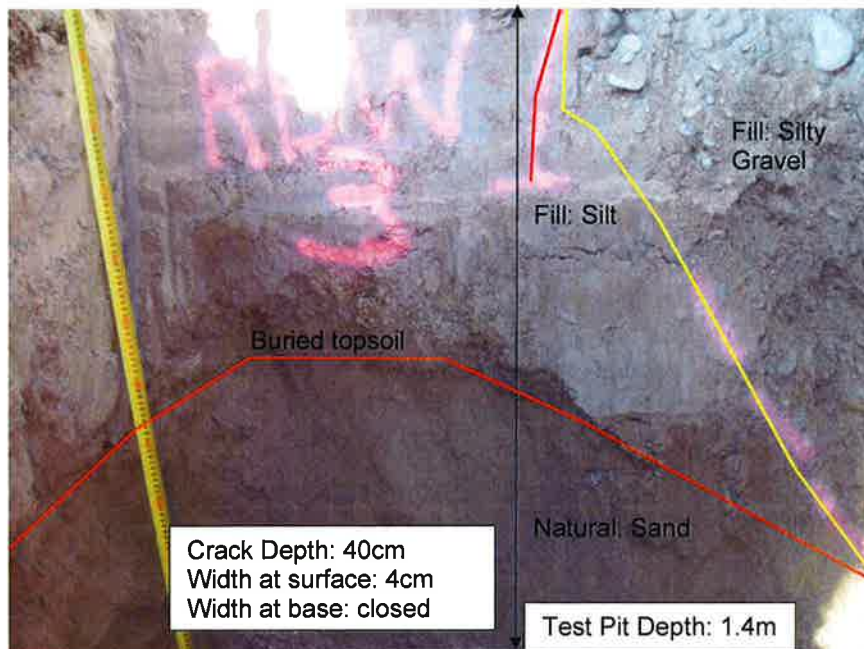


Ground Floor, 395 Madras Street,  
PO Box 4355, Christchurch  
Ph: 03 379 4402 Fax: 03 379 4403  
Email: riley@riley.co.nz

### Test Pit Photos Right Bank Waimakariri (RBW) 1 and 2

Scale: NTS

Date: 12/10/2010

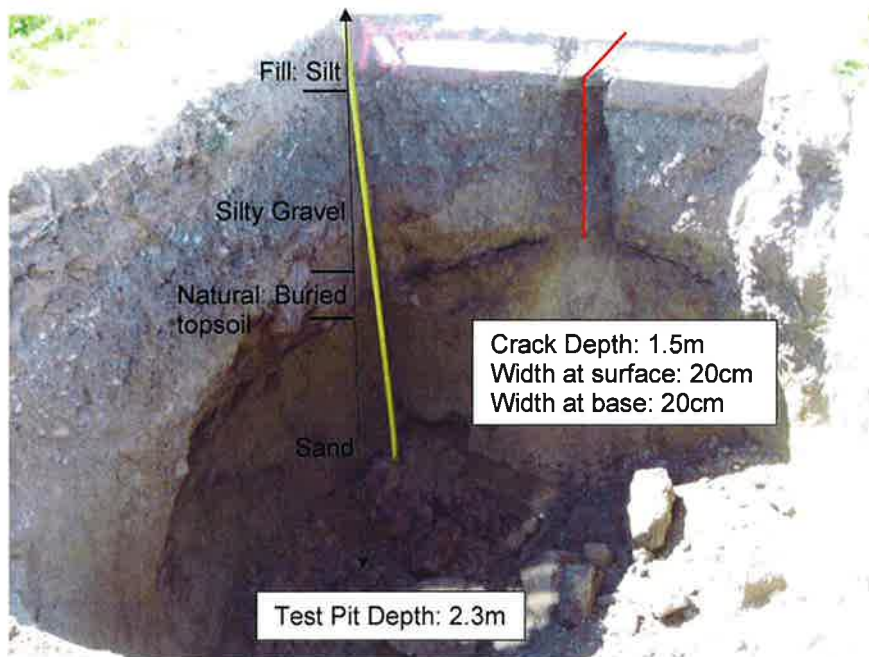
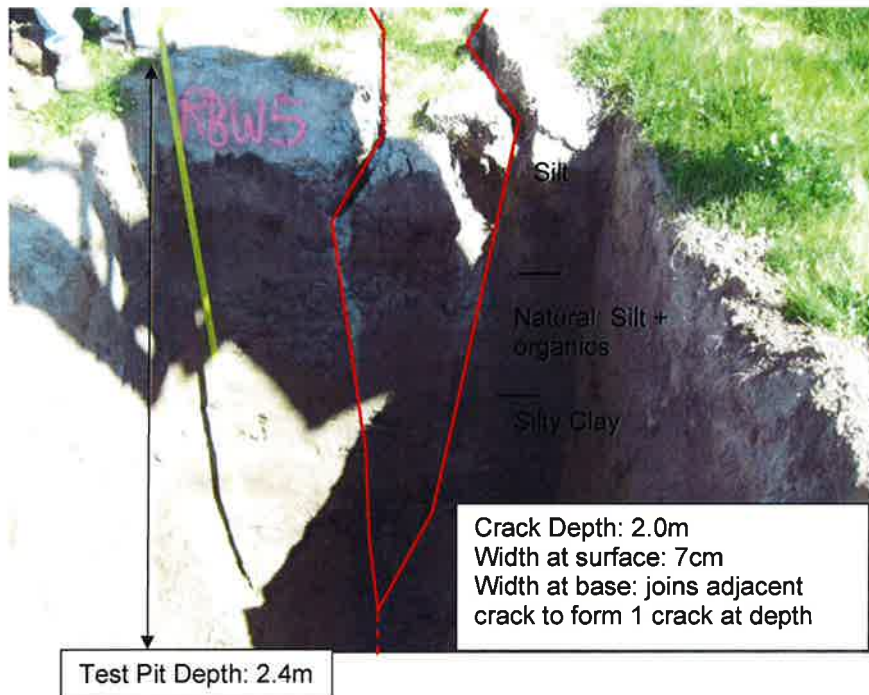


Ground Floor, 395 Madras Street,  
PO Box 4355, Christchurch  
Ph: 03 379 4402 Fax: 03 379 4403  
Email: [riley@riley.co.nz](mailto:riley@riley.co.nz)

### Test Pit Photos Right Bank Waimakariri (RBW) 3 and 4

Scale: NTS

Date: 12/10/2010



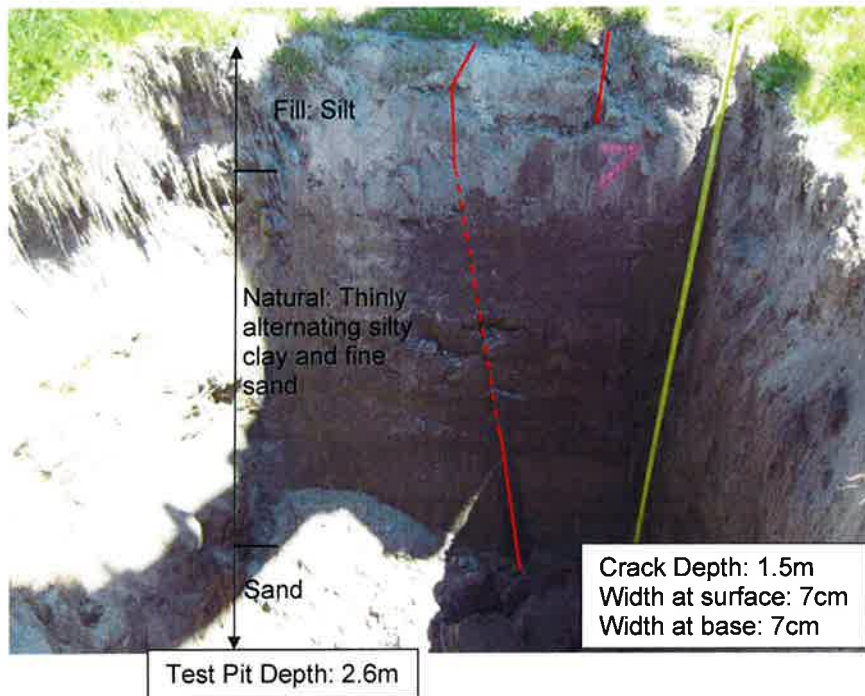
Ground Floor, 395 Madras Street,  
PO Box 4355, Christchurch  
Ph: 03 379 4402 Fax: 03 379 4403  
Email: [riley@riley.co.nz](mailto:riley@riley.co.nz)

### Test Pit Photos Right Bank Waimakariri (RBW) 5 and 6

Scale: NTS

Date: 12/10/2010



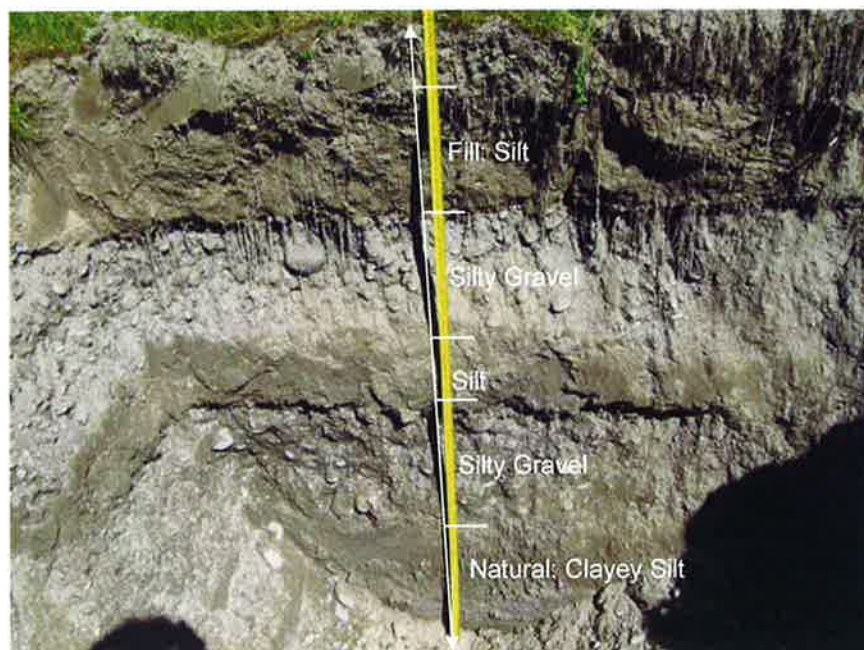
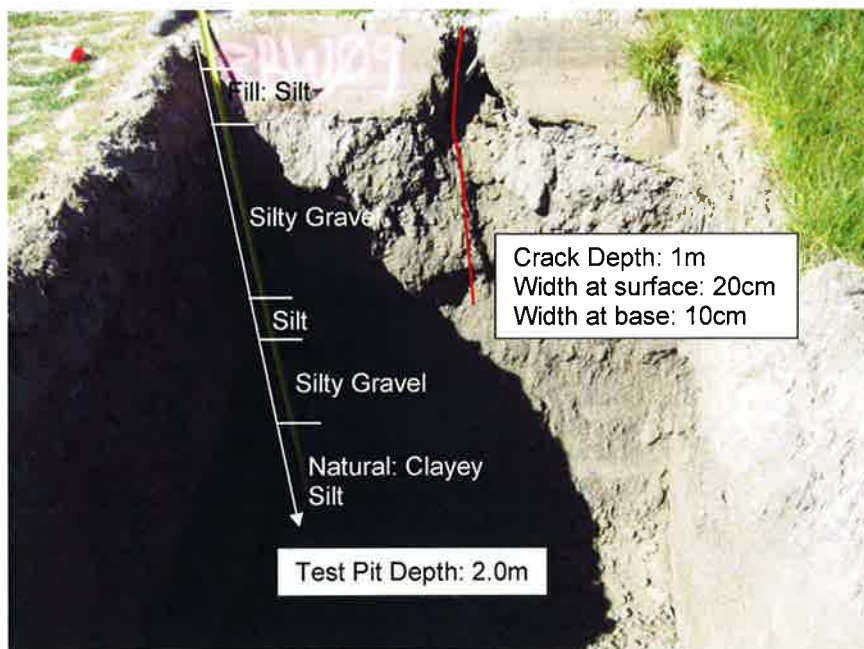


Ground Floor, 395 Madras Street,  
PO Box 4355, Christchurch  
Ph: 03 379 4402 Fax: 03 379 4403  
Email: riley@riley.co.nz

### Test Pit Photos Right Bank Waimakariri (RBW) 7 and 8

Scale: NTS

Date: 12/10/2010



Ground Floor, 395 Madras Street,  
PO Box 4355, Christchurch  
Ph: 03 379 4402 Fax: 03 379 4403  
Email: [riley@riley.co.nz](mailto:riley@riley.co.nz)

### Test Pit Photos Right Bank Waimakariri (RBW)

9

Scale: NTS

Date: 12/10/2010



# ***APPENDIX C***

## ***Test Pit Logs***





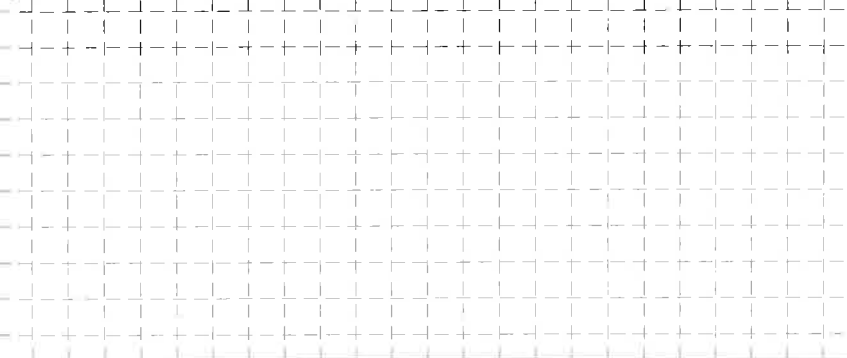
Riley Consultants Limited  
395 Madras Street  
Christchurch  
Tel: 03 3794402  
Fax: 03 3794403

## TEST PIT LOG

Project: Waimak Stopbank Condition Assessment		Location: Waimakariri Stopbank		Hole position:	No.: <b>LBW04</b>
Job No.: 10820	Start Date: 06-10-10 Finish Date: 06-10-10	Ground Level (m):	Co-Ordinates (): E 1,573,702.0 N 5,195,618.7		
Client: Environment Canterbury			Hole Depth: 1.00 m		Sheet: 1 of 1

Elevation (m)	Depth (m)	Geological Description <small>Soil Description: subordinate, particle size, MAJOR, minor, colour, structure, strength; moisture condition; grading; bedding; plasticity; sensitivity; major qualifications; weathering of clasts; subordinate qualifications; minor qualifications; additional structure; (GEOLOGICAL UNIT)</small>	Legend	Weathering <small>SW, S, SL, SH, V, W, U, UH, UH2</small>	Field Strength <small>SS, VL, CL, OL, SL, SH, V, W, U, UH, UH2</small>	Defect Description <small>(type, orientation, spacing, roughness, persistence, aperture, infilling etc)</small>	Groundwater	Samples	Tests
	0.20	Brown SILT, with abundant plant material / rootlets, firm to stiff, dry. (TOPSOIL)							
	1.00	Brown SILT. Non plastic, dry. (FILL)							
	EOH @ 1.00 m								
	2								
	3								
	4								
	5								

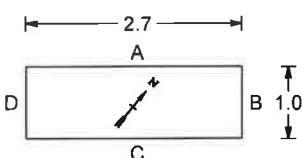
SKETCH:



MAP



Shoring/Support:  
Stability:



- Small Disturbed Sample
- Large Disturbed Sample
- U100 Undisturbed Sample
- ⬇ Permeability Test
- ▼ Clegg Hammer, test repetitions (IV)
- ✓ Insitu Vane Shear Strength (kPa)
- P=Peak, R=Residual, UTP=Unable to penetrate
- ▼ Scale Penetrometer - blows/50mm

GROUNDWATER

☒ None

☐ Slow Seep (depth)

☐ Rapid Inflow (depth)

PIT TERMINATED DUE TO:

☒ Target depth ☐ Collapse

☐ Refusal ☐ Machine limit

Remarks

All dimensions in metres  
Scale 1:50

Contractor:

Rig/Plant Used:  
CAT 312C

Logged by:  
AP

Checked by:



Riley Consultants Limited  
395 Madras Street  
Christchurch  
Tel: 03 3794402  
Fax: 03 3794403

## TEST PIT LOG

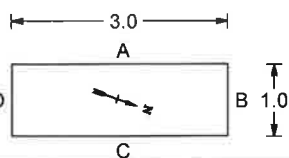
Project: Waimak Stopbank Condition Assessment		Location: Waimakariri Stopbank		Hole position:	No.: <b>LBW05</b>
Job No.: 10820	Start Date: 05-10-10 Finish Date: 05-10-10	Ground Level (m):	Co-Ordinates (): E 1,573,809.7 N 5,195,687.6		
Client: Environment Canterbury		Hole Depth: 1.85 m			Sheet: 1 of 1

Elevation (m)	Depth (m)	Geological Description <small>Soil Description: subordinate, particle size, MAJOR, minor, colour, structure, strength, moisture condition, grading, bedding, plasticity, sensitivity; major qualifications; weathering of clasts; subordinate qualifications, minor qualifications; additional structure; (GEOLOGICAL UNIT)</small>	Legend	Weathering <small>CS, V, W, M, F, S, U, N</small>	Field Strength <small>Soil   Rock S1, S2, S3, S4, S5, S6, S7, S8, S9, S10, S11, S12, S13, S14, S15, S16, S17, S18, S19, S20, S21, S22, S23, S24, S25, S26, S27, S28, S29, S30, S31, S32, S33, S34, S35, S36, S37, S38, S39, S40, S41, S42, S43, S44, S45, S46, S47, S48, S49, S50, S51, S52, S53, S54, S55, S56, S57, S58, S59, S60, S61, S62, S63, S64, S65, S66, S67, S68, S69, S70, S71, S72, S73, S74, S75, S76, S77, S78, S79, S80, S81, S82, S83, S84, S85, S86, S87, S88, S89, S90, S91, S92, S93, S94, S95, S96, S97, S98, S99, S100</small>	Defect Description <small>(type, orientation, spacing, roughness, persistence, aperture, infilling etc)</small>	Groundwater	Samples	Tests
	0.05	Brown SILT, with abundant plant material / rootlets, firm to stiff, dry. (TOPSOIL)	x						
	0.70	Brown silty fine SAND. Medium dense, dry. (FILL)	x						
	1	Brown fine SAND. Medium dense, dry							
	1.85	EOH @ 1.85 m							
	2								
	3								
	4								
	5								

SKETCH:

MAP

Shoring/Support:  
Stability:



- Small Disturbed Sample
- Large Disturbed Sample
- U100 Undisturbed Sample
- ⬇ Permeability Test
- ▼ Clegg Hammer, test repetitions (IV)
- ✓ Insitu Vane Shear Strength (kPa)
- P=Peak, R=Residual, UTP=Unable to penetrate
- ▼ Scala Penetrometer - blows/50mm

GROUNDWATER

☒ None

☐ Slow Seep (depth )

☐ Rapid Inflow (depth )

PIT TERMINATED DUE TO:

☒ Target depth ☐ Collapse

☐ Refusal ☐ Machine limit

Remarks

All dimensions in metres  
Scale 1:50

Contractor:

Rig/Plant Used:  
CAT 312C

Logged by:  
AP

Checked by:



Riley Consultants Limited  
395 Madras Street  
Christchurch  
Tel: 03 3794402  
Fax: 03 3794403

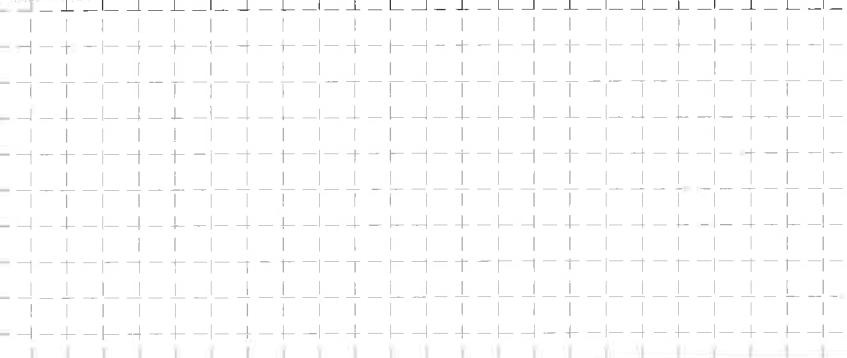
## TEST PIT LOG

Project: Waimak Stopbank Condition Assessment		Location: Waimakariri Stopbank		Hole position:	No.: <b>LBW06</b>
Job No.: 10820	Start Date: 05-10-10 Finish Date: 05-10-10	Ground Level (m):	Co-Ordinates (): E 1,573,715.8 N 5,195,622.9		
Client: Environment Canterbury		Hole Depth: 2.00 m			Sheet: 1 of 1

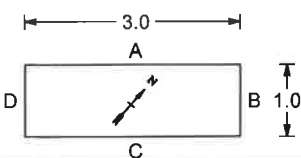
Elevation (m)	Depth (m)	Geological Description <small>Soil Description: subordinate, particle size, MAJOR, minor, colour, structure; strength; moisture condition; grading; bedding; plasticity, sensitivity; major qualifications; weathering of clasts; subordinate qualifications; minor qualifications; additional structure; (GEOLOGICAL UNIT)</small>	Legend	Weathering	Field Strength <small>Soil   Rock</small>	Defect Description <small>(type, orientation, spacing, roughness, persistence, aperture, infilling etc)</small>	Groundwater	Samples	Tests
	0.20	Brown SILT, with abundant plant material / rootlets, firm to stiff, dry. (TOPSOIL)							
	0.90	Brown SILT. Firm, dry. (FILL)							
1		Brown silty fine SAND. Medium dense, moist. (NATURAL)						LBW6 @ 1m	
2	2.00	EOH @ 2.00 m							
3									
4									
5									

SKETCH:

MAP



Shoring/Support:  
Stability:



- Small Disturbed Sample
- Large Disturbed Sample
- U100 Undisturbed Sample
- ⊥ Permeability Test
- ▼ Clegg Hammer, test repetitions (IV)
- ✓ Insitu Vane Shear Strength (kPa)
- P=Peak, R=Residual, UTP=Unable to penetrate
- ▼ Scala Penetrometer - blows/50mm

GROUNDWATER

☒ None

☐ Slow Seep (depth)

☐ Rapid Inflow (depth)

PIT TERMINATED DUE TO:

☒ Target depth

☐ Collapse

☐ Refusal

☐ Machine limit

Remarks

All dimensions in metres  
Scale 1:50

Contractor:

Rig/Plant Used:  
CAT 312C

Logged by:  
AP

Checked by:



Riley Consultants Limited  
395 Madras Street  
Christchurch  
Tel: 03 3794402  
Fax: 03 3794403

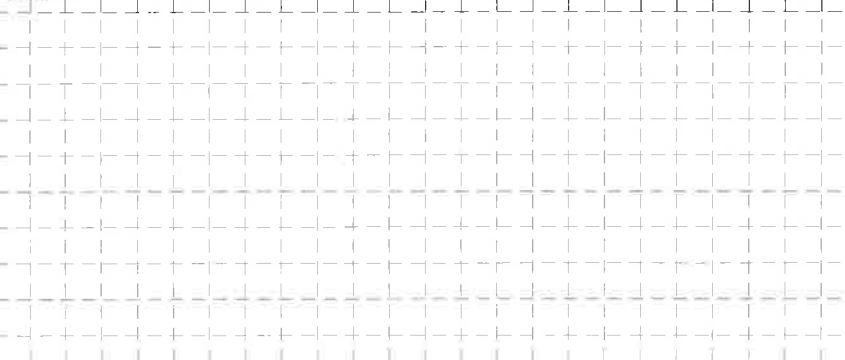
## TEST PIT LOG

Project: Waimak Stopbank Condition Assessment		Location: Waimakariri Stopbank		Hole position:	No.: <b>LBW07</b>
Job No.: 10820	Start Date: 05-10-10 Finish Date: 05-10-10	Ground Level (m):	Co-Ordinates (): E 1,573,809.2 N 5,195,737.0		Sheet: 1 of 1
Client: Environment Canterbury		Hole Depth: 1.90 m			

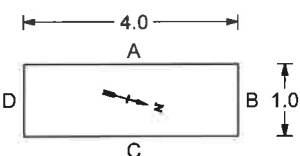
Elevation (m)	Depth (m)	Geological Description <small>Soil Description: subordinate, particle size, MAJOR, minor, colour, structure; strength, moisture condition, grading, bedding; plasticity, sensitivity; major qualifications; weathering of clasts; subordinate qualifications, minor qualifications; additional structure; (GEOLOGICAL UNIT)</small>	Legend	Field Strength <small>Soil   Rock</small>	Defect Description <small>(type, orientation, spacing, roughness, persistence, aperture, infilling etc)</small>	Groundwater	Samples	Tests
	0.30	Brown SILT, with abundant plant material / rootlets, firm to stiff, dry. (TOPSOIL)						
	1.00	Brown SILT, Firm, moist. (FILL)						
	1.90	Brown fine SAND, Medium dense, moist. (NATURAL)						
2		EOH @ 1.90 m						
3								
4								
5								

SKETCH:

MAP



Shoring/Support:  
Stability:



- Small Disturbed Sample
- Large Disturbed Sample
- U100 Undisturbed Sample
- ↓ Permeability Test
- ▼ Clegg Hammer; test repetitions (IV)
- ✓ Insitu Vane Shear Strength (kPa)
- P=Peak, R=Residual, UTP=Unable to penetrate
- ▼ Scala Penetrometer - blows/50mm

GROUNDWATER

☒ None

☐ Slow Seep (depth )

☐ Rapid Inflow (depth )

PIT TERMINATED DUE TO:

☒ Target depth

☐ Collapse

☐ Refusal

☐ Machine limit

Remarks

All dimensions in metres  
Scale 1:50

Contractor:

Rig/Plant Used:  
CAT 312C

Logged by:  
AP

Checked by:





Riley Consultants Limited  
395 Madras Street  
Christchurch  
Tel: 03 3794402  
Fax: 03 3794403

## TEST PIT LOG

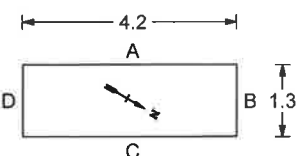
Project: Waimak Stopbank Condition Assessment		Location: Waimakariri Stopbank		Hole position:	No.:
Job No.: 10820	Start Date: 05-10-10 Finish Date: 05-10-10	Ground Level (m):	Co-Ordinates (): E 1,573,803.0 N 5,195,775.5		<b>LBW08</b>
Client: Environment Canterbury			Hole Depth: 1.45 m		Sheet: 1 of 1

Elevation (m)	Depth (m)	Geological Description <small>Soil Description: subordinate, particle size, MAJOR, minor, colour, structure, strength, moisture condition; grading; bedding; plasticity; sensitivity; major qualifications; weathering of clasts; subordinate qualifications, minor qualifications; additional structure; (GEOLOGICAL UNIT)</small>	Legend	Field Strength <small>Soil   Rock</small>	Defect Description <small>(type, orientation, spacing, roughness, persistence, aperture, infilling etc)</small>	Groundwater	Samples	Tests
	0.10							
	0.40	Brown SILT, with abundant plant material / rootlets, firm to stiff, dry. (TOPSOIL)						
	0.70	Brown SILT. Firm, non plastic, moist (FILL)						
	0.80							
	1	Brown clayey SILT. Firm, low plasticity, moist.						
	1.45	Brown / dark brown, mottled orange fine SAND. Medium dense, moist. Limonite stained (NATURAL?)					LBW8 @ 1.3m	
	2	Brown silty fine SAND. Medium dense, moist.						
		EOH @ 1.45 m						
	3							
	4							
	5							

SKETCH:

MAP

Shoring/Support:  
Stability:



- Small Disturbed Sample
- Large Disturbed Sample
- U100 Undisturbed Sample
- ⊥ Permeability Test
- ▼ Clegg Hammer, test repetitions (IV)
- ✓ Insitu Vane Shear Strength (kPa)
- P=Peak, R=Residual,
- UTP=Unable to penetrate
- ▼ Scala Penetrometer - blows/50mm

GROUNDWATER

☒ None

☐ Slow Seep (depth)

☐ Rapid Inflow (depth)

PIT TERMINATED DUE TO:

☒ Target depth ☐ Collapse

☐ Refusal ☐ Machine limit

Remarks

All dimensions in metres  
Scale 1:50

Contractor:

Rig/Plant Used:  
CAT 312C

Logged by:  
AP

Checked by:



Riley Consultants Limited  
395 Madras Street  
Christchurch  
Tel: 03 3794402  
Fax: 03 3794403

## TEST PIT LOG

Project: Waimak Stopbank Condition Assessment		Location: Waimakariri Stopbank		Hole position:	No.:
Job No.: 10820	Start Date: 05-10-10 Finish Date: 05-10-10	Ground Level (m):	Co-Ordinates (): E 1,573,562.7 N 5,195,906.5		<b>LBW09</b>
Client: Environment Canterbury			Hole Depth: 1.60 m		Sheet: 1 of 1

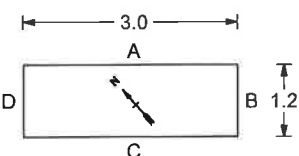
Elevation (m)	Depth (m)	Geological Description <small>Soil Description: subordinate, particle size, MAJOR, minor, colour, structure; strength; moisture condition; grading; bedding; plasticity; sensitivity; major qualifications; weathering of clasts; subordinate qualifications, minor qualifications; additional structure; (GEOLOGICAL UNIT)</small>	Legend	Field Strength <small>Soil   Rock</small>	Defect Description <small>(type, orientation, spacing, roughness, persistence, aperture, infilling etc)</small>	Groundwater	Samples	Tests
	0.10	Brown SILT, with abundant plant material / rootlets, firm to stiff, dry. (TOPSOIL)						
	0.60	Brown clayey SILT with some rootlets. Firm, non plastic, moist. (FILL)						
	1	Brown silty SAND. Medium dense, moist (NATURAL)						
	1.60	EOH @ 1.60 m						
	2							
	3							
	4							
	5							

SKETCH:

MAP



Shoring/Support:  
Stability:



- Small Disturbed Sample
- Large Disturbed Sample
- U100 Undisturbed Sample
- ⊥ Permeability Test
- ▼ Clegg Hammer, test repetitions (IV)
- ✓ Insitu Vane Shear Strength (kPa)
- P=Peak, R=Residual, UTP=Unable to penetrate
- ▼ Scala Penetrometer - blows/50mm

GROUNDWATER

☒ None

☐ Slow Seep (depth)

☐ Rapid Inflow (depth)

PIT TERMINATED DUE TO:

☒ Target depth ☐ Collapse

☐ Refusal ☐ Machine limit

Remarks

All dimensions in metres  
Scale 1:50

Contractor:

Rig/Plant Used:  
CAT 312C

Logged by:  
AP

Checked by:



Riley Consultants Limited  
395 Madras Street  
Christchurch  
Tel: 03 3794402  
Fax: 03 3794403

## TEST PIT LOG

Project: Waimak Stopbank Condition Assessment		Location: Waimakariri Stopbank		Hole position:	No.:
Job No.: 10820	Start Date: 05-10-10 Finish Date: 05-10-10	Ground Level (m):	Co-Ordinates (): E 1,573,719.9 N 5,195,849.4		<b>LBW10</b>
Client: Environment Canterbury			Hole Depth: 1.90 m		Sheet: 1 of 1

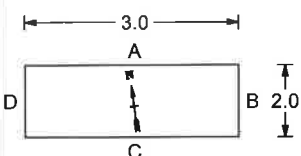
Elevation (m)	Depth (m)	Geological Description <small>Soil Description: subordinate, particle size, MAJOR, minor, colour, structure; strength; moisture condition; grading; bedding; plasticity; sensitivity; major qualifications; weathering of clasts; subordinate qualifications; minor qualifications; additional structure; (GEOLOGICAL UNIT)</small>	Legend	Field Strength <small>Soil   Rock</small>	Defect Description <small>(type, orientation, spacing, roughness, persistence, aperture, infilling etc)</small>	Groundwater	Samples	Tests
	0.10	Brown SILT, with abundant plant material / rootlets, firm to stiff, dry. (TOPSOIL)						
	0.70	Brown SILT. Firm, non plastic, moist. (NATURAL)						
	1	Brown silty fine SAND. Medium dense, moist						
	1.90	EOH @ 1.90 m						
	2							
	3							
	4							
	5							

SKETCH:

MAP



Shoring/Support:  
Stability:



- Small Disturbed Sample
- Large Disturbed Sample
- U100 Undisturbed Sample
- ↓ Permeability Test
- ▼ Clegg Hammer; test repetitions (IV)
- ✓ Insitu Vane Shear Strength (kPa)
- P=Peak, R=Residual, UTP=Unable to penetrate
- ▼ Scala Penetrometer - blows/50mm

GROUNDWATER

☒ None

☐ Slow Seep (depth )

☐ Rapid Inflow (depth )

PIT TERMINATED DUE TO:

☒ Target depth ☐ Collapse

☐ Refusal ☐ Machine limit

Remarks

All dimensions in metres  
Scale 1:50

Contractor:

Rig/Plant Used:  
CAT 312C

Logged by:  
AP

Checked by:



Riley Consultants Limited  
395 Madras Street  
Christchurch  
Tel: 03 3794402  
Fax: 03 3794403

## TEST PIT LOG

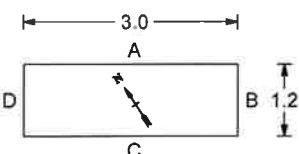
Project: Waimak Stopbank Condition Assessment		Location: Waimakariri Stopbank		Hole position:	No.:
Job No.: 10820	Start Date: 05-10-10 Finish Date: 05-10-10	Ground Level (m):	Co-Ordinates (): E 1,573,794.5 N 5,195,822.1		LBW11
Client: Environment Canterbury		Hole Depth: 2.90 m		Sheet: 1 of 1	

Elevation (m)	Depth (m)	Geological Description <small>Soil Description: subordinate, particle size, MAJOR, minor, colour, structure; strength; moisture condition; grading; bedding; plasticity; sensitivity; major qualifications; weathering of clasts; subordinate qualifications; minor qualifications; additional structure; (GEOLOGICAL UNIT)</small>	Legend	Weathering <small>ECV Low Med High Very High</small>	Field Strength <small>Soil   Rock ECV Low Med High Very High</small>	Defect Description <small>(type, orientation, spacing, roughness, persistence, aperture, infilling etc)</small>	Groundwater	Samples	Tests
	0.10								
	0.40	Brown SILT, with abundant plant material / rootlets, firm to stiff, dry. (TOPSOIL)							
	0.90	Brown SILT. Firm, non plastic, dry. (FILL)							
	1	Brown silty GRAVEL. Medium dense, moist							
	2	Brown clayey SILT. Firm, low plasticity, moist. (NATURAL)							
	2.90								
	3	EOH @ 2.90 m						LBW11 @ 2.8m	
	4								
	5								

SKETCH:

MAP

Shoring/Support:  
Stability:



- Small Disturbed Sample
- Large Disturbed Sample
- U100 Undisturbed Sample
- ⊥ Permeability Test
- ▼ Clegg Hammer, test repetitions (IV)
- ✓ Insitu Vane Shear Strength (kPa)
- P=Peak, R=Residual, UTP=Unable to penetrate
- ▼ Scala Penetrometer - blows/50mm

GROUNDWATER

☒ None

☐ Slow Seep (depth )

☐ Rapid Inflow (depth )

PIT TERMINATED DUE TO:

☒ Target depth ☐ Collapse

☐ Refusal ☐ Machine limit

Remarks

All dimensions in metres  
Scale 1:50

Contractor:

Rig/Plant Used:  
CAT 312C

Logged by:  
AP

Checked by:



Riley Consultants Limited  
395 Madras Street  
Christchurch  
Tel: 03 3794402  
Fax: 03 3794403

## TEST PIT LOG

Project: Waimak Stopbank Condition Assessment		Location: Waimakariri Stopbank		Hole position:	No.:
Job No.: 10820	Start Date: 07-10-10 Finish Date: 07-10-10	Ground Level (m):	Co-Ordinates (): E 1,575,779.4 N 5,195,931.3		<b>LBW12</b>
Client: Environment Canterbury			Hole Depth: 1.60 m		Sheet: 1 of 1

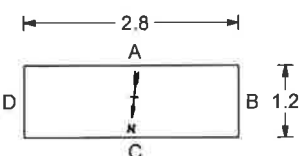
Elevation (m)	Depth (m)	Geological Description <small>Soil Description: subordinate, particle size, MAJOR, minor, colour, structure, strength, moisture condition, grading, bedding, plasticity, sensitivity; major qualifications; weathering of clasts; subordinate qualifications; minor qualifications; additional structure, (GEOLOGICAL UNIT)</small>	Legend	Weathering	Field Strength <small>Soil   Rock</small>	Defect Description <small>(type, orientation, spacing, roughness, persistence, aperture, infilling etc)</small>	Groundwater	Samples	Tests
	0.20	Brown / light brown clayey SILT. Firm, non plastic to low plasticity, dry, (FILL)							
	1.10	Brown gravelly SILT. Stiff, moist. Gravel; fine to coarse, subrounded.							
	1.60	Brown silty fine SAND. Medium dense, non plastic, moist (NATURAL)							
	2	EOH @ 1.60 m							
	3								
	4								
	5								

SKETCH:

MAP



Shoring/Support:  
Stability:



- Small Disturbed Sample
- Large Disturbed Sample
- U100 Undisturbed Sample
- ⊥ Permeability Test
- ▼ Clegg Hammer; test repetitions (IV)
- ✓ Insitu Vane Shear Strength (kPa)
- P=Peak, R=Residual, UTP=Unable to penetrate
- ▼ Scala Penetrometer - blows/50mm

GROUNDWATER

☒ None

☐ Slow Seep (depth )

☐ Rapid Inflow (depth )

PIT TERMINATED DUE TO:

☒ Target depth ☐ Collapse

☐ Refusal ☐ Machine limit

Remarks

Across the mouth of Kairaki Creek from the Kairaki Yacht Club

All dimensions in metres  
Scale 1:50

Contractor:

Rig/Plant Used:  
CAT 312C

Logged by: AP  
Checked by:





Riley Consultants Limited  
395 Madras Street  
Christchurch  
Tel: 03 3794402  
Fax: 03 3794403

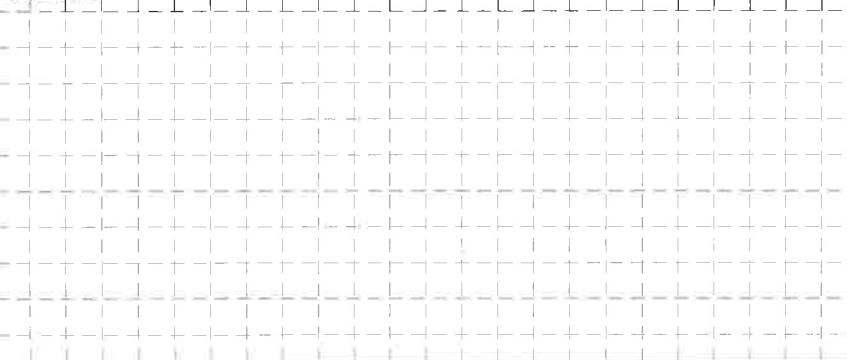
## TEST PIT LOG

Project: Waimak Stopbank Condition Assessment		Location: Waimakariri Stopbank		Hole position:	No.: <b>LBW13</b>
Job No.: 10820	Start Date: 07-10-10 Finish Date: 07-10-10	Ground Level (m):	Co-Ordinates (): E 1,575,755.5 N 5,195,930.5		
Client: Environment Canterbury		Hole Depth: 2.20 m			Sheet: 1 of 1

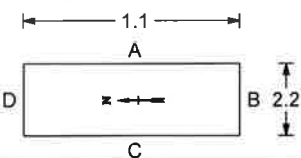
Elevation (m)	Depth (m)	Geological Description <small>Soil Description: subordinate, particle size, MAJOR, minor, colour, structure, strength; moisture condition; grading; bedding; plasticity; sensitivity; major qualifications, weathering of clasts; subordinate qualifications, minor qualifications; additional structure; (GEOLOGICAL UNIT)</small>	Legend	Weathering	Field Strength <small>Soil   Rock</small>	Defect Description <small>(type, orientation, spacing, roughness, persistence, aperture, infilling etc)</small>	Groundwater	Samples	Tests
	0.30	Brown / light brown clayey SILT. Firm, non plastic to low plasticity, dry (FILL)							
	1	Brown gravelly SILT. Stiff, moist. Gravel; fine to coarse, subrounded							
	1.30								
	2	Brown silty fine SAND with trace clay and partially decomposed organic material. Medium dense, non plastic, moist. (NATURAL)							
	2.20								
		EOH @ 2.20 m							
	3								
	4								
	5								

SKETCH:

MAP



Shoring/Support:  
Stability:



- Small Disturbed Sample
- Large Disturbed Sample
- U100 Undisturbed Sample
- ⬇ Permeability Test
- ▼ Clegg Hammer, test repetitions (IV)
- ✓ Insitu Vane Shear Strength (kPa)
- P=Peak, R=Residual, UTP=Unable to penetrate
- ▼ Scala Penetrometer - blows/50mm

GROUNDWATER

☒ None

- ☐ Slow Seep (depth)
- ☐ Rapid Inflow (depth)

PIT TERMINATED DUE TO:

- ☒ Target depth
- ☐ Collapse
- ☐ Refusal
- ☐ Machine limit

Remarks

Transverse crack opposite from Yacht Club

All dimensions in metres  
Scale 1:50

Contractor:

Rig/Plant Used:  
CAT 312C

Logged by:  
AP

Checked by:



Riley Consultants Limited  
395 Madras Street  
Christchurch  
Tel: 03 3794402  
Fax: 03 3794403

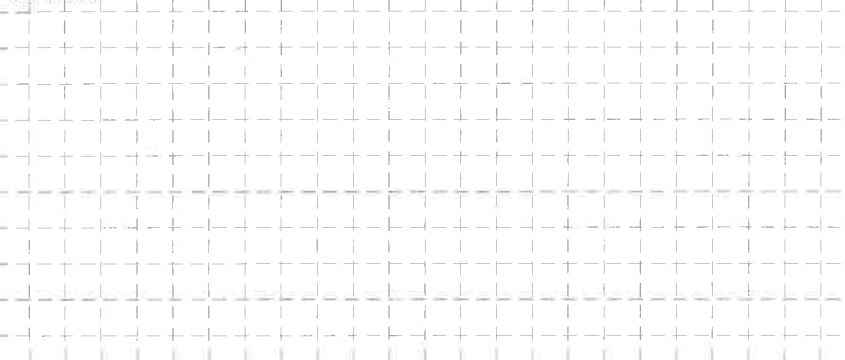
## TEST PIT LOG

Project: Waimak Stopbank Condition Assessment		Location: Waimakariri Stopbank		Hole position:	No.: <b>LBW14</b>
Job No.: 10820	Start Date: 07-10-10 Finish Date: 07-10-10	Ground Level (m):	Co-Ordinates (): E 1,575,717.2 N 5,195,931.5		
Client: Environment Canterbury		Hole Depth: 3.00 m			Sheet: 1 of 1

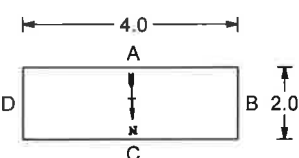
Elevation (m)	Depth (m)	Geological Description <small>Soil Description: subordinate, particle size, MAJOR, minor, colour, structure, strength, moisture condition, grading, bedding, plasticity, sensitivity, major qualifications, weathering of clasts; subordinate qualifications; minor qualifications; additional structure; (GEOLOGICAL UNIT)</small>	Legend	Weathering	Field Strength <small>Soil   Rock</small>	Defect Description <small>(type, orientation, spacing, roughness, persistence, aperture, infilling etc)</small>	Groundwater	Samples	Tests
	0.20	Brown SILT, with abundant plant material / rootlets, firm to stiff, dry (TOPSOIL)							
	1.00	Brown gravelly SILT. Stiff, moist. Gravel; fine to coarse, subrounded. (FILL)							
	1.20	Brown / orange sandy SILT. Firm, non plastic, moist Stained orange. (NATURAL)							
	2	Grey silty CLAY. Firm, low to medium plasticity, wet Stained orange.							
	3.00	EOH @ 3.00 m							
	4								
	5								

SKETCH:

MAP



Shoring/Support:  
Stability:



- Small Disturbed Sample
- Large Disturbed Sample
- U100 Undisturbed Sample
- ⬇ Permeability Test
- ▼ Clegg Hammer; test repetitions (IV)
- ✓ Insitu Vane Shear Strength (kPa)
- P=Peak, R=Residual, UTP=Unable to penetrate
- ▼ Scala Penetrometer - blows/50mm

GROUNDWATER

☒ None

- ☐ Slow Seep (depth)
- ☐ Rapid Inflow (depth)

PIT TERMINATED DUE TO:

- ☒ Target depth
- ☐ Collapse
- ☐ Refusal
- ☐ Machine limit

Remarks

Crack beside the gravel stockpile after the yacht club

All dimensions in metres  
Scale 1:50

Contractor:

Rig/Plant Used:  
CAT 312C

Logged by:  
AP

Checked by:



Riley Consultants Limited  
395 Madras Street  
Christchurch  
Tel: 03 3794402  
Fax: 03 3794403

## TEST PIT LOG

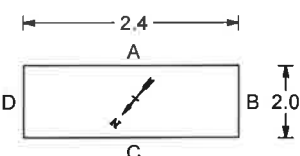
Project: Waimak Stopbank Condition Assessment		Location: Waimakariri Stopbank		Hole position:	No.: <b>LBW15</b>
Job No.: 10820	Start Date: 07-10-10 Finish Date: 07-10-10	Ground Level (m):	Co-Ordinates (): E 1,575,556.9 N 5,195,967.7		
Client: Environment Canterbury			Hole Depth: 1.50 m		Sheet: 1 of 1

Elevation (m)	Depth (m)	Geological Description <small>Soil Description: subordinate, particle size, MAJOR, minor, colour, structure, strength; moisture condition; grading; bedding; plasticity, sensitivity; major qualifications; weathering of clasts; subordinate qualifications; minor qualifications; additional structure; (GEOLOGICAL UNIT)</small>	Legend	Weathering <small>CLAY SILT SAND GRAVEL COBBLES Boulders</small>	Field Strength <small>Soil   Rock</small>	Defect Description <small>(type, orientation, spacing, roughness, persistence, aperture, infilling etc)</small>	Groundwater	Samples	Tests
	0.05	Brown SILT, with abundant plant material / rootlets, firm to stiff, dry (TOPSOIL)	x						
	0.50	Brown SILT. Firm, non plastic, dry. (FILL)	x						
	1.00	Brown gravelly SILT. Firm, non plastic, dry. Gravel subrounded.	x						
	1.20		x						
	1.30	Dark brown clayey SILT. Firm, low plasticity, moist (NATURAL)	x						
	1.50		x						
	2.00	Brown SILT. Firm, non plastic, moist							
		EOH @ 1.50 m							
	3.00								
	4.00								
	5.00								

SKETCH:

MAP

Shoring/Support:  
Stability:



- Small Disturbed Sample
- Large Disturbed Sample
- U100 Undisturbed Sample
- ⊥ Permeability Test
- ▼ Clegg Hammer, test repetitions (IV)
- ✓ Insitu Vane Shear Strength (kPa)
- P=Peak, R=Residual, UTP=Unable to penetrate
- ▼ Scala Penetrometer - blows/50mm

GROUNDWATER

☒ None

☐ Slow Seep (depth)

☐ Rapid Inflow (depth)

PIT TERMINATED DUE TO:

☒ Target depth ☐ Collapse

☐ Refusal ☐ Machine limit

Remarks

By the farmers access gate

All dimensions in metres  
Scale 1:50

Contractor:

Rig/Plant Used:  
CAT 312C

Logged by:  
AP

Checked by:



Riley Consultants Limited  
395 Madras Street  
Christchurch  
Tel: 03 3794402  
Fax: 03 3794403

## TEST PIT LOG

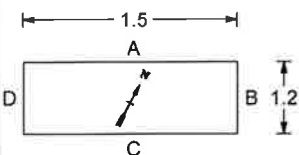
Project: Waimak Stopbank Condition Assessment		Location: Waimakariri Stopbank		Hole position:	No.: <b>RBK02</b>
Job No.: 10820	Start Date: 06-10-10 Finish Date: 06-10-10	Ground Level (m):	Co-Ordinates (°): E 1,575,871.9 N 5,196,657.6		
Client: Environment Canterbury			Hole Depth: 1.50 m		Sheet: 1 of 1

Elevation (m)	Depth (m)	Geological Description <small>Soil Description: subordinate, particle size, MAJOR, minor; colour, structure, strength; moisture condition; grading; bedding; plasticity; sensitivity; major qualifications; weathering of clasts; subordinate qualifications; minor qualifications; additional structure; (GEOLOGICAL UNIT)</small>	Legend	Field Strength <small>Soil   Rock</small>	Defect Description <small>(type, orientation, spacing, roughness, persistence, aperture, infilling etc)</small>	Groundwater	Samples	Tests
	0.20	Brown SILT, with abundant plant material / rootlets, firm to stiff, dry. (TOPSOIL)	X					
	0.60	Brown SILT. Firm, non plastic, dry. (FILL)	X					
	0.70		X					
	0.80	Dark brown SILT. Firm, non plastic, moist (buried topsoil?)	X					
	1.40	Brown SILT. Firm, non plastic, moist. (NATURAL)	X					
	1.50		X					
	2	Brown streaked dark brown clayey SILT. Firm, low plasticity, moist. With abundant decomposing organics.						
		Brown streaked grey SILT. Firm, low plasticity, moist.						
		EOH @ 1.50 m						
	3							
	4							
	5							

SKETCH:

MAP

Shoring/Support:  
Stability:



- Small Disturbed Sample
- Large Disturbed Sample
- U100 Undisturbed Sample
- Permeability Test
- ▼ Clegg Hammer, test repetitions (IV)
- ✓ Insitu Vane Shear Strength (kPa)
- P=Peak, R=Residual, UTP=Unable to penetrate
- ▼ Scala Penetrometer - blows/50mm

GROUNDWATER

☒ None

☐ Slow Seep (depth )

☐ Rapid Inflow (depth )

PIT TERMINATED DUE TO:

☒ Target depth

☐ Collapse

☐ Refusal

☐ Machine limit

Remarks

All dimensions in metres  
Scale 1:50

Contractor:

Rig/Plant Used:  
CAT 312C

Logged by:  
AP

Checked by:



Riley Consultants Limited  
395 Madras Street  
Christchurch  
Tel: 03 3794402  
Fax: 03 3794403

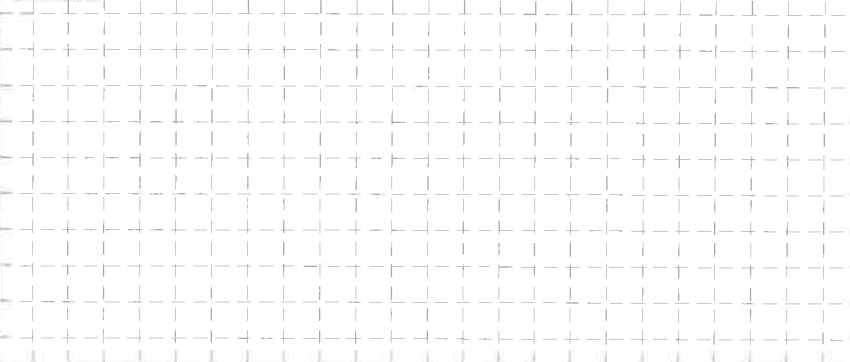
## TEST PIT LOG

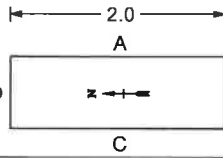
Project: Waimak Stopbank Condition Assessment		Location: Waimakariri Stopbank		Hole position:	No.: <b>RBK03</b>
Job No.: 10820	Start Date: 06-10-10 Finish Date: 06-10-10	Ground Level (m):	Co-Ordinates (): E 1,575,829.9 N 5,196,314.9		Sheet: 1 of 1
Client: Environment Canterbury		Hole Depth: 2.00 m			

Elevation (m)	Depth (m)	Geological Description <small>Soil Description: subordinate, particle size, MAJOR, minor, colour, structure, strength, moisture condition; grading, bedding; plasticity; sensitivity; major qualifications; weathering of clasts; subordinate qualifications, minor qualifications; additional structure; (GEOLOGICAL UNIT)</small>	Legend	Weathering	Field Strength <small>Soil   Rock</small>	Defect Description <small>(type, orientation, spacing, roughness, persistence, aperture, infilling etc)</small>	Groundwater	Samples	Tests
	0.30	Brown SILT. Firm to stiff, non plastic, dry. (FILL)							
	1.20	Grey silty SAND with minor clay. Loose, moist. Limonite stained.							
	2.00	Grey / brown silty CLAY with abundant decomposing plant material. Firm, wet. (NATURAL)							
	2.00	EOH @ 2.00 m							
	3								
	4								
	5								
	6								

SKETCH:

MAP





<b>Shoring/Support:</b> Stability: 		<ul style="list-style-type: none"><li>● Small Disturbed Sample</li><li>■ Large Disturbed Sample</li><li>■ U100 Undisturbed Sample</li><li>⊥ Permeability Test</li><li>▼ Clegg Hammer; test repetitions (IV)</li><li>✓ Insitu Vane Shear Strength (kPa)</li><li>P=Peak, R=Residual</li><li>UTP=Unable to penetrate</li><li>▼ Scala Penetrometer - blows/50mm</li></ul>	<b>GROUNDWATER</b> <input checked="" type="checkbox"/> None <input type="checkbox"/> Slow Seep (depth ) <input type="checkbox"/> Rapid Inflow (depth ) <b>PIT TERMINATED DUE TO:</b> <input checked="" type="checkbox"/> Target depth <input type="checkbox"/> Collapse <input type="checkbox"/> Refusal <input type="checkbox"/> Machine limit	<b>Remarks</b>
All dimensions in metres Scale 1:50		Contractor:	Rig/Plant Used: CAT 312C	Logged by: AP Checked by:



## TEST PIT LOG

Project: Waimak Stopbank Condition Assessment		Location: Waimakariri Stopbank		Hole position:	No.:  <b>RBK04</b>
Job No.: 10820	Start Date: 06-10-10 Finish Date: 06-10-10	Ground Level (m):	Co-Ordinates (): E 1,575,823.7 N 5,196,144.8		
Client: Environment Canterbury		Hole Depth: 1.80 m	Sheet: 1 of 1		

Elevation (m)	Depth (m)	Geological Description <small>Soil Description: subordinate, particle size, MAJOR, minor; colour, structure; strength; moisture condition; grading; bedding; plasticity; sensitivity; major qualifications; weathering of clasts; subordinate qualifications; minor qualifications; additional structure; (GEOLOGICAL UNIT)</small>	Legend	Weathering <small>W1 W2 W3 W4 W5</small>	Field Strength <small>Soil: S1, S2, S3, S4, S5, S6, S7, S8, S9, S10 Rock: R1, R2, R3, R4, R5, R6, R7, R8, R9, R10</small>	Defect Description <small>(type, orientation, spacing, roughness, persistence, aperture, infilling etc)</small>	Groundwater	Samples	Tests
	0.10	Brown SILT, with abundant plant material / rootlets, firm to stiff, dry. (TOPSOIL)							
	0.70	Brown SILT, Firm, non plastic, dry. (FILL)							
	0.80	Brown clayey SILT, Firm, non plastic, dry. With abundant fragments of wood and partially decomposed organics. (NATURAL)							
	1.80	Grey silty CLAY, Firm, moist. With abundant partially decomposed wood fragments. Organic stained.							
	2	EOH @ 1.80 m							
	3								
	4								
	5								

SKETCH:	MAP
	

<p>Shoring/Support: Stability:</p>	<ul style="list-style-type: none"> <li>● Small Disturbed Sample</li> <li>⬮ Large Disturbed Sample</li> <li>■ U100 Undisturbed Sample</li> <li>⬮ Permeability Test</li> <li>▼ Clegg Hammer; test repetitions (IV)</li> <li>✓ Insitu Vane Shear Strength (kPa)</li> <li>P=Peak, R=Residual, UTP=Unable to penetrate</li> <li>▼ Scale Penetrometer - blows/50mm</li> </ul>	<p>GROUNDWATER <input checked="" type="checkbox"/> None</p> <p><input type="checkbox"/> Slow Seep (depth )</p> <p><input type="checkbox"/> Rapid Inflow (depth )</p> <p>PIT TERMINATED DUE TO:</p> <p><input checked="" type="checkbox"/> Target depth <input type="checkbox"/> Collapse</p> <p><input type="checkbox"/> Refusal <input type="checkbox"/> Machine limit</p>	<p>Remarks</p>
--	---	---	----------------

All dimensions in metres Scale 1:50	Contractor:	Rig/Plant Used: CAT 312C	Logged by: AP	Checked by:
--	-------------	-----------------------------	------------------	-------------



Riley Consultants Limited  
395 Madras Street  
Christchurch  
Tel: 03 3794402  
Fax: 03 3794403

## TEST PIT LOG

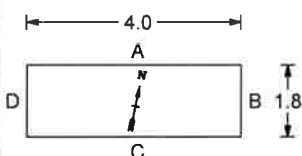
Project: Waimak Stopbank Condition Assessment		Location: Waimakariri Stopbank		Hole position:	No.: <b>RBW01</b>
Job No.: 10820	Start Date: 06-10-10 Finish Date: 06-10-10	Ground Level (m):	Co-Ordinates (): E 1,575,759.4 N 5,195,075.1		Sheet: 1 of 1
Client: Environment Canterbury		Hole Depth: 2.70 m			

Elevation (m)	Depth (m)	Geological Description <small>Soil Description: subordinate, particle size, MAJOR, minor, colour, structure, strength, moisture condition, grading, bedding, plasticity; sensitivity, major qualifications, weathering of clasts; subordinate qualifications, minor qualifications; additional structure; (GEOLOGICAL UNIT)</small>	Legend	Weathering	Field Strength <small>Soil   Rock</small>	Defect Description <small>(type, orientation, spacing, roughness, persistence, aperture, infilling etc)</small>	Groundwater	Samples	Tests
	0.10								
	0.40	Brown SILT, with abundant rootlets. Firm to stiff, dry. (TOPSOIL)	x x						
	0.60	Brown SILT. Firm, non plastic, dry. (FILL)	x x						
1		Brown gravelly SILT with rootlets. Firm, non plastic, dry. Gravel, subrounded.	x x						
		Brown / grey clayey SILT with abundant partially decomposed organic material. Firm, non plastic, moist (NATURAL)	x x						
2			x x						
	2.20		x x						
		Grey clayey SILT with abundant partially decomposed organic material. Firm, non plastic, moist. Discoloured brown.	x x						
	2.70		x x						
3		EOH @ 2.70 m							
4									
5									

SKETCH:

MAP

Shoring/Support:  
Stability:



- Small Disturbed Sample
- Large Disturbed Sample
- U100 Undisturbed Sample
- Permeability Test
- Clegg Hammer; test repetitions (IV)
- Insitu Vane Shear Strength (kPa)
- P=Peak, R=Residual, UTP=Unable to penetrate
- Scala Penetrometer - blows/50mm

GROUNDWATER

☒ None

☐ Slow Seep (depth)

☐ Rapid Inflow (depth)

PIT TERMINATED DUE TO:

☒ Target depth

☐ Collapse

☐ Refusal

☐ Machine limit

Remarks

All dimensions in metres  
Scale 1:50

Contractor:



Rig/Plant Used:  
CAT 312C

Logged by: AP  
Checked by:

## TEST PIT LOG

Project: Waimak Stopbank Condition Assessment		Location: Waimakariri Stopbank		Hole position:	No.:  <b>RBW02</b>
Job No.: 10820	Start Date: 06-10-10 Finish Date: 06-10-10	Ground Level (m):	Co-Ordinates (): E 1,575,717.5 N 5,195,079.5		
Client: Environment Canterbury		Hole Depth: 2.20 m			Sheet: 1 of 1

Elevation (m)	Depth (m)	Geological Description	Legend	Weathering	Field Strength	Defect Description (type, orientation, spacing, roughness, persistence aperture, infilling etc)	Groundwater	Samples	Tests
		Soil Description: subordinate, particle size, MAJOR, minor, colour, structure, strength, moisture condition; grading; bedding; plasticity; sensitivity; major qualifications; weathering of clasts; subordinate qualifications; minor qualifications; additional structure; (GEOLOGICAL UNIT)		Soil   Rock					
	0.10								
	0.40	Brown SILT, with abundant rootlets. Firm to stiff, dry. (TOPSOIL)							
	0.50								
	1.10	Brown SILT with some rootlets. Firm, non plastic, dry. (FILL)							
	2.10	Brown gravelly/cobbly SILT with rootlets. Firm, non plastic, dry. Gravel; subrounded.							
	2.20	Brown gravelly/cobbly SILT with abundant partially decomposed organic material. Firm, non plastic, moist. Gravel; subrounded.							
	2.20	Brown clayey SILT and fine SAND. Medium dense, moist. Mottled orange. (NATURAL)							
		Grey fine to medium SAND. Loose, saturated.							
	3	EOH @ 2.20 m							
	4								
	5								

SKETCH:	MAP
	

Shoring/Support: Stability:	● Small Disturbed Sample   Large Disturbed Sample ■ U100 Undisturbed Sample ▬ Permeability Test ▼ Clegg Hammer; test repetitions (IV) ✓ Insitu Vane Shear Strength (kPa) P=Peak, R=Residual, UTP=Unable to penetrate ▼ Scale Penetrometer - blows/50mm	GROUNDWATER <input type="checkbox"/> None <input type="checkbox"/> Slow Seep (depth ) <input type="checkbox"/> Rapid Inflow (depth ) PIT TERMINATED DUE TO: <input checked="" type="checkbox"/> Target depth <input type="checkbox"/> Collapse <input type="checkbox"/> Refusal <input type="checkbox"/> Machine limit	Remarks The crack is naturally filling. Crack likely to end at 2.1m because the material filling the crack is sourced from this layer
--------------------------------	--	---	--

All dimensions in metres Scale 1:50	Contractor:	Rig/Plant Used:	Logged by:	Checked by:
		CAT 312C	AP	

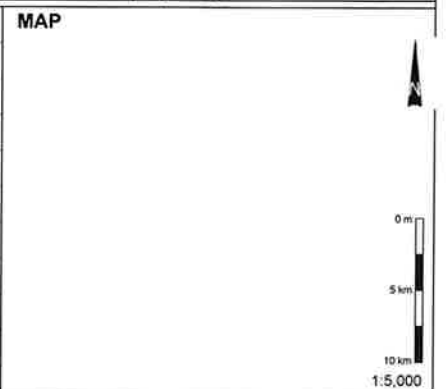
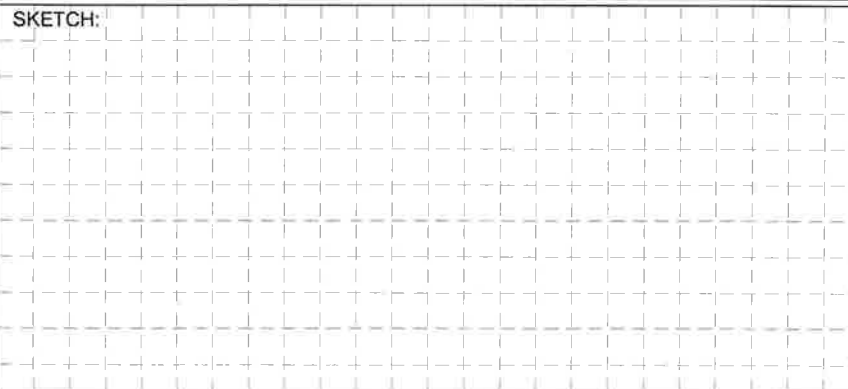


Riley Consultants Limited  
395 Madras Street  
Christchurch  
Tel: 03 3794402  
Fax: 03 3794403

## TEST PIT LOG

Project: Waimak Stopbank Condition Assessment		Location: Waimakariri Stopbank		Hole position:	No.: <b>RBW03</b>
Job No.: 10820	Start Date: 06-10-10 Finish Date: 06-10-10	Ground Level (m):	Co-Ordinates (): E 1,575,601.0 N 5,195,069.5		Sheet: 1 of 1
Client: Environment Canterbury		Hole Depth: 1.40 m			

Elevation (m)	Depth (m)	Geological Description <small>Soil Description: subordinate, particle size, MAJOR, minor, colour, structure; strength; moisture condition; grading; bedding; plasticity; sensitivity; major qualifications; weathering of clasts; subordinate qualifications; minor qualifications; additional structure; (GEOLOGICAL UNIT)</small>	Legend	Weathering <small>LOW MOD HIGH VERY HIGH</small>	Field Strength <small>Soil   Rock SAND GRAVEL CLAY SILT LOESS SAND GRAVEL CLAY SILT LOESS</small>	Defect Description <small>(type, orientation, spacing, roughness, persistence, aperture, infilling etc)</small>	Groundwater	Samples	Tests
	0.10	Dirt Road							
	0.80	Grey silty GRAVEL/COBBLES. Tightly packed, dense, moist (FILL)							
	1	Brown / light brown fine to medium SAND. Medium dense, moist. (NATURAL)							
	1.40	EOH @ 1.40 m							
	2								
	3								
	4								
	5								



<b>Shoring/Support Stability:</b>  All dimensions in metres Scale 1:50		<ul style="list-style-type: none"><li>Small Disturbed Sample</li><li>Large Disturbed Sample</li><li>U100 Undisturbed Sample</li><li>Permeability Test</li><li>Clegg Hammer; test repetitions (IV)</li><li>Insitu Vane Shear Strength (kPa)</li><li>P=Peak, R=Residual, UTP=Unable to penetrate</li><li>Scala Penetrometer - blows/50mm</li></ul>		<b>GROUNDWATER</b> <input checked="" type="checkbox"/> None <input type="checkbox"/> Slow Seep (depth ) <input type="checkbox"/> Rapid Inflow (depth ) <b>PIT TERMINATED DUE TO:</b> <input checked="" type="checkbox"/> Target depth <input type="checkbox"/> Collapse <input type="checkbox"/> Refusal <input type="checkbox"/> Machine limit		<b>Remarks</b>	
Contractor:		Rig/Plant Used: CAT 312C		Logged by: AP		Checked by:	



Riley Consultants Limited  
395 Madras Street  
Christchurch  
Tel: 03 3794402  
Fax: 03 3794403

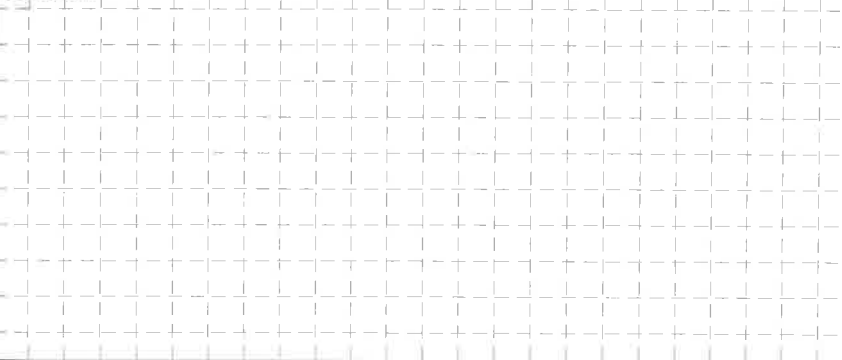
## TEST PIT LOG

Project: Waimak Stopbank Condition Assessment		Location: Waimakariri Stopbank		Hole position:	No.: <b>RBW04</b>
Job No.: 10820	Start Date: 06-10-10 Finish Date: 06-10-10	Ground Level (m):	Co-Ordinates (): E 1,575,497.0 N 5,195,059.4		
Client: Environment Canterbury			Hole Depth: 2.00 m		Sheet: 1 of 1

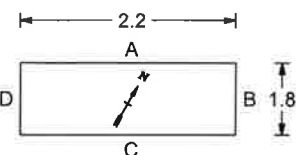
Elevation (m)	Depth (m)	Geological Description <small>Soil Description: subordinate, particle size, MAJOR, minor, colour, structure; strength; moisture condition; grading; bedding; plasticity; sensitivity; major qualifications; weathering of clasts; subordinate qualifications; minor qualifications; additional structure; (GEOLOGICAL UNIT)</small>	Legend	Weathering	Field Strength <small>Soil   Rock</small>	Defect Description <small>(type, orientation, spacing, roughness, persistence aperture, infilling etc)</small>	Groundwater	Samples	Tests
	0.10	Dirt Road							
	0.40								
	0.60	Brown silty GRAVEL. Medium dense, moist. Silt; non plastic. (FILL)							
	1.10	Brown fine SAND. Medium dense, moist							
	1.30								
	1.50	With thin isolated lenses of dark brown, wet SAND							
	2.00	Brown fine SAND. Medium dense, moist							
	2.00	Brown silty GRAVEL. Medium dense, wet. Silt; non plastic							
	3.00	Brown / orange fine SAND. Medium dense, moist. Limonite stained. (NATURAL)							
	3.00	EOH @ 2.00 m							
	4.00								
	5.00								

SKETCH:

MAP



Shoring/Support:  
Stability:



- Small Disturbed Sample
- Large Disturbed Sample
- U100 Undisturbed Sample
- ⬇ Permeability Test
- ▼ Clegg Hammer; test repetitions (IV)
- ✓ Insitu Vane Shear Strength (kPa)
- P=Peak, R=Residual, UTP=Unable to penetrate
- ▼ Scala Penetrometer - blows/50mm

GROUNDWATER

☒ None

- ☐ Slow Seep (depth)
- ☐ Rapid Inflow (depth)

PIT TERMINATED DUE TO:

- ☒ Target depth
- ☐ Collapse
- ☐ Refusal
- ☐ Machine limit

Remarks

All dimensions in metres  
Scale 1:50

Contractor:

Rig/Plant Used:  
CAT 312C

Logged by: AP  
Checked by:





Riley Consultants Limited  
395 Madras Street  
Christchurch  
Tel: 03 3794402  
Fax: 03 3794403

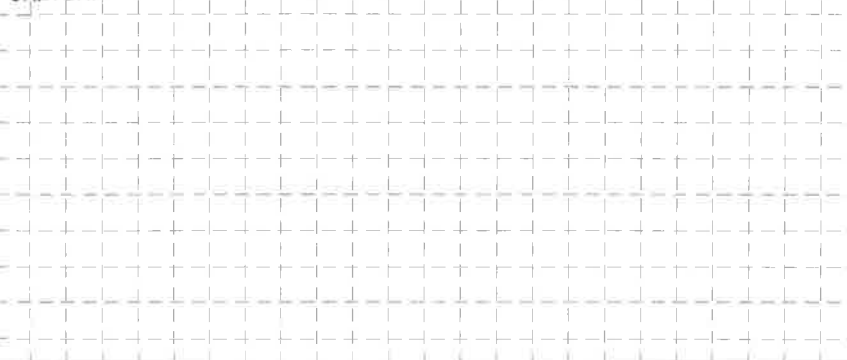
## TEST PIT LOG

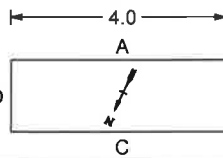
Project: Waimak Stopbank Condition Assessment		Location: Waimakariri Stopbank		Hole position:	No.: <b>RBW05</b>
Job No.: 10820	Start Date: 06-10-10 Finish Date: 06-10-10	Ground Level (m):	Co-Ordinates (): E 1,575,444.1 N 5,195,063.9		
Client: Environment Canterbury			Hole Depth: 2.40 m		Sheet: 1 of 1

Elevation (m)	Depth (m)	Geological Description <small>Soil Description: subordinate, particle size, MAJOR, minor, colour, structure, strength, moisture condition, grading, bedding, plasticity, sensitivity, major qualifications, weathering of clasts, subordinate qualifications, minor qualifications, additional structure, (GEOLOGICAL UNIT)</small>	Legend	Weathering	Field Strength <small>Soil   Rock</small>	Defect Description <small>(type, orientation, spacing, roughness, persistence, aperture, infilling etc)</small>	Groundwater	Samples	Tests
	0.10	Brown SILT, with abundant rootlets. Firm to stiff, dry. (TOPSOIL)							
	0.60	Brown SILT. Firm, dry. (FILL)							
	1.10	Brown SILT with some partially decomposed plant material. Firm, moist. (NATURAL)							
	2.40	Brown / orange silty CLAY with abundant partially decomposed organic material. Firm, moist							
	EOH @ 2.40 m								
	3								
	4								
	5								

SKETCH:

MAP



<b>Shoring/Support:</b> Stability: 	<ul style="list-style-type: none"><li>Small Disturbed Sample</li><li>Large Disturbed Sample</li><li>U100 Undisturbed Sample</li><li>Permeability Test</li><li>Clegg Hammer; test repetitions (IV)</li><li>Insitu Vane Shear Strength (kPa)</li><li>P=Peak, R=Residual, UTP=Unable to penetrate</li><li>Scala Penetrometer - blows/50mm</li></ul>	<b>GROUNDWATER</b> <input checked="" type="checkbox"/> None	<b>Remarks</b>	
		<input type="checkbox"/> Slow Seep (depth ) <input type="checkbox"/> Rapid Inflow (depth ) <b>PIT TERMINATED DUE TO:</b> <input checked="" type="checkbox"/> Target depth <input type="checkbox"/> Collapse <input type="checkbox"/> Refusal <input type="checkbox"/> Machine limit		
All dimensions in metres Scale 1:50	Contractor:	Rig/Plant Used: CAT 312C	Logged by: AP	Checked by:

# TEST PIT LOG

Project: Waimak Stopbank Condition Assessment		Location: Waimakariri Stopbank		Hole position:	No.:
Job No.: 10820	Start Date: 06-10-10 Finish Date: 06-10-10	Ground Level (m):	Co-Ordinates (): E 1,575,323.5 N 5,195,046.3		<b>RBW06</b>
Client: Environment Canterbury		Hole Depth: 2.30 m		Sheet: 1 of 1	

Elevation (m)	Depth (m)	Geological Description	Legend	Weathering	Field Strength	Defect Description	Groundwater	Samples	Tests
	0.10								
	0.30	Dirt Road							
		Brown SILT. Firm, non plastic, dry. (FILL)							
	0.80								
	0.90	Brown silty GRAVEL/COBBLES. Loosely packed, moist							
	1.00								
	1.50	Dark brown SAND with minor clay. Medium dense, moist (NATURAL)							
		Brown silty GRAVEL/COBBLES. Loosely packed, moist							
	2.00								
	2.30	Brown / dark brown fine to medium SAND. Loosely packed, moist to wet							
		EOH @ 2.30 m							
	3.00								
	4.00								
	5.00								

SKETCH:

MAP

1:5,000

Shoring/Support: Stability: <div style="display: flex; align-items: center;"> <div style="margin-right: 10px;"> </div> <div> <ul style="list-style-type: none"> <li>● Small Disturbed Sample</li> <li>■ Large Disturbed Sample</li> <li>■ U100 Undisturbed Sample</li> <li>⬆ Permeability Test</li> <li>▼ Clegg Hammer; test repetitions (IV)</li> <li>✓ Insitu Vane Shear Strength (kPa)</li> <li>P=Peak, R=Residual, UTP=Unable to penetrate</li> <li>▼ Scala Penetrometer - blows/50mm</li> </ul> </div> </div>		GROUNDWATER <input checked="" type="checkbox"/> None <div style="display: flex; flex-wrap: wrap;"> <div style="margin-right: 10px;"><input type="checkbox"/> Slow Seep (depth)</div> <div style="margin-right: 10px;"><input type="checkbox"/> Rapid Inflow (depth)</div> <div style="margin-right: 10px;"><input checked="" type="checkbox"/> Target depth</div> <div style="margin-right: 10px;"><input type="checkbox"/> Collapse</div> <div style="margin-right: 10px;"><input type="checkbox"/> Refusal</div> <div style="margin-right: 10px;"><input type="checkbox"/> Machine limit</div> </div>		Remarks		
PIT TERMINATED DUE TO:						
All dimensions in metres Scale 1:50		Contractor:		Rig/Plant Used: CAT 312C	Logged by: AP	Checked by:



Riley Consultants Limited  
395 Madras Street  
Christchurch  
Tel: 03 3794402  
Fax: 03 3794403

## TEST PIT LOG

Project: Waimak Stopbank Condition Assessment		Location: Waimakariri Stopbank		Hole position:	No.: <b>RBW07</b>
Job No.: 10820	Start Date: 06-10-10 Finish Date: 06-10-10	Ground Level (m):	Co-Ordinates (): E 1,575,207.7 N 5,195,053.2		Sheet: 1 of 1
Client: Environment Canterbury		Hole Depth: 2.60 m			

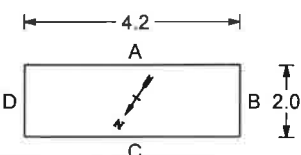
Elevation (m)	Depth (m)	Geological Description <small>Soil Description: subordinate, particle size, MAJOR, minor; colour, structure; strength; moisture condition; grading; bedding; plasticity; sensitivity; major qualifications; weathering of clasts; subordinate qualifications; minor qualifications; additional structure; (GEOLOGICAL UNIT)</small>	Legend	Field Strength		Defect Description <small>(type, orientation, spacing, roughness, persistence, aperture, infilling etc)</small>	Groundwater	Samples	Tests
				Soil	Rock				
	0.10								
	0.30	Brown SILT, with abundant rootlets. Firm to stiff, dry. (TOPSOIL)	x						
	0.80	Brown SILT with some rootlets. Firm, non plastic, dry. (FILL)	x						
1		Brown silty fine SAND. Loosely packed, dry							
2		Brown streaked dark brown / orange silty CLAY with partially decomposed organics. Firm, low plasticity, moist. Thinly interbedded with brown / light brown silty fine SAND. Sand; loosely packed. (NATURAL)							
2.30									
2.60		Blue / grey fine to medium SAND. Loose, saturated.							
3		EOH @ 2.60 m							
4									
5									

SKETCH:

MAP



Shoring/Support:  
Stability:



- Small Disturbed Sample
- Large Disturbed Sample
- U100 Undisturbed Sample
- Permeability Test
- Clegg Hammer, test repetitions (IV)
- Insitu Vane Shear Strength (kPa)
- P=Peak, R=Residual, UTP=Unable to penetrate
- Scala Penetrometer - blows/50mm

GROUNDWATER

☒ None

☐ Slow Seep (depth)

☐ Rapid Inflow (depth)

PIT TERMINATED DUE TO:

☒ Target depth ☐ Collapse

☐ Refusal ☐ Machine limit

Remarks

All dimensions in metres  
Scale 1:50

Contractor:



Rig/Plant Used:  
CAT 312C


Logged by: AP  
Checked by:

## TEST PIT LOG

Project: Waimak Stopbank Condition Assessment		Location: Waimakariri Stopbank		Hole position:	No.:  <b>RBW08</b>
Job No.: 10820	Start Date: 06-10-10 Finish Date: 06-10-10	Ground Level (m):	Co-Ordinates (): E 1,575,119.2 N 5,195,042.2		
Client: Environment Canterbury		Hole Depth: 1.80 m			Sheet: 1 of 1

Elevation (m)	Depth (m)	Geological Description <small>Soil Description: subordinate, particle size, MAJOR, minor, colour, structure, strength, moisture condition; grading, bedding, plasticity, sensitivity; major qualifications; weathering of clasts; subordinate qualifications; minor qualifications; additional structure; (GEOLOGICAL UNIT)</small>	Legend	Weathering <small>RS LW MW HW</small>	Field Strength <small>Soil Very Frag Weak Med Strong Rock Very Weak Weak Med Strong</small>	Defect Description <small>(type, orientation, spacing, roughness, persistence, aperture, infilling etc)</small>	Groundwater	Samples	Tests
	0.20	Brown SILT, with abundant rootlets. Firm to stiff, dry (TOPSOIL)							
	0.25		x						
	0.70	Dark brown SILT. Firm, moist. (FILL)	x						
	0.90		x						
	1	Brown SILT. Firm, non plastic, moist	x						
			x						
		Brown / grey silty GRAVEL. Loosely packed, moist	x						
			x						
	1.80	Brown streaked orange clayey SILT, with some partially decomposed organics. Firm, non plastic, moist (NATURAL)	x						
	2								
		EOH @ 1.80 m							
	3								
	4								
	5								

SKETCH:	MAP
	
	<p>0 m</p> <p>5 km</p> <p>10 km</p> <p>1:5,000</p>

<p>Shoring/Support: Stability:</p> 	<ul style="list-style-type: none"> <li>● Small Disturbed Sample</li> <li>⬮ Large Disturbed Sample</li> <li>■ U100 Undisturbed Sample</li> <li>⬇ Permeability Test</li> <li>⬇ Clegg Hammer, test repetitions (IV)</li> <li>✓ Insitu Vane Shear Strength (kPa)</li> <li>P=Peak, R=Residual, UTP=Unable to penetrate</li> <li>▼ Scala Penetrometer - blows/50mm</li> </ul>	<p>GROUNDWATER <input checked="" type="checkbox"/> None</p> <p><input type="checkbox"/> Slow Seep (depth )</p> <p><input type="checkbox"/> Rapid Inflow (depth )</p> <p>PIT TERMINATED DUE TO:</p> <p><input checked="" type="checkbox"/> Target depth <input type="checkbox"/> Collapse</p> <p><input type="checkbox"/> Refusal <input type="checkbox"/> Machine limit</p>	<p>Remarks</p>
--	---	---	----------------

All dimensions in metres Scale 1:50	Contractor:	Rig/Plant Used: CAT 312C	Logged by: AP	Checked by:
--	-------------	-----------------------------	------------------	-------------



Riley Consultants Limited  
395 Madras Street  
Christchurch  
Tel: 03 3794402  
Fax: 03 3794403

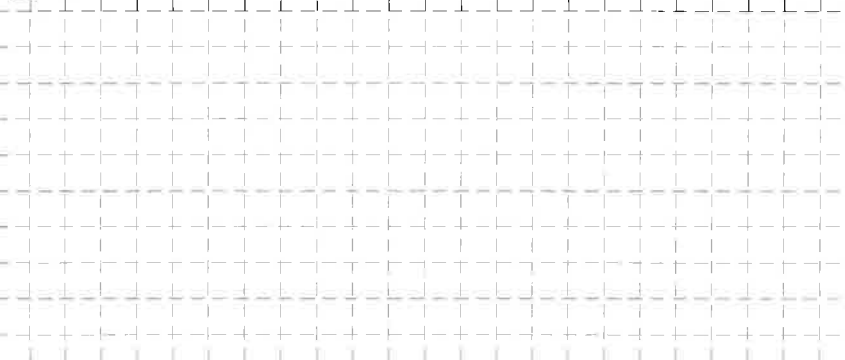
## TEST PIT LOG

Project: Waimak Stopbank Condition Assessment		Location: Waimakariri Stopbank		Hole position:	No.: <b>RBW09</b>
Job No.: 10820	Start Date: 06-10-10 Finish Date: 06-10-10	Ground Level (m):	Co-Ordinates (): E 1,575,164.5 N 5,195,045.4		Sheet: 1 of 1
Client: Environment Canterbury		Hole Depth: 2.00 m			

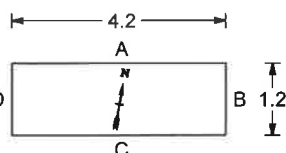
Elevation (m)	Depth (m)	Geological Description <small>Soil Description: subordinate, particle size, MAJOR, minor, colour, structure, strength, moisture condition, grading, bedding, plasticity, sensitivity, major qualifications; weathering of clasts; subordinate qualifications; minor qualifications; additional structure; (GEOLOGICAL UNIT)</small>	Legend	Weathering <small>W1 W2 W3 W4 W5 W6 W7 W8 W9 W10 W11 W12 W13 W14 W15 W16 W17 W18 W19 W20 W21 W22 W23 W24 W25 W26 W27 W28 W29 W30 W31 W32 W33 W34 W35 W36 W37 W38 W39 W40 W41 W42 W43 W44 W45 W46 W47 W48 W49 W50 W51 W52 W53 W54 W55 W56 W57 W58 W59 W60 W61 W62 W63 W64 W65 W66 W67 W68 W69 W70 W71 W72 W73 W74 W75 W76 W77 W78 W79 W80 W81 W82 W83 W84 W85 W86 W87 W88 W89 W90 W91 W92 W93 W94 W95 W96 W97 W98 W99 W100</small>	Field Strength <small>Soil Rock</small>	Defect Description <small>(type, orientation, spacing, roughness, persistence, aperture, infilling etc)</small>	Groundwater	Samples	Tests
	0.10	Brown SILT, with abundant plant rootlets. Firm to stiff, dry. (TOPSOIL)							
	0.50								
	0.55	Brown SILT. Firm, non plastic, dry. (FILL)							
	0.80								
	1.10	Dark brown SILT with abundant decomposed organic rootlets. Firm, non plastic, moist (buried topsoil?)							
	1.50	Brown / grey silty GRAVEL. Tightly packed, rounded to subrounded, moist. Silt; non plastic.							
	2.00	Brown SILT. Firm, non plastic, moist.							
		Brown silty fine to medium GRAVEL. Tightly packed, subrounded, moist. Silty; non plastic.							
		Brown / grey clayey SILT. Firm, non plastic, moist. (NATURAL)							
		EOH @ 2.00 m							
	3								
	4								
	5								

SKETCH:

MAP



Shoring/Support:  
Stability:



- Small Disturbed Sample
- Large Disturbed Sample
- U100 Undisturbed Sample
- ↓ Permeability Test
- ▼ Clegg Hammer; test repetitions (IV)
- ✓ Insitu Vane Shear Strength (kPa)
- P=Peak, R=Residual, UTP=Unable to penetrate
- ▼ Scala Penetrometer - blows/50mm

GROUNDWATER

☒ None

- ☐ Slow Seep (depth)
- ☐ Rapid Inflow (depth)

PIT TERMINATED DUE TO:

- ☒ Target depth
- ☐ Collapse
- ☐ Refusal
- ☐ Machine limit

Remarks

All dimensions in metres  
Scale 1:50

Contractor:

Rig/Plant Used:  
CAT 312C

Logged by:  
AP

Checked by:



---

## ***APPENDIX D***

### ***Laboratory Test Results***



# Material Test Report

Report No: MAT:CAN10S-06841

Issue No: 2

This report replaces all previous issues of report no 'MAT:CAN10S-06841'.

## Client:

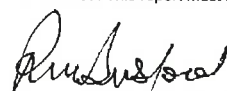
Riley Consultants Ltd  
PO Box 4355  
Christchurch Mail Centre

Christchurch 8140  
NZ

Project: QA Testing - Aggregates



The test (s) reported herein (unless indicated) have been performed in accordance with the laboratory's scope of accreditation. Results only apply to samples as received. This report must be reproduced in full.



Approved Signatory: Max Burford  
(Supervisor)  
IANZ Accreditation No:200  
Date of Issue: 19/10/10

## Sample Details

Sample ID: CAN10S-06841  
Client Sample ID: LBW 6 @ 1.0m  
Material: Silty SAND  
Sample Source: Field Sample [Taken From Site]  
Site/Sampled From: Left Bank Waimak Stopbank  
Date Sampled: 06/10/2010  
Specification: No Specification (fine all sieves)  
Sampled By: Ana Petaia  
Sampling Method: As Received - Not Accredited  
Date Tested: 11/10/2010  
Technician: Nader Guirguis  
Sampling Endorsed: Yes

## Other Test Results

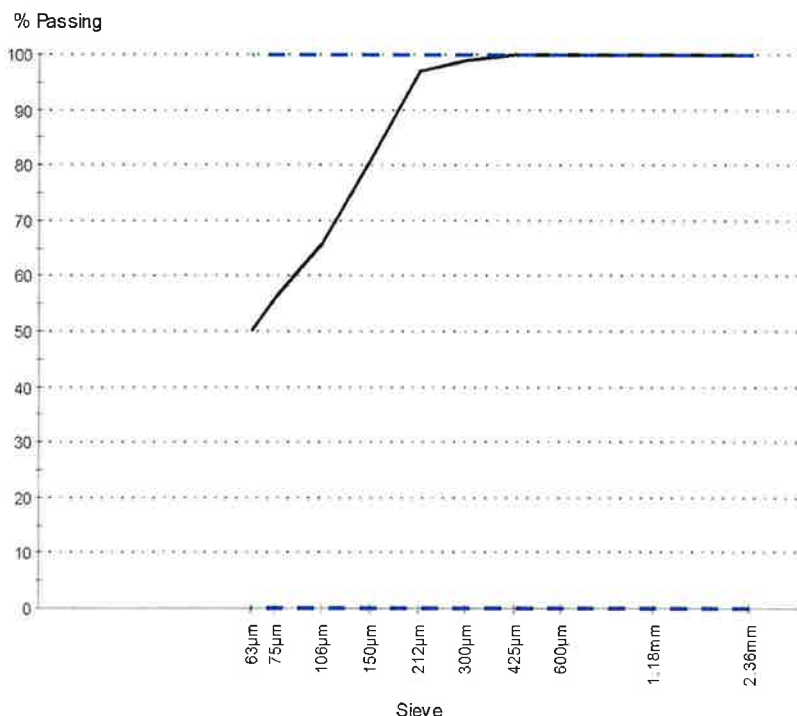
Description	Method	Result	Limits
Moisture Content (%)	NZS 4407:1991 Test 3.1	17.5	N/A

## Particle Size Distribution

Method: NZS 4407:1991 Test 3.8.1

Drying by: Oven

Note: Percentage passing the finest sieve was obtained by difference.



Sieve Size	% Passing	Limits
2.36mm	100	0 - 100
1.18mm	100	0 - 100
600µm	100	0 - 100
425µm	100	0 - 100
300µm	99	0 - 100
212µm	97	0 - 100
150µm	81	0 - 100
106µm	66	0 - 100
75µm	56	0 - 100
63µm	50	0 - 100

## Comments

Core Material of Stopbank and liquidified sand  
Report has been reissued with bore hole 6 and depth included

# Material Test Report

Report No: MAT:CAN10S-06842

Issue No: 2

This report replaces all previous issues of report no 'MAT:CAN10S-06842'

## Client:

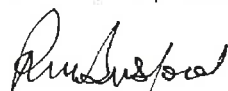
Riley Consultants Ltd  
PO Box 4355  
Christchurch Mail Centre

Christchurch 8140  
NZ

Project: QA Testing - Aggregates



The test(s) reported herein (unless indicated) have been performed in accordance with the laboratory's scope of accreditation. Results only apply to samples as received. This report must be reproduced in full.



Approved Signatory: Max Burford  
(Supervisor)  
IANZ Accreditation No:200  
Date of Issue: 18/10/10

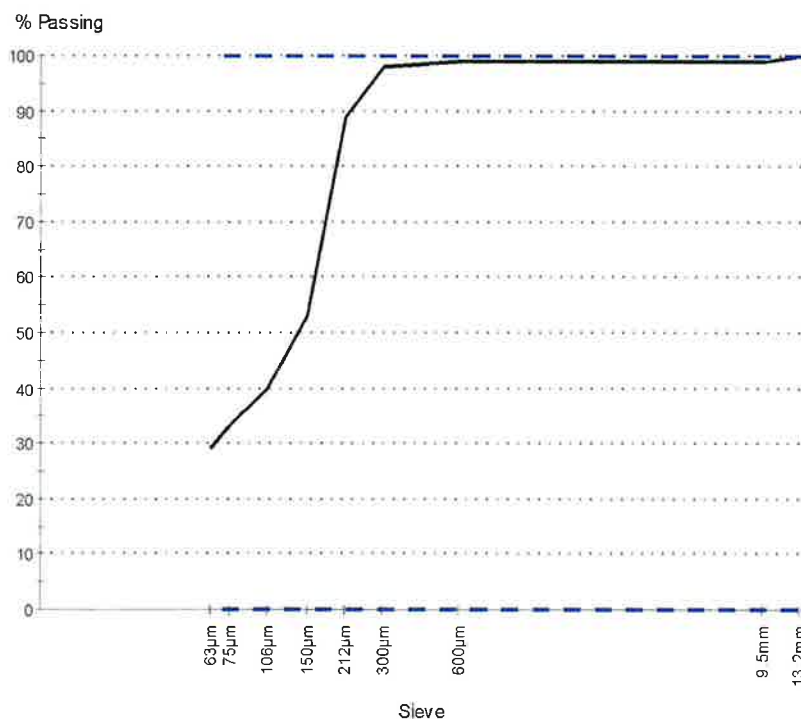
## Sample Details

Sample ID: CAN10S-06842  
Client Sample ID: O/N 11  
Material: Silty SAND  
Sample Source: Field Sample [Taken From Site]  
Site/Sampled From: Left Bank Waimak Stopbank  
Date Sampled: 06/10/2010  
Specification: No Specification (fine all sieves)  
Sampled By: Ana Petaia  
Sampling Method: As Received - Not Accredited  
Date Tested: 11/10/2010  
Technician: Nader Guirguis  
Sampling Endorsed: Yes

## Other Test Results

Description	Method	Result	Limits
Moisture Content (%)	NZS 4407:1991 Test 3.1	32.6	N/A

## Particle Size Distribution



Method: NZS 4407:1991 Test 3.8.1

Drying by: Oven

Note: Percentage passing the finest sieve was obtained by difference.

Sieve Size	% Passing	Limits
13.2mm	100	0 - 100
9.5mm	99	0 - 100
600µm	99	0 - 100
300µm	98	0 - 100
212µm	89	0 - 100
150µm	53	0 - 100
106µm	40	0 - 100
75µm	33	0 - 100
63µm	29	0 - 100

## Comments

Core Material of Stopbank and liquefied sand  
Report was reissued with RBW2 @ 3.1m added

Report No: MAT:CAN10S-06843

Issue No: 3

This report replaces all previous issues of report no 'MAT:CAN10S-06843'.

# Material Test Report

## Client:

Riley Consultants Ltd  
PO Box 4355  
Christchurch Mail Centre

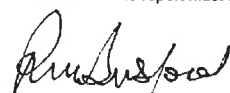
Christchurch 8140  
NZ

## Project:

QA Testing - Aggregates



The test(s) reported herein (unless indicated) have been performed in accordance with the laboratory's scope of accreditation. Results only apply to samples as received. This report must be reproduced in full.



Approved Signatory: Max Burford  
(Supervisor)  
IANZ Accreditation No:200  
Date of Issue: 19/10/10

## Sample Details

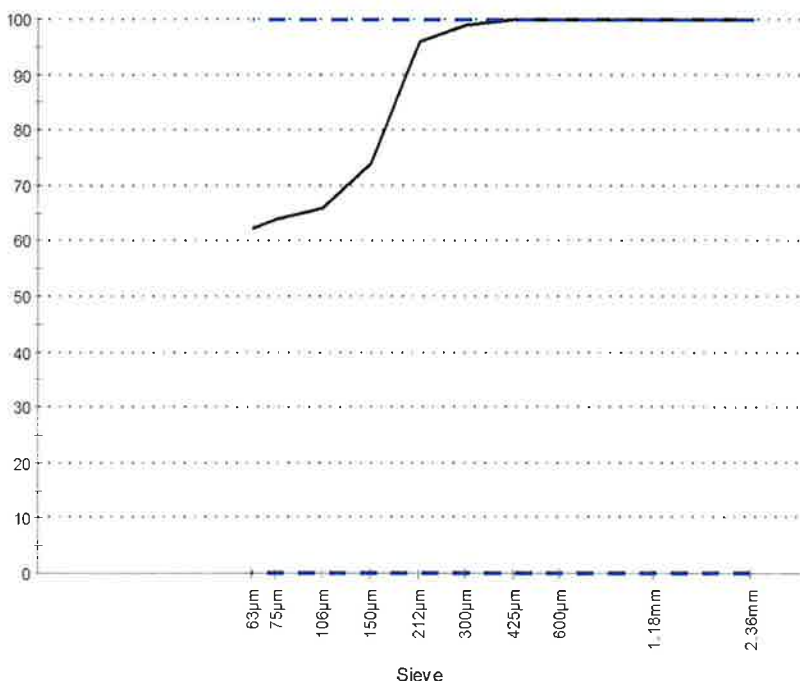
Sample ID: CAN10S-06843  
Client Sample ID: LBW 8 @ 1.3m  
Material: Silty SAND  
Sample Source: Field Sample [Taken From Site]  
Site/Sampled From: Left Bank Waimak Stopbank  
Date Sampled: 06/10/2010  
Specification: No Specification (fine all sieves)  
Sampled By: Ana Petaia  
Sampling Method: As Received - Not Accredited  
Date Tested: 11/10/2010  
Technician: Nader Guirguis  
Sampling Endorsed: Yes

## Other Test Results

Description	Method	Result	Limits
Moisture Content (%)	NZS 4407:1991 Test 3.1	17.5	N/A

## Particle Size Distribution

% Passing



Method: NZS 4407:1991 Test 3.8.1

Drying by: Oven

Note: Percentage passing the finest sieve was obtained by difference.

Sieve Size	% Passing	Limits
2.36mm	100	0 - 100
1.18mm	100	0 - 100
600µm	100	0 - 100
425µm	100	0 - 100
300µm	99	0 - 100
212µm	96	0 - 100
150µm	74	0 - 100
106µm	66	0 - 100
75µm	64	0 - 100
63µm	62	0 - 100

## Comments

Core Material of Stopbank and Liquefied Sand  
Report reissued with LBW8 @ 1.3m included

Report No: MAT:CAN10S-06844

Issue No: 1

# Material Test Report

## Client:

Riley Consultants Ltd  
PO Box 4355  
Christchurch Mail Centre

Christchurch 8140  
NZ

Project: QA Testing - Aggregates



The test (s) reported herein (unless indicated) have been performed in accordance with the laboratory's scope of accreditation. Results only apply to samples as received. This report must be reproduced in full.

*Max Burford*  
Approved Signatory: Max Burford  
(Supervisor)  
IANZ Accreditation No:200  
Date of Issue: 18/10/10

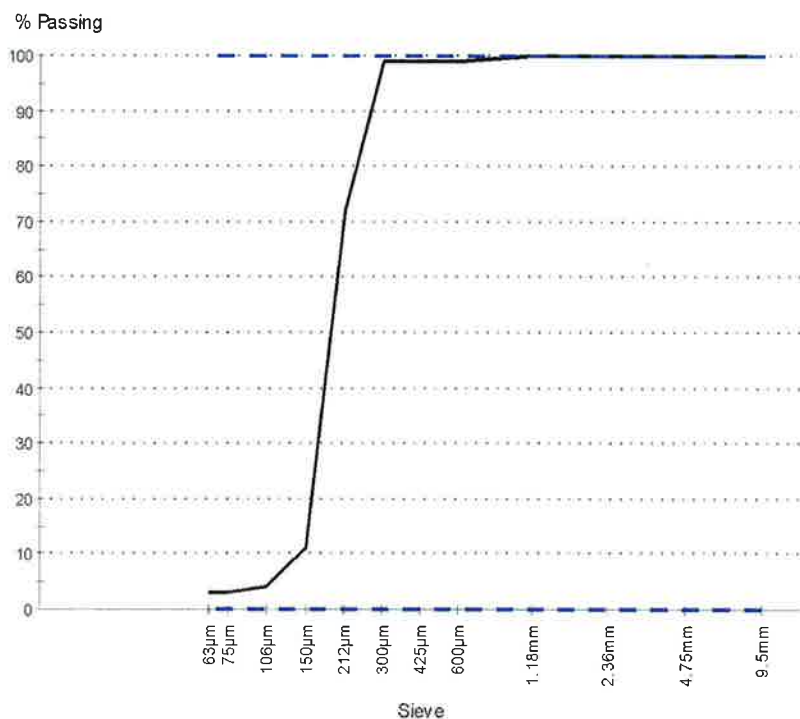
## Sample Details

Sample ID: CAN10S-06844  
Client Sample ID: O/N 11  
Material: Sand  
Sample Source: Field Sample [Taken From Site]  
Site/Sampled From: Left Bank Waimak Stopbank  
Date Sampled: 06/10/2010  
Specification: No Specification (fine all sieves)  
Sampled By: Ana Petaia  
Sampling Method: As Received - Not Accredited  
Date Tested: 11/10/2010  
Technician: Nader Guirguis  
Sampling Endorsed: Yes

## Other Test Results

Description	Method	Result	Limits
Moisture Content (%)	NZS 4407:1991 Test 3.1	3.2	N/A

## Particle Size Distribution



Method: NZS 4407:1991 Test 3.8.1

Drying by: Oven

Note: Percentage passing the finest sieve was obtained by difference.

Sieve Size	% Passing	Limits
9.5mm	100	0 - 100
4.75mm	100	0 - 100
2.36mm	100	0 - 100
1.18mm	100	0 - 100
600µm	99	0 - 100
425µm	99	0 - 100
300µm	99	0 - 100
212µm	72	0 - 100
150µm	11	0 - 100
106µm	4	0 - 100
75µm	3	0 - 100
63µm	3	0 - 100

## Comments

Core Material of Stopbank and Liquefied Sand  
RBW3 @ 1.0m



Report No: MAT:CAN10S-06845

Issue No: 1

# Material Test Report

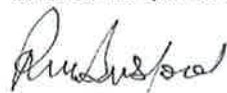
**Client:**

Riley Consultants Ltd  
PO Box 4355  
Christchurch Mail Centre

Christchurch 8140  
NZ

**Project:** QA Testing - Aggregates


The test (s) reported herein (unless indicated) have been performed in accordance with the laboratory's scope of accreditation. Results only apply to samples as received. This report must be reproduced in full.



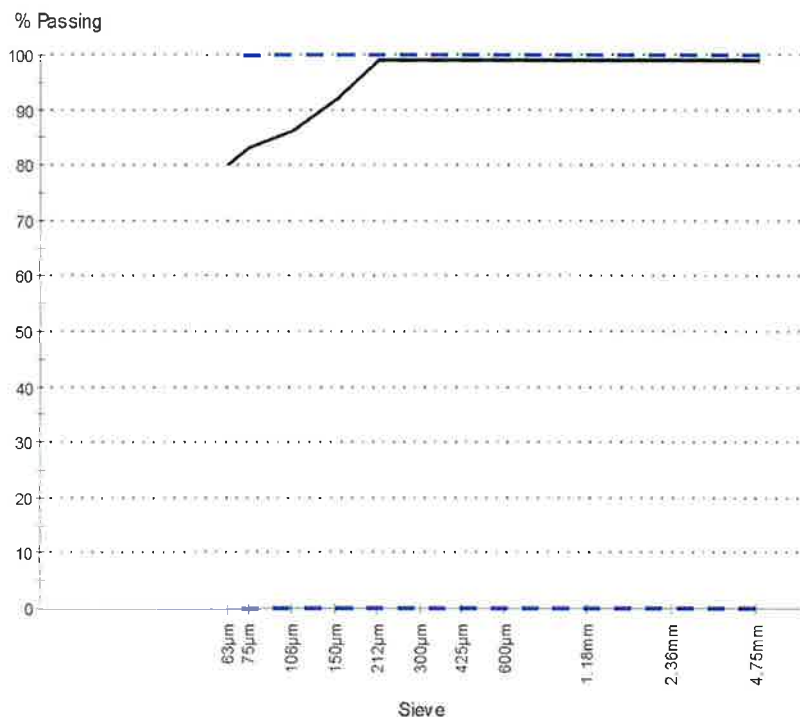
Approved Signatory: Max Burford  
(Supervisor)  
IANZ Accreditation No:200  
Date of Issue: 18/10/10

**Sample Details**

Sample ID: CAN10S-06845  
Client Sample ID: O/N 11  
Material: Sandy SILT  
Sample Source: Field Sample [Taken From Site]  
Site/Sampled From: Left Bank Waimak Stopbank  
Date Sampled: 06/10/2010  
Specification: No Specification (fine all sieves)  
Sampled By: Ana Petaia  
Sampling Method: As Received - Not Accredited  
Date Tested: 11/10/2010  
Technician: Nader Guirguis  
Sampling Endorsed: Yes

**Other Test Results**

Description	Method	Result	Limits
Moisture Content (%)	NZS 4407:1991 Test 3.1	29.1	N/A

**Particle Size Distribution**


Method: NZS 4407:1991 Test 3.8.1

Drying by: Oven

Note: Percentage passing the finest sieve was obtained by difference.

Sieve Size	% Passing	Limits
4.75mm	99	0 - 100
2.36mm	99	0 - 100
1.18mm	99	0 - 100
600µm	99	0 - 100
425µm	99	0 - 100
300µm	99	0 - 100
212µm	99	0 - 100
150µm	92	0 - 100
106µm	86	0 - 100
75µm	83	0 - 100
63µm	80	0 - 100

**Comments**

Core material of Stopbank and Liquefied Sand  
LBW 11 @ 2.8m

Report No: MAT:CAN10S-06846

Issue No: 1

# Material Test Report

Client:

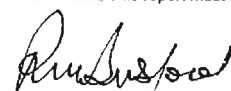
Riley Consultants Ltd  
PO Box 4355  
Christchurch Mail Centre

Christchurch 8140  
NZ

Project: QA Testing - Aggregates



The test (s) reported herein (unless indicated) have been performed in accordance with the laboratory's scope of accreditation. Results only apply to samples as received. This report must be reproduced in full.



Approved Signatory: Max Burford  
(Supervisor)  
IANZ Accreditation No:200  
Date of Issue: 18/10/10

## Sample Details

Sample ID: CAN10S-06846  
Client Sample ID: O/N 11  
Material: Sandy Gravel  
Sample Source: Field Sample [Taken From Site]  
Site/Sampled From: Left Bank Waimak Stopbank  
Date Sampled: 06/10/2010  
Specification: No Specification  
Sampled By: Ana Petaia  
Sampling Method: As Received - Not Accredited  
Date Tested: 11/10/2010  
Technician: Nader Guirguis  
Sampling Endorsed: No

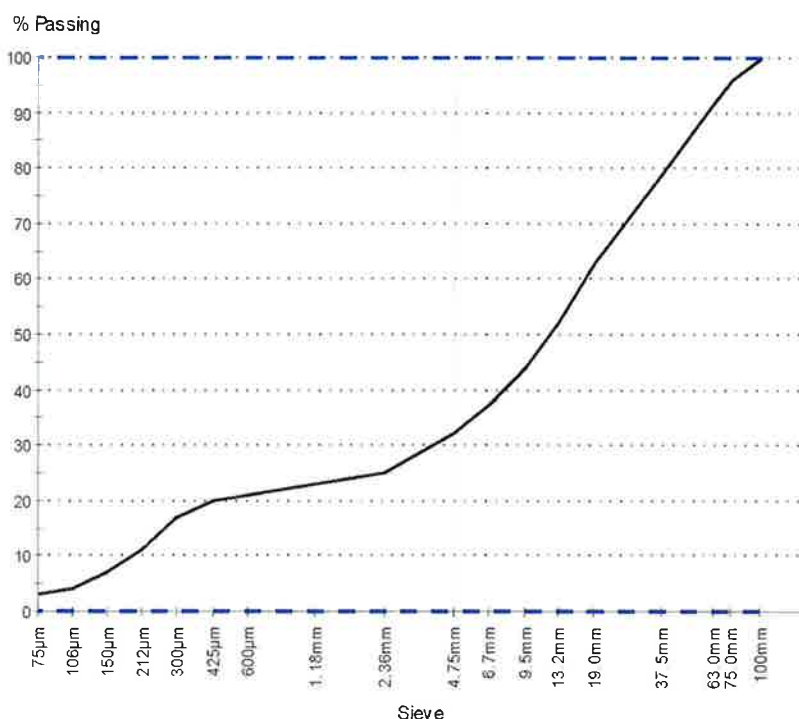
## Other Test Results

Description	Method	Result	Limits
Moisture Content (%)	NZS 4407:1991 Test 3.1	3.5	N/A

## Particle Size Distribution

Method: NZS 3111:1986 Test 6

Drying by: Oven



Sieve Size	% Passing	Limits
100mm	100	0 - 100
75.0mm	96	0 - 100
63.0mm	92	0 - 100
37.5mm	79	0 - 100
19.0mm	63	0 - 100
13.2mm	52	0 - 100
9.5mm	44	0 - 100
6.7mm	37	0 - 100
4.75mm	32	0 - 100
2.36mm	25	0 - 100
1.18mm	23	0 - 100
600µm	21	0 - 100
425µm	20	0 - 100
300µm	17	0 - 100
212µm	11	0 - 100
150µm	7	0 - 100
106µm	4	0 - 100
75µm	3	0 - 100
63µm	3	0 - 100

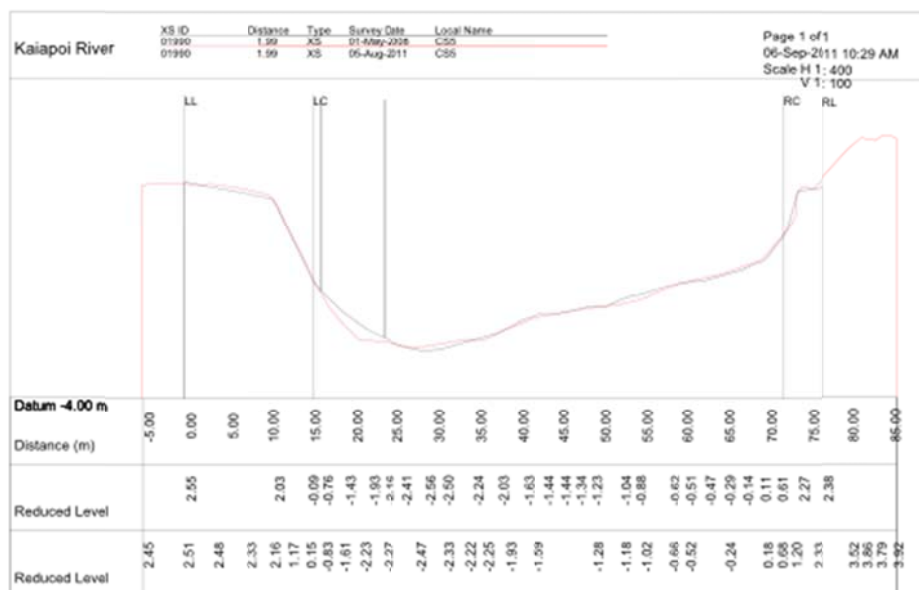
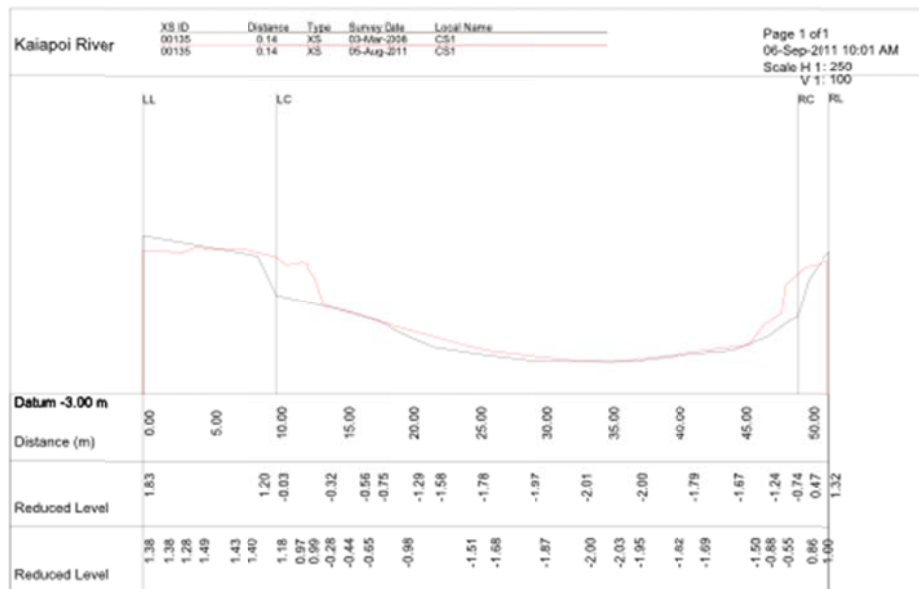
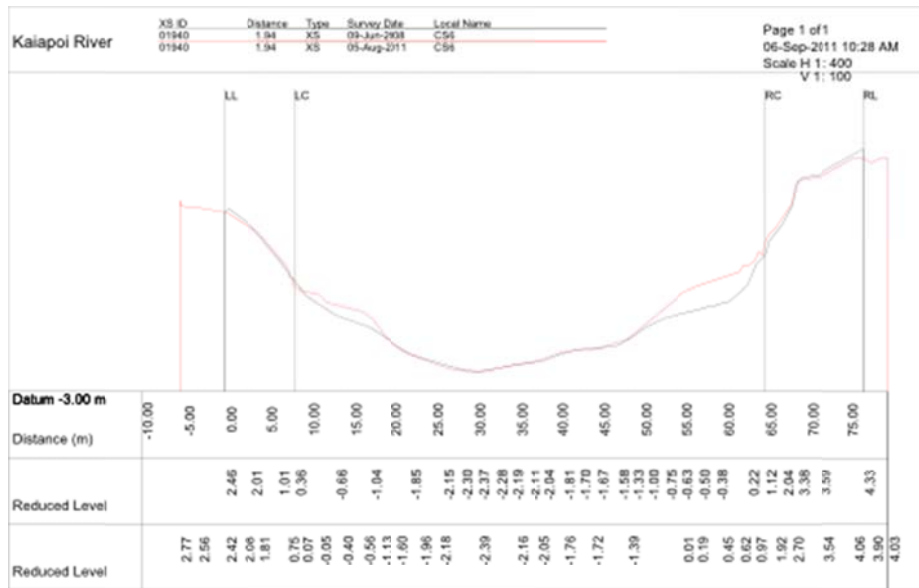
Comments

N/A

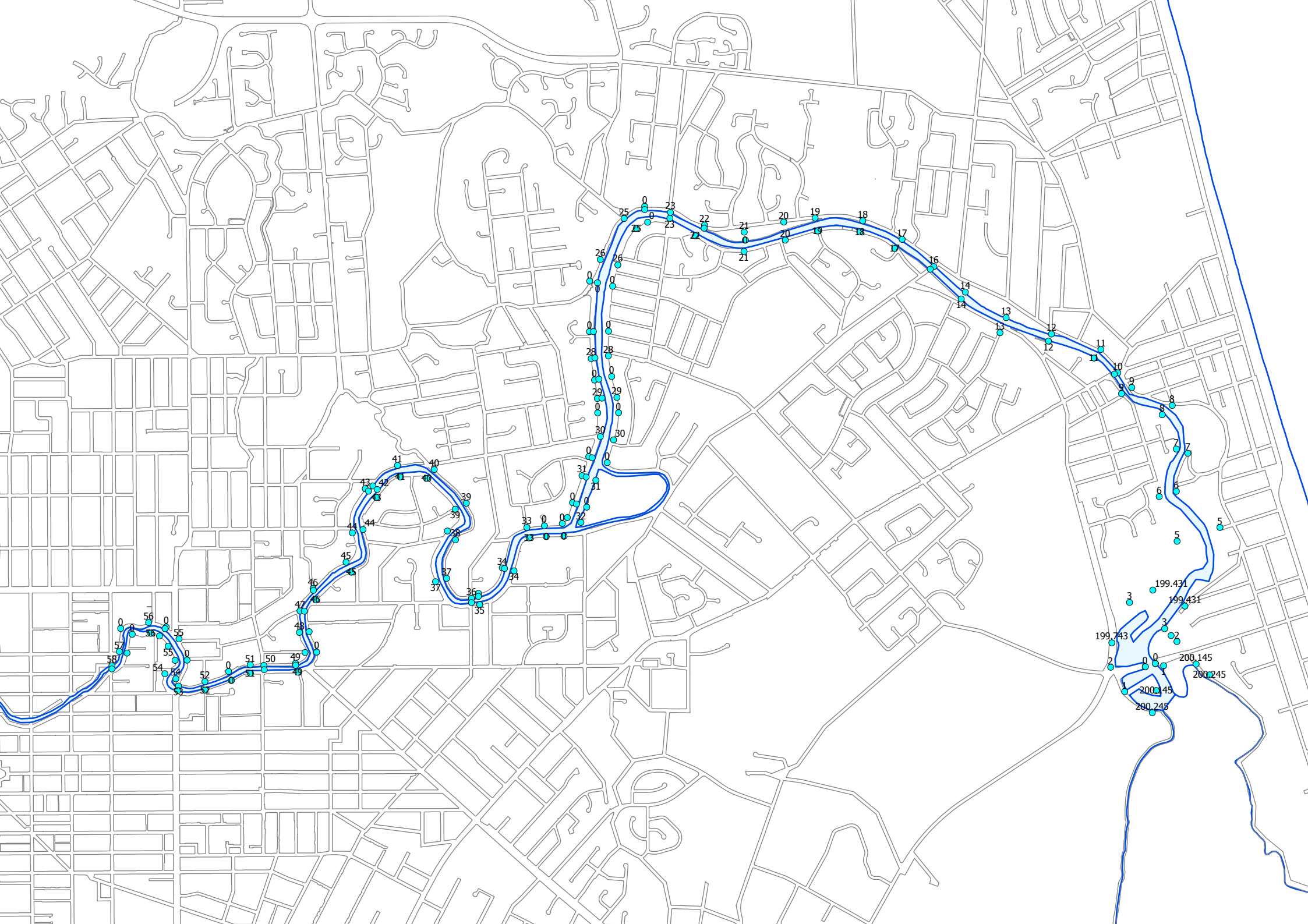
## **APPENDIX D:**

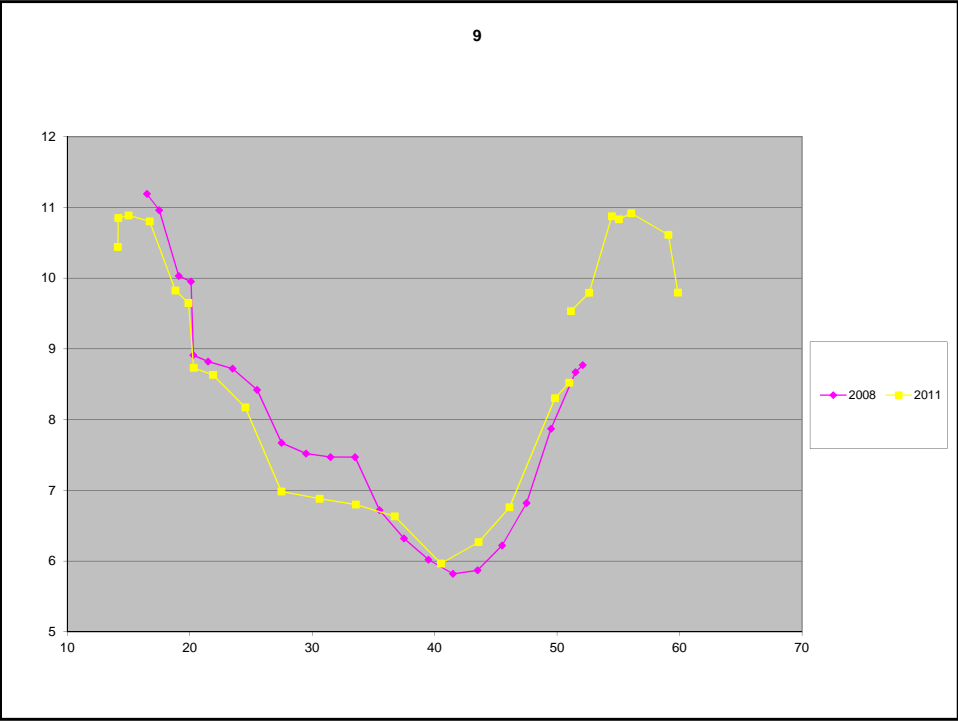
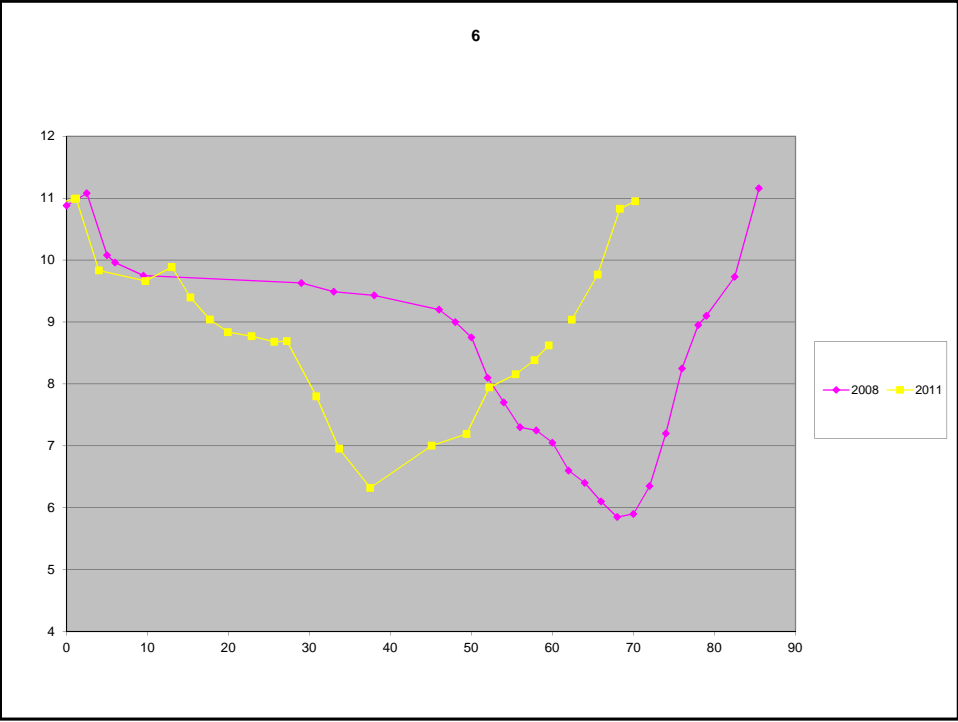
### **KAIAPOI AND AVON RIVER CROSS SECTIONS**



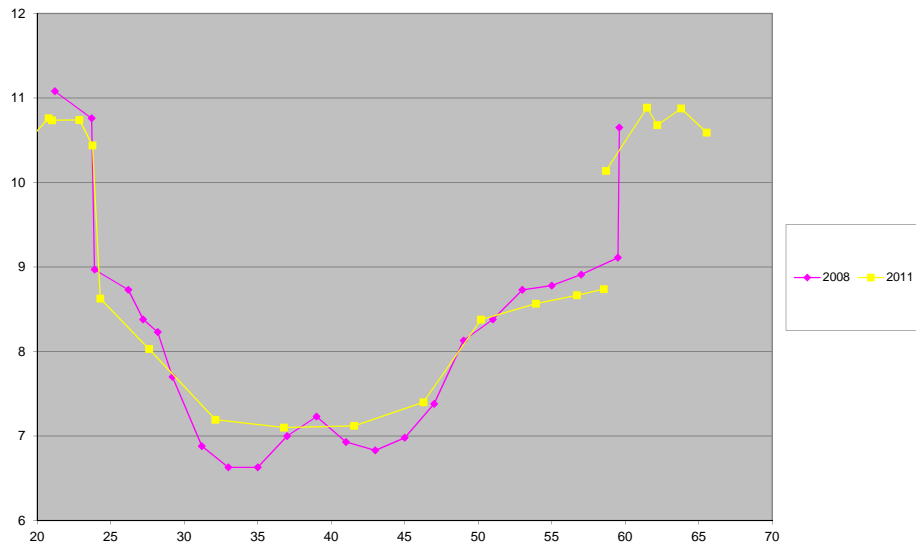




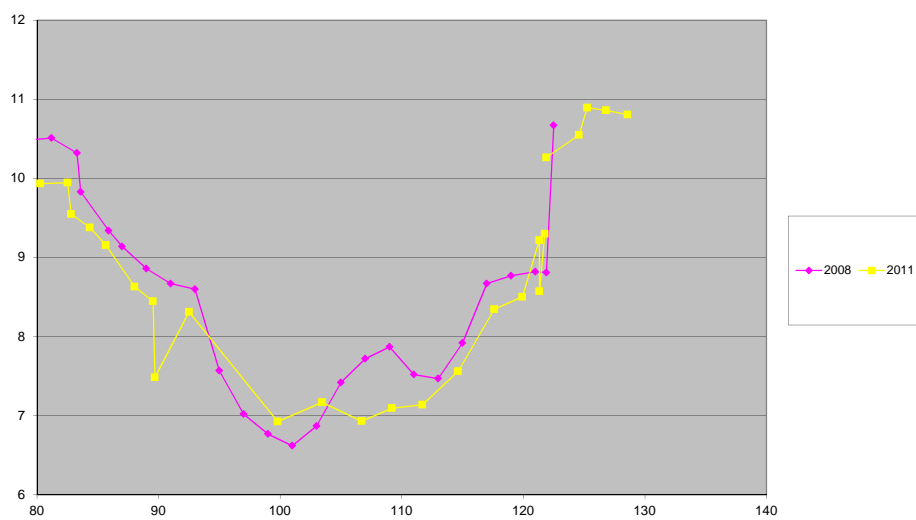




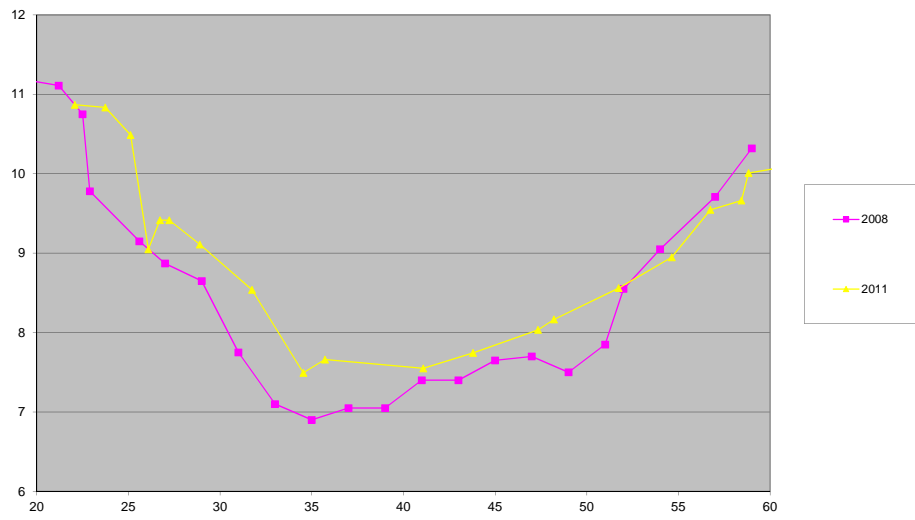
11



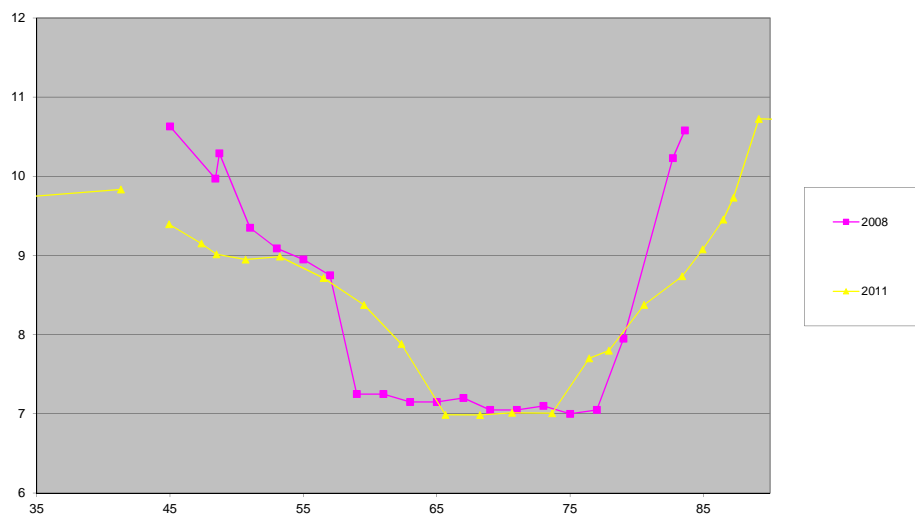
14



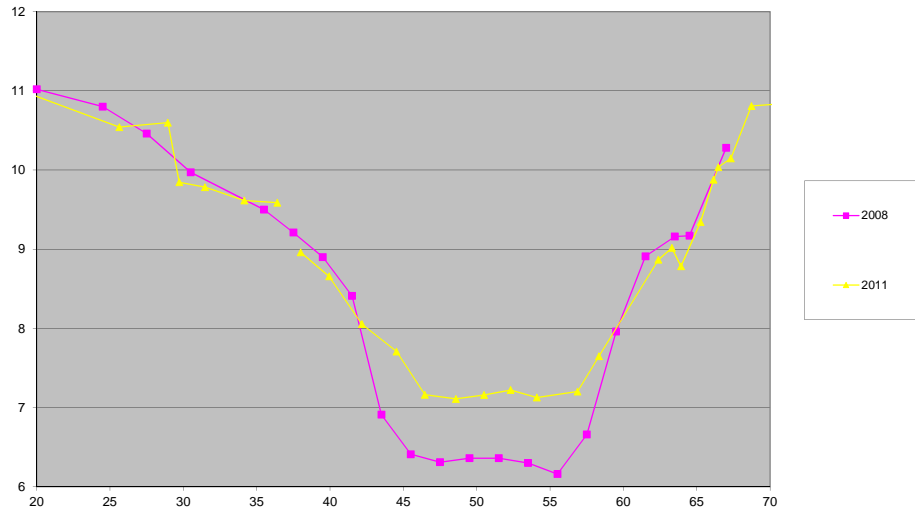
17



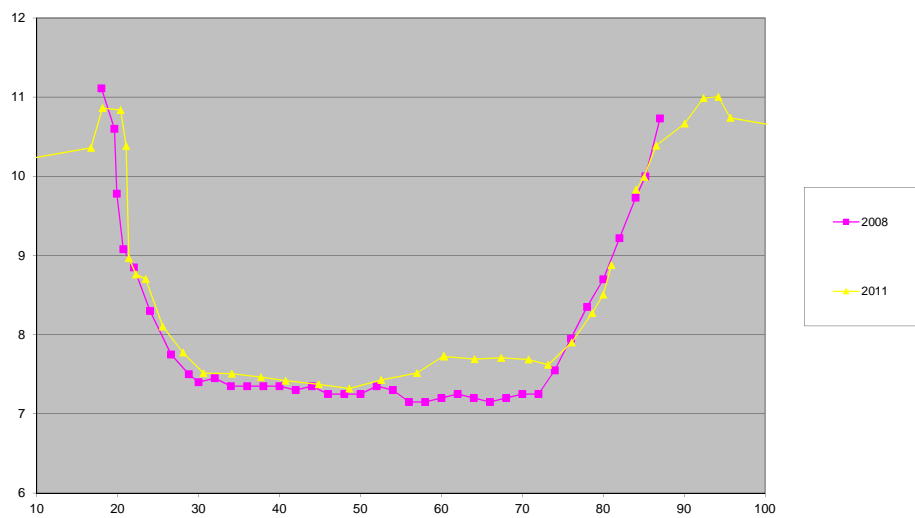
20



22

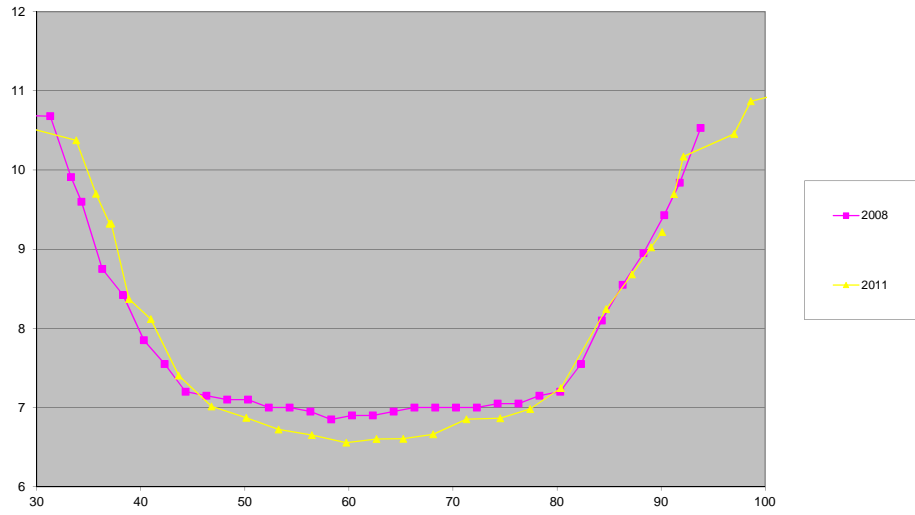


26

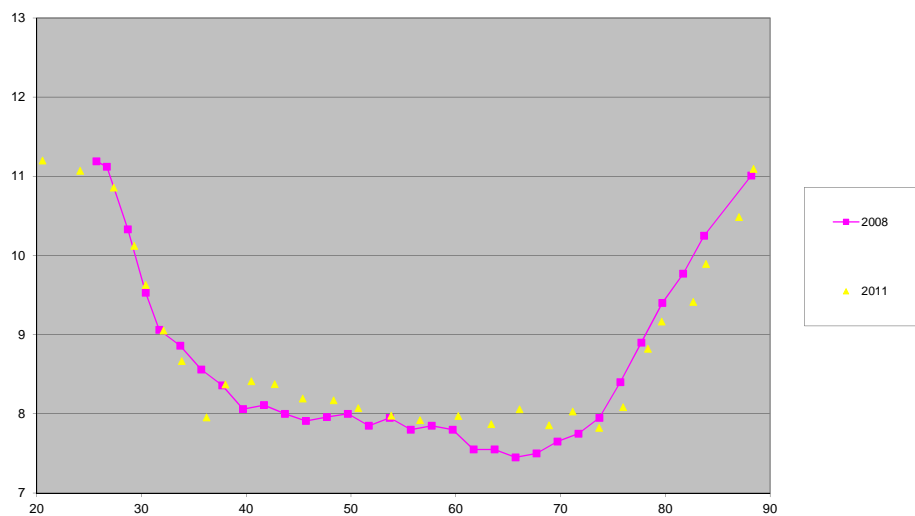


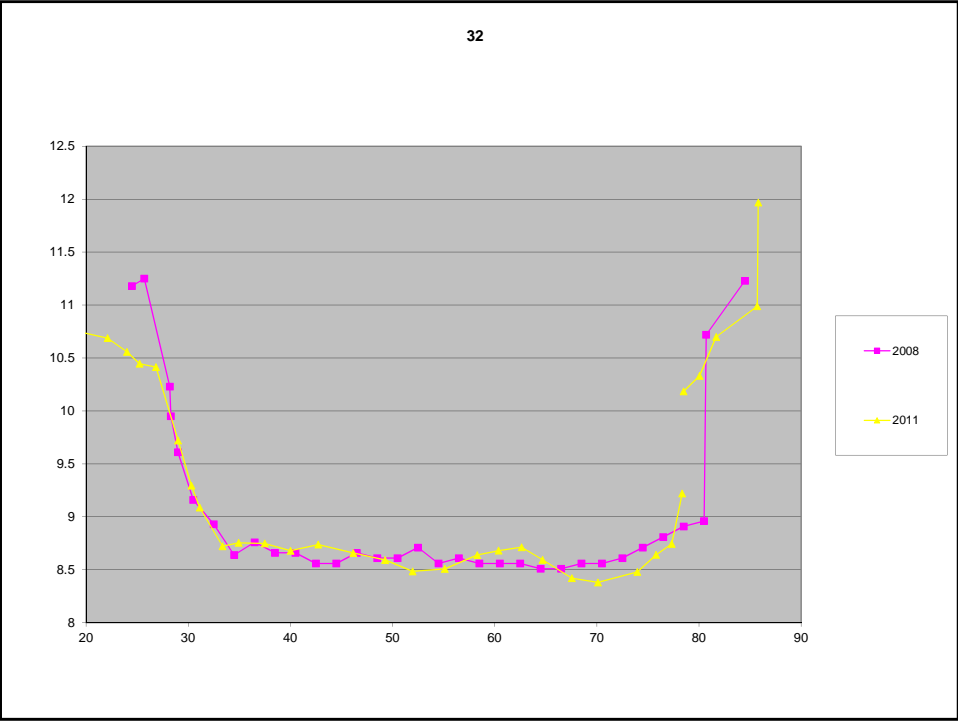
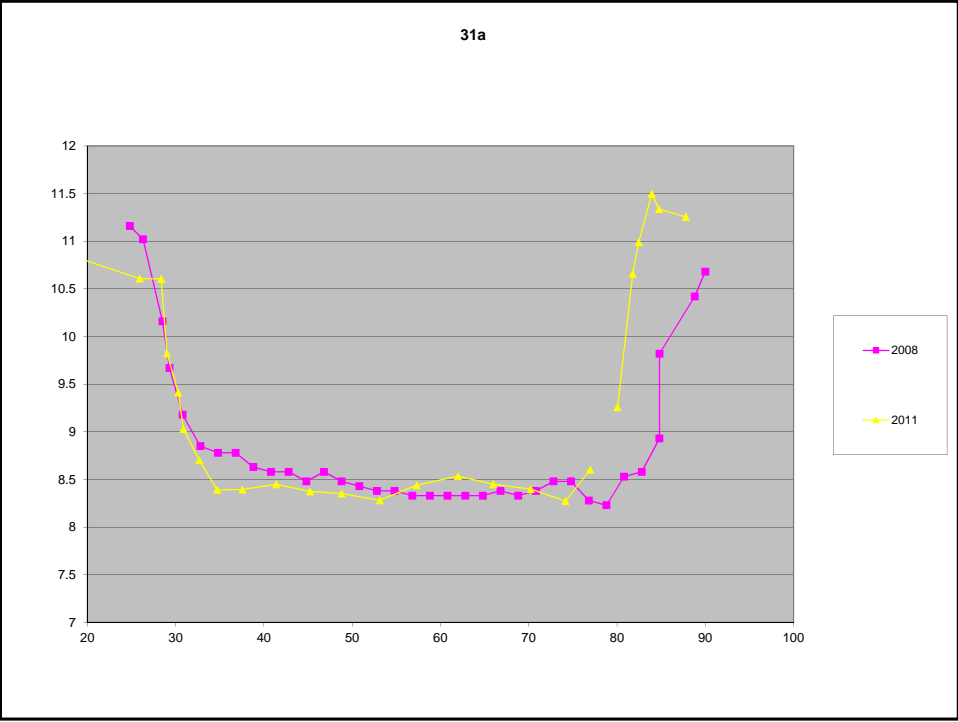


29

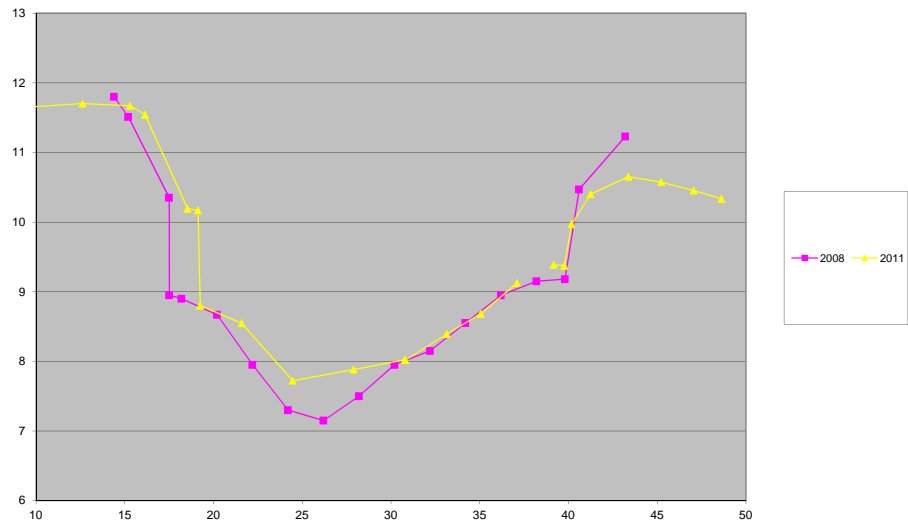


31

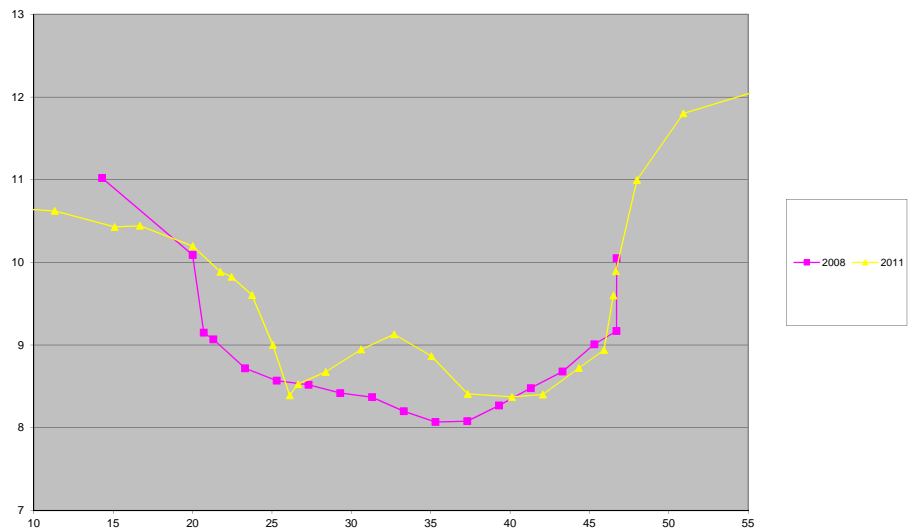


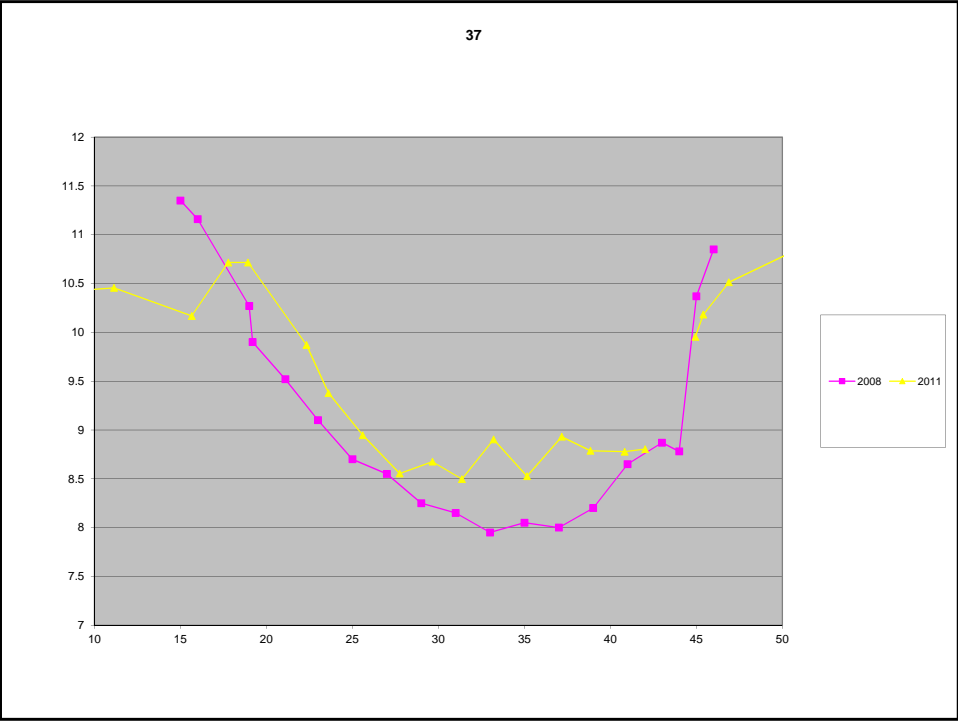
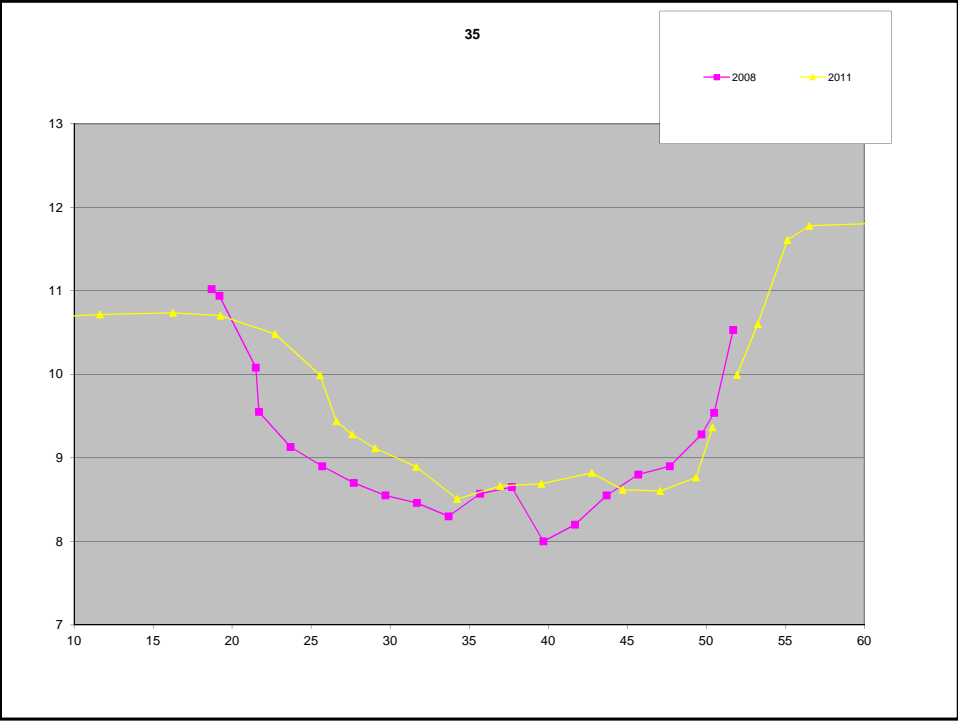


33

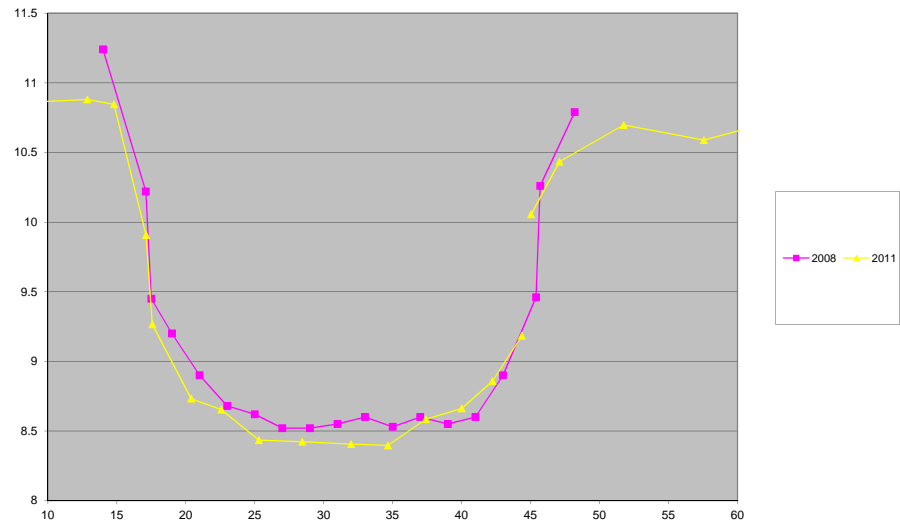


34 Near Torlesse

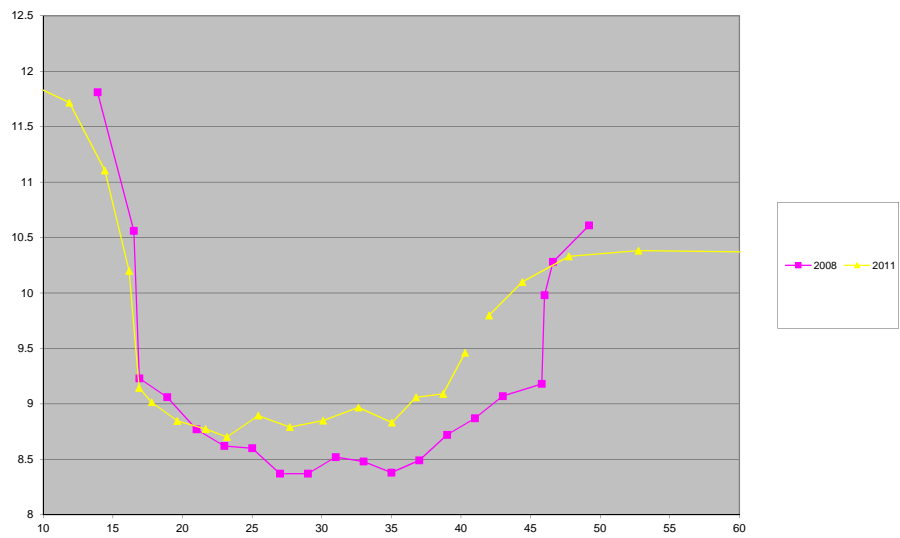




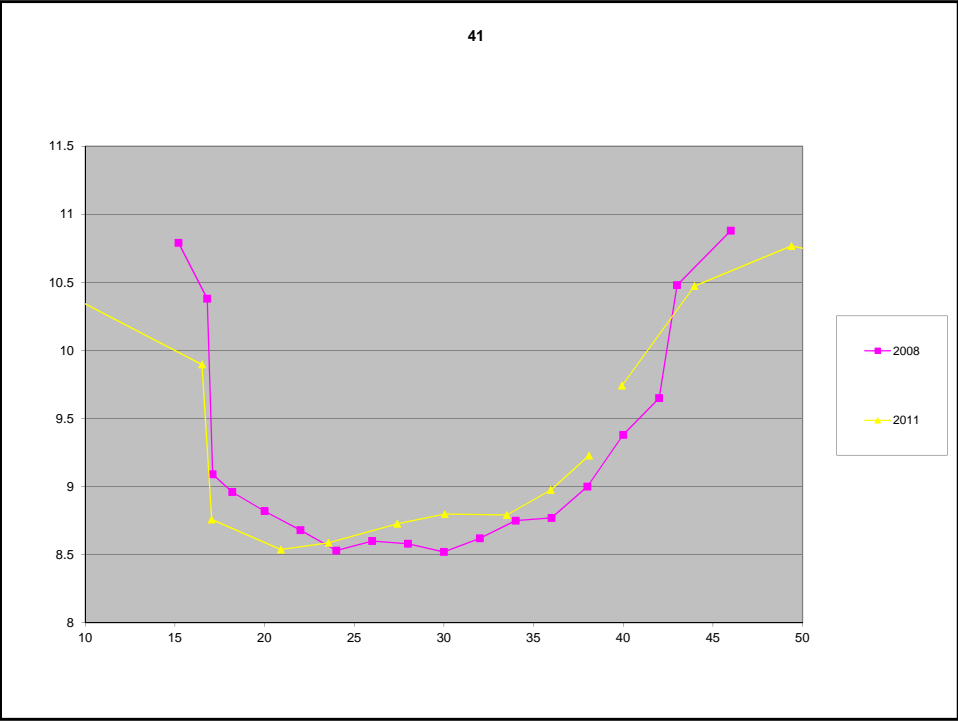
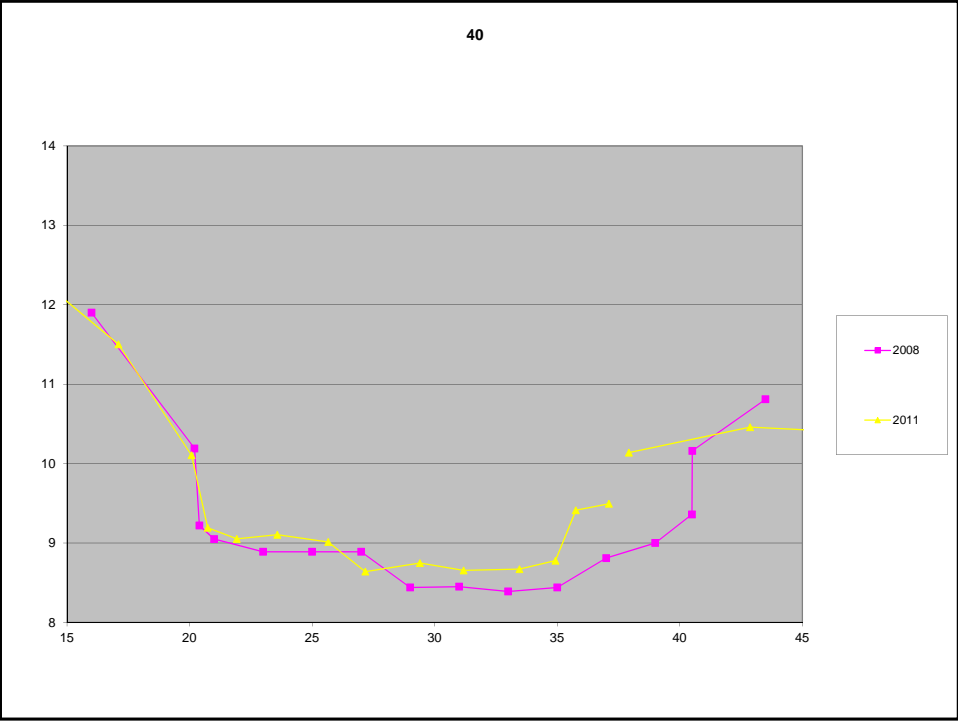
38



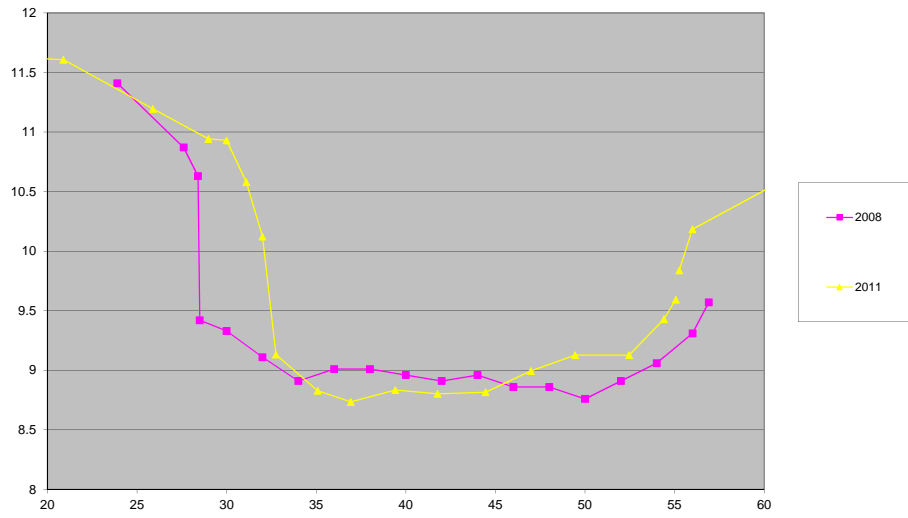
39



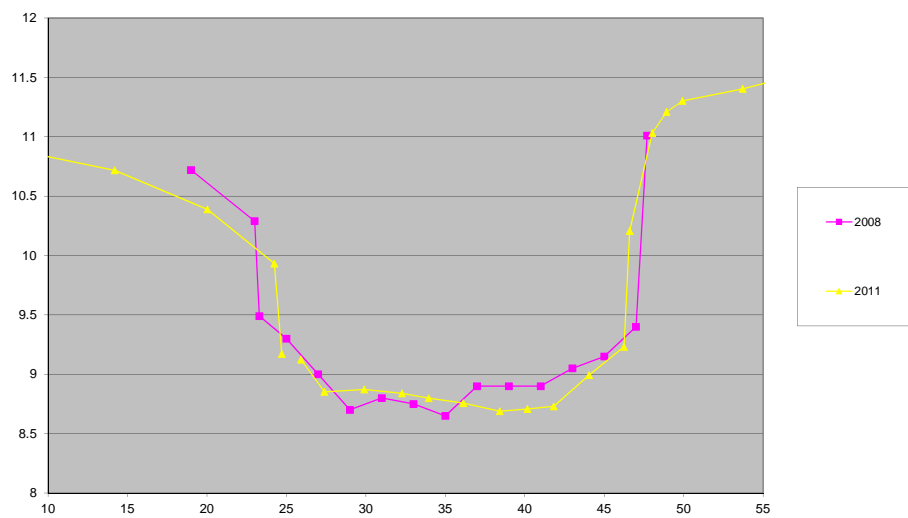




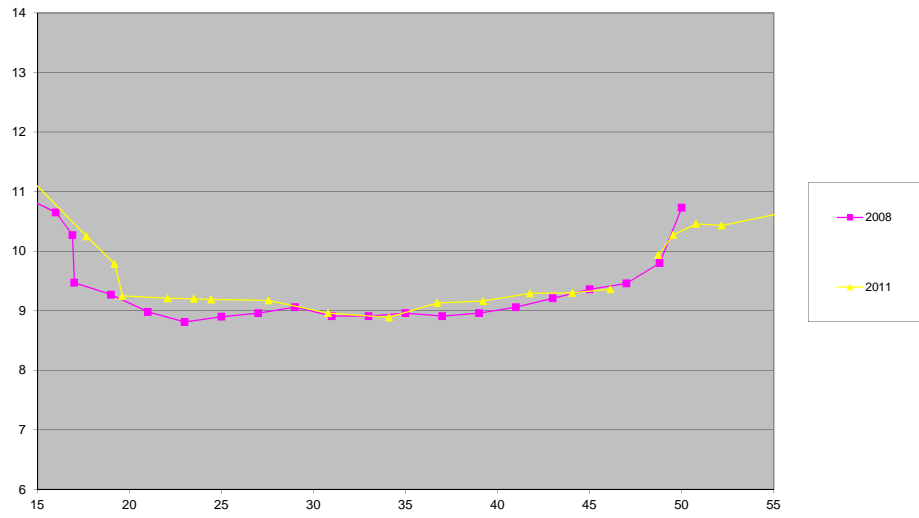
43



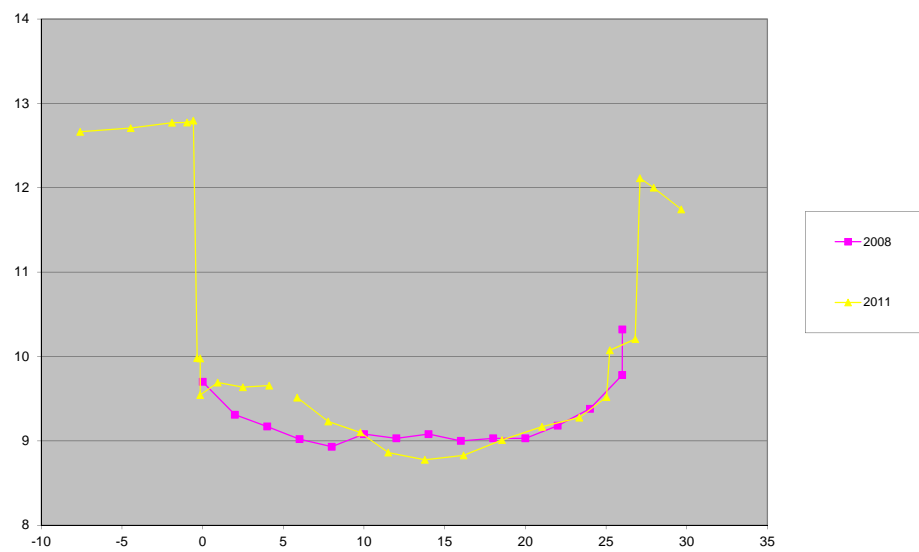
44

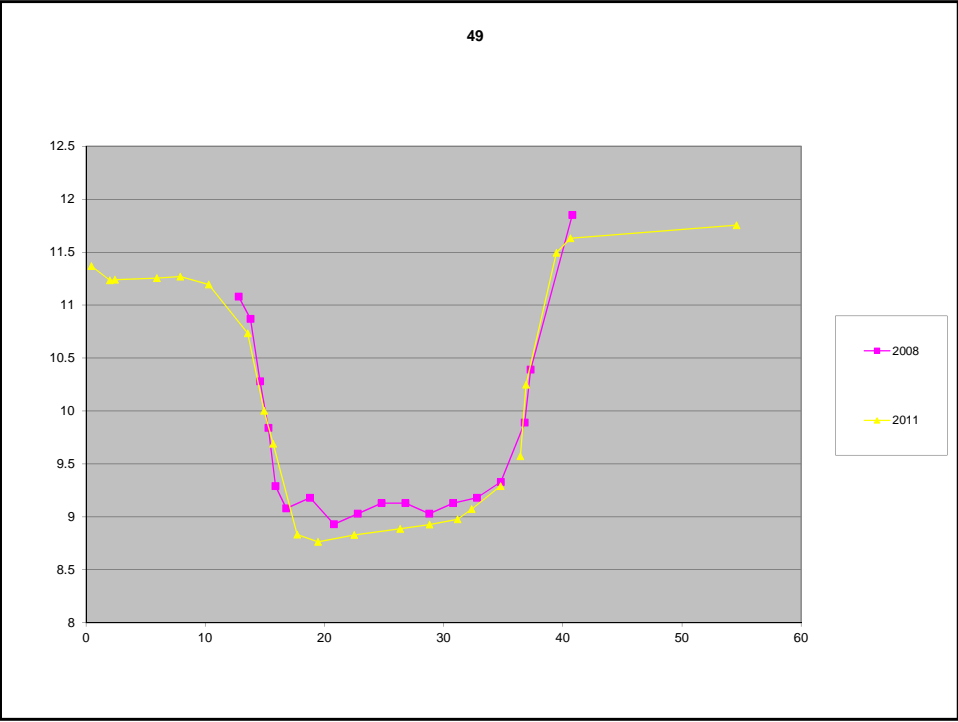
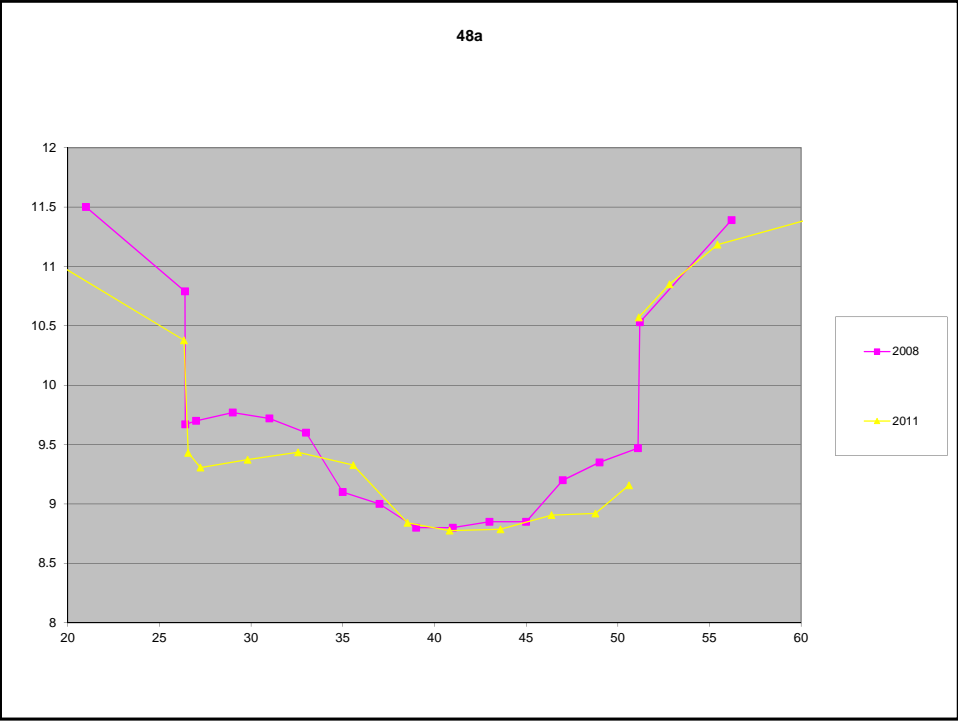


46

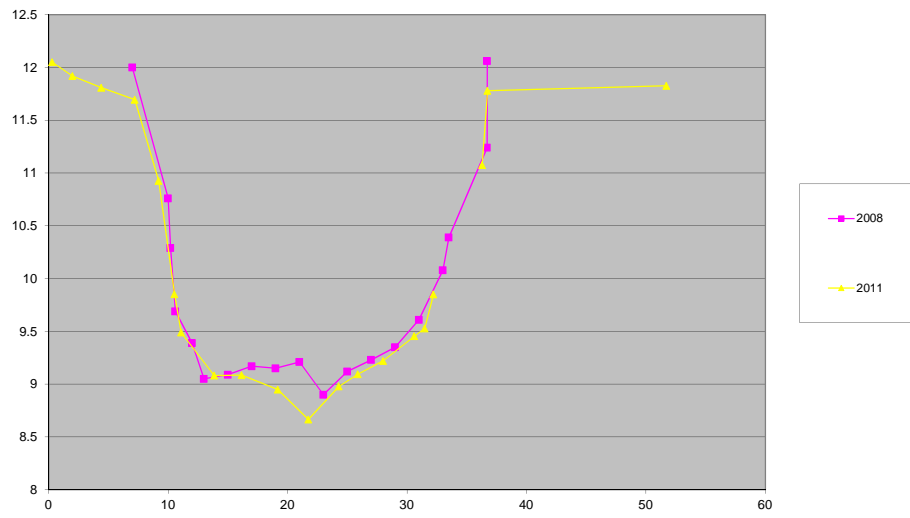


47

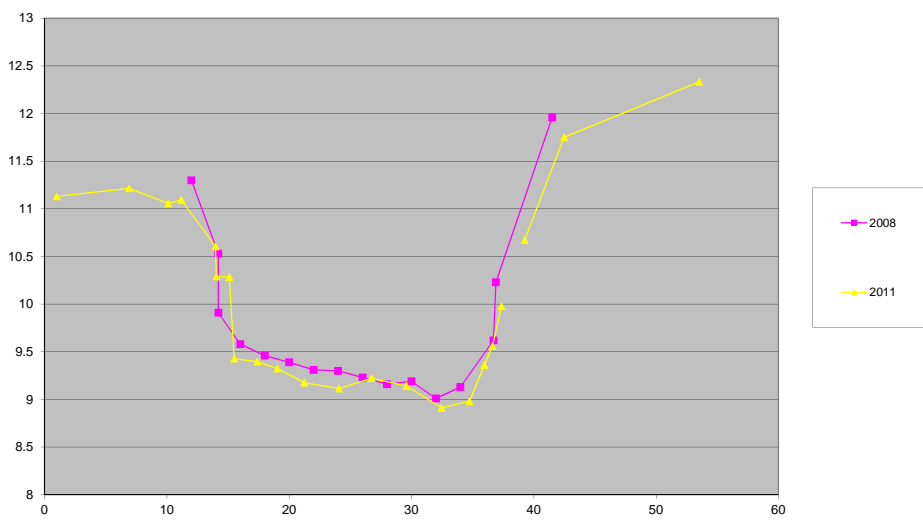




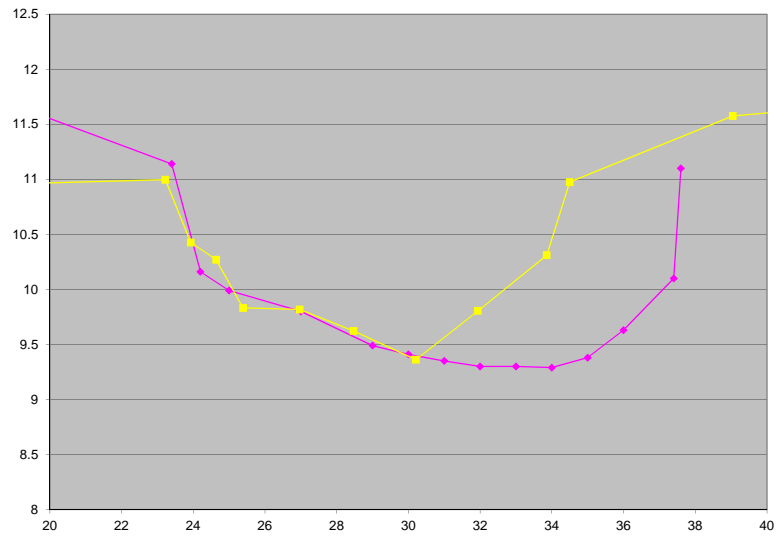
51



52







## **APPENDIX E:**

### **CPT LIQUEFACTION ANALYSIS**

**NORTH BANK KAIAPOI; NORTH BANK AVON**

**SOUTH BANK KAIAPOI; SOUTH BAK AVON**

## **APPENDIX F:**

### **COMPLETE ANALYSIS DATASET**